

# UNIVERSITETET I OSLO

Linn Neerbye Berntsen

## **Development of New Synthetic Methods for the Preparation of *N*-functionalized Hydantoins**

**Dissertation submitted for the degree of Philosophiae Doctor**

Department of Chemistry

Faculty of Mathematics and Natural Sciences

**2023**



© Linn Neerbye Berntsen, 2023

*Series of dissertations submitted to the  
Faculty of Mathematics and Natural Sciences, University of Oslo  
No. 2628*

ISSN 1501-7710

All rights reserved. No part of this publication may be  
reproduced or transmitted, in any form or by any means, without permission.

Cover: UiO.

Print production: Graphic Center, University of Oslo.

# Acknowledgements

The work presented in this dissertation was carried out at the Department of Chemistry, University of Oslo from 2018 to 2022 under the supervision of Dr. Alexander Harald Sandtorv, Dr. Ainara Nova Flores and associate professor Tore Bonge-Hansen. Financial support was provided by the same Department and is greatly acknowledged.

First, I would like to thank my previous main supervisor, Alexander Sandtorv, who trusted me enough to be the first PhD-candidate in a newly established group. You gave me the opportunity to work on an exciting project, the freedom to explore and create, and the opportunity to grow both as a person and a scientist. Your door was always open, and you were always up for lengthy discussions, scientific and non-scientific. I really appreciate your constant encouragement and support.

I would also like to thank Ainara Nova for taking the role as main supervisor in my final year. Also, thank you for the work we have done together and for introducing me to the glorious world of DFT calculations. Thank you, Tore Bonge-Hansen for all the support you gave when I needed it the most. Your endless positivity has really been helpful!

Thank you, past group members and present friends for contributing to making life on the 3<sup>rd</sup> floor just a little bit better. I would like to mention Karolina Filipowicz, Jeroen Ketele, Thomas Nordbø Solvi, Kristian Sørnes, Inga Schmidtke and Sara Peeters.

I would also like to express my gratitude towards the talented people contributing to the work presented in this dissertation; Kristian Sørnes, Thomas Nordbø Solvi, Brian Gilmour and Fiona Hagen; thank you! Dr. David Wragg, thank you for performing X-ray diffraction analyses, and an additional thanks for having the patience to teach me how to perform my analyses. Thank you, Inga Schmidtke, Håkon Gulbrandsen, Ainara Nova and Alexander Sandtorv for providing invaluable feedback on the dissertation.

Professor Frode Rise and Dirk Petersen; thank you for the incredible job you do running the NMR lab. Osamu Sekiguchi, Sverre Løyland and Erlend Steinvik; thank you for performing MS-analyses, and Massoud Kaboli; thank you for making teaching in the organic course lab fun!

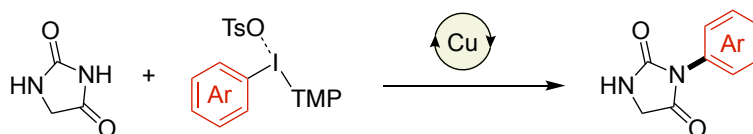
I would also like to extend my gratitude to my mom, dad, sister, extended family and friends for your unconditional love and support throughout this PhD. Lastly, thank you, my Rado. I'm eternally grateful for your everyday love and support, and sincerely grateful for the motivation and encouragement you have given me to push through to complete this journey. I could not have done this without you.

Linn Neerbye Berntsen

Oslo, March 2023.

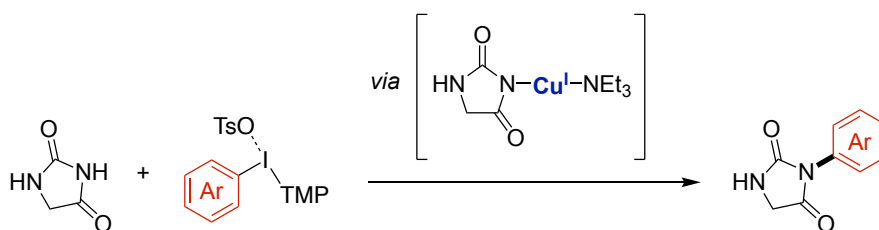
# Abstract

When new, synthetic challenges arise and the old, synthetic tools no longer suffice, the development of new methodologies are desired. The work in this dissertation focuses on expanding the synthetic toolbox by developing new strategies for C-N coupling of imides, with the focus being on the hydantoin framework. Being less reactive than many other *N*-nucleophiles, the imide functional group presents a challenging task for functionalizing the nitrogen atom and often requires assistance from a metal.



- Regio- and chemoselective
- Broad substrate scope
- Derivatization of pharmaceuticals

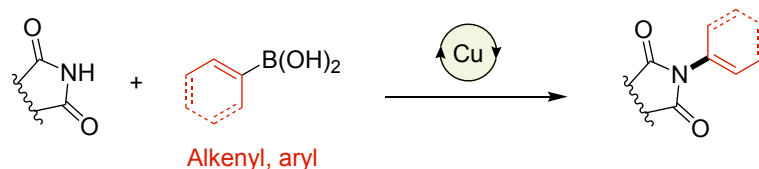
The applications and previous synthetic strategies for hydantoin functionalization is summarized in Chapter 1. Chapter 2 describes the development of a new methodology for the Cu-catalyzed and regioselective *N*-3-arylation of hydantoin. The protocol utilizes unsymmetrical diaryliodonium salts as arylating agents in the presence of triethylamine and a catalytic amount of a simple Cu-salt. The method is compatible with structurally diverse hydantoin and arenes bearing weakly electron donating- or withdrawing substituents. The method is applicable for late-stage functionalization of pharmaceutically relevant hydantoin. Parts of this chapter is published in **Paper I**.



- DFT calculations and experiments
- Origin of observed selectivities and product yields

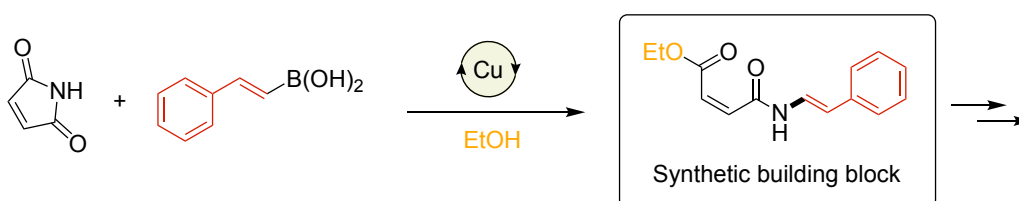
The computational investigation of the reaction in Chapter 2 is described in Chapter 3. Based on density functional theory (DFT) calculations and experimental observations, a Cu<sup>I</sup>/Cu<sup>III</sup>-catalytic cycle is proposed for the *N*-3-arylation of hydantoin. Our results suggest that deprotonation of hydantoin proceeds the oxidative addition of aryl(TMP)iodonium tosylate to a Cu<sup>I</sup>-imido intermediate. The rate-determining step of the reaction depends on the properties of the transferred aryl groups. The mechanism

agrees with species observed by  $^1\text{H}$  NMR spectroscopy, a kinetic isotope experiment, and the product yields observed. A completed manuscript for the work presented in this chapter is appended in this dissertation as **Paper II**.



- Mild and practical
- High FG tolerance
- (*E*)-alkenyl- and arylboronic acids

Chapter 4 covers the development of a general Cu-catalyzed  $\text{C}(\text{sp}^2)$ -N bond forming strategy for *N*-functionalization of hydantoins and other cyclic imides using boronic acids as coupling partners. The simple and practical method includes the use of (*E*)-alkenylboronic acids for the formation of (*E*)-enimides, with full retention of the double-bond configuration. The method is also operable with arylboronic acid, yielding *N*-arylimides. A large range of cyclic imides are allowed under the conditions, including pharmaceutically relevant hydantoins and uracils. Parts of this work is published in **Paper III**.



- One-pot
- Access to new *N*-substituted maleamates
- Synthon for synthetic transformations

In Chapter 5, the study of an unexpected reaction discovered in Chapter 4 is described. Using maleimide as a cyclic imide under the conditions described in Chapter 4 led to the formation of a linear molecule through a ring-opening mechanism. The use of the *N*-alkenylated maleamate (boxed) as a building block is demonstrated through exploration of synthetic transformations. The results indicate that EtOH is the preferred alcohol for ring-opening, and that transformations ranging from double bond isomerization and ester hydrolysis to intramolecular ring-formations were feasible. The work presented in this chapter is unpublished.

# List of papers

- I.** Cu-catalyzed *N*-3-arylation of Hydantoins Using Diaryliodonium Salts  
Linn Neerbye Berntsen, Ainara Nova, David S. Wragg, Alexander H. Sandtorv.  
*Org. Lett.* **2020**, *22* (7), 2687–2691.
  
- II.** A Mechanistic Study of the Cu-catalyzed *N*-arylation of Hydantoin with Aryl(TMP)iodonium salts.  
Linn Neerbye Berntsen, Ainara Nova.  
*Manuscript included in the Appendix.*
  
- III.** Cu-catalyzed C(sp<sup>2</sup>)-N-bond Coupling of Boronic Acids and Cyclic Imides  
Linn Neerbye Berntsen, Thomas Nordbø Solvi, Kristian Sørnes, David S. Wragg, Alexander H. Sandtorv.  
*Chem. Commun.* **2021**, *57*, 11851-11854.

# List of contributors

## Paper I

Linn Neerbye Berntsen: Experimental work and manuscript writing.

Ainara Nova: Proposal of mechanism, manuscript writing.

David Wragg: X-ray diffraction analyses (measurement and refinement).

Fiona X. Hagen: Experimental work (supplementary controls to optimization study).

Brian C. Gilmour: Experimental work (synthesis of diaryliodonium salts, Scheme 2.6).

Alexander H. Sandtorv: Supervision and manuscript writing.

## Paper II

Linn Neerbye Berntsen: Experimental work, computational (calculations with other substrates for the preferred pathway) and manuscript writing.

Ainara Nova: Supervision, computational work (calculations on pathway I and II with phenyl as substrate) and manuscript writing.

## Paper III

Linn Neerbye Berntsen: Experimental work, X-ray diffraction analyses and manuscript writing.

David S. Wragg: X-ray diffraction analyses (measurement and refinement).

Kristian Sørnes: Experimental work (synthesis of arylhydantoins, Scheme 4.8).

Thomas Nordbø Solvi: Experimental work (synthesis of arylhydantoins, Scheme 4.8).

Alexander H. Sandtorv: Supervision and manuscript writing.



# Abbreviations

Abbreviations and acronyms used throughout this dissertation are in agreement with the standards in the field\*. Non-standard abbreviations used in the text are included herein.

2,4-TZD	2,4-Thiazolidinedione
3c-4e	3-center-4-electron (bond)
APPI	Atmospheric pressure photoionization
BPin	Boronic acid pinacol ester
<i>t</i> -BuOK	Potassium <i>tert</i> -butoxide
<i>t</i> -BuONa	Sodium <i>tert</i> -butoxide
chxn	(±)- <i>trans</i> -1,2-Cyclohexanediamine
DBDMH	1,3-Dibromo-5,5-dimethylhydantoin
dd	Doublet of doublets (spectral)
ddd	Doublet of doublet of doublets (spectral)
DG	Directing group
DIPA	Diisopropylamine
DIPEA	<i>N,N</i> -Diisopropylethylamine
DMA	<i>N,N</i> -Dimethylaniline
DMAc	<i>N,N</i> -Dimethylacetamide
DMCyDa	<i>trans-N,N'</i> -dimethylcyclohexane-1,2-diamine
DMEDA	1,2-Dimethylethylenediamine
dq	Doublet of quartets (spectral)
dt	Doublet of triplets (spectral)
DTBP	2,6-Di- <i>tert</i> -butylpyridine
EDG	Electron donating group
EWG	Electron withdrawing group
FG	Functional group
hept	Heptet (spectral)
IS	Internal standard
KIE	Kinetic isotope effect
L	Ligand
LFA-1	Lymphocyte function-associated antigen 1
LiHMDS	Lithium bis(trimethylsilyl)amide

MeCN	Acetonitrile
met	2-Methylallyl
MIDA	<i>N</i> -Methyliminodiacetic acid
MW	Microwave
nd	Not detected
NMPPR	<i>N</i> -Methylpiperidine
OAc	Acetate
OEt	Ethoxy
OTf	Triflate
OTs	Tosylate
PEM	2,3-Bis(phenylethynyl)maleimide
PET	Positron emission tomography
Phen	1,10-Phenanthroline
PIDA	Phenyliodine(III)diacetate
PPR	Piperidine
Pro	Proline
SARM	Selective androgen receptor modulator
td	Triplet of doublets (spectral)
TEA/Et <sub>3</sub> N	Triethylamine
TfOH	Trifluoromethanesulfonic acid
TMA	Trimethylamine
TMHD	2,2,6,6-Tetramethyl-3,5-heptanedione
TMP	1,3,5-Trimethoxyphenyl
TMP-H	1,3,5-Trimethoxybenzene
TPA	Triisopropylamine
TsOH	<i>para</i> -Toluenesulfonic acid
tt	Triplet of triplets (spectral)

\* The ACS Style Guide: Effective Communication of Scientific Information. 3rd ed.; Coghill, A. M., Garson, L. R., Eds.; American Chemical Society: Washington, DC, 2006.

# Table of Contents

Acknowledgements .....	i
Abstract .....	iii
List of papers .....	v
List of contributors .....	vi
Abbreviations.....	vii
<b>Chapter 1: Introduction.....</b>	<b>1</b>
1.1 Hydantoins: General introduction and chemistry .....	1
1.1.1 Notable reactions and stability of the hydantoin ring.....	2
1.2 Applications of the hydantoin scaffold.....	3
1.3 Synthetic methods to access hydantoins .....	6
1.3.1 Classical methods .....	7
1.3.2 Non-classical methods .....	9
1.4 Cu-catalysis: A tool to form C-N bonds.....	10
1.4.1 Cu-catalysis in coupling reactions: Ullmann and Chan-Lam reactions.....	11
1.4.2 Cu-catalysis in <i>N</i> -functionalization of hydantoins.....	13
1.5 Objectives .....	16
<b>Chapter 2: Development of a methodology for the <i>N</i>-3-arylation of hydantoins using unsymmetrical diaryliodonium salts .....</b>	<b>19</b>
2.1 Introduction .....	19
2.1.1 Diaryliodonium salts.....	19
2.2 Development of a method for <i>N</i> -3-arylation of hydantoins.....	24
2.2.1 Initial hits and screening of bases and ligands .....	25
2.2.2 Catalyst screening .....	27
2.2.3 Can we eliminate the formation of the bis-arylated product? .....	30
2.2.4 Screening of the diaryliodonium salt counter anions .....	31
2.2.5 Screening of concentration, temperature and solvents .....	33
2.2.6 Screening of reaction stoichiometry .....	35
2.2.7 Screening of auxiliaries: TMP <i>vs.</i> Mes .....	36

2.2.8	Attempts to develop a protocol for bis-arylation .....	37
2.2.9	Final optimized conditions for the <i>N</i> -3-arylation reaction.....	38
2.2.10	Synthesis of aryl(TMP)iodonium tosylates .....	38
2.2.11	Scope and limitations of the developed reaction .....	40
2.3	Conclusion.....	44
2.4	Experimental.....	45

**Chapter 3: A mechanistic study of the Cu-catalyzed *N*-arylation of hydantoin using aryl(TMP)iodonium salts .....** 81

3.1	Introduction .....	81
3.2	Summary of important findings in the mechanistic study .....	83
3.3	Conclusion.....	86

**Chapter 4: Development of a methodology for Cu-catalyzed C(sp<sup>2</sup>)-N cross-coupling of cyclic imides and boronic acids .....** 87

4.1	Introduction .....	87
4.1.1	Access to enimides through <i>N</i> -alkenylation reactions.....	87
4.1.2	Boronic acids as coupling partners in cross-coupling reactions .....	90
4.2	Development of a method for <i>N</i> -alkenylation of imides .....	92
4.2.1	Screening of reaction conditions .....	93
4.2.2	Scope and limitations of the developed reaction .....	97
4.2.3	C(sp <sup>2</sup> )-N coupling reactions with other boronic acid derivatives.....	105
4.2.4	Reaction mechanism: Proposal of a catalytic cycle .....	106
4.3	Conclusion.....	108
4.4	Experimental.....	108

**Chapter 5: Simple access to *N*-substituted maleamates *via* one-pot C(sp<sup>2</sup>)-N cross-coupling and ring-opening of maleimides.....** 119

5.1	Introduction .....	119
5.2	Formation of maleamic acids and esters from maleimides .....	119
5.2.1	Strategies to access <i>N</i> -substituted maleamic acids and esters .....	120
5.3	Exploration of the formation and reactivity of ( <i>E</i> )- <i>N</i> -styryl ethyl maleamate.....	121
5.3.1	Optimization of reaction conditions for the one-pot C-(sp <sup>2</sup> )-N coupling and ring-opening reaction.....	121
5.3.2	Can we produce other esters by changing the solvent?.....	123

5.3.3	Changing the maleimide or the coupling partner: how will it affect the reaction? .....	124
5.3.4	( <i>E</i> )- <i>N</i> -styryl ethyl maleamate (11b) as synthon in synthetic transformations.....	125
5.4	Conclusion.....	127
5.5	Experimental.....	128
<b>Chapter 6: Future prospects.....</b>		<b>153</b>
6.1	Chapter 2 and 3: <i>N</i> -3-arylation of hydantoins .....	153
6.2	Chapter 4: <i>N</i> -alkenylation of cyclic imides with boronic acids.....	155
6.3	Chapter 5: <i>N</i> -alkenylation and ring-opening of maleimides .....	156
<b>References.....</b>		<b>159</b>
<b>Appendix: Paper I-III.....</b>		<b>181</b>



# Chapter 1: Introduction

## 1.1 Hydantoins: General introduction and chemistry

Hydantoin (2,4-imidazolidinedione) **1a** (Figure 1.1) is a five-membered heterocyclic compound first discovered by Adolf von Baeyer in 1861.<sup>1</sup> During his work with uric acid he isolated hydantoin as a hydrogenation product of allantoin, hence the name. The conformation of the newly discovered substance was however unclear until 1870 when Adolph Strecker<sup>2</sup> proposed the now-accepted cyclic structure. Designation of positions in the hydantoin ring has, however, differed over the years.<sup>3</sup> The general consensus nowadays is as displayed in Figure 1.1.

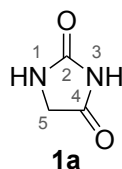
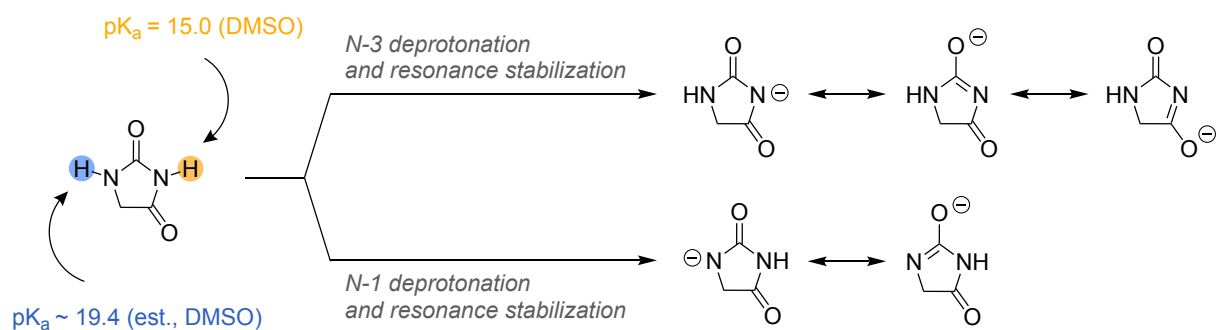


**Figure 1.1.** Hydantoin core structure with numbering.

Comprised of two nitrogen atoms, two carbonyl groups and an  $\alpha$ -carbonyl carbon, the hydantoin framework provides multiple reactive positions. The N-1, N-3 and C-5 positions are considered the primary points of functionalization,<sup>4,5</sup> whereas the carbonyl positions only partake in some reactions.<sup>3</sup> The two N-H sites and the electron withdrawing ability of the carbonyl groups helps explain the weakly acidic nature of hydantoins.<sup>6</sup>  $pK_a$  values of 9.0-9.1 in water<sup>7,8</sup> and 15.0 in DMSO<sup>9</sup> have been determined for the proton in the N-3 position of unsubstituted hydantoin, making it the most acidic site. The N-3 position can be regarded as an imide (with two carbonyl groups) where resonance stabilization of the negative charge (as a result of deprotonation) is greatest (Scheme 1.1).

The  $pK_a$  of the amidic N-1 proton has been estimated to 19.4 in DMSO.<sup>10</sup> The ability to stabilize a negative charge is lesser in this position, hence the weaker acidity. Situated alpha to a carbonyl group, the C-5 protons can also be considered very weakly acidic. Based on other  $\alpha$ -carbonyl amide protons,<sup>11</sup> a very rough estimate of  $pK_a \approx 30$  can be made.



**Scheme 1.1.**  $\text{p}K_a$ -values of the N-3- and N-1 protons, deprotonation and resonance stabilization of the negative charge.

Intramolecular proton transfers cause hydantoin to exhibit tautomerism. Several tautomeric forms have been suggested (Figure 1.2). Liquid- and solid state studies confirm the predominance of the imido-tautomer **I**.<sup>12</sup> Additional support from more recent density functional theory (DFT) calculations confirm the stability of conformer **I**, both isolated and in solution.<sup>13, 14</sup> However, the importance of tautomers **II-VII** are reflected in various reactions of hydantoin and hydantoin analogs.<sup>3</sup> For example, racemization of optically active hydantoin can only be explained by the enolization of conformer **IV**, **V** or **VI**.

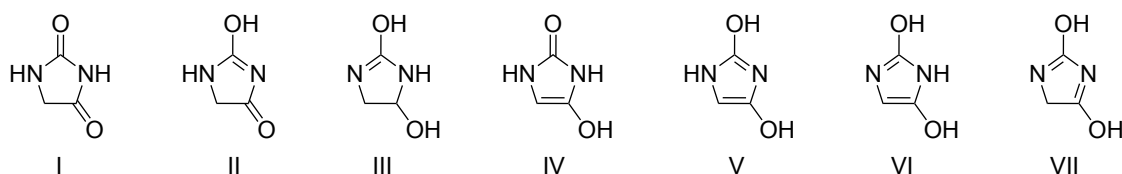
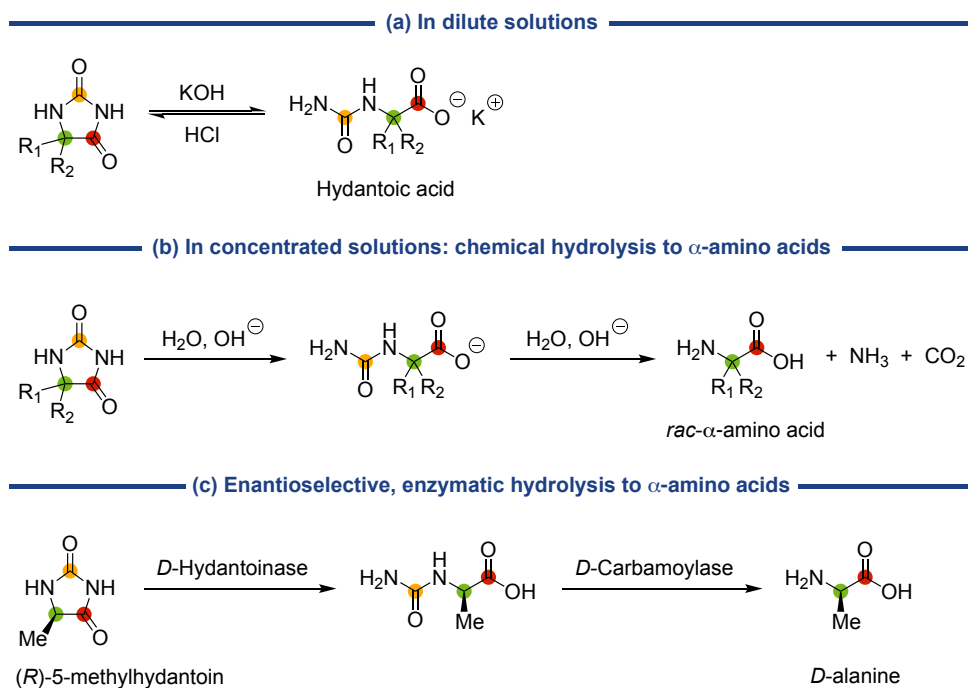


**Figure 1.2.** Hydantoin tautomers.

### 1.1.1 Notable reactions and stability of the hydantoin ring

In the presence of alkali salts in hot, dilute solutions, the hydantoin ring is cleaved and converted to salts of hydantoic acid (Scheme 1.2a). The reverse reaction, cyclization, can be realized with hot, dilute hydrochloric acid<sup>3, 15</sup> (Scheme 1.2a). The reaction is not reversible in concentrated alkali- or (mineral)acidic solutions.<sup>16</sup> Instead, the hydantoin ring is hydrolyzed to its corresponding  $\alpha$ -amino acid (Scheme 1.2b). Amino acid synthesis by hydantoin hydrolysis is a highly valuable synthetic tool as both natural and unnatural amino acids can be obtained. However, chemically induced reactions typically give racemic mixtures. For enantioselective production of *D*- and *L*-amino acids, enzymatic routes involving the use of biocatalysts are used (Scheme 1.2c).<sup>17-19</sup>





**Scheme 1.2.** Reactions involving cleavage of the hydantoin ring.

Ring stability is highly influenced by the substituents on the ring atoms. Generally, substituted hydantoins are more stable than unsubstituted ones with regards to hydrolysis of the ring and the ease of formation from hydantoic acid. The stability is apparent with substituents at either nitrogen atoms or at C-5 and typically increases with the number of substituents.<sup>3, 15</sup> Substituents also affect the acidic character of hydantoins, generally by increasing the acidity. As an example, the  $pK_a$  of 5,5-diphenylhydantoin is 8.3 in water,<sup>20</sup> which is 7-8 times stronger than unsubstituted hydantoin.

## 1.2 Applications of the hydantoin scaffold

Hydantoins have several applications areas (Figure 1.3) due to its intrinsic properties and tunable nature. The combination of several sites of functionalization and numerous possible substitution patterns provides endless possibilities to regulate its features; introduction of substituents in the C-5 position allows for altering flexibility/rigidity and chirality while the presence of hydrogen bond donors- and acceptors allows for adjusting hydrophilicity/lipophilicity.<sup>21, 22</sup>

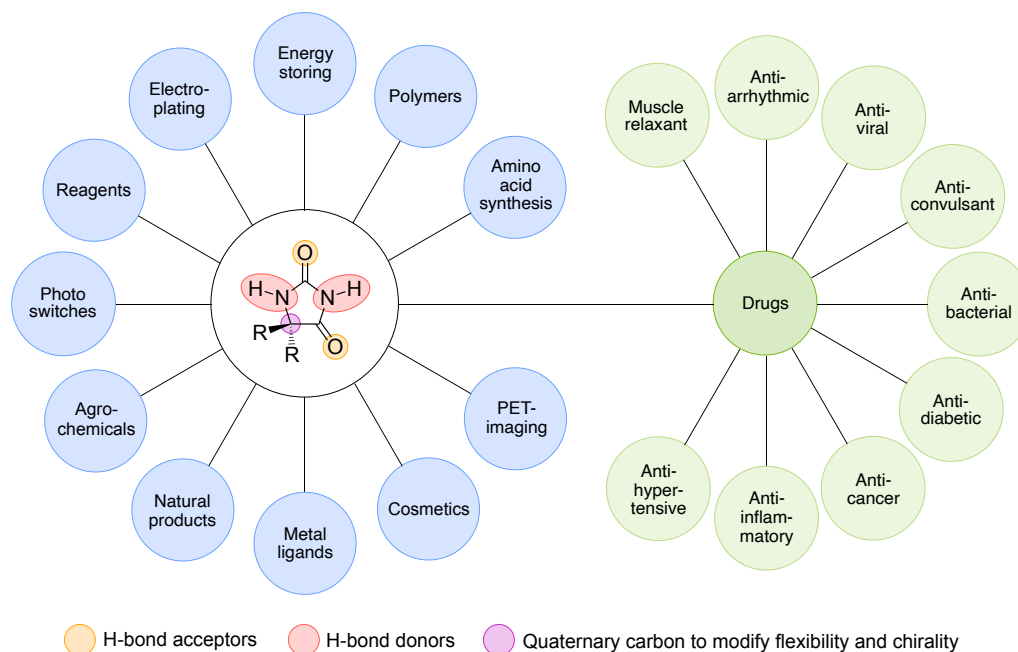


**Figure 1.3.** Applications and structural properties of hydantoin. Adapted from reference 21 and 22.

The versatile heterocycle can be found in molecular photo switches,<sup>23, 24</sup> energy storing materials,<sup>25</sup> polymers,<sup>26, 27</sup> agrochemicals (pesticides)<sup>28</sup> and as preservatives in cosmetics.<sup>29</sup> Figure 1.4 displays examples where the hydantoin core is embedded in such structures. Substituted hydantoin can be utilized as reagents in synthesis.<sup>30-32</sup> By introducing halogens on both nitrogen atoms, they can serve as electrophilic halogenation agents.<sup>33-35</sup> For example, 1,3-dibromo-5,5-dimethylhydantoin (DBDMH) ( $X = \text{Br}$  in Figure 1.4) is a cheap and convenient alternative to the more popular *N*-bromosuccinimide (NBS) as they exhibit similar reactivities.

Due to their chelating abilities, hydantoin is used as ligands in transition metal complexes.<sup>36-41</sup> The coordination modes differ with the metal and the overall conditions with N-3 and/or O-4 coordination being the most dominant (Figure 1.4). Their complexing aptitude is evident in *e.g.* electroplating of silver.<sup>42, 43</sup>

Owing to the many advances made in the preparation of hydantoin by cyclization (see Section 1.3.1.1), a variety of isotope labelled atoms can be directly introduced into the hydantoin ring.<sup>44</sup> Depending on the isotopic labelling, they can be utilized as radiotracers in PET-imaging<sup>45, 46</sup> (Figure 1.4). Moreover, hydantoin cyclization reactions have been exploited in derivatization of natural plant-extract in the synthesis of natural product like hydantoin.<sup>47</sup> Hydantoin-containing molecules have also been directly isolated from natural sources<sup>48-50</sup> (Figure 1.4).

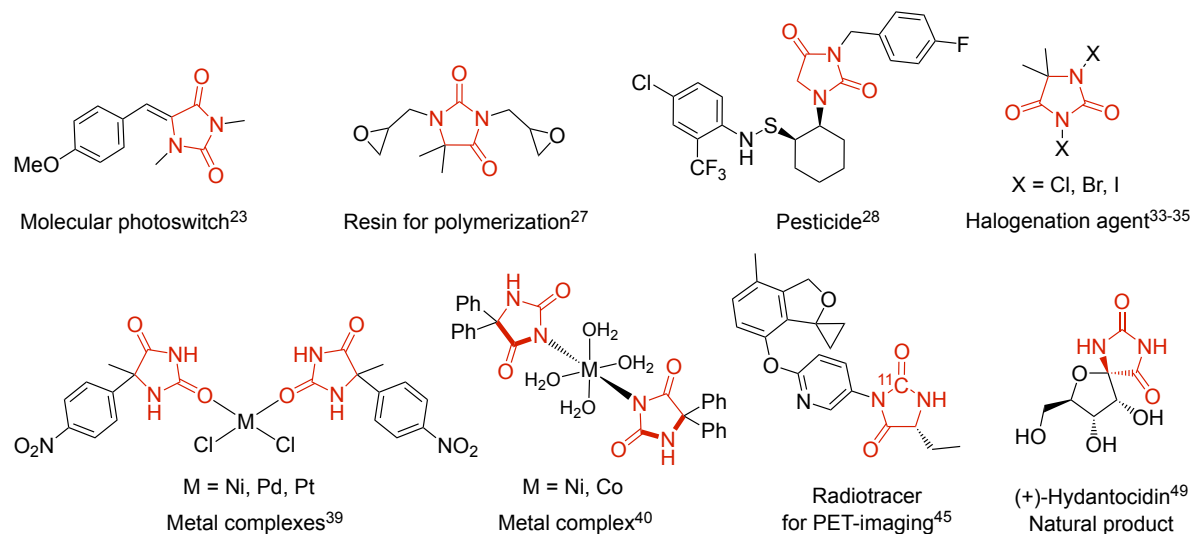


**Figure 1.4.** The hydantoin ring in structures with a wide range of applications.

As seen in Section 1.1.1, hydrolysis of the hydantoin ring can be used in the production of both natural- and unnatural amino acids.<sup>17, 19</sup> Despite the many properties and uses of hydantoin, most notable are the broad biological and pharmacological properties and hence its appearance in wide range of drugs<sup>51-59</sup> (Figure 1.4).

Hydantoin is considered a privileged scaffold in medicinal chemistry being an integral part of several bioactive compounds.<sup>60, 61</sup> The wide range of biological activities can be attributed to the ease of modifications on the hydantoin ring, making them highly attractive candidates for drug discovery. A vast number of hydantoin-containing compounds have been led through clinical trials and several of them are clinically approved and commercialized (Figure 1.5). Some representative examples are the marketed drugs phenytoin (anticonvulsant), dantrolene (muscle relaxant) nitrofurantoin (antibacterial) and nilutamide (antiandrogen). Clinical candidates include the selective androgen receptor modulators (SARMs) GLPG-0492<sup>62</sup> and PS178990 (previously known as BMS-564929)<sup>63</sup>, as well as leukocyte function-associated antigen-1 (LFA-1) antagonists BMS-587101<sup>64</sup> and BIRT377.<sup>65</sup>

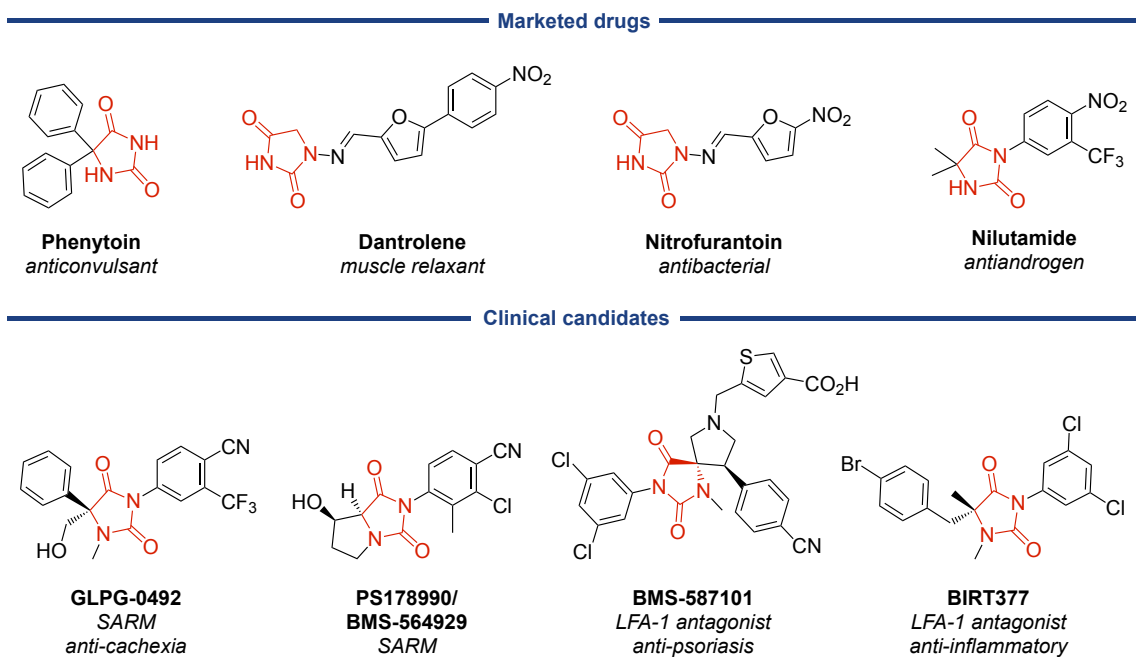


Figure 1.5. Hydantoin marketed drugs and clinical candidates.

### 1.3 Synthetic methods to access hydantoin

Numerous methods have been developed to access the hydantoin scaffold.<sup>5, 66</sup> The previously mentioned C-5, N-1 and N-3 positions suggest a variety of possible substitution patterns and give rise to several classes of mono-, di-, tri- and/or tetrasubstituted hydantoins.

In the following subsections, the synthetic methods for accessing substituted hydantoins will be divided into “classical” and “non-classical”. The classical approaches include cyclization reactions from linear precursors or direct functionalization of the ring by the means of substitution (*e.g.* condensation and nucleophilic substitution). Easily accessible starting materials with a high number of diversity points, the ease of the reactions and the possibility to obtain nearly any desired substituted hydantoin make the classical cyclization methods extremely attractive from a synthetic perspective. Some limitations are, however, associated with these methods. The apparent drawbacks are the harsh conditions and toxic reagents often used, combined with the invariable C-5 substitution. Additionally, long reaction times, solubility problems and poor yields have been reported.<sup>22, 67</sup>

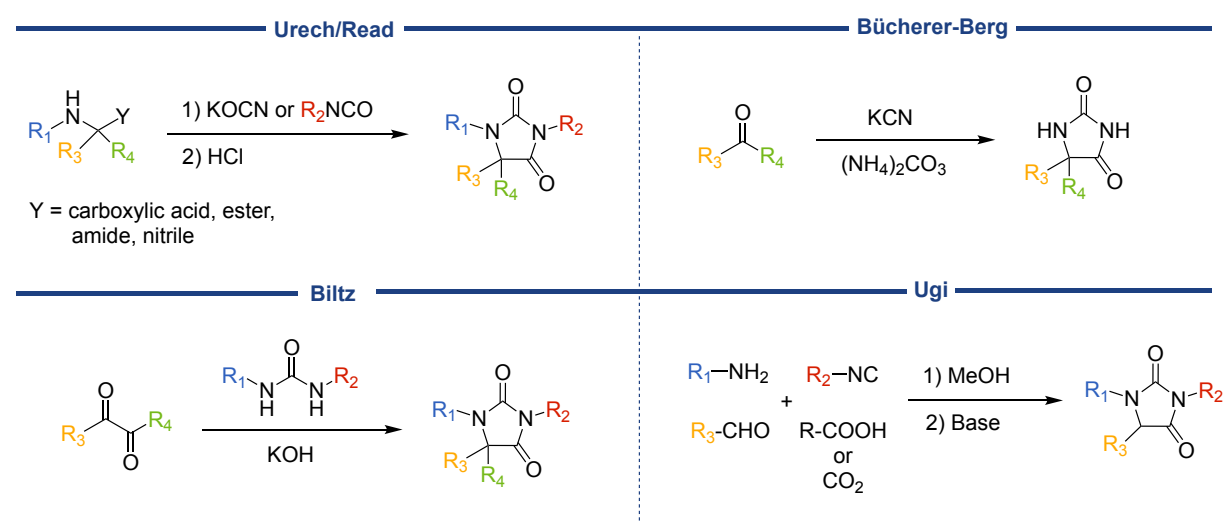
To overcome some of the limitations associated with the classical linear methods, direct functionalization offers an alternative solution to access substituted hydantoins. In a

direct route, the substituents are chemo- or regioselectively put onto the ring itself. This strategy offers many advantages; it is potentially faster, cheaper, allows for divergent modification and late-stage functionalization of the hydantoin core. Despite the diversity the classical methods offer, limitations exist. Unaddressed synthetic challenges include the direct and selective functionalization where the classical strategies fall short. The non-classical methods rely on new synthetic methodologies, in particular on advances made in transition metal catalysis.

### 1.3.1 Classical methods

#### 1.3.1.1 Cyclization reactions

The first methods developed for hydantoin ring synthesis were dedicated to the preparation of 5-substituted and 5,5-disubstituted hydantoins.<sup>5</sup> Urech<sup>68</sup> reported the first constructive synthetic route for 5-methylhydantoin in 1873, which still remains as one of the most prominent approaches to access 5-substituted hydantoins. It involves a two-step condensation-cyclization of amino acids in the presence of potassium cyanate and hydrochloric acid (Scheme 1.3). Equally impactful methods are: (1) Read<sup>69</sup> synthesis (Scheme 1.3), using Urech conditions, but starting from  $\alpha$ -aminonitriles, (2) the Bücherer-Berg<sup>70</sup> reaction starting from carbonyl compounds, potassium cyanate and ammonium carbonate to generate 5-substituted or 5,5-disubstituted hydantoins (Scheme 1.3) and (3) the Biltz<sup>71</sup> synthesis utilizing 1,2-dicarbonyl compounds and urea under strong basic conditions to obtain 5,5-disubstituted hydantoins (Scheme 1.3).

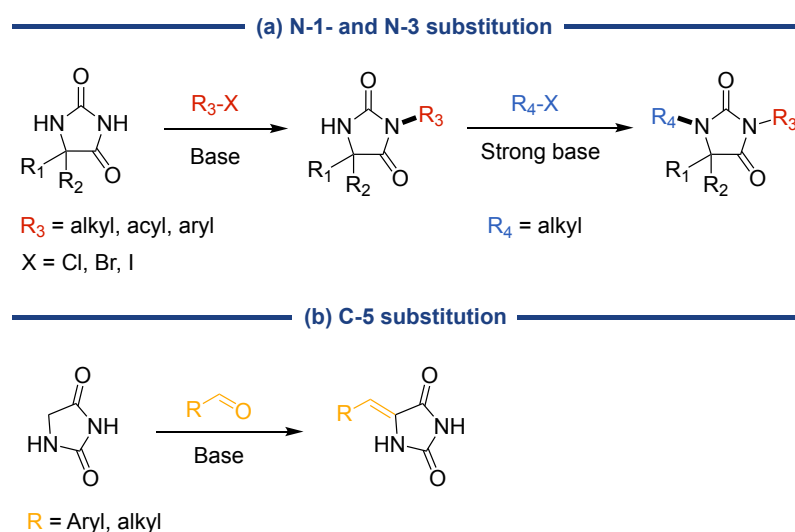


**Scheme 1.3.** Classical approaches to substituted hydantoins, including the Urech/Read, Bücherer-Berg, Biltz and Ugi-type condensation reactions.

The primary access point for *N*-substituted hydantoins also include linear synthesis or multicomponent reactions (MCRs). Improvements and variations of the classical conditions have been extensively reported over the years.<sup>3, 5, 66</sup> They include substituents on the amino-nitrogen in the amino acid derivative in a Urech/Read type reaction giving rise to *N*-1-substituted hydantoins.<sup>58, 59, 72-74</sup> The use of substituted isocyanates instead of cyanate salts results in substituents in the N-3 position.<sup>72, 75-79</sup> Following Biltz method, substituted ureas have been used to access hydantoins with substituents in N-1<sup>80, 81</sup> or N-3<sup>82-84</sup> (or both) positions depending on the conditions. Another well-established approach used is the Ugi condensation reaction where primary amines, aldehydes, isocyanides and carboxylic acid (or carbon dioxide) react to give 1,3,5-substituted hydantoins.<sup>85-89</sup> Besides the aforementioned methods, a plethora of other synthetic routes have been developed to furnish various substituted hydantoins.<sup>5</sup>

### 1.3.1.2 Direct functionalization by substitution and addition reactions

Derivatization of the hydantoin scaffold in either nitrogen position is predominantly accomplished through alkylation and acylation reactions (Scheme 1.4). The most usual way is by reaction with alkyl- and acyl halides in alkaline solutions, where the more acidic N-3 position is the preferred site of reaction.<sup>30, 90-99</sup> Similar conditions have also been implemented in arylation reactions where aryl halides undergo nucleophilic aromatic substitution to furnish *N*-3-arylated hydantoins (Scheme 1.4a). The method is, however, restricted to electron deficient aryl halides, which limits the general applicability of the strategy. Phenytoin<sup>100, 101</sup> and nilutamide<sup>102-104</sup> (Figure 1.4) analogs have been prepared using such methods.



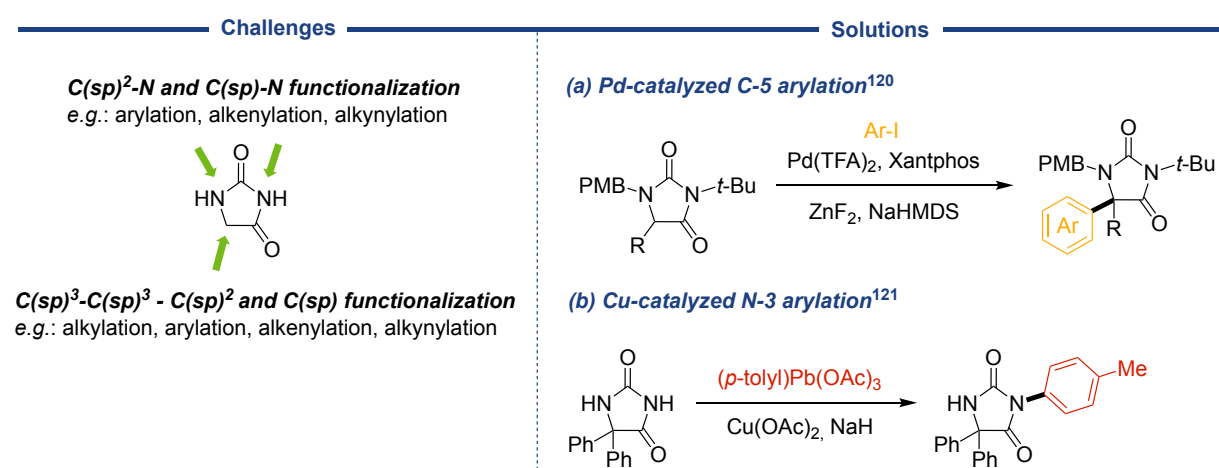
**Scheme 1.4.** Classical approaches for direct functionalization of hydantoins.

Introduction of alkyl groups at the N-1 nitrogen is generally only possible when N-3 is already substituted, and often requires harsher conditions (use of a stronger base and/or longer reaction times) (Scheme 1.4a). However, some cases of direct N-1-alkylation (without N-3-substitution) have been reported under similar, basic conditions.<sup>105, 106</sup> Selective acylation of the less basic, but more nucleophilic N-1 position is considered less challenging than alkylation and commonly performed with acid anhydrides.<sup>107-113</sup>

While most saturated C-5 substituents are introduced through cyclization reactions, unsaturated substituents are introduced directly on the ring (Scheme 1.4b). Depending on the R-group, they are referred to as aryl- or alkylidenehydantoin and are predominantly accessed through the Knoevenagel condensation reaction with aldehydes.<sup>114-118</sup>

### 1.3.2 Non-classical methods

The previously untackled challenges from the classical methods include direct and selective functionalization of N-1, N-3 and C-5 (Scheme 1.5, left). Functionalizations include, but are not limited to, arylations, alkenylations and alkynylations. For the C-5 position, alkylation is also a challenge that requires other tools (than those provided by the classical methods) to be conquered. Some of these matters have already been dealt with,<sup>119</sup> most often by the aid of transition metals<sup>120, 121</sup> (Scheme 1.5, right).



**Scheme 1.5.** Challenges for direct and selective functionalization of hydantoin and two reported non-classical strategies to handle them.

A direct Pd-catalyzed C-5 arylation was reported for the first time by Clayden and co-workers in 2015<sup>120</sup> (Scheme 1.5a). The use of palladium as a transition metal catalyst allowed for the coupling of a sp<sup>2</sup>-carbon with the C-5 carbon, furnishing 5,5-disubstituted hydantoins. The first example of selective *N*-3-functionalization of hydantoins with a metal was reported for the first time in 1992<sup>121</sup> (Scheme 1.5b). In this reaction, arylation with a slightly electron rich arene was accomplished with the assistance of a Cu-catalyst.

As will be shown in later sections, some advances have been made for the direct- and transition metal-catalyzed *N*-arylation reactions. Of particular interest in this work are the *N*-3-functionalization (including arylations) of hydantoins. The following sections will shed light on how these challenges can be met and what tools can be utilized to successfully handle them.

## 1.4 Cu-catalysis: A tool to form C-N bonds

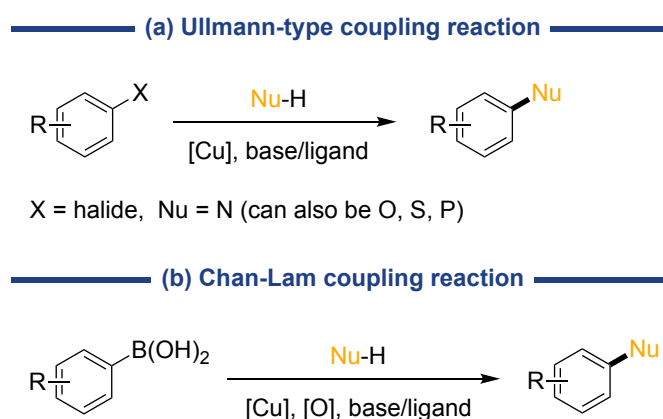
Copper has emerged as one of the most important transition metals in various transformations of organic molecules owing to its high abundance, low price, low toxicity and chemical diversity.<sup>122</sup> Its versatility stems from the accessible Cu<sup>0</sup>, Cu<sup>I</sup>, Cu<sup>II</sup>, Cu<sup>III</sup> oxidation states, allowing it to catalyze both polar- (two-electron) and radical (one-electron) processes.<sup>123</sup> Additionally, copper coordinates easily to heteroatoms,  $\pi$ -bonds and terminal alkynes, providing the ability for a wide range of transformations.

Copper has proven to be an important tool in the construction of C-N bonds.<sup>124</sup> The discovery of Cu-promoted cross-coupling reactions started with Ullmann and Goldberg in the early 1900s<sup>125-127</sup> (Scheme 1.6a). Almost a century later Chan<sup>128</sup> and Lam<sup>129</sup> reported the well-known Chan-Lam cross-coupling reaction (Scheme 1.6b). Besides the Pd-catalyzed Buchwald-Hartwig cross-coupling, these are considered the main routes to form C-N bonds.<sup>130</sup>



### 1.4.1 Cu-catalysis in coupling reactions: Ullmann and Chan-Lam reactions

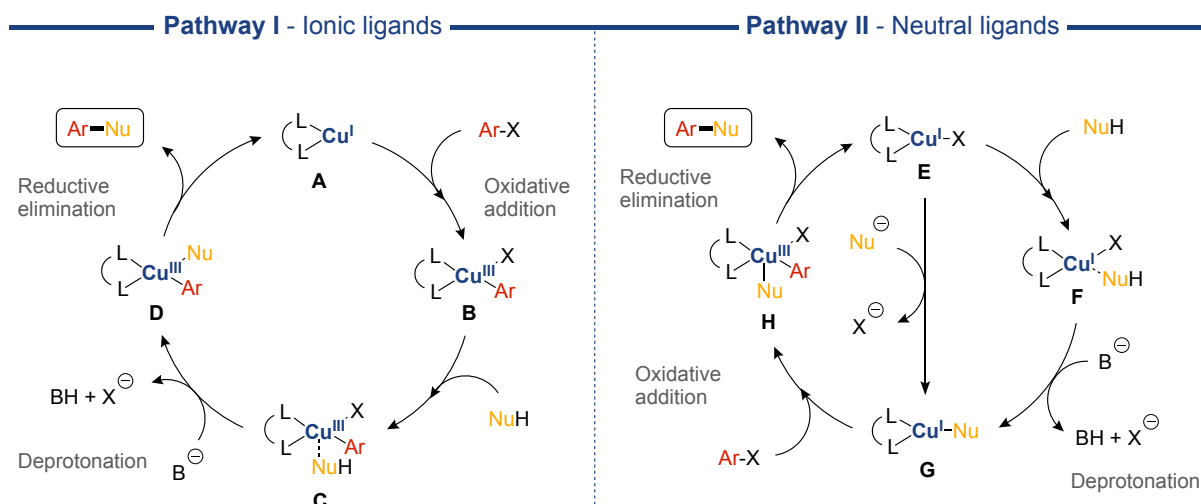
Ullmann-type conditions typically involve the coupling of an aryl halide (electrophile) with a nucleophile in the presence of a copper-salt and a base, often at high temperatures (Scheme 1.6a). The Chan-Lam reaction uses arylboronic acids (nucleophiles) instead of aryl halides and requires an additional oxidation source (Scheme 1.6b).



**Scheme 1.6.** General conditions for the Ullmann- and Chan-Lam cross-coupling reactions.

Several advances have been made over the years towards improving and expanding the original conditions of these reactions. Recent developments include the use of other arylating agents, including more reactive ones, and expansion of possible coupling partners to include alkynyl-, alkenyl- and alkyl halides and boron-based analogs, and the use of chelating ligands to promote couplings.<sup>124, 131-133</sup> Additionally, the scope of *N*-nucleophiles has been extended from the original amines to amides, sulfonamides, carbamates, imides, hydrazines, and azides.<sup>124, 133</sup>

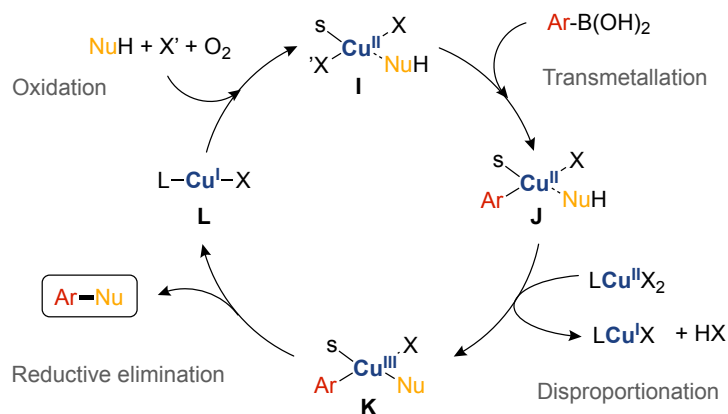
Several possible mechanisms have been proposed for the Ullmann-type reaction, but the Cu<sup>I</sup>/Cu<sup>III</sup> catalytic cycles (Scheme 1.7) are considered the most accepted ones.<sup>124, 134</sup> The detailed reaction pathway is, however, highly dependent on the nature of the ligands. For ionic ligands (pathway I, Scheme 1.7), the active catalytic Cu<sup>I</sup>-species **A** undergoes oxidative addition with an aryl halide to form Cu<sup>III</sup>-complex **B**. Coordination of the nucleophile with **B** results in the intermediate Cu<sup>III</sup>-complex **C**, then deprotonation by a base affords Cu<sup>III</sup>-complex **D**. Reductive elimination generates the arylated nucleophile (Ar-Nu) and regenerates **A**.



**Scheme 1.7.** Suggested general  $\text{Cu}^{\text{I}}/\text{Cu}^{\text{III}}$  catalytic cycles for the Ullmann-reaction. L = ligand, X = halide, B = base. Adapted from reference 124 and 134.

For neutral ligands (pathway II, Scheme 1.7), coordination of the nucleophile with active catalytic  $\text{Cu}^{\text{I}}$ -species **E** provides intermediate  $\text{Cu}^{\text{I}}$ -complex **F**. Upon reaction with a base,  $\text{Cu}^{\text{I}}$ -complex **G** is formed. Complex **G** could alternatively be generated directly by substitution with an anionic nucleophile. **G** undergoes oxidative addition with an aryl halide to form  $\text{Cu}^{\text{III}}$ -complex **H**. Reductive elimination generates the arylated nucleophile ( $\text{Ar-Nu}$ ) and regenerates **E**.

The detailed mechanistic understanding of the Chan-Lam reaction remains underdeveloped due to its complicated nature.<sup>130</sup> However, recent efforts have been made to thoroughly investigate the catalytic cycle.<sup>135</sup> A  $\text{Cu}^{\text{I}}/\text{Cu}^{\text{II}}/\text{Cu}^{\text{III}}$  cycle has been suggested based on the standard Chan-Lam conditions where copper(II)acetate ( $\text{Cu}(\text{OAc})_2$ ) and triethylamine ( $\text{Et}_3\text{N}$ ) are used (Scheme 1.8). The active  $\text{Cu}^{\text{II}}$ -species **I** is formed in a reaction with the pre-catalyst and its ligands, the solvent, the and the nucleophile. Transmetalation by the boronic acid results in the formation of  $\text{Cu}^{\text{II}}$ -complex **J**. A second  $\text{Cu}^{\text{II}}$ -source is used in the disproportionation reaction to furnish  $\text{Cu}^{\text{III}}$ -complex **K**. Reductive elimination generates the arylated nucleophile ( $\text{Ar-Nu}$ ) while simultaneously generating  $\text{Cu}^{\text{I}}$ -complex **L**. **I** is regenerated using an oxidant ( $\text{O}_2$  is most commonly used).



**Scheme 1.8.** Suggested general Cu<sup>I</sup>/Cu<sup>II</sup>/Cu<sup>III</sup> catalytic cycle for the Chan-Lam reaction. L = ligand, X/X' = anionic ligand, s = solvent. Adapted from reference 130 and 135.

### 1.4.2 Cu-catalysis in *N*-functionalization of hydantoins

The Cu-promoted C-N bond-forming reactions are potentially a highly relevant tool in the development of methods to functionalize the nitrogen atoms of hydantoins. Despite of the several advantages, the direct, selective functionalization strategy remains underdeveloped. The lack of attention from the synthetic community towards these reactions is imaginably due to their challenging nature. With the help of the Ullmann and Chan-Lam methodology, the disadvantages of the classical methods have been partly defeated in the pursuit to access, in particular, *N*-arylhydantoins.

A brief retrosynthetic analysis of the *N*-3-arylation of hydantoins demonstrates the possible ways in which they can be synthesized (Figure 1.6). Two fragments are obtained from breaking the C-N bond. Nucleophilic hydantoin-synthon **S-1** can be prepared by the reaction with a base. The electrophilic aryl-synthon **S-2** can be formed through interactions of an aryl- and copper-source, potentially in combination with a ligand. Some widely used copper-sources, bases and ligands are displayed, along with potential coupling partners.<sup>131, 134</sup>

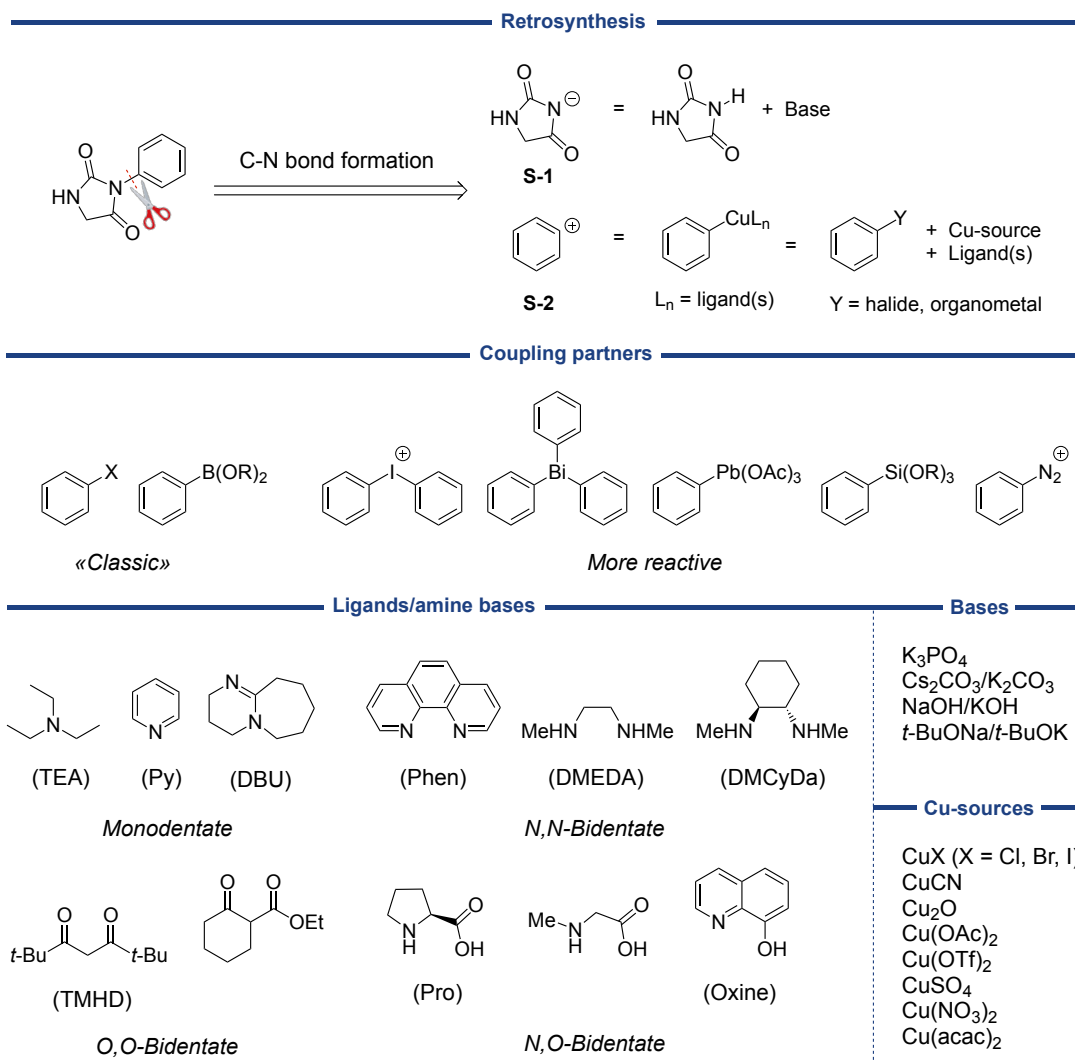
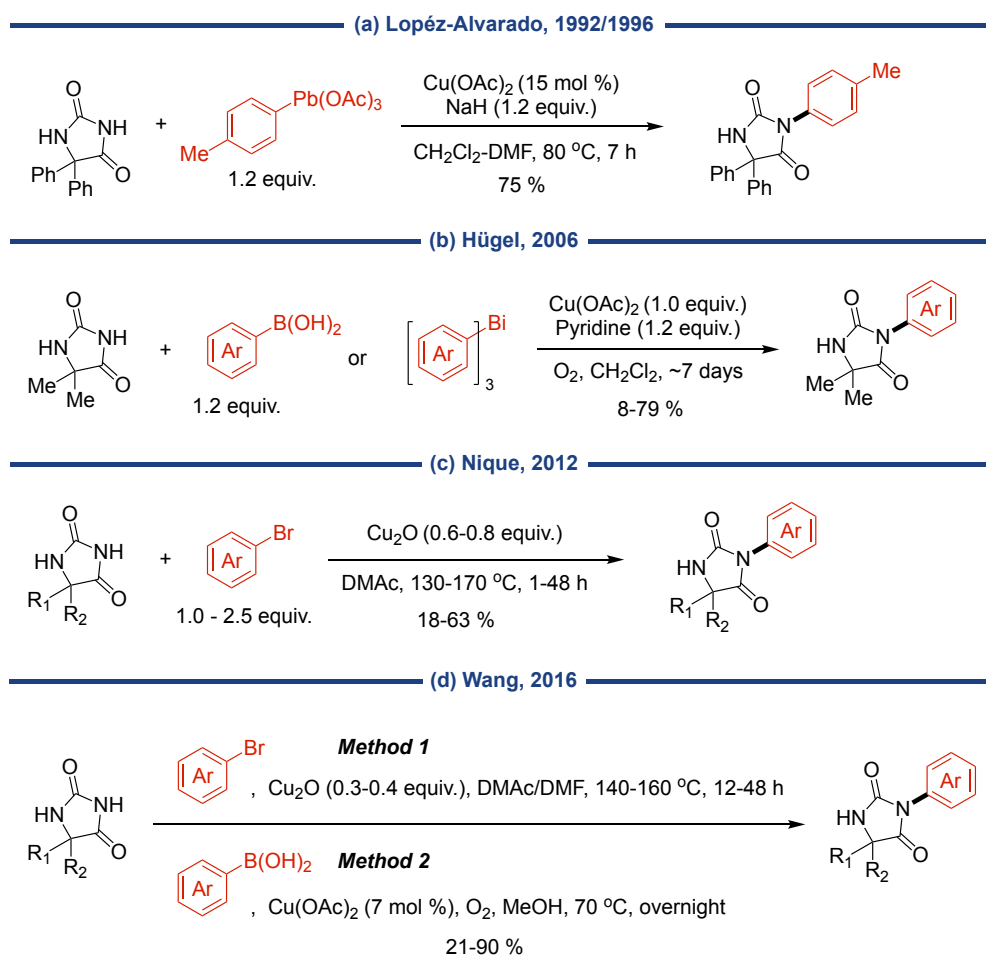


**Figure 1.6.** Retrosynthesis of 3-phenylhydantoin and some common aryl-, ligand-, base- and copper-sources used in C-N bond-forming reactions.

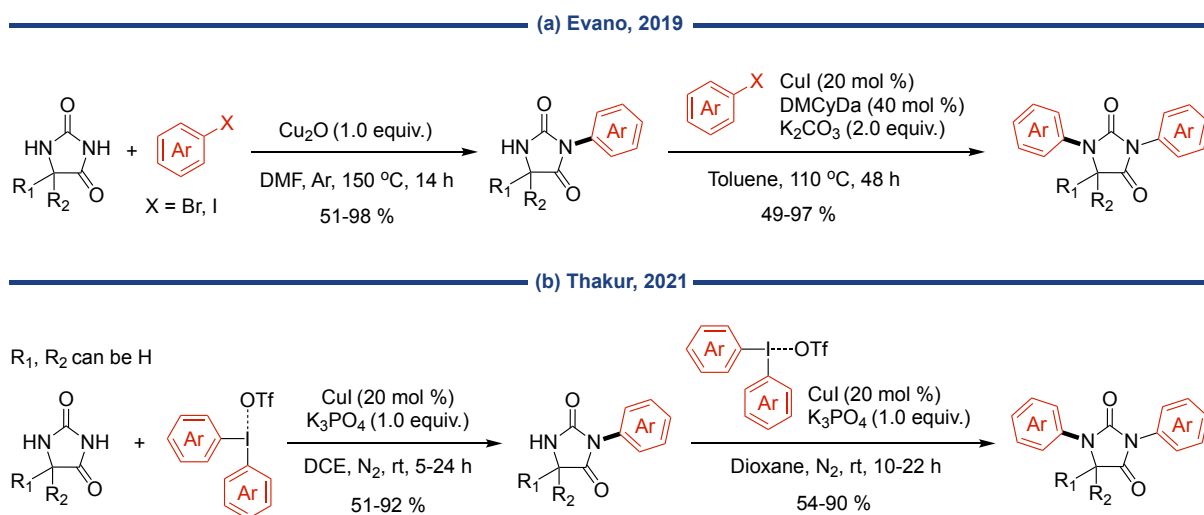
López-Alvarado and co-workers pioneered the Cu-catalyzed *N*-3-arylation of hydantoins using *p*-tolyllead triacetate<sup>121, 136</sup> (Scheme 1.9a). However, only the arylation of phenytoin was reported. Later, Hügel *et al.* developed a protocol utilizing arylboronic acids and triarylbismuthanes as arylating agents (Scheme 1.9b) in a Cu-mediated arylation.<sup>137</sup> Aryl halides were employed in the same Cu-mediated fashion by Nique<sup>73</sup> and Wang<sup>138</sup> (Scheme 1.9c and d) in the search for novel clinical trial candidates. The latter author (and co-workers) also explored the use of arylboronic acids in order to obtain all desired analogs.



**Scheme 1.9.** Cu-promoted *N*-3-arylations of 5,5-disubstituted hydantoin.

The above-mentioned methods only include highly specialized substrates. A more general and comprehensive procedure was recently reported by Evano's group.<sup>139</sup> They revisited the Cu-mediated regioselective *N*-3-arylation using aryl halides, followed by a subsequent Cu-catalyzed *N*-1-arylation protocol to access *N,N*-diarylated hydantoin (Scheme 1.10a). The method allows for a wide range of aryl groups (except *ortho*-substituted) to be transferred to both nitrogen atoms in good to excellent yields. However, regioselectivity was lost by removal of one or both C-5 substituents, rendering the method only applicable for 5,5-disubstituted hydantoin. Even more recently<sup>a</sup>, a fully Cu-catalyzed *N*-3- and subsequent *N*-1-arylation using symmetrical and unsymmetrical diaryliodonium salts was published by Thakur and co-workers<sup>140</sup> (Scheme 1.10b). A major advantage with this method is the possibility to transfer *ortho*-substituted arenes. Additionally, there are no demands for 5,5-disubstituted hydantoin.

<sup>a</sup> This work was published *after* our work "Cu-catalyzed *N*-3-arylation of hydantoin using diaryliodonium salts" (paper I).



**Scheme 1.10.** *N*-3- and subsequent *N*-1-arylation of hydantoin.

## 1.5 Objectives

New synthetic methods are needed to overcome challenges not met by present methods. Method development often seeks to solve a specific task, but with the desire for the method to be simple, more general, less sensitive and greener. Nowadays, the synergy between experimental and computational chemistry is used to reach these goals.

The main objective of the work presented herein is the development of methods for direct, regioselective C(sp<sup>2</sup>)-*N*-3-functionalization of unsubstituted hydantoin, with a focus on using lower catalysts loadings. The developed methods should be applicable to substituted hydantoin and other compounds containing the imide-functionality as the overall purpose of this work is to help to expand the synthetic toolbox.

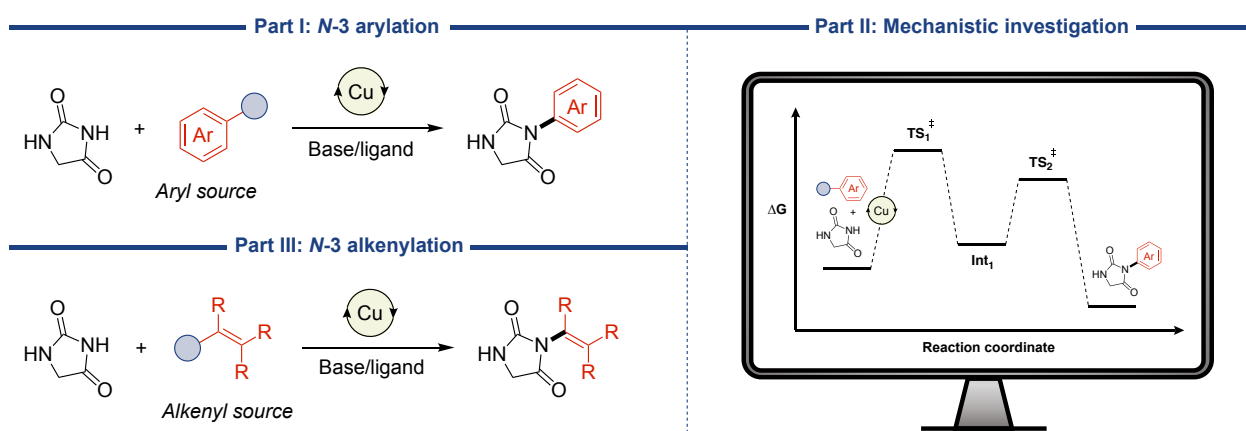


**Figure 1.7.** Objectives of the work presented.

The previously reported *N*-3-arylation reactions rely on 5,5-disubstituted hydantoins and (mostly) high catalyst loadings. The regioselective arylation of unsubstituted hydantoins still remains elusive. The key challenge of interest, and the first part of this dissertation aimed to tackle the regioselective *N*-3-arylation of unsubstituted hydantoins using lower catalyst loadings (Figure 1.7, part I).

The second part of this thesis is dedicated to determine the mechanism of the reaction developed in part I using DFT calculations (Figure 1.7, part II). Although method-dependent, no detailed mechanistic investigation of *N*-3-hydantoin arylations have so far been reported.

Most direct *N*-functionalization of hydantoins include arylations reactions. The last part of this work aimed to expand the pool of C(sp<sup>2</sup>)-coupling partners in the *N*-functionalization scope to include alkenyl groups (Figure 1.7, part III). Except for three isolated examples,<sup>141-143</sup> no such protocol has been reported for hydantoins.





# Chapter 2: Development of a methodology for the *N*-3-arylation of hydantoins using unsymmetrical diaryliodonium salts

## 2.1 Introduction

This chapter covers the development of a protocol for regioselective *N*-3-arylation of hydantoins using diaryliodonium salts as coupling partners. The work presented in this chapter is mainly covered in Paper I, but additional unpublished results are included as well. Prior to the method development, a brief introduction to diaryliodonium salts is given, where unsymmetrical salts are in focus.

### 2.1.1 Diaryliodonium salts

Diaryliodonium salts (diaryl- $\lambda^3$ -iodanes) (Figure 2.1) are a class of hypervalent iodine<sup>III</sup>-compounds first discovered in 1894.<sup>144</sup> They possess a T-shape where the apical ligands ( $\text{Ar}_2$  and X as drawn in Figure 2.1b) share a 3c-4e (hypervalent) bond.<sup>145</sup> Their exact geometry in solution, however, is still debated and may depend on both on the identity of the solvent and the counter anion.<sup>145, 146</sup>

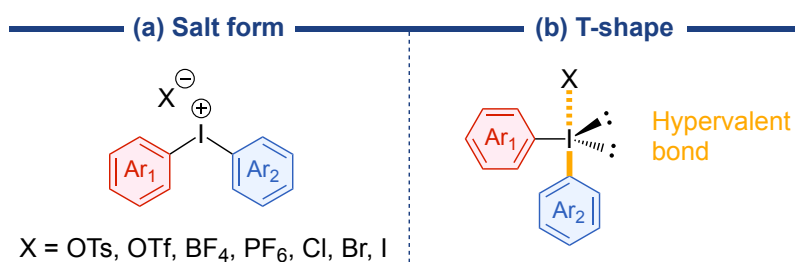


**Figure 2.1.** Structure of diaryliodonium salts.  $\text{Ar}_1 = \text{Ar}_2$  for symmetrical salts.  $\text{Ar}_1 \neq \text{Ar}_2$  for unsymmetrical salts.

Diaryliodonium salts have emerged a powerful source of arylating reagents over the past decades, owing to their high electrophilicity and the excellent leaving group ability of iodoarenes.<sup>147-151</sup> They are applicable in a variety of transformations as they possess the ability transfer aryl groups to both carbon- and heteroatom nucleophiles, metal-free<sup>152-155</sup> (as aryl cation equivalents, aryl radicals or arynes) and transition metal-catalyzed.<sup>156-158</sup> In particular, the use of copper<sup>159</sup> or palladium<sup>156</sup> as a transition metal-catalyst has proven to facilitate aryl transfer efficiently. Additional traits to their reactivity include good selectivity, low toxicity and stability in air and moisture.<sup>147</sup>

Diaryliodonium salts are either symmetrical ( $\text{Ar}_1 = \text{Ar}_2$ ) or unsymmetrical ( $\text{Ar}_1 \neq \text{Ar}_2$ ), and their use is accompanied by advantages and disadvantages. In reactions with nucleophiles, both aryl groups can theoretically be transferred. Thus, from a selectivity point of view, symmetrical salts are superior as selectivity issues in these reactions are avoided. The use of unsymmetrical salts is thus accompanied with potential chemoselectivity issues. The observed chemoselectivities are influenced by steric- and electronic properties of the arenes and the nature of the nucleophile. In transition-metal catalyzed reactions, the most electron-rich or the least bulky arene is preferentially transferred to the metal (then to the nucleophile).<sup>157, 160, 161</sup> In fact, sterically cumbersome arenes are often used as auxiliary groups (often referred to as “dummy ligands”) to help facilitate transfer of the desired (smaller) aryl group. In metal-free reactions the most electron-deficient arene is usually transferred. The steric effects, however, are highly dependent on the nucleophile. *ortho*-substituted aryl groups are often preferred transferred, even though being more electron-rich. This is commonly known as the “*ortho*-effect”. The *ortho*-effect is observed for heteroatom-nucleophiles (including N, O, S and F) where the bulkier aryl moiety is transferred.<sup>148, 155, 162</sup> The opposite is observed for B- and C-nucleophiles where the less bulky arene is transferred<sup>148, 155</sup> (Figure 2.2).

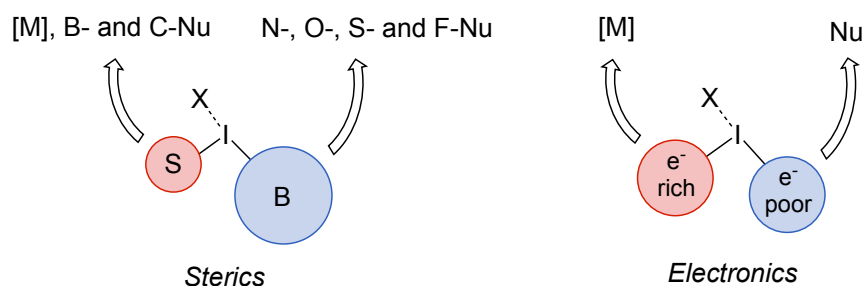
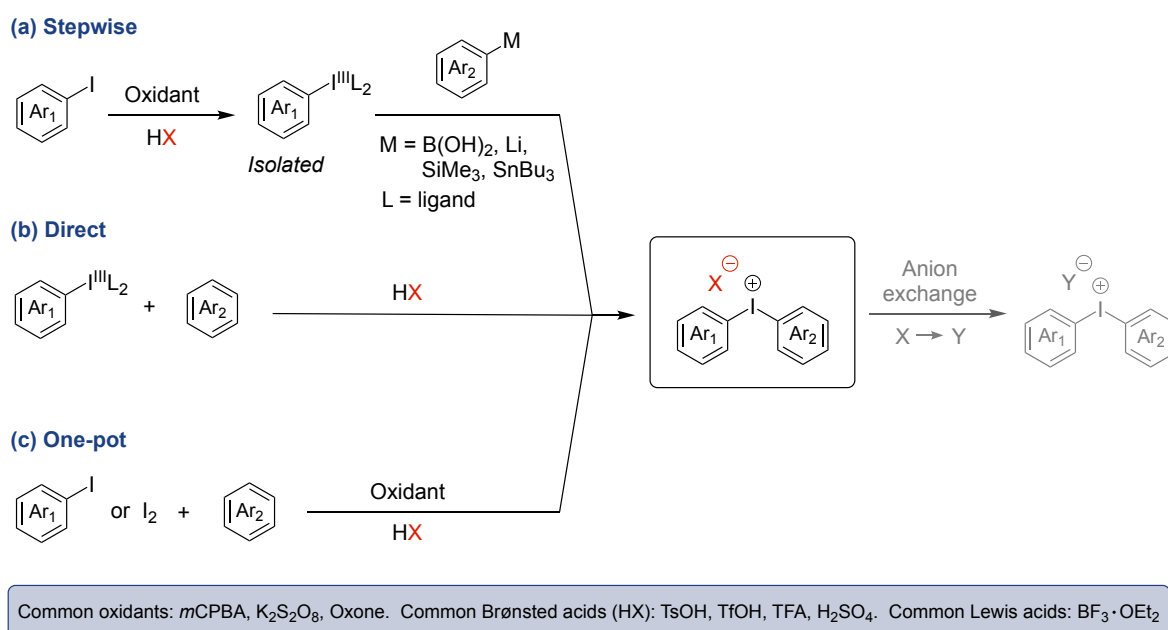


**Figure 2.2.** Stereoelectronic effects and chemoselectivity of unsymmetrical diaryliodonium salts in metal-catalyzed and metal-free aryl transfer reactions. S = small, B = bulky, [M] = transition metal.

From a synthetic perspective, the preparation of unsymmetrical salts is often more facile. Salts containing one electron-poor and one electron-rich arene are more readily prepared than symmetric salts containing two equally electron-rich or electron-poor moieties.<sup>163</sup> Lastly, if an expensive aryl group is being transferred, the possibility to use a cheaper dummy ligand is especially lucrative as waste of expensive aryl iodides can be avoided.

### 2.1.1.1 Preparation of unsymmetrical diaryliodonium salts

Diaryliodonium salts require synthesis prior to use<sup>b</sup>, which is a disadvantage compared to using, for example, aryl iodides or arylboronic acids as coupling partners. However, the preparation of unsymmetrical salts is often feasible and not too time-consuming. A plethora of synthetic strategies to access unsymmetrical diaryliodonium salts exist.<sup>147</sup> An overview over some common strategies is presented in Scheme 2.1. In the stepwise route (Scheme 2.1a), iodoarenes are first oxidized to iodine<sup>III</sup>-species in the presence of an acid (HX), then isolated. The diaryliodonium salts are obtained by subsequent ligand exchange with arenes or metalarenes.<sup>164, 165</sup> The direct route (Scheme 2.1b) involves preformed/commercially available iodine<sup>III</sup>-reagents that reacts with HX and an arene to furnish the salts.



**Scheme 2.1.** General synthetic strategies towards unsymmetrical diaryliodonium salts. Sketched in grey is the anion exchange process necessary in some cases.

Recently, convenient and efficient one-pot procedures have been developed (Scheme 2.1c) by the groups of Olofsson,<sup>166-171</sup> Stuart,<sup>172, 173</sup> Zhdankin<sup>174, 175</sup> and others.<sup>176, 177</sup> This strategy involves the formation of diaryliodonium salts by oxidation and ligand exchange of iodoarenes (or molecular iodine) and arenes. The ligand exchange step of arenes on the iodine<sup>III</sup>-intermediates is formally considered an electrophilic aromatic substitution implying certain limitations of salts possible to produce by these methods.

<sup>b</sup> Several diaryliodonium salts are commercially available, but often expensive.

### 2.1.1.2 Controlling chemoselectivity: 2,4,6-trimethoxyphenyl as auxiliary

The concept of dummy groups/auxiliaries was briefly introduced in Section 2.1.1. The chemoselectivity of aryl transfers can be (sterically or electronically) controlled with careful selection of the non-transferred arene, *i.e.* the dummy group. Diaryliodonium salts bearing a 2,4,6-trimethoxyphenyl (TMP) moiety have displayed remarkable selectivity in reactions with several nucleophiles.<sup>152, 163, 166, 172, 178-181</sup> Other frequently used dummy ligands include 2,4,6-trimethylphenyl (Mes), anisyl and phenyl.<sup>155, 163</sup> Recent efforts in the development of one-pot reactions have made aryl(TMP)iodonium salts easily accessible. These advantages make them highly attractive candidates in arylation reactions.

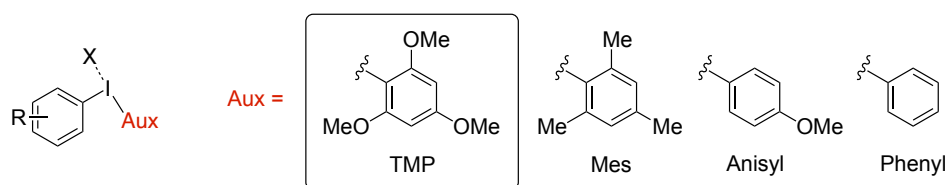


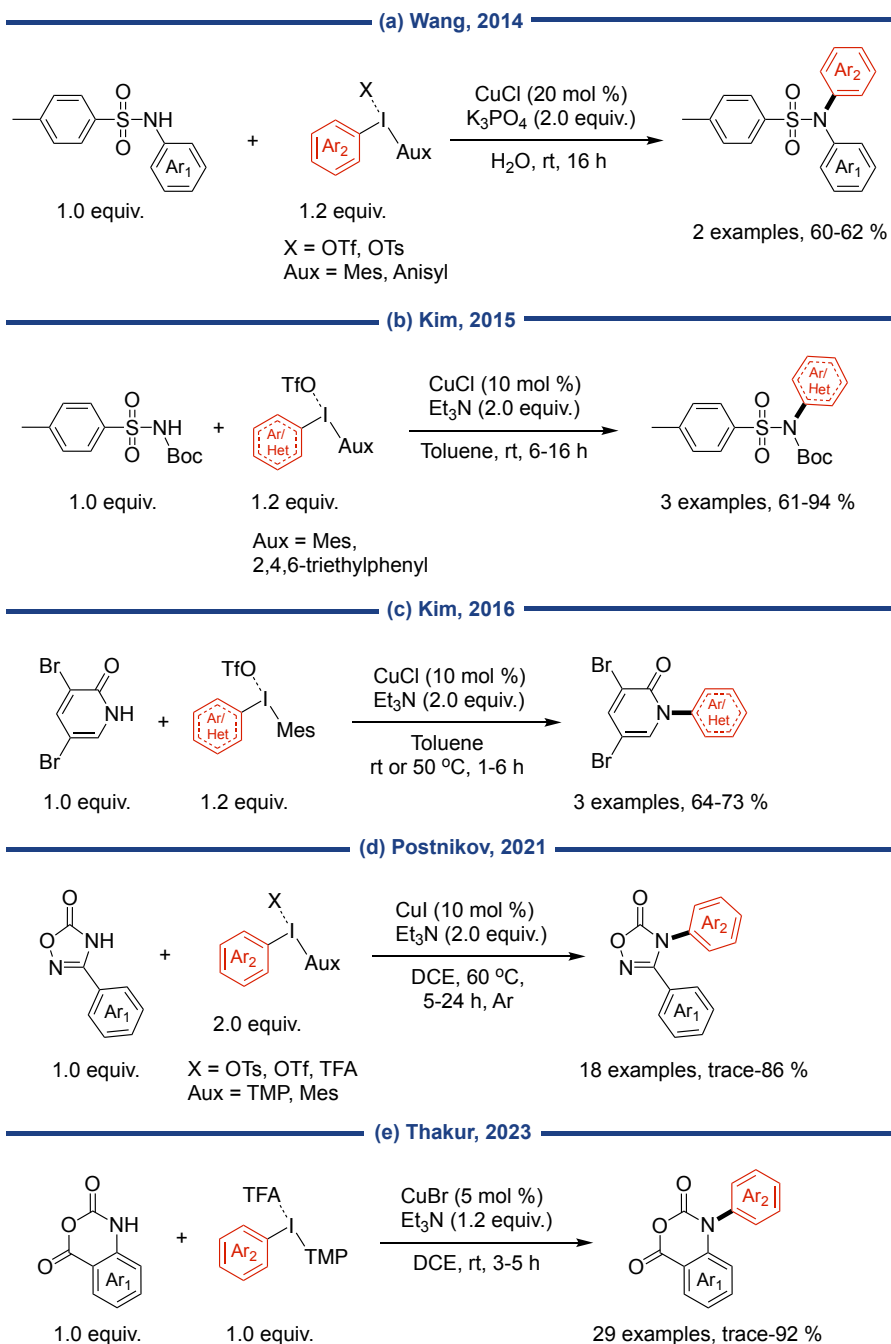
Figure 2.3. Common dummy ligands.

### 2.1.1.3 Cu-catalyzed *N*-arylations with unsymmetrical diaryliodonium salts

Various *N*-nucleophiles have been successfully arylated with diaryliodonium salts. Both symmetrical and unsymmetrical salts have been used for that purpose, including metal-free and metal-catalyzed processes. However, less reactive *N*-nucleophiles, such as amides and imides, often require the assistance of a metal-catalyst to overcome limitations in reactivity.<sup>182-187</sup> Moreover, a metal-catalyst is often needed to ensure selectivity in substrates with multiple nucleophilic sites.<sup>188-192</sup>

This section focuses specifically on reactions catalyzed by copper using unsymmetrical diaryliodonium salts. The pool of nucleophiles is also limited to include only *N*-nucleophiles with similar *N*-character as hydantoins like imides<sup>c</sup>, amides, sulfonamides. The nitrogen lone-pair of these nucleophiles are less available due to delocalization and are thus weaker nucleophiles than *e.g.* amines.

<sup>c</sup> No Cu-catalyzed *N*-arylation of imides using unsymmetrical diaryliodonium salts were reported prior to our work.



**Scheme 2.2.** Some examples of Cu-catalyzed *N*-arylations of weak nucleophiles using unsymmetrical diaryliodonium salts.

In 2014, Wang *et al.* published an *N*-arylation of *N*-arylsulfonamides in water using in the presence of a simple copper salt and a base (Scheme 2.2a).<sup>182</sup> Symmetrical diaryliodonium salts were mostly used in the study, but two examples using unsymmetrical salts were reported. Selective transfer of the phenyl group was accomplished using phenyl(Mes)iodonium triflate. Electron-deficient *p*-nitrophenyl was selectively transferred using anisyl as auxiliary and tosylate as counter anion.

A year later, Kim and co-workers also published a study concerning the *N*-arylation of *N*-arylsulfonamides (Scheme 2.2b).<sup>184</sup> CuCl was also used a catalyst in their procedure but with lower catalyst loading. Triethylamine was used as a base/ligand and toluene as solvent. Unsymmetrical salts containing either Mes or its ethyl analog (2,4,6-ethylphenyl) were only used in the transfer of an electron-deficient aryl- and two heteroaryl groups. The following year, the same group reported an *N*-arylation of 2-pyridones using the same conditions as in their previous work (Scheme 2.2c).<sup>183</sup> The same strategy was also employed concerning the transfer of an electron-deficient and two heteroarenes.

The group of Postnikov reported *N*-arylation of oxadiazolones in 2021, using both symmetric and unsymmetrical diaryliodonium salts (Scheme 2.2d).<sup>185</sup> The reaction took place in 1,2-dichloroethane employing CuI as a catalyst and triethylamine as a base/ligand. They evaluated the effect of reactivity of the symmetrical and unsymmetrical salts. It was discovered that by using Mes as an auxiliary, the yield of the *N*-phenylated oxadiazolone was increased compared to using the symmetric diphenyl-salt. When electron-withdrawing groups were present on the arene being transferred, TMP was the superior auxiliary in terms of yield and avoidance of side-product formation (*O*-arylation). In cases were sterically hindered *ortho*-substituents were present in the TMP-salts, only small amounts of product were obtained.

Diaryliodonium salts using TMP as auxiliary and trifluoroacetate (TFA) as counter anion facilitated the *N*-arylation of isatoic anhydrides (Scheme 2.2e).<sup>193</sup> The use of a simple Cu-salt in combination with triethylamine in DCE proved yet again to be an efficient system for such transformation.

## 2.2 Development of a method for *N*-3-arylation of hydantoins

Based on the previously reported *N*-arylations of hydantoins (Chapter 1, Scheme 1.9 and 1.10), we saw an unexploited potential where the development of a new method could enable us to reach our goal (Chapter 1, Figure 1.7). We reasoned that our conditions should include a copper salt, a base and/or ligand and heat. Considering the weak nucleophilicity of hydantoins N-3 position, we postulated that diaryliodonium salts would be a suitable coupling partner owing to its high electrophilicity. More specifically, aryl(TMP)iodonium salts were chosen for reasons already described in Section 2.1.

A small selection of the exploratory study is already included in Paper I. The following sections includes additional unpublished results as some interesting results were discovered during the study. Reaction parameters evaluated during the optimization include bases, ligands, catalysts and catalyst loading, solvents, concentration, temperature, stoichiometry, auxiliaries and counter anions of the diaryliodonium salts. To simplify the reading experience, the screening of reaction parameters is divided into subsections. It should be noted that the order presented here is not chronological.

### 2.2.1 Initial hits and screening of bases and ligands

We decided to start the study using unsubstituted hydantoin **1a**, a slight excess of phenyl(TMP)iodonium tosylate **2a** and catalytic amounts of CuI. Working with the assumption that deprotonation is paramount for product formation, we initiated the optimization with an excess of the base, triethylamine (Et<sub>3</sub>N). Toluene was chosen as solvent, and the reaction was carried out at 70° C. This resulted in 47 % of the desired product **3a** and 9 % of the bis-arylated **3c** (Figure 2.4). The latter was present to a certain extent in all our reactions. The *N*-1-arylated **3b** was only detected in a few reactions in around 5 %. Transfer of TMP to hydantoin was not seen in any of the reactions.

A series of primary, secondary and tertiary amine bases were then tested to in an attempt to increase formation of **3a** and reduce formation of **3c** (Figure 2.4). None of the bases outperformed triethylamine, but identical results were obtained with *N*-methylpiperidine (NMPPR). DBU and diisopropylamine (DIPA) both produced **3a** in 30 % yield and **3c** in 1 %. Pyrrolidine gave similar results (28 % of **3a** and 3 % of **3c**), while ethylamine and piperidine (PPR) gave 17 % of **3a** and 3 % of **3c**. Trimethylamine (TMA), triisopropylamine (TPA) and dimethylaniline (DMA) were least effective amine bases only yielding 5-7 % of the *N*-3-arylated **3a**.

Common inorganic bases were also screened (NaH, K<sub>2</sub>CO<sub>3</sub> and K<sub>3</sub>PO<sub>4</sub>). No reaction occurred in any of the instances. The bidentate amine ligands 1,2-dimethylethylenediamine (DMEDA) and *trans*-1,2-diaminocyclohexane (chxn) were tested in catalytic amounts but were incapable to furnish any product. The combination of K<sub>3</sub>PO<sub>4</sub> and chxn were ineffective, as was the phosphorus-based ligand triphenylphosphine (PPh<sub>3</sub>).

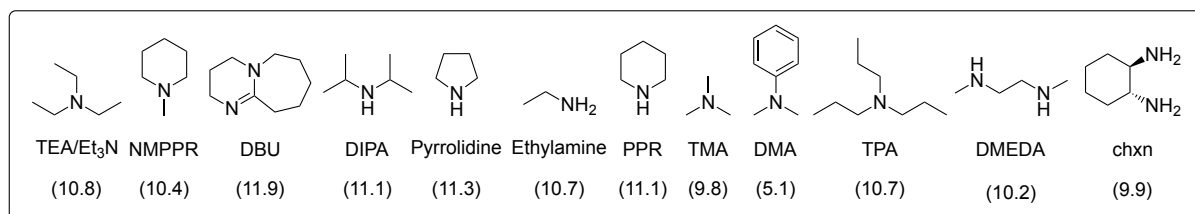
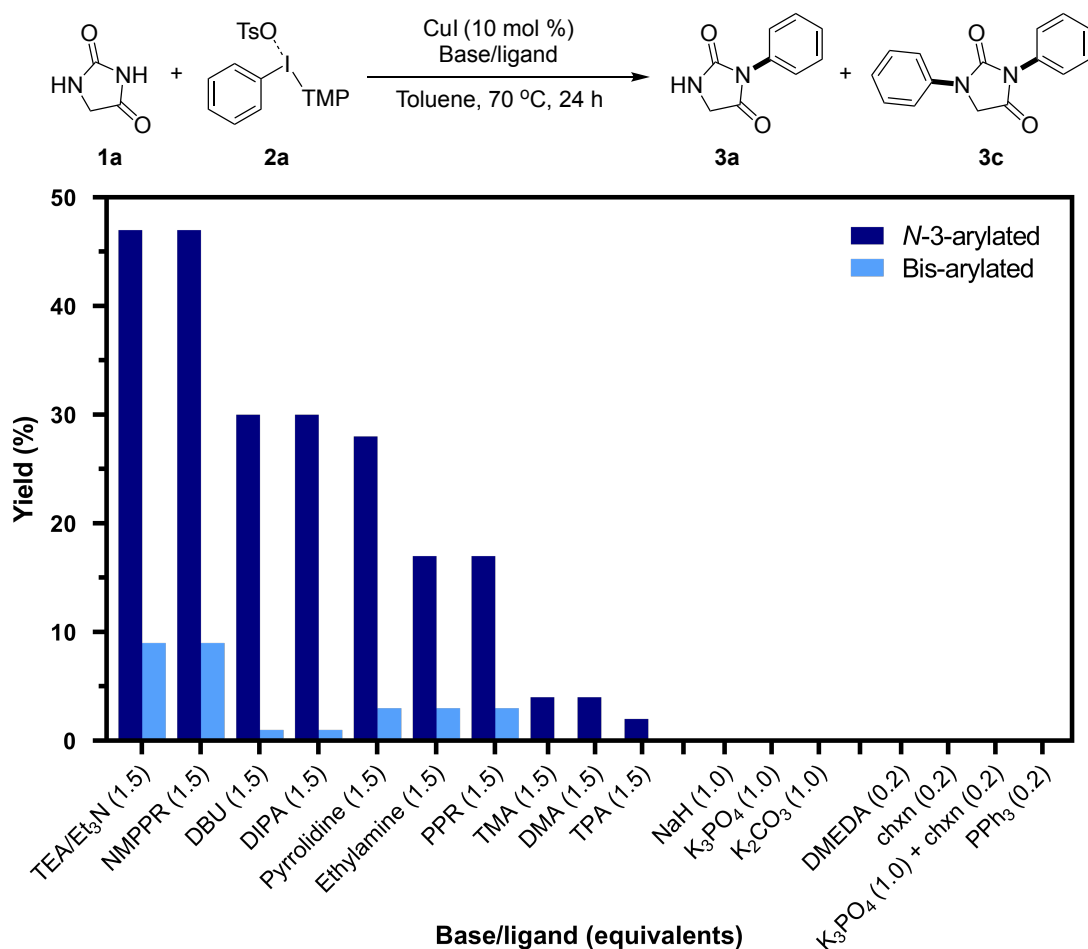


**Figure 2.4.** Graphical presentation of the base/ligand screening.  $pK_a$ -values<sup>194-196</sup> (in water) of amine bases are given in parentheses. Conditions: Hydantoin **1a** (0.2 mmol, 1.0 equiv.), PhI(TMP)OTs **2a** (0.3 mmol, 1.5 equiv.), CuI (0.02 mmol, 0.1 equiv.), base/ligand (as specified) and toluene (2 mL). Yields were measured using mesitylene (Mes) as an internal standard (IS) in <sup>1</sup>H NMR spectroscopic analyses.

The results clearly indicate the reaction being aided by the presence of an amine. The results from the amine-screening, however, cannot be explained based solely on basicity ( $pK_a$ -values are listed in Figure 2.4). Assuming hydantoin deprotonation prior to aryl transfer is a rate limiting step, the best results would have been yielded by the stronger base (DBU or NaH). Moreover, no clear trend can be extrapolated from their structural features as both the most (TEA and NMPPR) and the least (TMA, DMA and TPA) favorable results were provided by tertiary amines. Considering the lack of product formation using strong, inorganic bases and the affinity of amines towards Cu-ligation, we propose a dual role for the amines; as Cu-ligand and base.



## 2.2.2 Catalyst screening

Having shown that the *N*-3-arylation of hydantoin could be performed with CuI as a catalyst, we wanted to explore other transition metals. Catalysts based on copper, nickel, iron and palladium were tested in the hydantoin arylation reaction (Table 2.1).

**Table 2.1.** Screening of catalysts.

#	[M]	Base/ligand/additive (equiv.)	Yield 3a (%) <sup>[a]</sup>	Yield 3c (%) <sup>[a]</sup>
1	CuI	Et <sub>3</sub> N (1.5)	47 <sup>[b]</sup>	9
2	CuCl	Et <sub>3</sub> N (1.5)	45	10
3	Cu <sub>2</sub> O	Et <sub>3</sub> N (1.5)	41	6
4	CuOAc	Et <sub>3</sub> N (1.5)	28	4
5	Cu <sub>2</sub> SO <sub>4</sub>	Et <sub>3</sub> N (1.5)	16	2
6	Cu(OTf) <sub>2</sub>	Et <sub>3</sub> N (1.5)	65, 60 <sup>[b]</sup>	12
7	Cu(OAc) <sub>2</sub> · H <sub>2</sub> O	Et <sub>3</sub> N (1.5)	59	8
8	CuCl <sub>2</sub> · 2H <sub>2</sub> O	Et <sub>3</sub> N (1.5)	61 <sup>[b]</sup>	8
9 <sup>[c]</sup>	Cu(NO <sub>3</sub> ) <sub>2</sub> · 2.5 H <sub>2</sub> O	Et <sub>3</sub> N (1.5)	66	7
10 <sup>[c]</sup>	Cu(NO <sub>3</sub> ) <sub>2</sub> · 2.5 H <sub>2</sub> O	Et <sub>3</sub> N (0.2) and NaH (1.1)	67	14
11	Cu(OTf) <sub>2</sub>	Et <sub>3</sub> N (1.5) and H <sub>2</sub> O (1.0)	78 <sup>[b]</sup>	10
12	CuI	Et <sub>3</sub> N (1.5) and H <sub>2</sub> O (1.0)	62	6
<b>Other metals</b>				
13	NiCl <sub>2</sub>	Et <sub>3</sub> N (1.5)	nd	nd
14	Fe(OC <sub>4</sub> ) <sub>2</sub> · H <sub>2</sub> O	Et <sub>3</sub> N (1.5)	nd	nd
15	Pd(OAc) <sub>2</sub>	Et <sub>3</sub> N (1.5)	nd	nd
16	Pd(OAc) <sub>2</sub>	PPh <sub>3</sub> (0.2)	nd	nd

Conditions: Hydantoin **1a** (0.2 mmol, 1.0 equiv.), PhI(TMP)OTs **2a** (0.3 mmol, 1.5 equiv.), catalyst (as specified, 0.02 mmol, 0.1 equiv.), base/ligand/additive (as specified) and toluene (2 mL). [a] <sup>1</sup>H NMR yield using Mes as IS. [b] Isolated yield. [c] 1.1 equiv. of PhI(TMP)OTs **2a** was used.

A range of Cu-based catalysts were investigated with varying success (Table 2.1, entries 1-9) Similar results as using CuI (Table 2.1, entry 1) were obtained with CuCl and Cu<sub>2</sub>O (Table 2.1, entries 2 and 3), while CuOAc and Cu<sub>2</sub>SO<sub>4</sub> (Table 2.1, entries 4 and 5) did not perform well under the conditions (28 % and 16 % yield, respectively). Increased yields of **3a** were obtained with Cu(OTf)<sub>2</sub> and the hydrated salts (Table 2.1, entries 6-9), ranging from 59 % to 66 %.

Cu(NO<sub>3</sub>)<sub>2</sub> · 2.5 H<sub>2</sub>O (66 % yield, Table 2.1, entry 9) was used further in reaction with NaH and Et<sub>3</sub>N to investigate whether the role of Et<sub>3</sub>N could be dual, operating as both a base and a ligand (Table 2.1, entry 10). We theorized that in the reaction, NaH would work as base (being the stronger of the two) while Et<sub>3</sub>N would primarily work as a ligand for the catalyst. 67 % yield of the product was obtained from this reaction compared to 66 % using only Et<sub>3</sub>N, which suggest the possibility for the theory being valid.

The highest yields from the catalyst screening were seen with hydrated Cu-salts. Considering the yields using Cu(OTf)<sub>2</sub> were obtained without water<sup>d</sup>, 1.0 equivalent of water was added to the reaction mixture (Table 2.1, entry 11). Not surprisingly, an increase in yield of **3a** (78 %) was observed. A “control” experiment with CuI and water (Table 2.1, entry 12) verified the increase in yield of **3a** from 47 to 62 %. We speculated whether the water contributes to solubility or proton transfer but did not warrant it any further investigation.

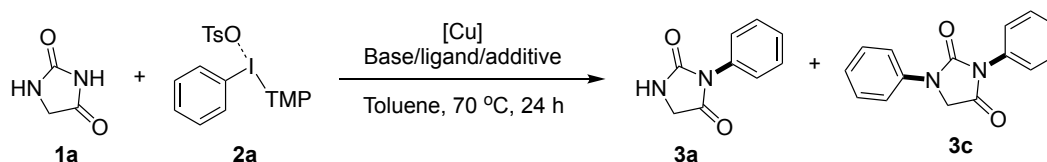
At the point of the discovery, the conditions from entry 11 (Table 2.1) were the best at hand. Hence, several of the optimization reactions in later sections include the use of these conditions. However, these were *not* the final, optimized conditions used further in the scoping of coupling partners and substrates for several reasons. As will be seen later, they failed to furnish the transfer of substituted arenes in desirable yields (Section 2.2.10.2, Scheme 2.7). Also, the addition of 1.0 equivalent of water to each reaction was impractical due to the low volume added (3.6 μL). Additionally, the hygroscopic nature of Cu(OTf)<sub>2</sub> left us with too many uncertainties concerning the amount of water added to each reaction.

---

<sup>d</sup> Cu(OTf)<sub>2</sub> is hygroscopic to a certain degree, and no measurement were taken to ensure moisture-free reaction conditions.

The catalyst loadings were evaluated for the two catalysts yielding the best results from the catalyst screening in Table 2.1. A decrease in loading from 10 mol % to 5 % Cu(OTf)<sub>2</sub> (Table 2.2, entries 1 and 2), produced **3a** in only 58 % yield and increased the yield of the undesired **3c** to 21 %. An increase in loading from 10 to 20 mol % (Table 2.2, entry 3) the reaction was unfavorably affected producing only 42 % of **3a**.

**Table 2.2.** Screening of catalyst loading.



#	[Cu] (mol %)	Base/additive (equiv.)	Yield <b>3a</b> (%) <sup>[a]</sup>	Yield <b>3c</b> (%) <sup>[a]</sup>
1	Cu(OTf) <sub>2</sub> (10)	Et <sub>3</sub> N (1.5) and H <sub>2</sub> O (1.0)	78 <sup>[b]</sup>	10
2	Cu(OTf) <sub>2</sub> (5)	Et <sub>3</sub> N (1.5) and H <sub>2</sub> O (1.0)	58	21
3	Cu(OTf) <sub>2</sub> (10)	Et <sub>3</sub> N (1.5) and H <sub>2</sub> O (1.0)	42	3
4	Cu(NO <sub>3</sub> ) <sub>2</sub> · 2.5 H <sub>2</sub> O (10)	Et <sub>3</sub> N (1.5)	66 <sup>[b]</sup>	7
5	Cu(NO <sub>3</sub> ) <sub>2</sub> · 2.5 H <sub>2</sub> O (5)	Et <sub>3</sub> N (1.5)	70	9
6	Cu(NO <sub>3</sub> ) <sub>2</sub> · 2.5 H <sub>2</sub> O (2.5)	Et <sub>3</sub> N (1.5)	66	8
7	Cu(NO <sub>3</sub> ) <sub>2</sub> · 2.5 H <sub>2</sub> O (100)	Et <sub>3</sub> N (1.5)	7	nd

Conditions: Hydantoin **1a** (0.2 mmol, 1.0 equiv.), PhI(TMP)OTs **2a** (0.3 mmol, 1.5 equiv.), catalyst (as specified) base/ligand/additive (as specified) and toluene (2 mL). [a] <sup>1</sup>H NMR yield using Mes as IS. [b] Isolated yield.

Varying the catalyst loading of Cu(NO<sub>3</sub>)<sub>2</sub> · 2.5 H<sub>2</sub>O did not impact the reaction as significantly as with Cu(OTf)<sub>2</sub>. A decrease in loading from 10 % mol (Table 2.2, entry 4) to 5 mol % (Table 2.2, entry 5) gave a slight increase in yield of **3a** from 66 % to 70 %. Further reduction of the loading to 2.5 mol % gave the same results as with 10 mol % (Table 2.2, entry 6).

Complete conversion of hydantoin was not achieved under our best conditions thus far. We wanted to explore the possibility of full hydantoin conversion using stoichiometric amounts of copper, seeing that several *N*-3 hydantoin arylations have been reported with stoichiometric amounts of catalyst.<sup>73, 137, 139</sup> However, such high loadings failed under our conditions as only 7 % of **3a** was afforded (Table 2.2, entry 7).

### 2.2.3 Can we eliminate the formation of the bis-arylated product?

We desired to investigate the formation of the unwanted bis-arylated **3c** into more detail. We speculated additional deprotonation of the N-1 position (after N-3 deprotonation) and hence formation of **3c** with the excess of Et<sub>3</sub>N used. Consequently, the amount of Et<sub>3</sub>N was evaluated (Figure 2.5). The red dots represent the reactions with the addition of water, while no water was added in the reaction represented by the blue dots. In both cases, 1.5 equivalents of Et<sub>3</sub>N (with respect to hydantoin **1a**) was the optimal amount concerning product formation. By reducing the amount of Et<sub>3</sub>N to 1.1 equivalent, a decrease in yield of N-3-arylated **3a** was apparent; from 78 % to 66 % (red) and 65 % to 60 % (blue). By reducing to 1.0 equivalent (blue only), a more significant reduction was seen when only 45 % of the desired product was yielded. Additionally, 7 % of the bis-arylated product was formed. A further reduction of Et<sub>3</sub>N gave a further reduction in yield. Surprisingly, an increase to 2.0 equivalents Et<sub>3</sub>N affected the reaction negatively. The formation of bis-arylated **3c** could not be eliminated regardless of the amount of Et<sub>3</sub>N, but a more favorable **3a:3c** ratio was obtained with the addition of water. The addition of more than 1.0 equivalent was, however, not favorable.

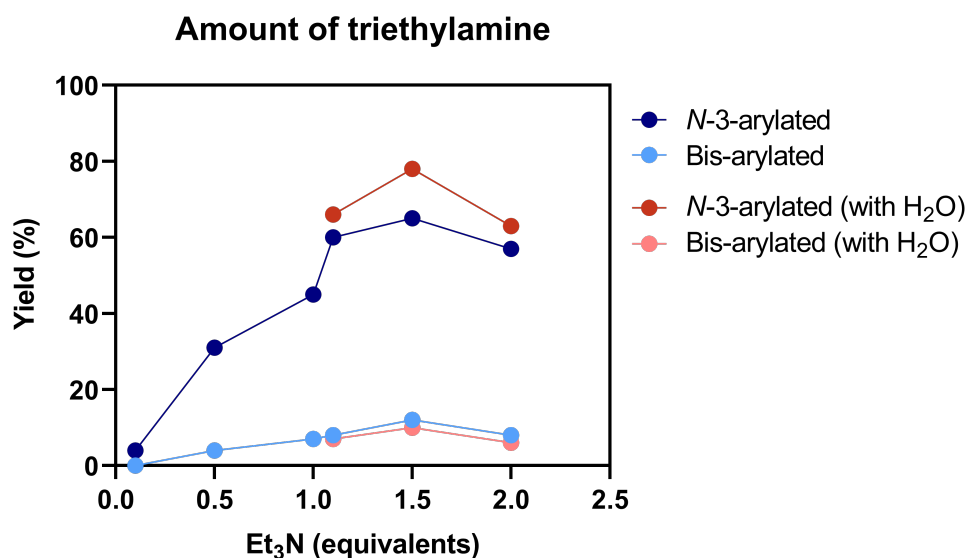
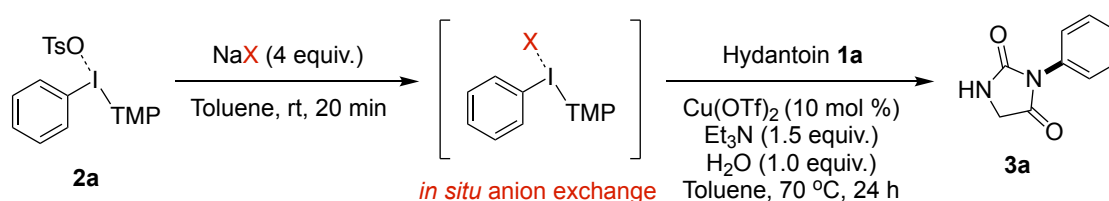


**Figure 2.5.** Screening of the amount of triethylamine in reactions employing Cu(OTf)<sub>2</sub> as a catalyst, with (dark- and light red) and without (dark- and light blue) the addition of 1.0 equiv. H<sub>2</sub>O. Conditions: Hydantoin **1a** (0.2 mmol, 1.0 equiv.), PhI(TMP)OTs **2a** (0.3 mmol, 1.5 equiv.), Cu(OTf)<sub>2</sub> (0.02 mmol, 0.1 equiv.), Et<sub>3</sub>N (as specified) and toluene (2 mL). Yields were measured using Mes as IS in <sup>1</sup>H NMR spectroscopic analyses.

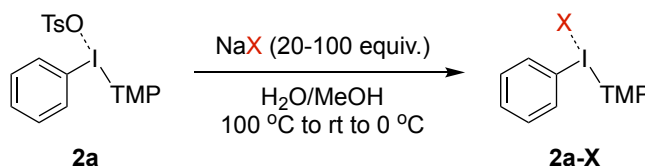
## 2.2.4 Screening of the diaryliodonium salt counter anions

The counter anion of diaryliodonium salts exerts a dramatic effect on reactivity<sup>197</sup> and reaction selectivity.<sup>197, 198</sup> Hence, it is an important variable to evaluate in an optimization process. In order to screen a wide range of counter anions and avoid synthesizing each individual salt, an “admix approach”<sup>197</sup> was used. In this approach, the diaryliodonium salt is mixed with an excess of sodium salt containing the counter anion of interest prior to addition of nucleophile and additives (Scheme 2.3).



**Scheme 2.3.** The admix approach. Excess NaX is added to facilitate *in situ* exchange of the counter anion.

To verify the results of *N*-arylation using this approach, two of the diaryliodonium salts (**2a-BF<sub>4</sub>** and **2a-OTf**) were pre-synthesized by “classical” counter anion exchange reactions (Scheme 2.4).<sup>172</sup>



**Scheme 2.4.** Anion exchange reaction.

The results of the screening (Table 2.3) show a great variety in the outcome of each reaction using different counter anions. Formation of bis-arylated **3c** could not be suppressed in any of the reactions where reasonable yields of **3a** were obtained (Table 2.3, entries 1-4 and 10). The original conditions using OTs<sup>-</sup> as a counter anion (Table 2.3, entry 1) proved to be optimal affording **3a** in 78 %.

The reaction proceeded well using F<sup>-</sup>, BF<sub>4</sub><sup>-</sup> and NO<sub>3</sub><sup>-</sup> as counter anions (Table 2.3, entries 2-4) producing **3a** in 66 %, 64 % and 61 % yields, respectively. Only 26 % of the desired product was obtained employing PF<sub>6</sub><sup>-</sup> (Table 2.3, entry 5), while the reaction barely proceeded using OAc<sup>-</sup>, Br<sup>-</sup> and Cl<sup>-</sup> (Table 2.3, entries 6-8). OTf have frequently been used as a counter anion in several successful arylation reactions<sup>182-185</sup>, but surprisingly, no product was obtained when triflate was used under our conditions

(Table 2.3, entry 9). The result was confirmed starting from the pre-exchanged triflate salt **2a-OTf** (Table 2.3, entry 10). The result in entry 3 (Table 2.3) was also confirmed by starting from the pre-exchanged tetrafluoroborate salt **2a-BF<sub>4</sub>** (Table 2.3, entry 11), yielding 62 % of **3a**.

A direct connection between the nature of the anion and the reactivity of the diaryliodonium salts have been difficult to establish. In metal-free reactions, the effects of the counter anions are often attributed to their leaving group ability or nucleophilicity (as competing nucleophiles).<sup>197-199</sup> The presence of a Cu-salt under the conditions tested adds another complicating factor as the anions could additionally interact with the metal center.

**Table 2.3.** Screening of counter anions.

#	Anion (X)	Alkali salt (equiv.)	Yield <b>3a</b> (%) <sup>[a]</sup>	Yield <b>3c</b> (%) <sup>[a]</sup>
1	OTs	-	78	10
2	OTs	NaF (4.4)	66	5
3	OTs	NaBF <sub>4</sub> (4.4)	64	3
4	OTs	NaNO <sub>3</sub> (4.4)	61	5
5	OTs	KPF <sub>6</sub> (4.4)	26	1
6	OTs	NaOAc (4.4)	7	0
7	OTs	NaBr (4.4)	7	0
8	OTs	NaCl (4.4)	5	0
9	OTs	NaOTf (4.4)	0	0
10 <sup>[b]</sup>	OTf	-	0	0
11 <sup>[c]</sup>	BF <sub>4</sub>	-	62	3

Conditions: PhI(TMP)OTs **2a** (0.22 mmol, 1.1 equiv.), alkali salt (0.44 mmol, 4.4 equiv.), hydantoin **1a** (0.2 mmol, 1.0 equiv.), Cu(OTf)<sub>2</sub> (0.02 mmol, 0.1 equiv.), Et<sub>3</sub>N (0.3 mmol, 1.5 equiv.) and toluene (2 mL). [a] <sup>1</sup>H NMR yield using Mes as IS. [b] PhI(TMP)OTf **2a-OTf** (0.22 mmol, 1.1 equiv.) was used, [c] PhI(TMP)BF<sub>4</sub> **2a-BF<sub>4</sub>** (0.22 mmol, 1.1 equiv.) was used.

## 2.2.5 Screening of concentration, temperature and solvents

The insolubility of the starting materials (except Et<sub>3</sub>N) in toluene encouraged us assess whether it was the ideal solvent for the reaction. A series of solvents were screened, and the results are summarized in Figure 2.6. The optimal concentration was determined prior to the solvent screening. A 0.1 M concentration was used during the entire optimization process, which also proved to be the optimal one. Yields of **3a** comparable to those obtained in toluene (78 %) were seen in DMSO (76 %), DMF (74 %) and 1,4-dioxane (73 %). The ratio of *N*-3-arylated **3a** to bis-arylated **3c** were most favorable in the reaction where acetonitrile was used, but the yield was considerably lower with only 66 %. To our surprise, the reaction proceeded to some extent in all the solvents tested, including heptane.

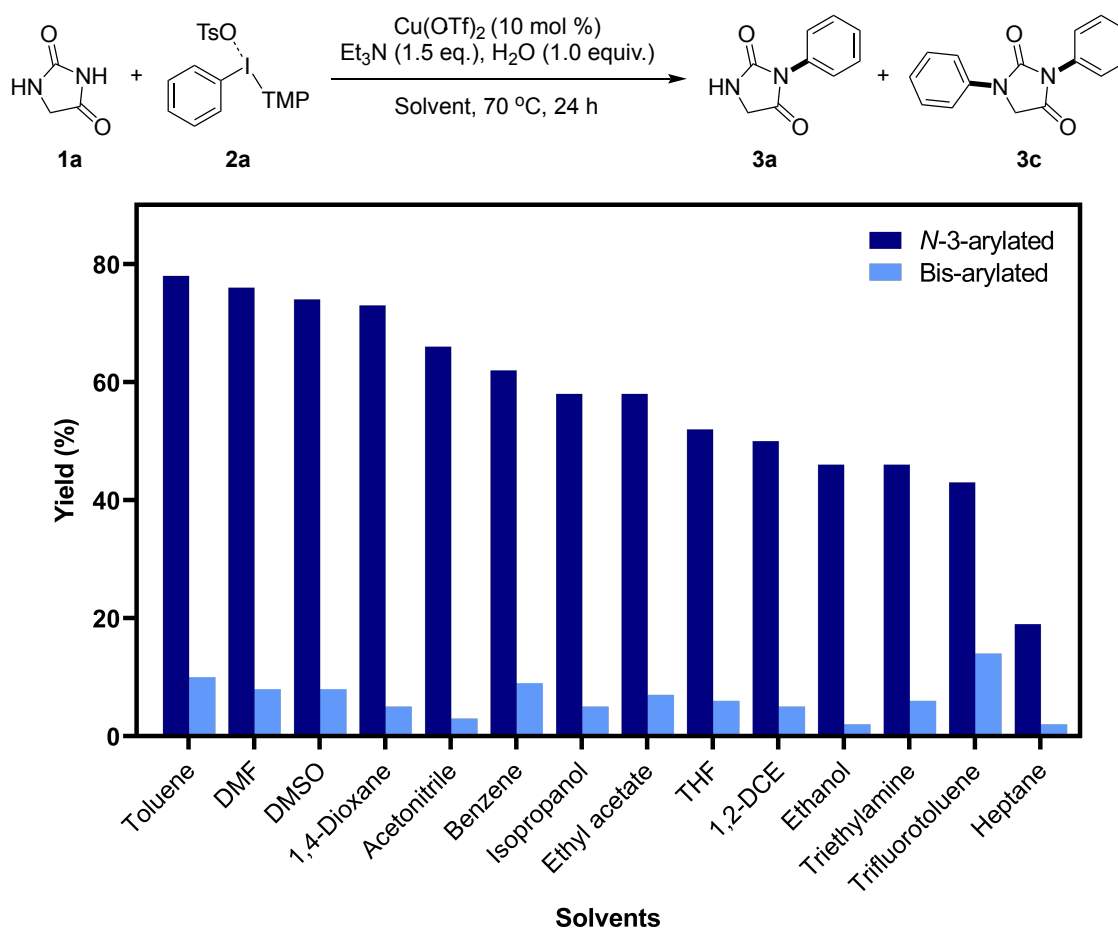


**Figure 2.6.** Screening of solvents. Conditions: Hydantoin **1a** (0.2 mmol, 1.0 equiv.), PhI(TMP)OTs **2a** (0.3 mmol, 1.5 equiv.), Cu(OTf)<sub>2</sub> (0.02 mmol, 0.1 equiv.), Et<sub>3</sub>N (0.3 mmol, 1.5 equiv.) and solvent (2 mL). Yields were measured using Mes as IS in <sup>1</sup>H NMR spectroscopic analyses.

Temperature can assert a dramatic effect on a chemical reaction in terms of reaction rate and possible thermal decomposition of the diaryliodonium salts. Five sets of reactions were run at different temperatures to investigate the effect (Figure 2.7, dark blue line). Increasing the temperature from 70 °C to 80 °C had no effect on product formation as the yields were the same (72 % and 73 %, respectively). By increasing the temperature to 90 °C and 100 °C, reaction rates were visibly faster as the reaction completion could be reached after 8 hours. However, less product was formed with only 67 % and 54 %, respectively. No residual salt **2a** was detected by <sup>1</sup>H NMR spectroscopic analysis of the post-reaction mixture, indicating possible thermal decomposition (and hence less product formation). DSC-TGA<sup>e</sup> analysis have shown reduced thermal stability of diaryliodonium salts bearing electron-rich aromatic rings.<sup>200</sup> Additionally, Cu-complexes of diaryliodonium salts also displayed lower decomposition temperatures (down to 70 °C). With an electron-rich TMP-moiety and Cu-complexation during the reaction, thermal decomposition around the temperatures tested are not unlikely.

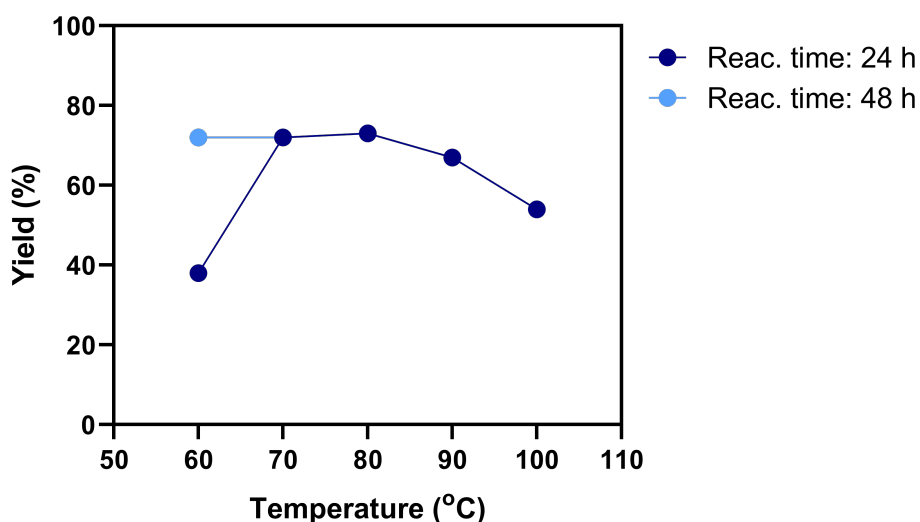


**Figure 2.7.** Effect of the reaction temperature. Conditions: Hydantoin **1a** (0.2 mmol, 1.0 equiv.), PhI(TMP)OTs **2a** (0.3 mmol, 1.5 equiv.), Cu(OTf)<sub>2</sub> (0.02 mmol, 0.1 equiv.), Et<sub>3</sub>N (0.3 mmol, 1.5 equiv.) and toluene (2 mL). Yields were obtained from isolation of the products.

Conversion of hydantoin **1a** was not particularly efficient at 60 °C as only 38 % of **3a** was produced. Residual salt **2a** was detected in the post-reaction mixture by <sup>1</sup>H NMR spectroscopy, indicating potential increase in yield with prolonged reaction times. Certainly, a twofold increase in reaction time (Figure 2.7, pale blue line) yielded 72 % of the product.

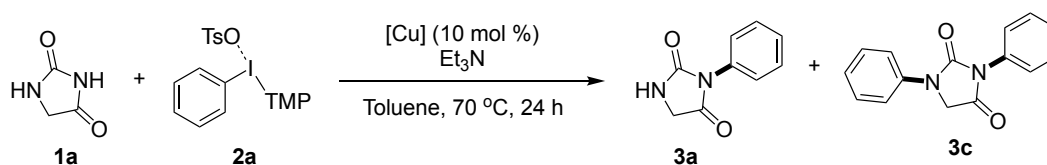
<sup>e</sup> DSC = Differential Scanning Calorimetry, TGA = Thermogravimetric Analysis. DSC-TGA measures heat flow and mass changes in a compound as a function of temperature.



## 2.2.6 Screening of reaction stoichiometry

It has been demonstrated that a slight excess of diaryliodonium salt provide good yields of the *N*-3-arylated product. However, we thought a brief exploration of reaction stoichiometry was warranted; either by increasing the amount of arylating agent to produce more of **3a**, or reversing the stoichiometry, having an excess of hydantoin. Reversing the stoichiometry and ultimately reducing the amount of diaryliodonium salt employed would improve the atom economy as less I-TMP is wasted.

**Table 2.4.** Screening of reaction stoichiometry.



#	[Cu]	<b>2a</b> (equiv.)	<b>1a</b> (equiv.)	<b>Et<sub>3</sub>N</b> (equiv.)	<b>Yield 3a</b> (%) <sup>[a]</sup>	<b>Yield 3c</b> (%) <sup>[a]</sup>
<b>Excess salt</b>						
1	Cu(OTf) <sub>2</sub>	1.1	1.0	1.5	66, 78 <sup>[b,c]</sup>	10
2	Cu(OTf) <sub>2</sub>	1.5	1.0	1.5	65	8
3	Cu(NO <sub>3</sub> ) <sub>2</sub> · 2.5 H <sub>2</sub> O	1.1	1.0	1.5	66 <sup>[b]</sup>	8
4	Cu(NO <sub>3</sub> ) <sub>2</sub> · 2.5 H <sub>2</sub> O	1.5	1.0	1.5	72	10
5	Cu(NO <sub>3</sub> ) <sub>2</sub> · 2.5 H <sub>2</sub> O	2.0	1.0	1.5	72	10
6 <sup>[d]</sup>	Cu(NO <sub>3</sub> ) <sub>2</sub> · 2.5 H <sub>2</sub> O	3.0	1.0	1.5	79 <sup>[b]</sup>	11
<b>Excess hydantoin</b>						
7	Cu(NO <sub>3</sub> ) <sub>2</sub> · 2.5 H <sub>2</sub> O	1.0	1.1	1.5	64	6
8	Cu(NO <sub>3</sub> ) <sub>2</sub> · 2.5 H <sub>2</sub> O	1.0	1.5	1.5	51	4
9	Cu(NO <sub>3</sub> ) <sub>2</sub> · 2.5 H <sub>2</sub> O	1.0	2.0	1.5	52	3
10	Cu(NO <sub>3</sub> ) <sub>2</sub> · 2.5 H <sub>2</sub> O	1.0	2.0	3.0	48	2
11 <sup>[e]</sup>	Cu(OTf) <sub>2</sub>	1.0	2.0	3.0	29	2

Conditions: Hydantoin **1a**, PhI(TMP)OTs **2a**, and Et<sub>3</sub>N as specified, Cu-catalyst (0.02 mmol, 0.1 equiv.) and toluene (2 mL). [a] <sup>1</sup>H NMR yield using Mes as IS. [b] Isolated yield. [c] H<sub>2</sub>O (1.0 equiv.) was added. [d] 5 mol % catalyst was employed.

The results from screening are summed up in Table 2.4, where entries 1-4 are included for easier comparison. Increasing the amount of salt from 1.5 to 2.0 equivalents did not influence the product formation as the same results were obtained (72 % of **3a** and 10 % of **3c**, Table 2.4, entry 5). A further increase to 3.0 equivalents (and using 5 mol %

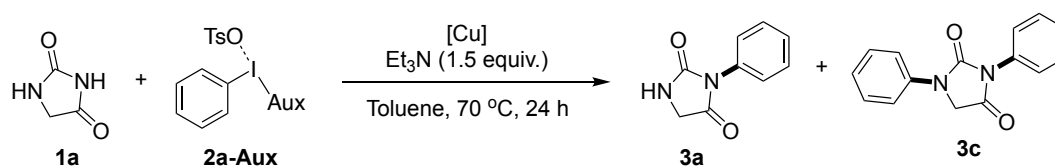
loading of  $\text{Cu}(\text{NO}_3)_2 \cdot 2.5 \text{H}_2\text{O}$ ), however, gave a boost in the yield of **3a** to 79 %, which were the best result obtained thus far (Table 2.4, entry 6).

We theorized that by reversing the stoichiometry, an excess of hydantoin could hamper the formation of bis-arylated product. Using an excess of hydantoin ranging from 1.1-2.0 equivalents did in fact reduce the bis-formation but did also impede the formation of **3c** (Table 2.4, entries 7-9). An excess of base was added to compensate for the increased amount of hydantoin (Table 2.4, entries 10 and 11), but in neither case the yield was satisfactory.

### 2.2.7 Screening of auxiliaries: TMP *vs.* Mes

Using mesityl (Mes, briefly mentioned in Section 2.1.1.2) as an auxiliary for selective arene transfer is well established in the literature.<sup>155, 160, 189, 201-206</sup> A short study was conducted to investigate the effect using Mes in place of TMP as auxiliary (Table 2.5).

**Table 2.5.** Screening of auxiliaries: TMP and Mes.



#	[Cu] (mol %)	2a-Aux (equiv.)	Yield 3a (%) <sup>[a]</sup>	Yield 3c (%)
1	CuI (10)	TMP (1.5)	47	11 <sup>[b]</sup>
2	CuI (10)	Mes (1.5)	30	7 <sup>[c]</sup>
3	$\text{Cu}(\text{NO}_3)_2 \cdot 2.5 \text{H}_2\text{O}$ (5)	TMP (3.0)	79	11 <sup>[b]</sup>
4	$\text{Cu}(\text{NO}_3)_2 \cdot 2.5 \text{H}_2\text{O}$ (5)	Mes (3.0)	60 <sup>[c]</sup>	4 <sup>[c]</sup>

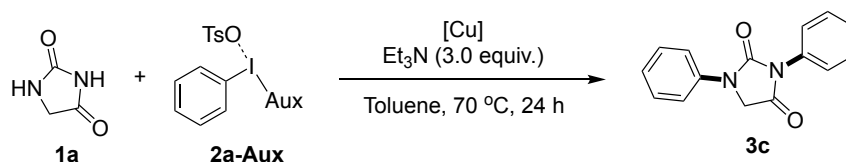
Conditions: Hydantoin **1a** (0.2 mmol, 1.0 equiv.), PhI(TMP)OTs **2a** or PhI(Mes)OTs **2a-Mes** (as specified), Cu-catalyst (as specified),  $\text{Et}_3\text{N}$  (0.3 mmol, 1.5 equiv.) and toluene (2 mL). [a] Isolated yield. [b] <sup>1</sup>H NMR yield using Mes as IS. [c] <sup>1</sup>H NMR yield using TMP-H as IS.

Phenyl transfer selectivity was retained as no transfer of Mes was detected. However, a reduction in overall yield was seen. Using CuI as a catalyst, 47 % of **3a** was produced with TMP as auxiliary and only 30 % with Mes (Table 2.5, entries 1 and 2). With  $\text{Cu}(\text{NO}_3)_2 \cdot 2.5 \text{H}_2\text{O}$ , a reduction from 79 % to 60 % (Table 2.5, entries 3 and 4) was seen with Mes. The reduced conversion is an indication that a more electron rich auxiliary is favorable.

## 2.2.8 Attempts to develop a protocol for bis-arylation

Complete suppression of bis-arylation was not achieved under our conditions. No direct (one-pot) *N,N*-bis-arylation, where hydantoin is arylated at both nitrogen atoms concomitantly, have been reported. We decided to optimize the conditions in an attempt to develop a procedure. We began the optimization similar to the optimization for *N*-3-arylation, but 3.0 equivalents of both coupling partner and base was used to ensure bis-arylation. Employing CuI as a catalyst and TMP as the auxiliary furnished 65 % of the bis-arylated **3c** (Table 2.6, entry 1) Exchanging TMP for Mes gave a reduction in yield and only 37 % was obtained (entry 2). These results are consistent with previous results where Mes was used as an alternative to TMP (see Table 2.5).

**Table 2.6.** Optimization of bis-arylation.



#	[Cu] (mol %)	<b>2a-Aux</b> (equiv.)	Additive (equiv.)	Atm	Yield <b>3c</b> (%) <sup>[a]</sup>
1	CuI (10)	TMP (3.0)	-	Argon	65 <sup>[c]</sup>
2	CuI (10)	Mes (3.0)	-	Argon	37 <sup>[b]</sup>
3	Cu(OTf) <sub>2</sub> (10)	TMP (3.0)	H <sub>2</sub> O (1.0)	Air	42
4	Cu(OTf) <sub>2</sub> (10)	TMP (3.0)	-	Air	72
5 <sup>[d]</sup>	Cu(OTf) <sub>2</sub> (10)	TMP (3.0)	-	Argon	59
6	Cu(OTf) <sub>2</sub> (5)	TMP (3.0)	-	Air	63 <sup>[c]</sup>
7	Cu(NO <sub>3</sub> ) <sub>2</sub> · 2.5 H <sub>2</sub> O (10)	TMP (3.0)	-	Air	44
8	Cu(NO <sub>3</sub> ) <sub>2</sub> · 2.5 H <sub>2</sub> O (10)	TMP (5.0)	-	Air	60

Conditions: Hydantoin **1a** (0.2 mmol, 1.0 equiv.), PhI(TMP)OTs **2a** or PhI(Mes)OTs **2a-Mes** (as specified) catalyst (as specified), Et<sub>3</sub>N (0.6 mmol, 3.0 equiv.) and toluene (2 mL). [a] <sup>1</sup>H NMR yield using Mes as IS. [b] <sup>1</sup>H NMR yield using TMP-H as IS. [c] Isolated yield. [d] Cu(OTf)<sub>2</sub> was dried in the oven, then under high vacuum prior to the reaction. Additionally, anhydrous toluene was used.

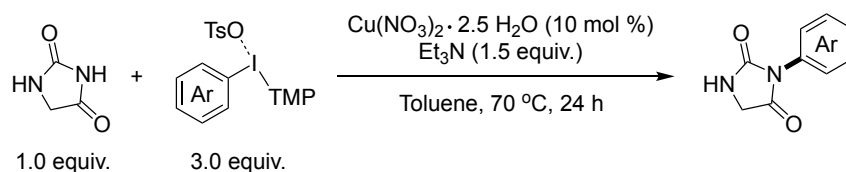
Previous results also showed a reduction of **3c** produced when Cu(OTf)<sub>2</sub> and H<sub>2</sub>O was used. Without addition of water, 72 % of **3c** was obtained, compared to 42 % where water was included (Table 2.6, entries 3 and 4). Rationally, we then tried to ensure moisture-free conditions by drying the catalyst and using an anhydrous solvent (Table

2.6, entry 5). The reaction was performed under inert atmosphere as previous results did not indicate any negative impact of excluding air. However, only 59 % of **3c** was afforded. From the screening of catalyst loading (Table 2.2), a lower load of Cu(OTf)<sub>2</sub> lead to more of the bis-arylated product. 5 mol % Cu(OTf)<sub>2</sub> yielded **3c** in 63 % under normal conditions (Table 2.6, entry 6). Substituting Cu(OTf)<sub>2</sub> for Cu(NO<sub>3</sub>)<sub>2</sub> · 2.5 H<sub>2</sub>O did not yield a satisfactory outcome as only 44 % and 60 % of **3c** was afforded (Table 2.6, entries 7 and 8). The latter with a large excess of salt (5.0 equivalents).

Unfortunately, reproducibility of the best results was not achieved, likely due to uncontrollable effects. Pinpointing the culprits of the failed reproducibility were not the focus of this study, and it was decided not to proceed any further.

### 2.2.9 Final optimized conditions for the *N*-3-arylation reaction

After an extensive optimization study, the optimized conditions for the reaction were finally determined (Scheme 2.5) and include Aryl(TMP)iodonium tosylate (3.0 equivalents), Cu(NO<sub>3</sub>)<sub>2</sub> · 2.5 H<sub>2</sub>O (10 mol %) and Et<sub>3</sub>N (1.5 equivalents) in toluene at 70 °C for 24 hours.



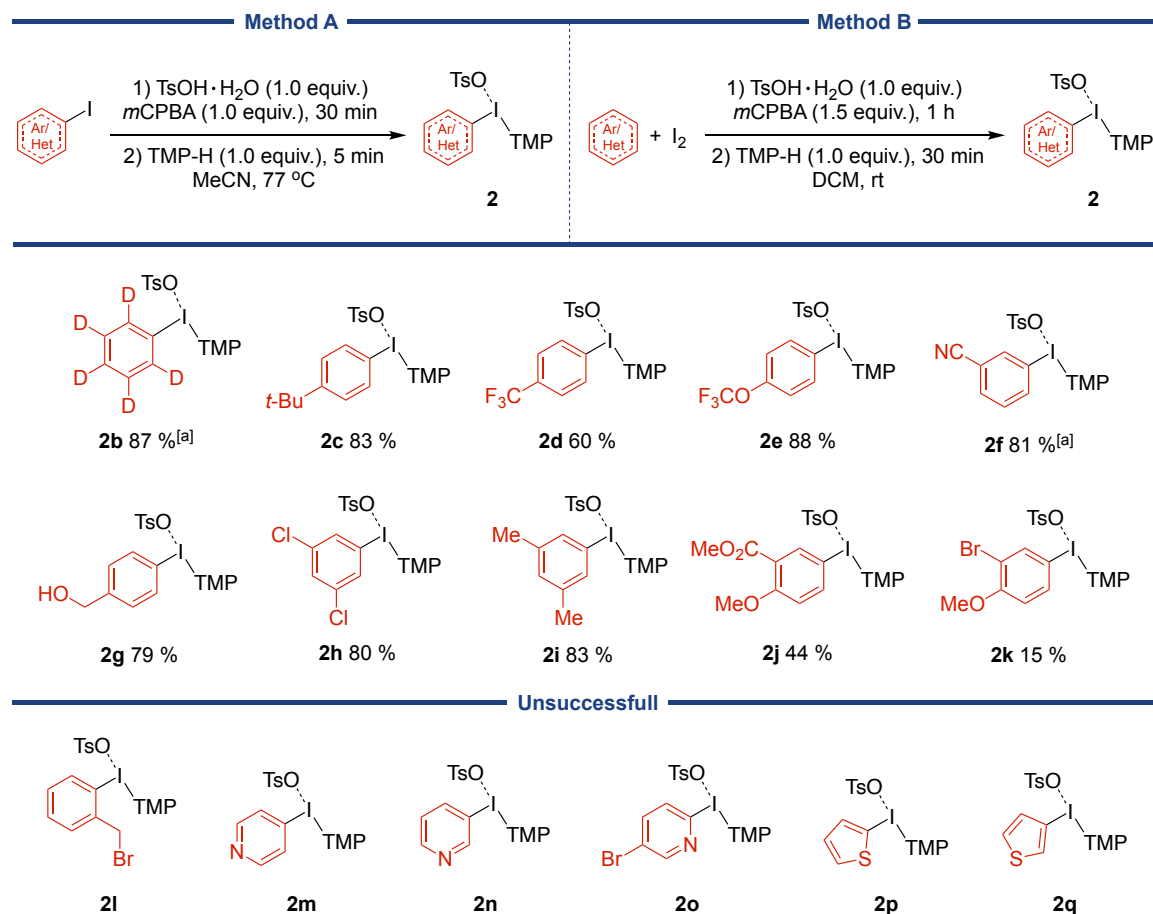
Scheme 2.5. Optimized conditions.

### 2.2.10 Synthesis of aryl(TMP)iodonium tosylates

With the final optimized conditions, a natural next step is to explore the scope and limitations of the reaction. Prior to this, the preparation of the diaryliodonium salts is presented. Most of the salts included in the upcoming scope tables are included in Paper I. The following section will include the synthesis of unpublished salts, in addition to unsuccessful attempts. The majority of the salts presented were used further in the coupling reactions with hydantoin.

A number of substituted aryl(TMP)iodonium tosylates were synthesized according to procedures reported by Stuart (method A)<sup>172</sup> and Olofsson (method B)<sup>166</sup> (Scheme 2.6). Method A have demonstrated tolerance towards a variety of diverse steric- and electronic effects. As such, it was the primary method of choice for preparation of the

salts. Salt **2b-2i** was smoothly synthesized and isolated in very good yields (60-88 %) using this method.



**Scheme 2.6.** Substrate scope of unpublished aryl(TMP)iodonium tosylates. Salt **2b-2i** were synthesized using **method A**,<sup>172</sup> conditions: **1**) aryl iodide (5.0 mmol, 1.0 equiv.), TsOH·H<sub>2</sub>O (5.0 mmol, 1.0 equiv.), *m*CPBA (5.0 mmol, 1.0 equiv.), MeCN, 77 °C, 30 min. **2**) Trimethoxybenzene (TMP-H) (5 mmol, 1.0 equiv.), 5 min. Salt **2j** and **2k** were synthesized using **method B**,<sup>166</sup> conditions: **1**) arene (1.1 mmol, 1.0 equiv.), iodine (0.55 mmol, 0.5 equiv.), TsOH·H<sub>2</sub>O (1.1 mmol, 1.0 equiv.), *m*CPBA (1.7 mmol, 1.5 equiv.), DCM, rt, 1 h. **2**) TMP-H (1.1 mmol, 1.0 equiv.), 30 min. [a] synthesized using method A on a 2 mmol scale.

In method B, the iodoarene is generated in situ from an arene and molecular iodine. This method was used in the preparation of salt **2j** and **2k**. Challenges in purification process gave these salts in only 44 % and 15 %, respectively. Aryl- and heteroaryl iodides were subjected to the conditions of method A, but the reactions were unsuccessful (**2l-2q**). The milder method B was tested using thiophene, were regioisomers **2p** and **2q** potentially could form, but no product was obtained from the reaction. No other methods were tried in the preparation of these salts as they were merely attempts to get an insight in the limitations of the methods.

### 2.2.11 Scope and limitations of the developed reaction

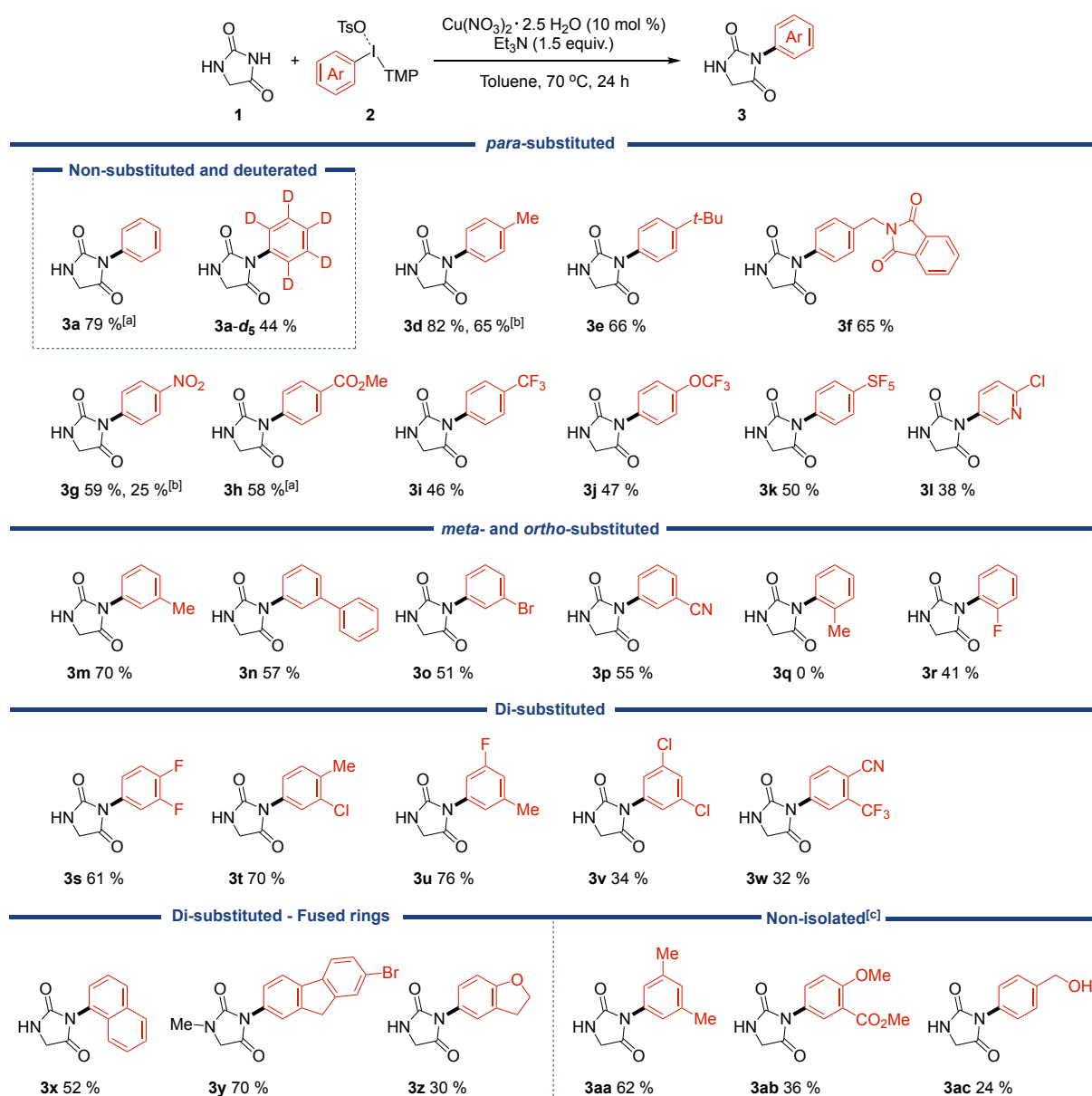
With a selection aryl(TMP)iodonium tosylates and various *N*-nucleophiles (hydantoins and imides), the scope and limitations of the reactions were explored. Most of the structures are included in Paper I, but **3a-d**, **3c**, **3e**, **3i-j**, **3p**, **3v**, **3aa-3ac**, and **6c** are additional structures included herein.

#### 2.2.11.1 Substrate scope: Diaryliodonium salts

Using the optimized conditions, aryl(TMP)iodonium salts with different electronic- and steric properties were tested in the *N*-3-arylation reaction to investigate the scope and limitations of the substrates (Scheme 2.7). To our surprise, the performance of deuterated salt **2b** was mediocre. Only 44 % of **3a-d** was obtained from the reaction, presumably due to the presence of a kinetic isotope effect (KIE). Aryl groups bearing weakly electron-donating groups (EDGs) in the *para*-position were efficiently transferred, yielding **3d** in 82 %, **3e** in 66 % and **3f** in 65 %. Substituting the weakly EDGs with electron withdrawing-groups (EWGs) reduced the efficiency of the aryl transfer and *p*-NO<sub>2</sub> substituted **3g** and *p*-CO<sub>2</sub>Me **3h** were afforded in moderate yields.

Replacing Cu(NO<sub>3</sub>)<sub>2</sub> · 2.5 H<sub>2</sub>O with Cu(OTf)<sub>2</sub> and H<sub>2</sub>O (frequently reoccurring conditions in the optimization study) gave unexpected results in the transfer of *p*-Me- and *p*-NO<sub>2</sub> substituted arenes. Only 65 % of **3d** and 25 % of **3g** was obtained, indicating an unforeseen electronic sensitivity in aryl transfer with Cu(OTf)<sub>2</sub>.

The fluorinated *p*-CF<sub>3</sub> **3i**, *p*-OCF<sub>3</sub> **3j**, and *p*-SF<sub>5</sub> **3k** were also afforded in moderate yields (46-50 %). Recently, the latter two “exotic” groups have been of high interest in the quest for new drugs.<sup>207, 208</sup> Despite the moderate outcome, the method helps expand accessibility of potential biologically active hydantoins containing these groups. The increased electron deficiency of the pyridine analog also had a negative impact on the outcome and **3l** was only isolated in modest yields (38 %).



**Scheme 2.7.** Diaryliodonium salt substrate scope. Conditions: Hydantoin **1a** or 1-methylhydantoin **1b** (0.2 mmol, 1.0 equiv.), ArI(TMP)OTs **2** (0.6 mmol, 3.0 equiv.), Cu(NO<sub>3</sub>)<sub>2</sub> · 2.5 H<sub>2</sub>O (0.02 mmol, 0.1 equiv.), Et<sub>3</sub>N (0.3 mmol, 1.5 equiv.), toluene (2 mL). [a] 5 mol % of catalyst employed [b] Cu(OTf)<sub>2</sub> (10 mol %) and H<sub>2</sub>O (1.0 equiv.) was used instead of Cu(NO<sub>3</sub>)<sub>2</sub>·2.5 H<sub>2</sub>O. [c] <sup>1</sup>H NMR yield determined by using Mes as IS.

*meta*-Substituted arenes were also tolerated under our conditions. Similar trends in terms of electronic effects were also observed for **3m-3p**. The more electron-rich *m*-Me substituted **3m** was afforded in 70 %, while 51 % to 57 % of **3n-3p** were afforded. Our method was notably sensitive to substituents in *ortho*-position. The effect can likely be attributed to steric crowding around the Cu-center in the catalytic process,<sup>209, 210</sup> increasing the energy needed for effective aryl transfer. *o*-Me substituted **3q** was too

sterically congested and no product formation was observed. The smaller fluorine atom was tolerated and 41 % of **3r** was isolated.

Di-substituted aryl moieties **3s-3u** were transferred smoothly (61-76 %), while transfer of the more electron-deficient **3v** and **3w** were, not surprisingly, less efficient. The fused naphthyl- and fluorene-rings **3x** and **3y** were obtained in moderate and good yields (52 % and 70 %, respectively). As with the very electron-poor, the method was also ineffective for very electron-rich substrates. To demonstrate the fact, dihydrobenzofuran **3z** was only isolated in 30 %.

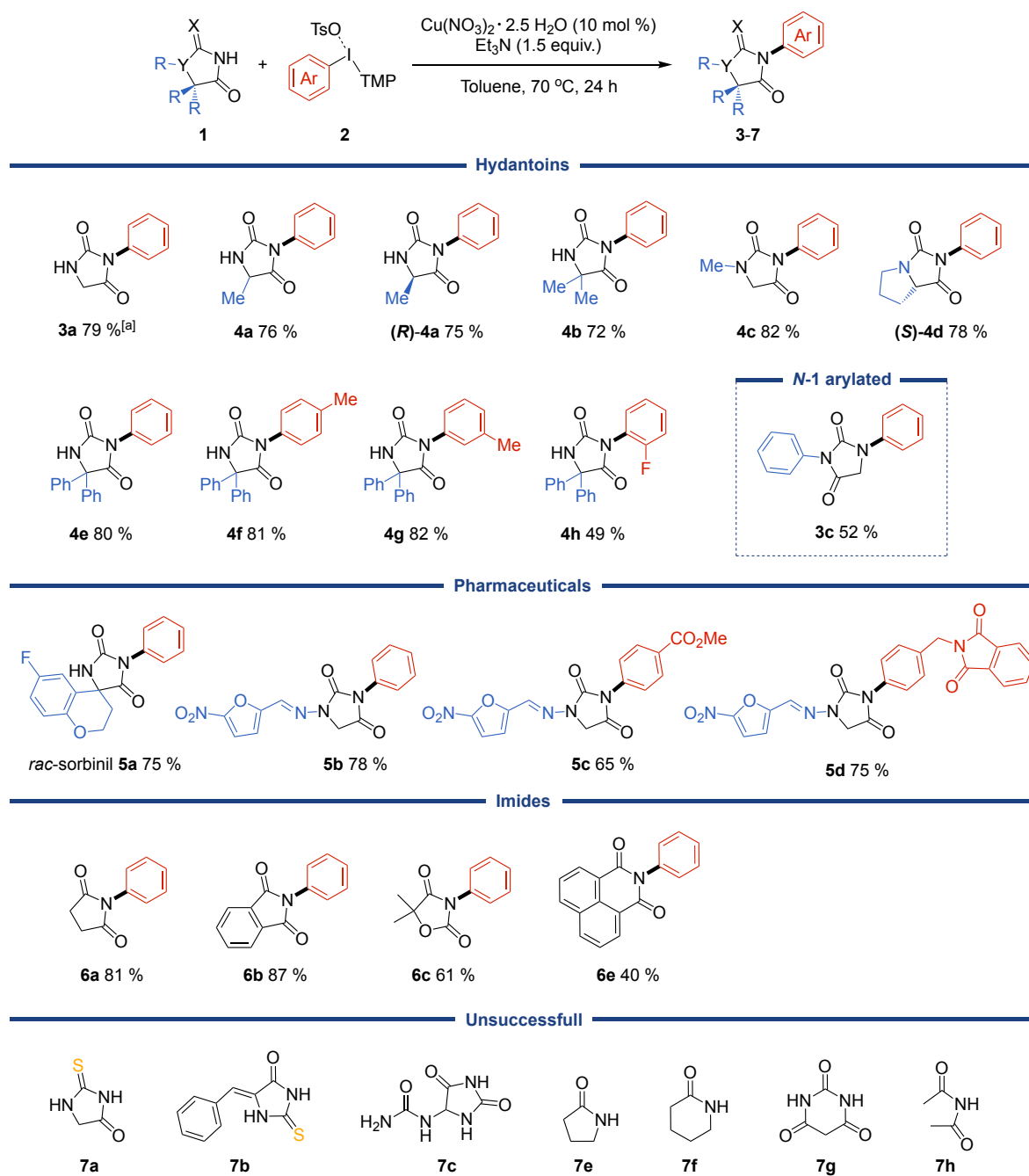
The three arylated hydantoins **3aa-3ac** were synthesized, but not isolated due to unsatisfactory yields. Thus, their yields were determined by <sup>1</sup>H NMR analysis of the crude reaction mixture. In addition to the bis-arylated byproduct, the *N*-1-arylated was present in 12 % in the reaction with the *m*-xylene salt, only affording 62 % of **3aa**. Compared to the other methylated arenes (see **3d**, **3t** and **3u**), higher yields were expected in this reaction. The free hydroxy group of salt **2g** survived our conditions, but only 24 % of **3ac** was detected.

#### 2.2.11.2 Substrate scope: Hydantoins and other imides

Next, we wanted to investigate the *N*-3-arylation of hydantoins with substituents on *N*-1 and *C*-5 (Scheme 2.8). Introducing a methyl group on *C*-5 did not affect yield significantly (76 % of **4a** vs. 79 % of unsubstituted **3a**). Pleasingly, our conditions did not cause epimerization in the *C*-5 position, allowing for controlled, stereoretentive couplings. (*R*)-**4a** was afforded in equal yields to **4a**. Introducing yet another methyl group did not affect the reaction notably either as 72 % of 5,5-dimethylated **4b** was isolated. As expected, *N*-1-substitution was beneficial, blocking potential *N*-1-aryl transfer and hence bis-arylation. A slight increase in yield (82 %) was seen for 1-methylated **4c**. Arylation of hydantoin with substituents in 1- and 5 position was also successful. *L*-proline-derived hydantoin (*S*)-**4d** was obtained in 78 % yield and retention of stereochemistry was observed.

The bulkier 5,5-diphenylated hydantoin were subjected to arylation with a small series of diaryliodonium salts. Phenyl, *p*-Me- and *m*-Me-substituted **4e-4g** were, expectantly, obtained in very good yields (80-82 %), while the yield severely reduced with the *ortho*-substituted *o*-F **4h**. Similar trends were seen with the *C*-5 unsubstituted **3d**, **3m**, **3q** and **3r**.





**Scheme 2.8.** Hydantoin- and imide scope. Conditions: Hydantoin or imide **1** (0.2 mmol, 1.0 equiv), ArI(TMP)OTs **2** (0.3 mmol, 1.5 equiv), Cu(NO<sub>3</sub>)<sub>2</sub> · 2.5 H<sub>2</sub>O (0.02 mmol, 0.1 equiv), Et<sub>3</sub>N (0.3 mmol, 1.5 equiv), toluene (2 mL). [a] 5 mol % of catalyst employed.

Evano *et al.* reported a subsequent *N*-1-arylation (Chapter 1, Scheme 1.10a) after *N*-3-arylation. The reaction required a different set of (harsher) conditions for the more demanding *N*-1-arylation to proceed. We subjected *N*-3-arylated (**3a**) hydantoin to *N*-1-arylation using our original conditions. Only 52 % of **3c** was obtained, clearly demonstrating the more challenging arylation of the *N*-1 position.

To demonstrate the usefulness of the method, marketed hydantoin-containing pharmaceuticals were arylated. The racemate of sorbinil<sup>211</sup> (an aldose reductase inhibitor) was pleasingly arylated in good yields (**5a**, 75 %). Arylation of the well-known antibacterial nitrofurantoin provided a nitrofurantoin-derivatives **5b-5c** also in good yields. These examples illustrate the possibility of late-stage functionalization of pharmaceuticals, thereby highlight the advantage of direct functionalization.

To further expand the structural space, a small selection of cyclic imides were exposed to our conditions. Aryl transfer proved to efficient for succinimide and phthalimide producing **6a** and **6b** in 81 % and 87 %, respectively. The method was less productive for the 2,4-oxazolidinedione (hereby referred to as “oxohydantoin”) **6c** and the 6-membered imide (naphthalimide) **6d**.

Unfortunately, several of the substrates tested were not compatible with our method. The failure of thiohydantoins **7a** and **7b** can likely be attributed their preference for a thio-enol configuration<sup>3, 212</sup> (see Chapter 1, Figure 1.2, tautomer II). Decomposition of allantoin **7c** in the presence of Cu(II) have been reported,<sup>213</sup> but no decomposition was detected under our conditions. Regardless, coupling with **7c** was unsuccessful, presumably due to Cu-coordination. The method was not applicable to lactams **7e** and **7f**, barbituric acid **7g**, and and the linear imide **7h** as no reaction was detected.

## 2.3 Conclusion

A general and efficient Cu-catalyzed method for regioselective *N*-3-arylation of hydantoins has been developed. The method utilizes unsymmetrical diaryliodonium salts, a simple Cu-salt in catalytic amounts and triethylamine as a base/ligand. The chemoselective nature of unsymmetrical aryl(TMP)iodonium salts was displayed in the aryl transfers, providing a broad scope of arylated hydantoins in moderate to very good yields. The method operates best with, but are not limited to, weakly EWGs and EDGs. Structurally diverse hydantoins are well tolerated, including unsubstituted hydantoins and chiral hydantoins where the stereogenic center is retained. The method developed is useful for diversification of pharmaceutically relevant agents such as phenytoin, *rac*-sorbinil and nitrofurantoin.

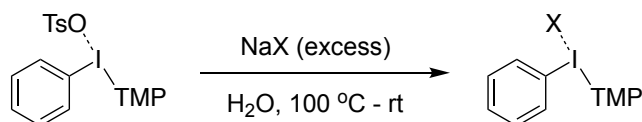
## 2.4 Experimental

Experimental details and data for compounds not included in Paper I are described herein. Information about reagents, solvents and instrumentation are mostly covered in the supporting information to Paper I. Additional information included here are: Spectra using CD<sub>3</sub>CN as solvent were calibrated using the residual solvent peak (<sup>1</sup>H NMR: 1.94 ppm and <sup>13</sup>C NMR: 1.32 ppm/118.26 ppm).

### Synthesis and characterization of diaryliodonium salts

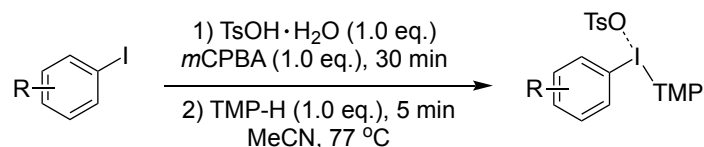
Diaryliodonium salts **2a**, **2a-BF<sub>4</sub>**, **2a-OTf**, **2a-Mes** and **2b-2k** were prepared according to literature procedures.<sup>166, 172</sup>

#### General procedure for anion exchange<sup>172</sup>



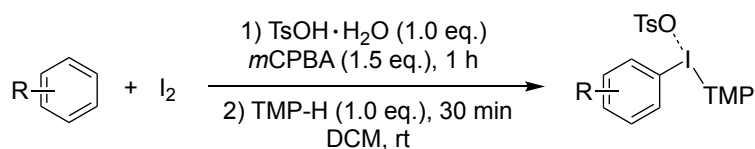
Phenyl(2,4,6-trimethoxyphenyl)iodonium tosylate (**2a**) (0.651 g, 1.20 mmol, 1.00 equiv.) was added to 50 mL boiling water in a 100 mL round-bottom flask. As the salt did not fully dissolve after 2 min, methanol was added dropwise until the solution had a homogenous appearance. NaBF<sub>4</sub> (13.2 g, 120 mmol, 100 equiv.) was added and the solution was stirred for 2 minutes at 100 °C. The resulting solution was left to cool to ambient temperature before chilling further in an ice-bath. The mixture was then vacuum filtered, and the filter cake was washed with cold water (3 x 30 mL), dried under suction for 15-20 min, and then washed with diethyl ether (3 x 30 mL). The sample was further dried under high vacuum to afford the final product.

### General procedure A: preparation of aryl(TMP)iodonium tosylates from iodoarenes



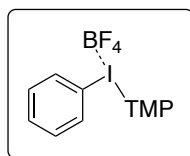
Following a reported procedure,<sup>172</sup> aryl iodide (5.0 mmol, 1.0 equiv.) and acetonitrile (5 mL) were added to a 50 mL round-bottom flask and equipped with a magnetic stir bar. *p*-Toluenesulfonic acid monohydrate (TsOH·H<sub>2</sub>O) (5.0 mmol, 1.0 equiv.) was added in one portion at room temperature, followed by *m*-chloroperbenzoic acid (*m*CPBA) (5.0 mmol, 1.0 equiv.). The flask was lowered into a pre-heated heating block set at 77 °C and stirred for 30 minutes. 1,3,5-trimethoxybenzene (TMP-H) (5.0 mmol, 1.0 equiv.) was then added and the resulting solution was stirred for 5 minutes at 77 °C. The flask was cooled to ambient temperature before acetonitrile was removed under reduced pressure. The resulting crude oil was triturated with Et<sub>2</sub>O (40 mL). The precipitate was isolated by vacuum filtration with a fritted funnel and rinsed with Et<sub>2</sub>O (3 x 20 mL), then dried further under high vacuum to obtain the product in analytic purity.

### General procedure B: preparation of aryl(TMP)iodonium tosylates from arenes and iodide



With slight modifications from the original procedure,<sup>166</sup> iodine (0.55 mmol, 0.50 equiv.) and DCM (40 mL) were added to a 100 mL round-bottom flask and equipped with a magnetic stir bar. *m*-chloroperbenzoic acid (*m*CPBA) (1.7 mmol, 1.5 equiv.), arene (1.1 mmol, 1.0 equiv.) and *p*-toluenesulfonic acid monohydrate (TsOH·H<sub>2</sub>O) (1.1 mmol, 1.0 equiv.) were added sequentially, and the reaction mixture was stirred at rt for 1 h. The mixture gradually change color from deep purple to clear yellow. 1,3,5-trimethoxybenzene (TMP-H) (1.1 mmol, 1.0 equiv.) was then added and the resulting solution was stirred for 30 min at rt. The solution was triturated with Et<sub>2</sub>O (60 mL), the mixture was stirred for 30 min and then kept in the freezer for an addition 30 min. The resulting solid was filtered off, washed three times with Et<sub>2</sub>O, dried under water suction and then dried further under high vacuum to afford the desired product.

### Phenyl(2,4,6-trimethoxyphenyl)iodonium tetrafluoroborate (**2a-BF<sub>4</sub>**)<sup>214</sup>



Phenyl(2,4,6-trimethoxyphenyl)iodonium tosylate (**2a**) (0.651 g, 1.20 mmol, 1.00 equiv.) and NaBF<sub>4</sub> (13.2 g, 120 mmol, 100 equiv.) were used in the preparation of **2a-BF<sub>4</sub>** according to the general procedure for anion exchange. Some product was suspected lost during the filtration step, as such, the filtrate was extracted three times with DCM. The combined organic layers were dried with MgSO<sub>4</sub>, filtered and DCM was removed under reduced pressure. The two batches were combined and dried under high vacuum. **2a-BF<sub>4</sub>** was afforded as a grey-brown solid (0.221 g, 40 %).

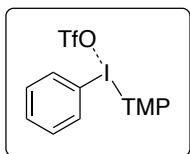
<sup>1</sup>H NMR (600 MHz, DMSO-*d*<sub>6</sub>): δ 7.92 (dd, *J* = 8.4, 1.2 Hz, 2H), 7.61 (t, *J* = 7.5 Hz, 1H), 7.47 (t, *J* = 7.8 Hz, 2H), 6.47 (s, 2H), 3.95 (s, 6H), 3.87 (s, 3H).

<sup>13</sup>C NMR (151 MHz, DMSO-*d*<sub>6</sub>): δ 166.2, 159.4, 134.3, 131.6 (2C), 116.1, 92.1, 87.0, 57.3, 56.2.

<sup>19</sup>F NMR (376 MHz, DMSO-*d*<sub>6</sub>): δ -148.23 (from [<sup>10</sup>BF<sub>4</sub>]<sup>-</sup>), -148.29 (from [<sup>11</sup>BF<sub>4</sub>]<sup>-</sup>)

HRMS (ESI) *m/z* [M - BF<sub>4</sub>]<sup>+</sup>: Calcd. for C<sub>15</sub>H<sub>16</sub>IO<sub>3</sub><sup>+</sup>: 371.0139, found: 371.0138.

### Phenyl(2,4,6-trimethoxyphenyl)iodonium triflate (**2a-OTf**)<sup>163, 215</sup>



Phenyl(2,4,6-trimethoxyphenyl)iodonium tosylate (**2a**) (0.543 g, 1.00 mmol, 1.0 equiv.) and NaOTf (3.45 g, 20.0 mmol, 20.0 equiv.) were used in the preparation of **2a-OTf** according to the general procedure for anion exchange. **2a-OTf** was afforded as a white solid (0.298 g, 57 %).

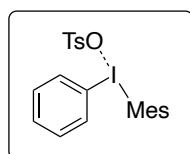
<sup>1</sup>H NMR (600 MHz, DMSO-*d*<sub>6</sub>): δ 7.92 (dd, *J* = 8.4, 1.2 Hz, 2H), 7.63 – 7.59 (m, 1H), 7.47 (t, *J* = 7.8 Hz, 2H), 6.47 (s, 2H), 3.95 (s, 6H), 3.87 (s, 3H).

<sup>13</sup>C NMR (151 MHz, DMSO-*d*<sub>6</sub>): δ 166.2, 159.4, 134.4, 131.6, 120.7 (q, *J*<sub>C-F</sub> = 322.6 Hz), 116.1, 92.1, 87.0, 57.3, 56.2.

<sup>19</sup>F NMR (376 MHz, DMSO-*d*<sub>6</sub>): δ -77.7.

HRMS (ESI) *m/z* [M - OTf]<sup>+</sup>: Calcd. for C<sub>15</sub>H<sub>16</sub>IO<sub>3</sub><sup>+</sup>: 371.0139, found: 371.0139.

## Phenyl(2,4,6-trimethylphenyl)iodonium tosylate (**2a-Mes**)<sup>216</sup>



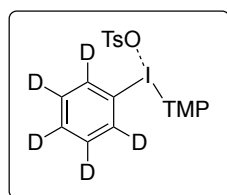
**2a-Mes** was prepared according to general procedure A with modifications. In stage 2), 1,3,5-trimethylbenzene (mesitylene) (765  $\mu\text{L}$ , 5.50 mmol, 1.10 equiv.) was added in place of TMP-H and the reaction time was extended from 5 min to 12 h. **2a-Mes** was afforded as a white solid (2.17 g, 88 %).

<sup>1</sup>H NMR (600 MHz, DMSO-*d*<sub>6</sub>):  $\delta$  7.97 (dd,  $J = 8.5, 1.1$  Hz, 2H), 7.64 – 7.61 (m, 1H), 7.51 – 7.48 (m, 2H), 7.48 – 7.45 (m, 2H), 7.21 (d,  $J = 0.7$  Hz, 2H), 7.10 (dd,  $J = 8.5, 0.7$  Hz, 2H), 2.59 (s, 6H), 2.29 (s, 3H), 2.28 (s, 3H).

<sup>13</sup>C NMR (151 MHz, DMSO-*d*<sub>6</sub>):  $\delta$  145.7, 143.0, 141.5, 137.6, 134.4, 131.8, 131.7, 129.7, 128.0, 125.5, 122.6, 114.5, 26.3, 20.8, 20.5.

HRMS (ESI)  $m/z$  [M - OTs]<sup>+</sup>: Calcd. for C<sub>15</sub>H<sub>16</sub>I<sup>+</sup>: 323.0291, found: 323.0292.

## Phenyl-*d*<sub>5</sub>-(2,4,6-trimethoxyphenyl)iodonium tosylate (**2b**)



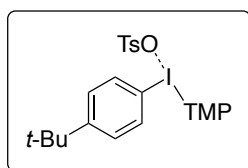
**2b** was prepared to general procedure A on a 2.0 mmol scale and obtained as a pale, pink solid (1.10 g, 87 %).

<sup>1</sup>H NMR (600 MHz, DMSO-*d*<sub>6</sub>):  $\delta$  7.47 (d,  $J = 8.0$  Hz, 2H), 7.10 (d,  $J = 7.8$  Hz, 2H), 6.47 (s, 2H), 3.94 (s, 6H), 3.87 (s, 3H), 2.28 (s, 3H).

<sup>13</sup>C NMR (151 MHz, DMSO-*d*<sub>6</sub>):  $\delta$  166.2, 159.4, 145.8, 137.6, 133.9 (t,  $J = 25.7$  Hz), 131.1 (t,  $J = 24.5$  Hz), 128.0, 125.5, 115.8, 92.1, 87.0, 57.3, 56.2, 20.8. One triplet was not visible in the spectrum, but visible the spectrum of the coupled product (**3a-d<sub>5</sub>**).

HRMS (ESI)  $m/z$  [M - OTs]<sup>+</sup>: Calcd. for C<sub>15</sub>H<sub>11</sub>D<sub>5</sub>INO<sub>3</sub><sup>+</sup>: 376.0453, found: 376.0452.

**(4-(*tert*-butyl)phenyl)(2,4,6-trimethoxyphenyl)iodonium tosylate (2c)<sup>172</sup>**



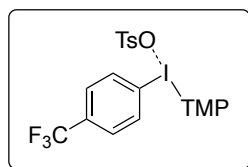
**2c** was prepared according to general procedure A on a 5 mmol scale and obtained as an off-white powder (1.84 g, 83 %).

<sup>1</sup>H NMR (600 MHz, DMSO-*d*<sub>6</sub>): δ 7.83 (d, *J* = 8.7 Hz, 2H), 7.49 – 7.46 (m, 4H), 7.12 – 7.09 (m, 2H), 6.47 (s, 2H), 3.95 (s, 6H), 3.87 (s, 3H), 2.28 (s, 3H), 1.24 (s, 9H).

<sup>13</sup>C NMR (151 MHz, DMSO-*d*<sub>6</sub>): δ 166.1, 159.4, 154.6, 145.8, 137.5, 134.1, 128.6, 127.9, 125.5, 112.5, 92.0, 86.9, 57.3, 56.1, 34.8, 30.7, 20.7.

HRMS (ESI) *m/z* [M - OTs]<sup>+</sup>: Calcd. for C<sub>19</sub>H<sub>24</sub>IO<sub>3</sub><sup>+</sup>: 423.0765, found: 423.0764.

**4-(Trifluoromethyl)phenyl(2,4,6-trimethoxyphenyl)iodonium tosylate (2d)<sup>172</sup>**



**2d** was prepared according to general procedure A on a 5 mmol scale and obtained as a pale, pink powder (1.28 g, 60 %).

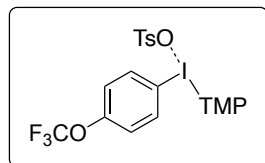
<sup>1</sup>H NMR (600 MHz, DMSO-*d*<sub>6</sub>): δ 8.11 (d, *J* = 8.2 Hz, 2H), 7.82 (d, *J* = 8.4 Hz, 2H), 7.47 (d, *J* = 8.1 Hz, 2H), 7.10 (d, *J* = 7.8 Hz, 2H), 6.49 (s, 2H), 3.94 (s, 6H), 3.88 (s, 3H), 2.28 (s, 3H).

<sup>13</sup>C NMR (151 MHz, DMSO-*d*<sub>6</sub>): δ 166.4, 159.4, 145.7, 137.6, 135.0, 131.4 (q, *J*<sub>C-F</sub> = 32.5 Hz), 128.1 (q, *J*<sub>C-F</sub> = 3.7 Hz), 128.0, 125.5, 123.4 (q, *J*<sub>C-F</sub> = 272.8 Hz), 120.3, 92.2, 87.0, 57.4, 56.2, 20.7.

<sup>19</sup>F NMR (376 MHz, DMSO-*d*<sub>6</sub>): δ -61.7.

HRMS (ESI) *m/z* [M - OTs]<sup>+</sup>: Calcd. for C<sub>16</sub>H<sub>15</sub>F<sub>3</sub>IO<sub>3</sub><sup>+</sup>: 439.0013, found: 439.0013.

**4-(Trifluoromethoxy)phenyl(2,4,6-trimethoxyphenyl)iodonium tosylate (2e)**<sup>217</sup>



**2e** was prepared according to general procedure A on a 5 mmol scale and obtained as a white powder (2.85 g, 88 %).

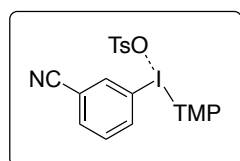
<sup>1</sup>H NMR (600 MHz, DMSO-*d*<sub>6</sub>): δ 8.03 (d, *J* = 9.1 Hz, 2H), 7.47 (d, *J* = 8.3 Hz, 4H), 7.10 (d, *J* = 8.4 Hz, 2H), 6.48 (s, 2H), 3.95 (s, 6H), 3.87 (s, 3H), 2.28 (s, 3H).

<sup>13</sup>C NMR (151 MHz, DMSO-*d*<sub>6</sub>): δ 166.3, 159.4, 150.2, 145.8, 137.5, 136.7, 128.0, 125.5, 123.8, 119.8 (q, *J*<sub>C-F</sub> = 258.2 Hz), 113.7, 92.1, 87.2, 57.4, 56.2, 20.7.

<sup>19</sup>F NMR (376 MHz, DMSO-*d*<sub>6</sub>): δ -56.8.

HRMS (ESI) *m/z* [M - OTs]<sup>+</sup>: Calcd. for C<sub>16</sub>H<sub>15</sub>F<sub>3</sub>IO<sub>4</sub><sup>+</sup>: 454.9962, found: 454.9961.

**3-Cyanophenyl(2,4,6-trimethoxyphenyl)iodonium tosylate (2f)**<sup>172</sup>



**2f** was prepared according to general procedure A on a 2 mmol scale and obtained as a pale, pink powder (0.920 g, 81 %).

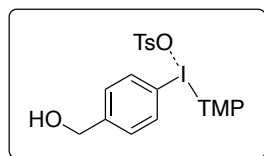
<sup>1</sup>H NMR (600 MHz, DMSO-*d*<sub>6</sub>): δ 8.45 (t, *J* = 1.7 Hz, 1H), 8.19 (ddd, *J* = 8.2, 1.9, 1.1 Hz, 1H), 8.06 (dt, *J* = 7.8, 1.3 Hz, 1H), 7.64 (t, *J* = 8.0 Hz, 1H), 7.46 (d, *J* = 8.2 Hz, 2H), 7.10 (d, *J* = 7.9 Hz, 2H), 6.47 (s, 2H), 3.94 (s, 6H), 3.87 (s, 3H), 2.28 (s, 3H).

<sup>13</sup>C NMR (151 MHz, DMSO-*d*<sub>6</sub>): δ 166.4, 159.4, 145.5, 138.9, 137.7, 137.4, 135.2, 132.3, 128.1, 125.5, 117.0, 116.2, 113.6, 92.1, 87.2, 57.4, 56.2, 20.8.

HRMS (ESI) *m/z* [M - OTs]<sup>+</sup>: Calcd. for C<sub>16</sub>H<sub>15</sub>INO<sub>3</sub><sup>+</sup>: 396.0091, found: 396.0090.



#### 4-(hydroxymethyl)phenyl(2,4,6-trimethoxyphenyl)iodonium tosylate (**2g**)<sup>172</sup>



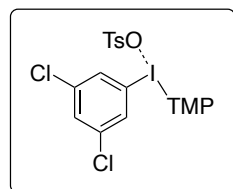
**2g** was prepared according to general procedure A on a 5 mmol scale and obtained as a pink powder (2.26 g, 79 %).

<sup>1</sup>H NMR (600 MHz, DMSO-*d*<sub>6</sub>): δ 7.87 (d, *J* = 8.4 Hz, 2H), 7.47 (d, *J* = 8.1 Hz, 2H), 7.38 (d, *J* = 8.7 Hz, 1H), 7.11 (d, *J* = 7.9 Hz, 2H), 6.45 (s, 2H), 5.70-4.70 (br s, 1H), 4.52 (s, 2H), 3.94 (s, 6H), 3.86 (s, 3H), 2.28 (s, 3H).

<sup>13</sup>C NMR (151 MHz, DMSO-*d*<sub>6</sub>): δ 166.1, 159.3, 146.6, 145.7, 137.6, 134.3, 129.2, 128.0, 125.5, 113.6, 92.0, 87.2, 62.0, 57.3, 56.2, 20.8.

HRMS (ESI) *m/z* [M - OTs]<sup>+</sup>: Calcd. for C<sub>16</sub>H<sub>18</sub>INO<sub>4</sub><sup>+</sup>: 401.0244, found: 401.0244.

#### 3,5-Dichlorophenyl(2,4,6-trimethoxyphenyl)iodonium tosylate (**2h**)<sup>172</sup>



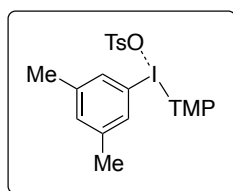
**2h** was prepared according to general procedure A on a 5 mmol scale with the following deviations: (I) The reaction mixture was removed from heat 10 min before stage 2; (II) Stage 2 was ran for 10 min at room temperature. **2h** was obtained as a white powder (2.44 g, 80 %).

<sup>1</sup>H NMR (600 MHz, DMSO-*d*<sub>6</sub>): δ 7.96 (d, *J* = 1.9 Hz, 2H), 7.89 (t, *J* = 1.8 Hz, 1H), 7.46 (d, *J* = 8.0 Hz, 2H), 7.10 (d, *J* = 7.8 Hz, 2H), 6.49 (s, 2H), 3.95 (s, 6H), 3.88 (s, 3H), 2.28 (s, 3H).

<sup>13</sup>C NMR (151 MHz, DMSO-*d*<sub>6</sub>): δ 166.5, 159.4, 145.6, 137.6, 135.6, 132.2, 131.6, 128.0, 125.5, 116.5, 92.2, 87.2, 57.4, 56.2, 20.8.

HRMS (ESI) *m/z* [M - OTs]<sup>+</sup>: Calcd. for C<sub>15</sub>H<sub>14</sub>Cl<sub>2</sub>IO<sub>3</sub><sup>+</sup>: 438.9359, found: 438.9359.

### 3,5-Dimethylphenyl(2,4,6-trimethoxyphenyl)iodonium tosylate (**2i**)<sup>172</sup>



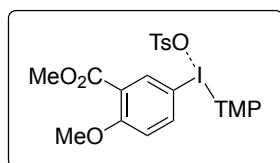
**2i** was prepared according to general procedure A on a 5 mmol scale and obtained as a white powder (2.37 g, 83 %).

<sup>1</sup>H NMR (600 MHz, DMSO-*d*<sub>6</sub>): δ 7.55 – 7.54 (m, 2H), 7.47 (d, *J* = 8.1 Hz, 2H), 7.24 – 7.22 (m, 1H), 7.10 (d, *J* = 7.8 Hz, 1H), 6.46 (s, 2H), 3.95 (s, 6H), 3.87 (s, 3H), 2.28 (s, 3H), 2.27 (s, 6H).

<sup>13</sup>C NMR (151 MHz, DMSO-*d*<sub>6</sub>): δ 166.1, 159.4, 145.8, 141.0, 137.5, 133.0, 131.7, 128.0, 125.5, 115.6, 92.1, 86.8, 57.3, 56.1, 20.7, 20.6.

HRMS (ESI) *m/z* [M - OTs]<sup>+</sup>: Calcd. for C<sub>17</sub>H<sub>20</sub>IO<sub>3</sub><sup>+</sup>: 399.0452, found: 399.0452.

### 4-Methoxy-3-(methoxycarbonyl)phenyl(2,4,6-trimethoxyphenyl)iodonium tosylate (**2j**)<sup>166</sup>



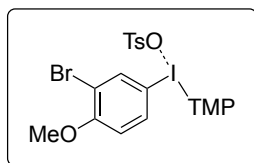
**2j** was prepared according to general procedure B on a 0.55 mmol scale and obtained as a white powder (0.305 g, 44 %).

<sup>1</sup>H NMR (600 MHz, DMSO-*d*<sub>6</sub>): δ 8.17 (d, *J* = 2.4 Hz, 1H), 8.03 (dd, *J* = 9.0, 2.4 Hz, 1H), 7.46 (d, *J* = 8.1 Hz, 2H), 7.22 (d, *J* = 9.1 Hz, 1H), 7.10 (d, *J* = 7.8 Hz, 2H), 6.46 (s, 2H), 3.95 (s, 6H), 3.86 (s, 3H), 3.85 (s, 3H), 3.81 (s, 3H), 2.28 (s, 3H).

<sup>13</sup>C NMR (151 MHz, DMSO-*d*<sub>6</sub>): δ 166.1, 164.3, 160.2, 159.2, 145.8, 137.5, 136.9, 128.0, 125.5, 122.3, 115.8, 104.5, 92.1, 87.6, 57.3, 56.4, 56.2, 52.5, 20.8.

HRMS (ESI) *m/z* [M - OTs]<sup>+</sup>: Calcd. for C<sub>18</sub>H<sub>20</sub>IO<sub>6</sub><sup>+</sup>: 459.0299, found: 459.0299.

### 3-Bromo-4-methoxyphenyl(2,4,6-trimethoxyphenyl)iodonium tosylate (2jk)<sup>166</sup>



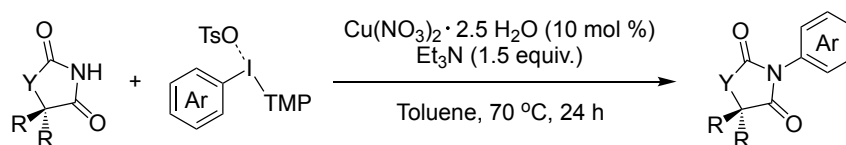
**2k** was prepared according to general procedure B on a 0.55 mmol scale and obtained as a white powder (0.107 g, 15 %).

<sup>1</sup>H NMR (600 MHz, DMSO-*d*<sub>6</sub>): 8.11 (d, *J* = 2.3 Hz, 1H), 7.87 (dd, *J* = 8.9, 2.2 Hz, 1H), 7.47 (d, *J* = 8.1 Hz, 2H), 7.17 (d, *J* = 9.0 Hz, 1H), 7.10 (d, *J* = 7.8 Hz, 2H), 6.46 (s, 2H), 3.95 (s, 6H), 3.86 (d, *J* = 1.9 Hz, 6H), 2.28 (s, 3H).

<sup>13</sup>C NMR (151 MHz, DMSO-*d*<sub>6</sub>): 166.2, 159.3, 158.0, 145.7, 138.0, 137.7, 135.8, 128.1, 125.5, 115.4, 112.3, 105.2, 92.1, 87.7, 57.3, 56.8, 56.2, 20.8.

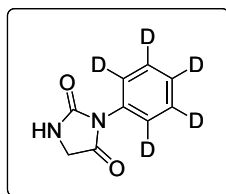
HRMS (ESI) *m/z* [M - OTs]<sup>+</sup>: Calcd. for C<sub>16</sub>H<sub>17</sub>BrIO<sub>4</sub><sup>+</sup>: 478.9349, found: 478.9348.

### Synthesis and characterization of arylhydantoin



Hydantoin (0.2 mmol, 1.0 equiv.), aryl(TMP)iodonium tosylate (0.6 mmol, 3.0 equiv.) and Cu(NO<sub>3</sub>)<sub>2</sub> · 2.5 H<sub>2</sub>O (4.7 mg, 0.020 mmol, 0.10 equiv.) were added to a 7 mL screw cap vial equipped with a magnetic stir bar. Toluene (2 mL) was added and the vial was placed in a pre-heated vial insert heating block set to 70 °C. Triethylamine (42 μL, 0.30 mmol, 1.5 equiv.) was added via a syringe, and the suspension was stirred for 24 hours at 70 °C. The resulting mixture (typically colored orange, brown or black) was allowed to cool to room temperature before it was concentrated under reduced pressure. The crude mixture was purified by column chromatography using silica gel and eluent system as specified. The desired product was dried under high vacuum for several hours.

### 3-Phenyl-*d*<sub>5</sub>-hydantoin (**3a-d<sub>5</sub>**)



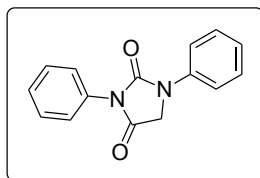
**3a-d<sub>5</sub>** was prepared according to the general procedure. The crude reaction mixture was purified by column chromatography using gradient elution (hexane:acetone [9:1 → 8:2 → 7:3]) to afford **3a-d<sub>5</sub>** as a colorless solid (15.9 mg, 44 %).

<sup>1</sup>H NMR (600 MHz, CD<sub>3</sub>CN): δ 6.23 (br s, 1H), 3.99 (d, *J* = 1.3 Hz, 2H).

<sup>13</sup>C NMR (151 MHz, CD<sub>3</sub>CN): δ 172.0, 158.0, 133.3, 129.4 (t, *J*<sub>C-D</sub> = 24.7 Hz), 128.5 (t, *J*<sub>C-D</sub> = 24.6 Hz), 127.4 (t, *J*<sub>C-D</sub> = 25.0 Hz), 47.2.

HRMS (ESI) *m/z* [M + Na]<sup>+</sup>: Calcd. for C<sub>9</sub>H<sub>3</sub>D<sub>5</sub>N<sub>2</sub>NaO<sub>2</sub><sup>+</sup>: 204.0792, found: 204.0792.

### 1,3-Diphenylhydantoin (**3c**)<sup>218</sup>



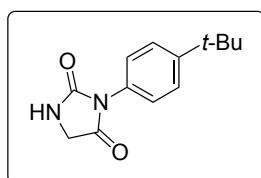
**3c** was prepared according to the general procedure starting from 3-phenylhydantoin **3a**. The crude reaction mixture was purified by column chromatography (pentane:EtOAc [4:1]) to afford **3c** as a colorless solid (26.2 mg, 52 %).

<sup>1</sup>H NMR (600 MHz, CDCl<sub>3</sub>): δ 7.65 – 7.61 (m, 2H), 7.52 – 7.49 (m, 2H), 7.47 – 7.45 (m, 2H), 7.44 – 7.40 (m, 3H), 7.20 (tt, *J* = 7.4, 1.1 Hz, 1H), 4.47 (s, 2H).

<sup>13</sup>C NMR (151 MHz, CDCl<sub>3</sub>): δ 167.3, 153.2, 137.4, 131.3, 129.4, 129.2, 128.5, 126.3, 124.7, 118.6, 49.8.

HRMS (ESI) *m/z* [M + Na]<sup>+</sup>: Calcd. for C<sub>15</sub>H<sub>12</sub>N<sub>2</sub>NaO<sub>2</sub><sup>+</sup>: 275.0791, found: 275.0790.

### 3-(4-*tert*-butylphenyl)hydantoin (**3e**)



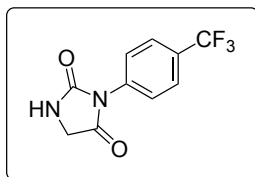
**3e** was prepared according to the general procedure. The crude reaction mixture was purified by column chromatography using gradient elution (hexane:acetone [9:1 → 4:1]) to afford **3e** as a colorless solid (30.9 mg, 66 %).

<sup>1</sup>H NMR (600 MHz, CDCl<sub>3</sub>): δ 7.48 (dt, *J* = 8.7, 2.6 Hz, 2H), 7.28 (dt, *J* = 8.6, 2.6 Hz, 2H), 6.92 (br s, 1H), 4.06 (d, *J* = 1.2 Hz, 2H), 1.31 (s, 9H).

<sup>13</sup>C NMR (151 MHz, CDCl<sub>3</sub>): δ 170.4, 158.0, 151.5, 128.5, 126.3, 125.7, 46.5, 34.7, 31.2.

HRMS (ESI) *m/z* [M + Na]<sup>+</sup>: Calcd. for C<sub>13</sub>H<sub>16</sub>N<sub>2</sub>NaO<sub>2</sub><sup>+</sup>: 255.1104, found: 255.1103.

### 3-(4-trifluoromethylphenyl)hydantoin (**3i**)<sup>45, 219</sup>



**3i** was prepared according to the general procedure. The crude reaction mixture was purified by column chromatography using gradient elution (hexane:chloroform:acetone [9:9:1 → 3:3:1]) to afford **3i** as a colorless solid (22.8 mg, 46 %).

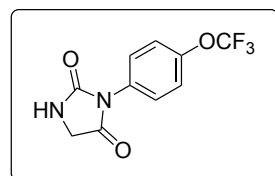
<sup>1</sup>H NMR (600 MHz, CDCl<sub>3</sub>): δ 7.75 (d, *J* = 8.4 Hz, 2H), 7.61 (d, *J* = 8.3 Hz, 2H), 6.80 (br s, 1H), 4.15 (d, *J* = 1.2 Hz, 2H).

<sup>13</sup>C NMR (151 MHz, CDCl<sub>3</sub>): δ 169.6, 156.9, 134.5, 130.2 (q, *J*<sub>C-F</sub> = 32.9 Hz), 126.2 (q, *J*<sub>C-F</sub> = 3.8 Hz), 126.0, 123.5 (d, *J*<sub>C-F</sub> = 272.5 Hz), 46.4.

<sup>19</sup>F NMR (376 MHz, CDCl<sub>3</sub>): δ -62.7.

HRMS (ESI) *m/z* [M + Na]<sup>+</sup>: Calcd. for C<sub>10</sub>H<sub>7</sub>F<sub>3</sub>N<sub>2</sub>NaO<sub>2</sub><sup>+</sup>: 267.0352, found: 267.0351.

### 3-(4-trifluoromethoxyphenyl)hydantoin (**3j**)<sup>220</sup>



**3j** was prepared according to the general procedure. The crude reaction mixture was purified by column chromatography using gradient elution (hexane:acetone [9:1 → 7:3]) to afford **3j** as a colorless solid (24.7 mg, 47 %).

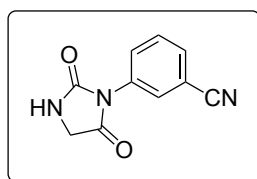
<sup>1</sup>H NMR (600 MHz, CDCl<sub>3</sub>): δ 7.46 (d, *J* = 9.0 Hz, 2H), 7.31 (d, *J* = 8.0 Hz, 2H), 6.73 (br s, 1H), 4.11 (d, *J* = 1.1 Hz, 2H).

<sup>13</sup>C NMR (151 MHz, CDCl<sub>3</sub>): δ 169.8, 157.2, 148.5 (q, *J*<sub>C-F</sub> = 2.0 Hz), 129.7, 127.5, 121.7, 120.34 (d, *J*<sub>C-F</sub> = 257.9 Hz), 46.4.

<sup>19</sup>F NMR (376 MHz, CDCl<sub>3</sub>): δ -57.9.

HRMS (ESI) *m/z* [M + Na]<sup>+</sup>: Calcd. for C<sub>10</sub>H<sub>7</sub>F<sub>3</sub>N<sub>2</sub>NaO<sub>3</sub><sup>+</sup>: 283.0301, found: 283.0301.

### 3-(3-cyanophenyl)hydantoin (**3p**)



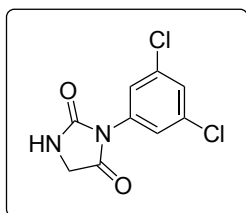
**3p** was prepared according to the general procedure. The crude reaction mixture was purified by column chromatography using gradient elution (hexane:acetone [9:1 → 7:3]) to afford **3p** as a colorless solid (21.8 mg, 55 %).

$^1\text{H}$  NMR (600 MHz,  $\text{CD}_3\text{CN}$ ):  $\delta$  7.78 (t,  $J = 1.9$  Hz, 1H), 7.75 – 7.71 (m, 2H), 7.64 (t,  $J = 7.9$  Hz, 1H), 6.35 (br s, 1H), 4.02 (d,  $J = 1.3$  Hz, 2H).

$^{13}\text{C}$  NMR (150 MHz,  $\text{CD}_3\text{CN}$ ):  $\delta$  171.5, 157.1, 134.3, 132.4, 131.9, 131.0, 130.6, 118.9, 113.6, 47.2.

HRMS (ESI)  $m/z$   $[\text{M} + \text{Na}]^+$ : Calcd. for  $\text{C}_{10}\text{H}_7\text{N}_3\text{NaO}_2^+$ : 224.0430, found: 224.0430.

### 3-(3,5-Dichlorophenyl)hydantoin (**3v**)<sup>221, 222</sup>



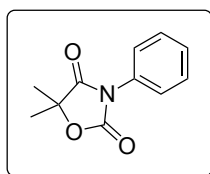
**3v** was prepared according to the general procedure. The crude reaction mixture was purified by column chromatography using gradient elution (hexane:chloroform:acetone [9:9:1 → 3:3:1]) to afford **3v** as a colorless solid (16.5 mg, 34 %).

$^1\text{H}$  NMR (600 MHz,  $\text{CDCl}_3$ ):  $\delta$  7.43 (d,  $J = 1.9$  Hz, 2H), 7.38 (t,  $J = 1.9$  Hz, 1H), 6.36 (br s, 1H), 4.14 (d,  $J = 1.1$  Hz, 2H).

$^{13}\text{C}$  NMR (150 MHz,  $\text{CDCl}_3$ ):  $\delta$  169.1, 156.2, 135.3, 133.1, 128.4, 124.3, 46.3.

HRMS (ESI)  $m/z$   $[\text{M} + \text{Na}]^+$ : Calcd. for  $\text{C}_9\text{H}_6\text{Cl}_2\text{N}_3\text{NaO}_2^+$ : 266.9699, found: 266.9698.

### 5,5-Dimethyl-3-phenyl-2,4-oxazolidinedione (**6c**)<sup>223</sup>



**6c** was prepared according to the general procedure starting from 5,5-dimethyl-2,4-oxazolidinedione. The crude reaction mixture was purified by column chromatography (hexane:chloroform [7:3]), followed by hot recrystallization from MeOH (0.5 mL) to afford **6c** as a colorless solid (24.9 mg, 61 %).

$^1\text{H}$  NMR (600 MHz,  $\text{CDCl}_3$ ):  $\delta$  7.51 – 7.48 (m, 2H), 7.45 – 7.40 (m, 3H), 1.69 (s, 6H).

$^{13}\text{C}$  NMR (150 MHz,  $\text{CDCl}_3$ ):  $\delta$  174.9, 153.3, 130.9, 129.3, 128.8, 125.5, 83.4, 23.8.

HRMS (ESI)  $m/z$   $[\text{M} + \text{Na}]^+$ : Calcd. for  $\text{C}_{11}\text{H}_{11}\text{NNaO}_3^+$ : 228.0631, found: 228.0631.

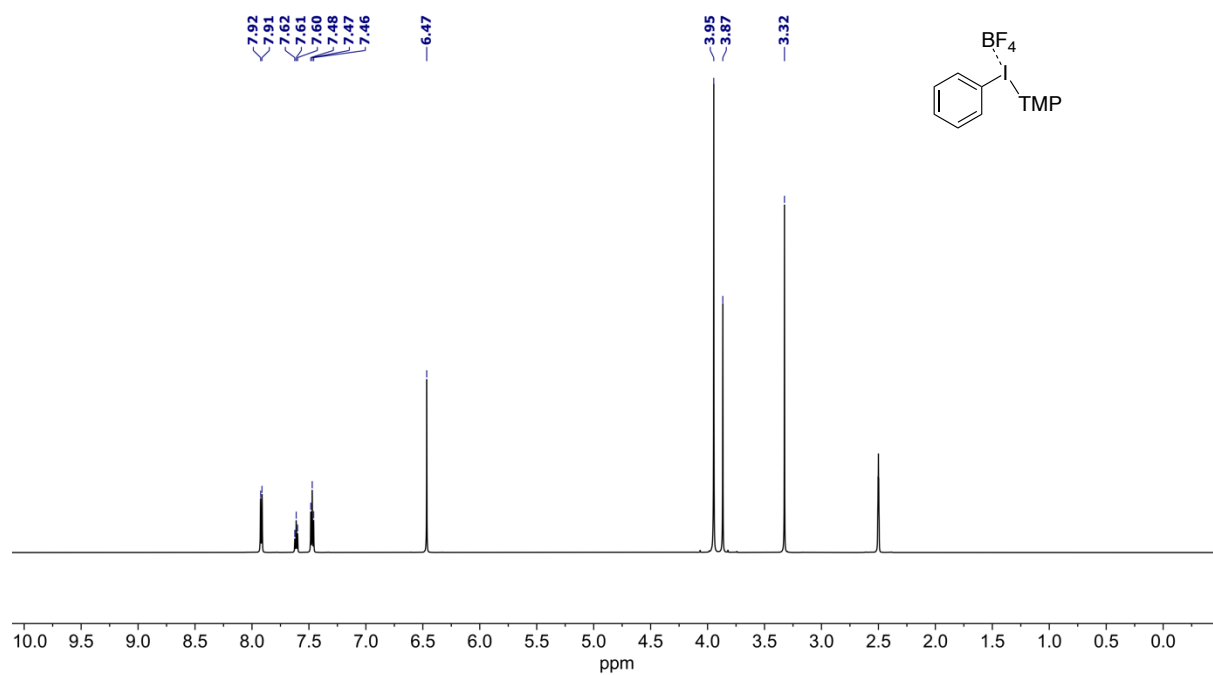


**Figure 2.8.**  $^1\text{H}$  NMR (600 MHz,  $\text{DMSO-}d_6$ ) spectrum of **2a-BF<sub>4</sub>**.

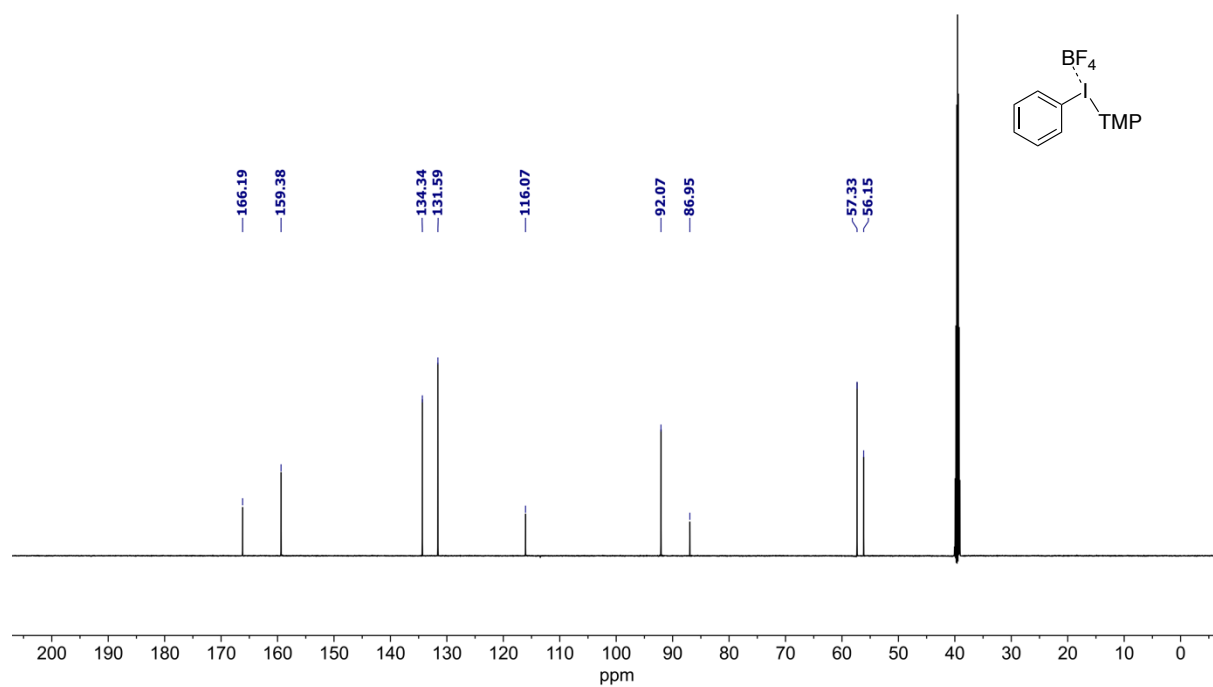


**Figure 2.9.**  $^{13}\text{C}$  NMR (151 MHz,  $\text{DMSO-}d_6$ ) spectrum of **2a-BF<sub>4</sub>**.

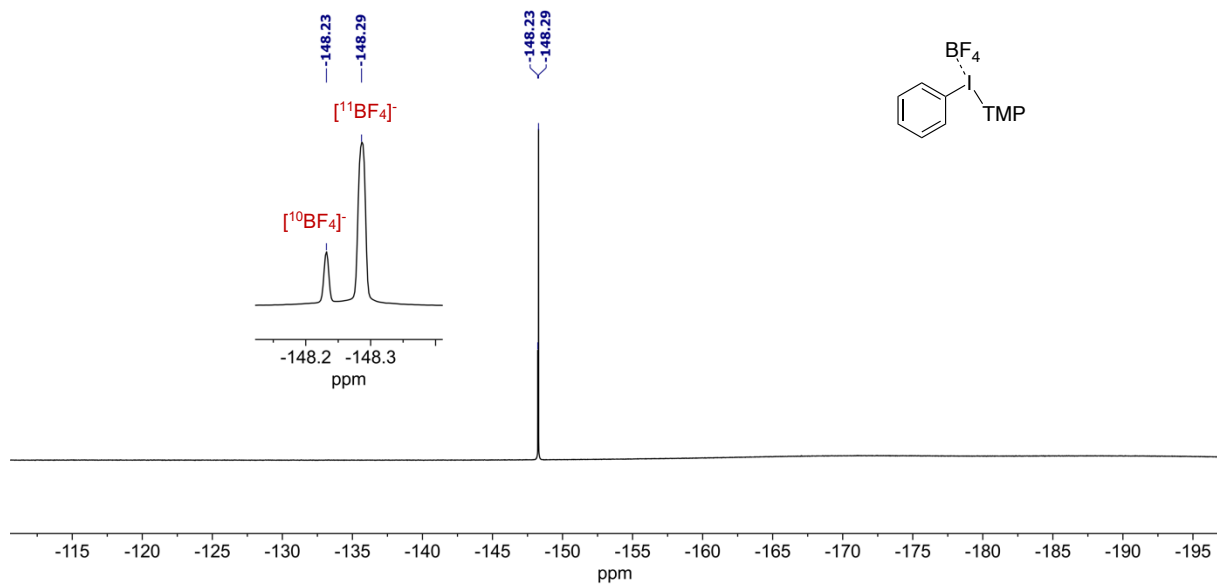


**Figure 2.10.**  $^{19}\text{F}$  NMR (376 MHz,  $\text{DMSO-}d_6$ ) spectrum of **2a-BF<sub>4</sub>**.

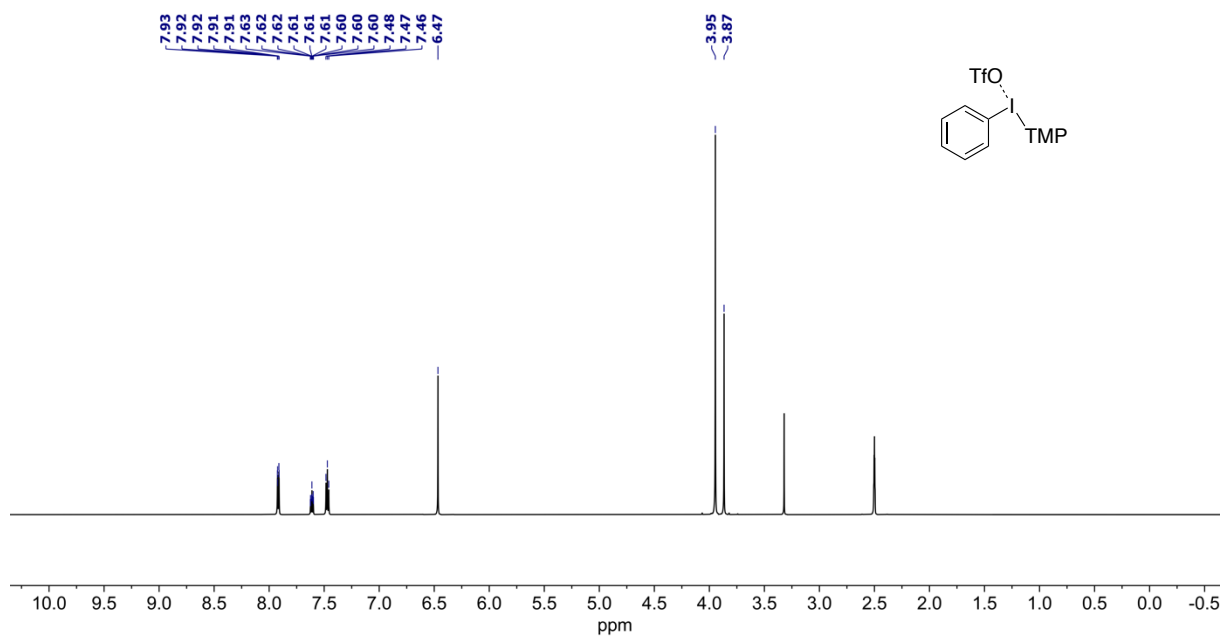


**Figure 2.11.**  $^1\text{H}$  NMR (600 MHz,  $\text{DMSO-}d_6$ ) spectrum of **2a-OTf**.



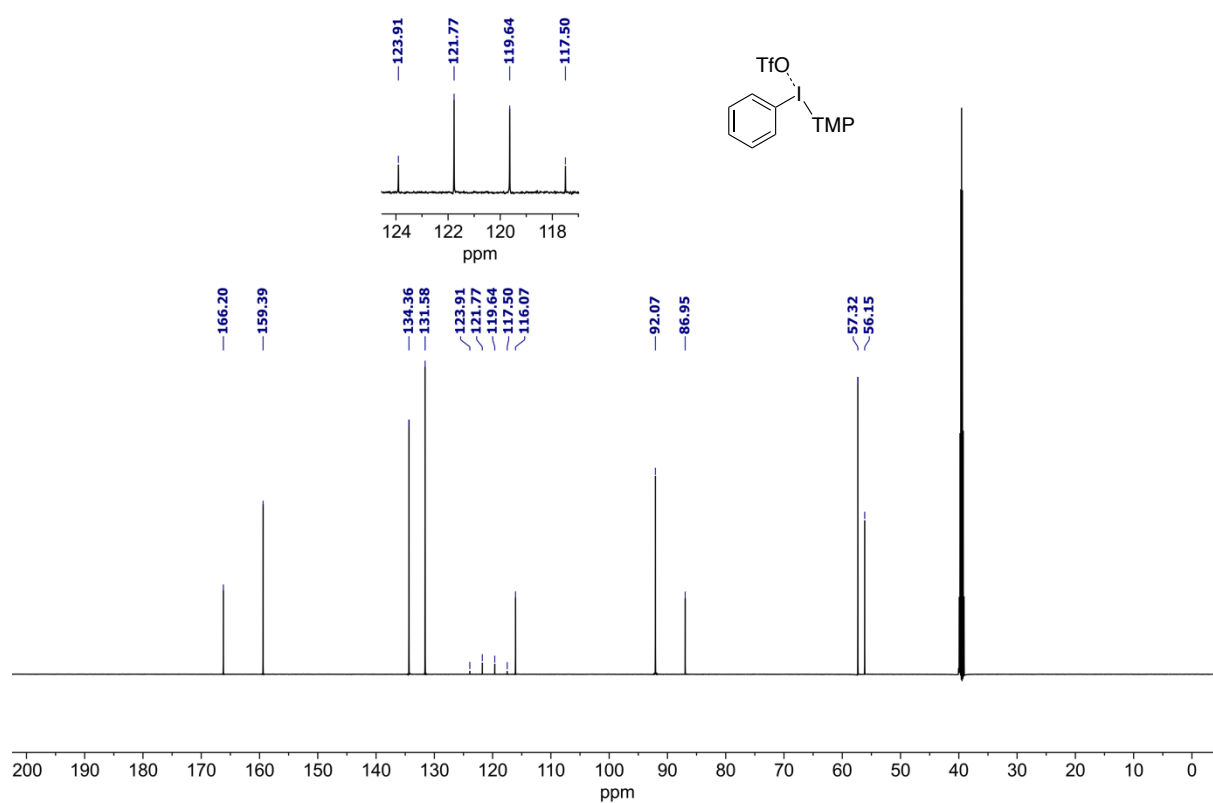


**Figure 2.12.**  $^{13}\text{C}$  NMR (151 MHz,  $\text{DMSO-}d_6$ ) spectrum of **2a-OTf**.

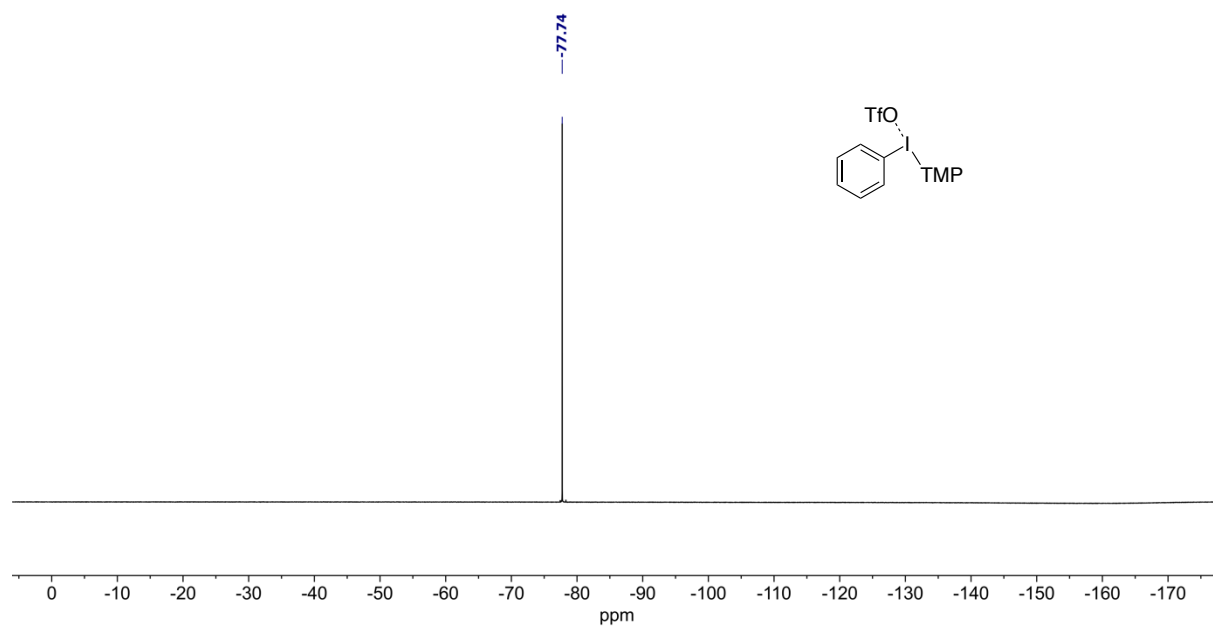


**Figure 2.13.**  $^{19}\text{F}$  NMR (376 MHz,  $\text{DMSO-}d_6$ ) spectrum of **2a-OTf**.

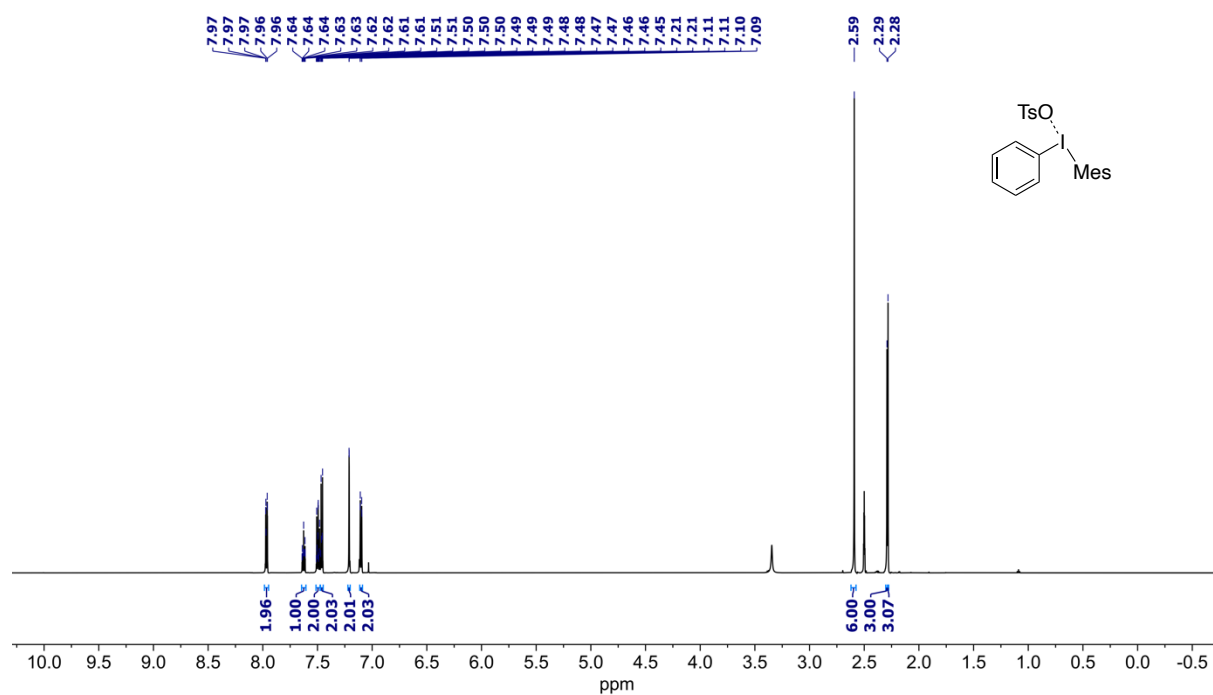


Figure 2.14. <sup>1</sup>H NMR (600 MHz, DMSO-*d*<sub>6</sub>) spectrum of **2a-Mes**.

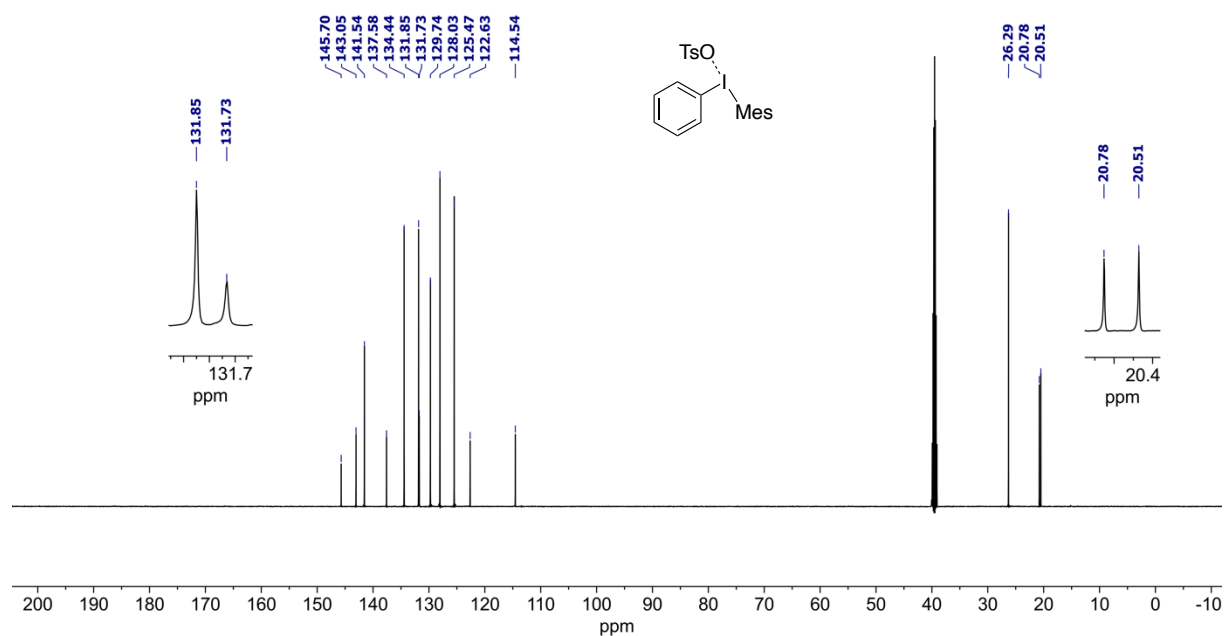


Figure 2.15. <sup>13</sup>C NMR (151 MHz, DMSO-*d*<sub>6</sub>) spectrum of **2a-Mes**.

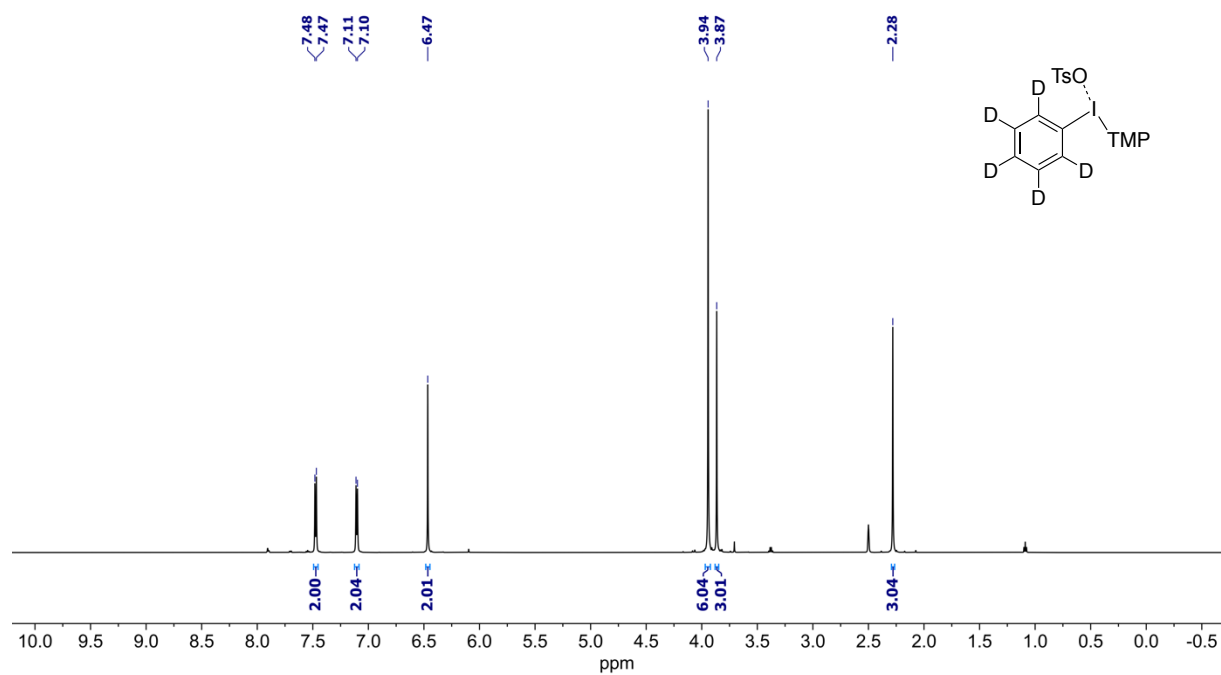


Figure 2.16.  $^1\text{H}$  NMR (600 MHz,  $\text{DMSO-}d_6$ ) spectrum of **2b**.

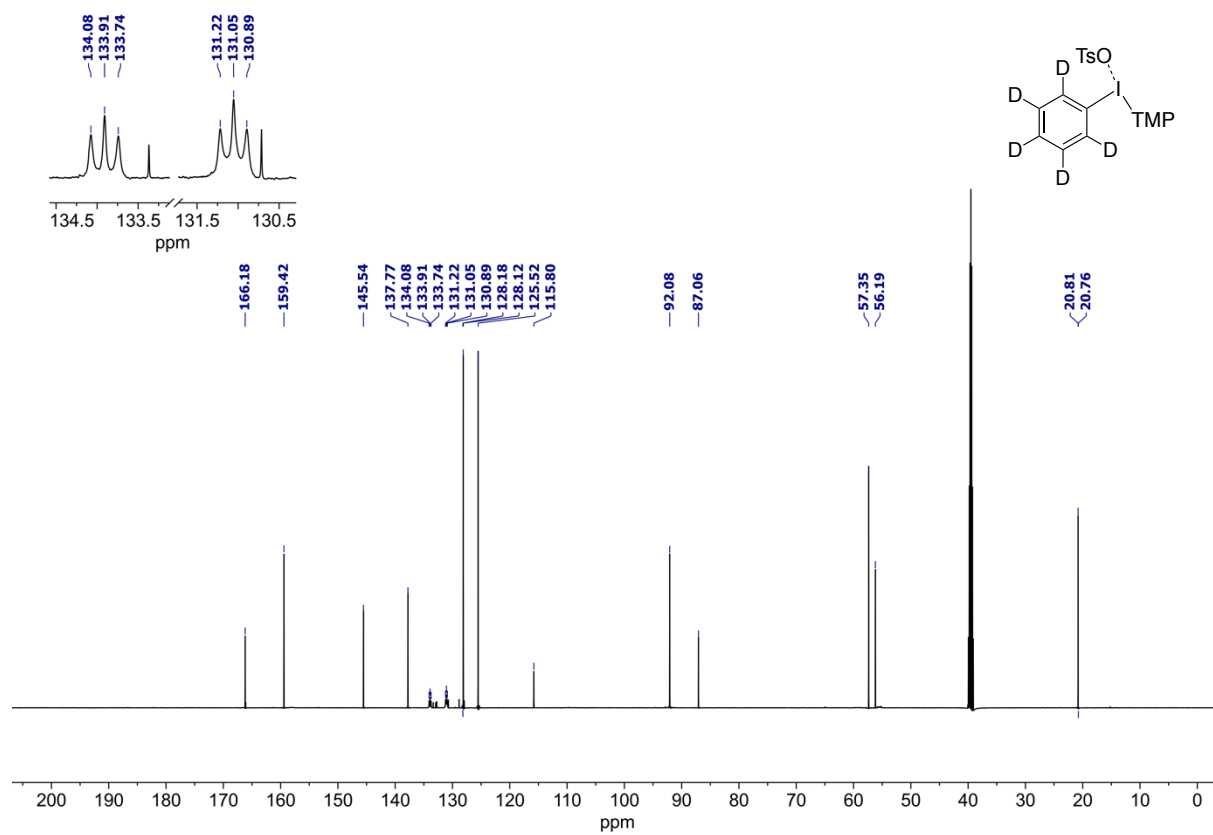
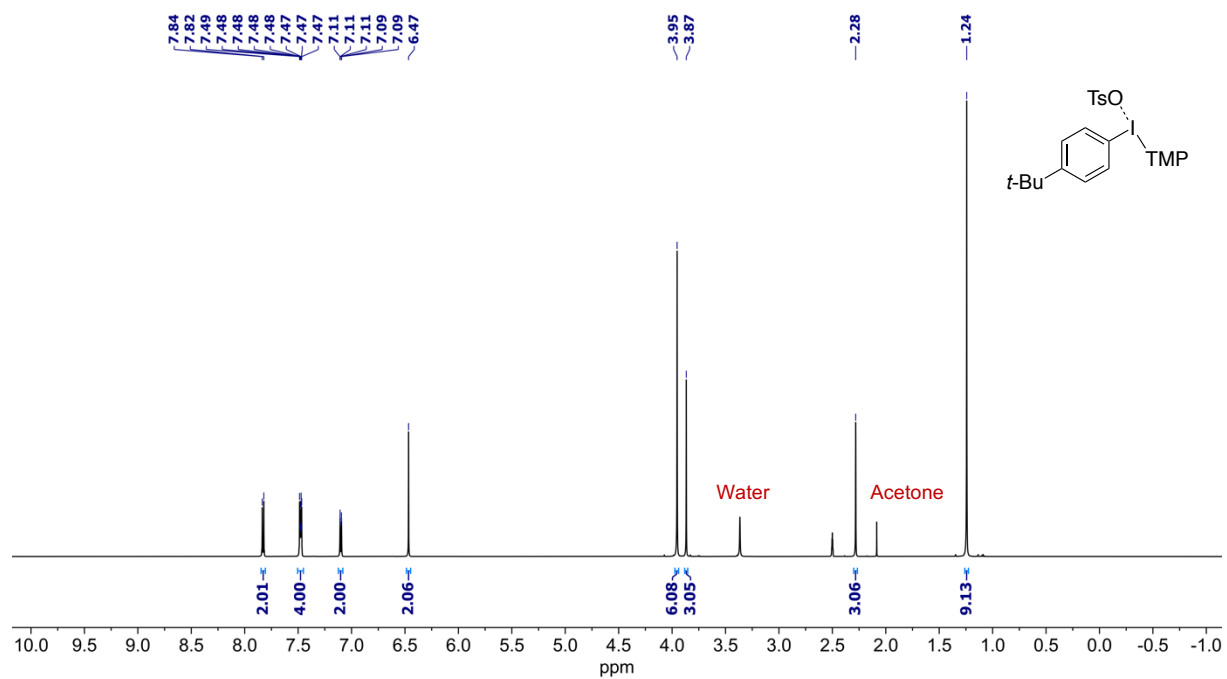
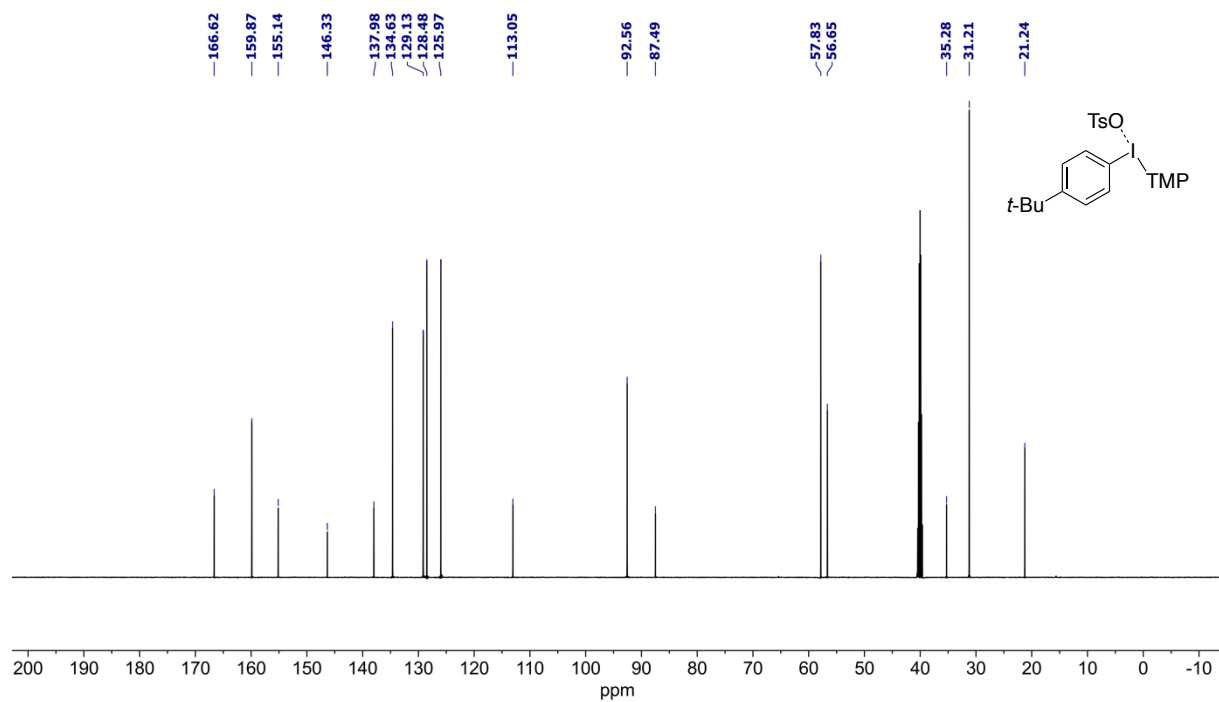


Figure 2.17.  $^{13}\text{C}$  NMR (151 MHz,  $\text{DMSO-}d_6$ ) spectrum of **2b**.



**Figure 2.18.** <sup>1</sup>H NMR (600 MHz, DMSO-*d*<sub>6</sub>) spectrum of **2c**.



**Figure 2.19.** <sup>13</sup>C NMR (151 MHz, DMSO-*d*<sub>6</sub>) spectrum of **2c**.

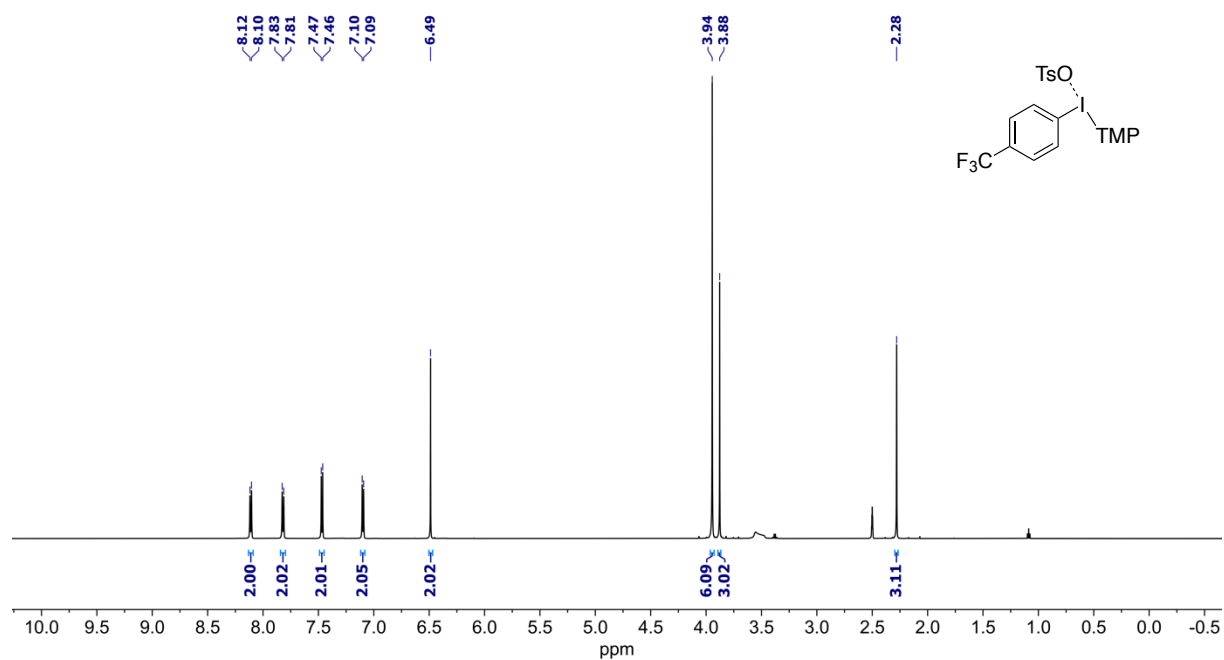


Figure 2.20.  $^1\text{H}$  NMR (600 MHz,  $\text{DMSO-}d_6$ ) spectrum of **2d**.

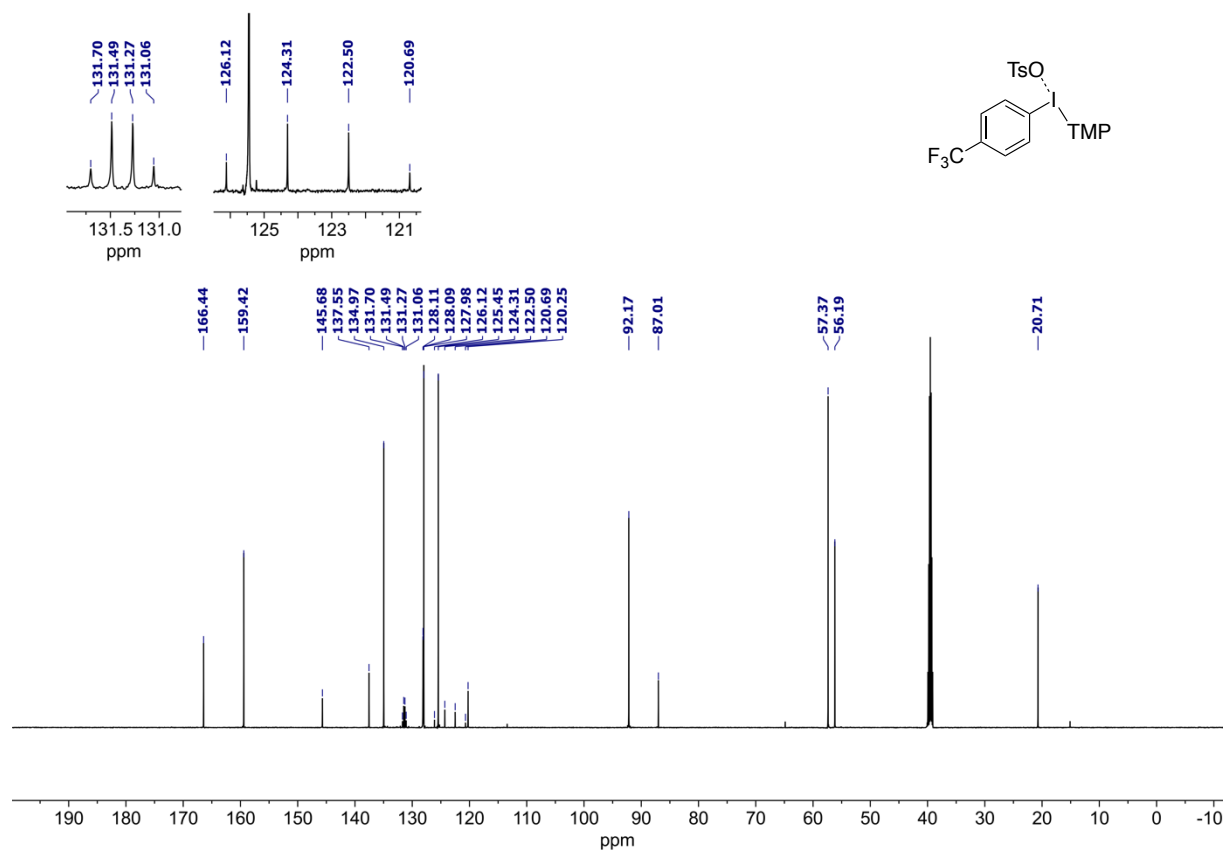
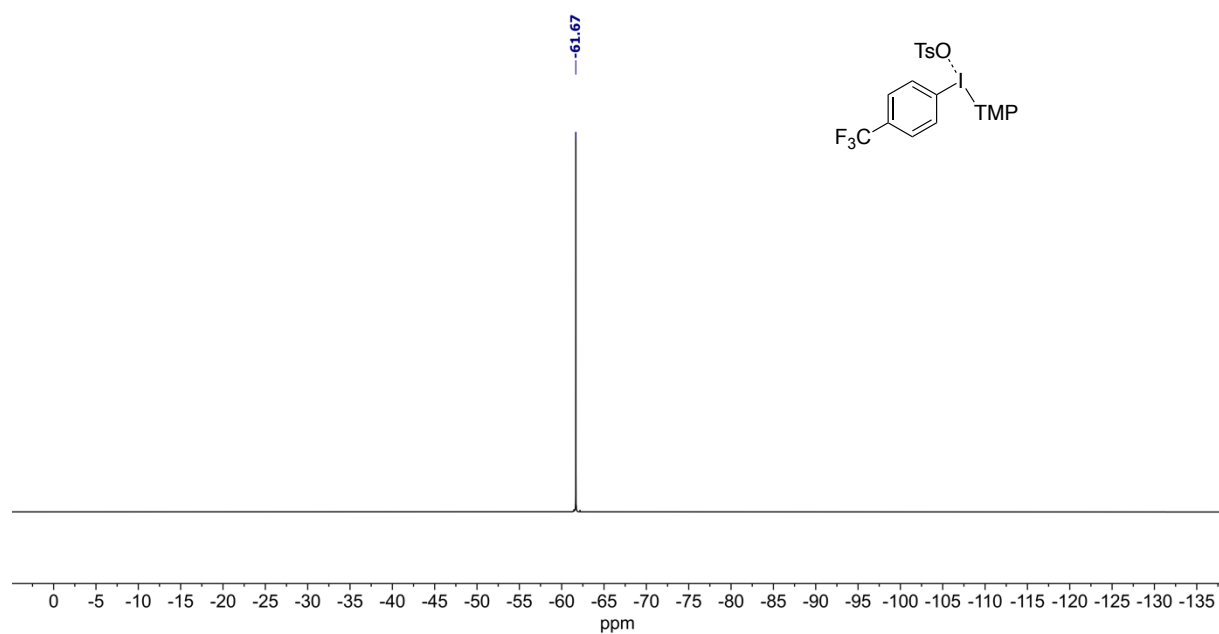
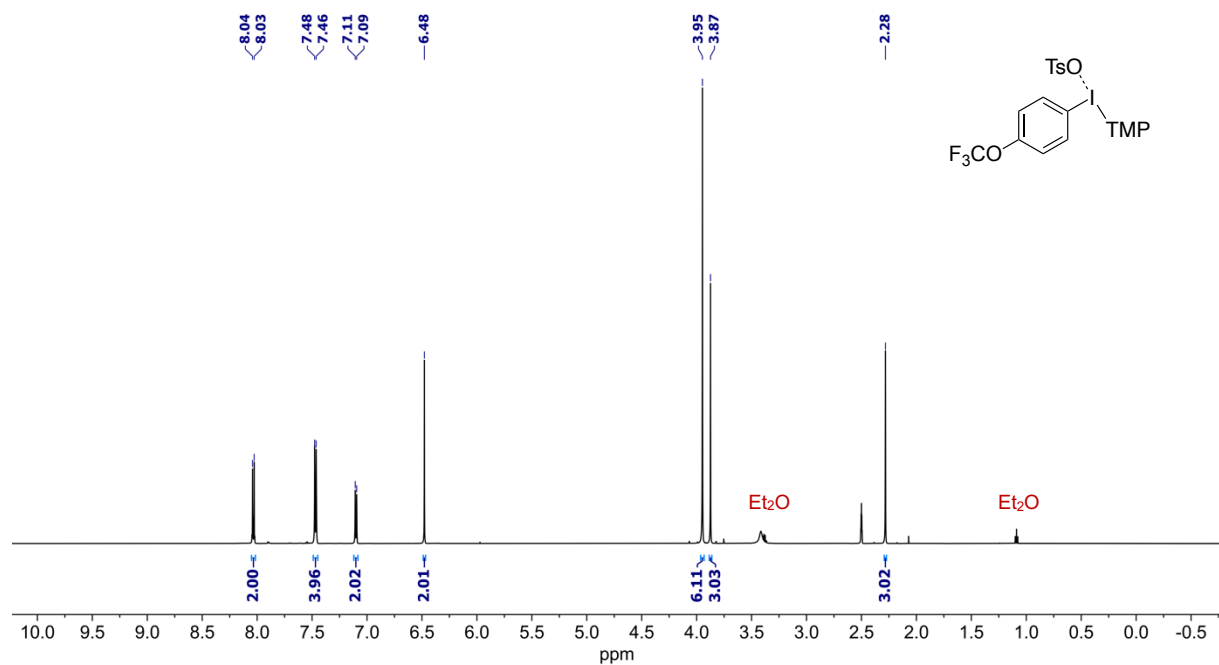


Figure 2.21.  $^{13}\text{C}$  NMR (151 MHz,  $\text{DMSO-}d_6$ ) spectrum of **2d**.



**Figure 2.22.**  $^{19}\text{F}$  NMR (376 MHz,  $\text{DMSO-}d_6$ ) spectrum of **2d**.



**Figure 2.23.**  $^1\text{H}$  NMR (600 MHz,  $\text{DMSO-}d_6$ ) spectrum of **2e**.

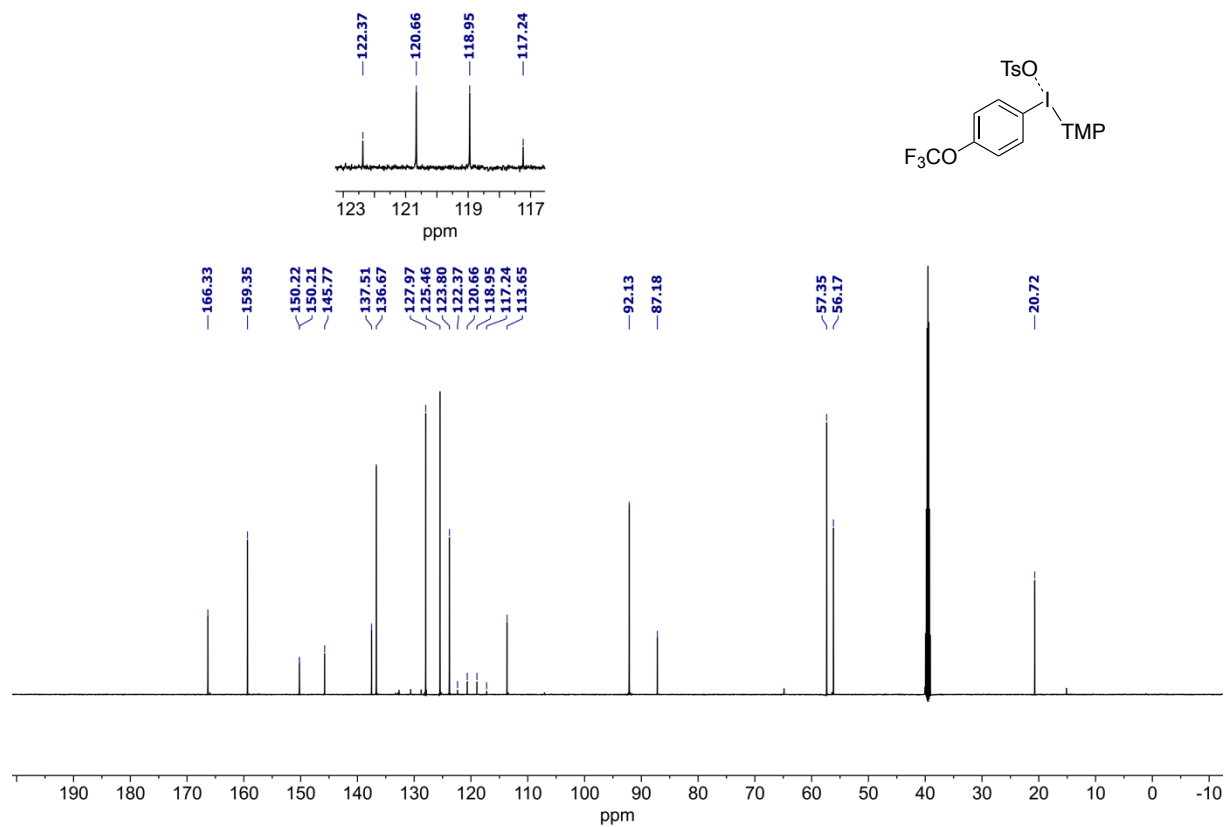


**Figure 2.24.**  $^{13}\text{C}$  NMR (151 MHz,  $\text{DMSO-}d_6$ ) spectrum of **2e**.

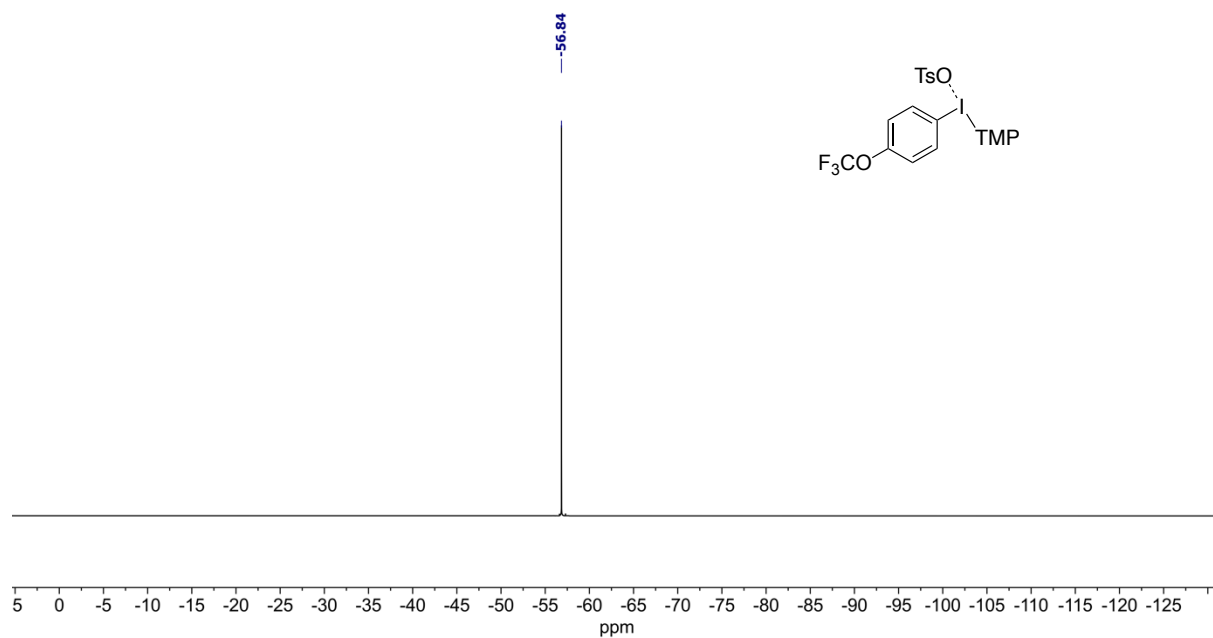


**Figure 2.25.**  $^{19}\text{F}$  NMR (376 MHz,  $\text{DMSO-}d_6$ ) spectrum of **2e**.

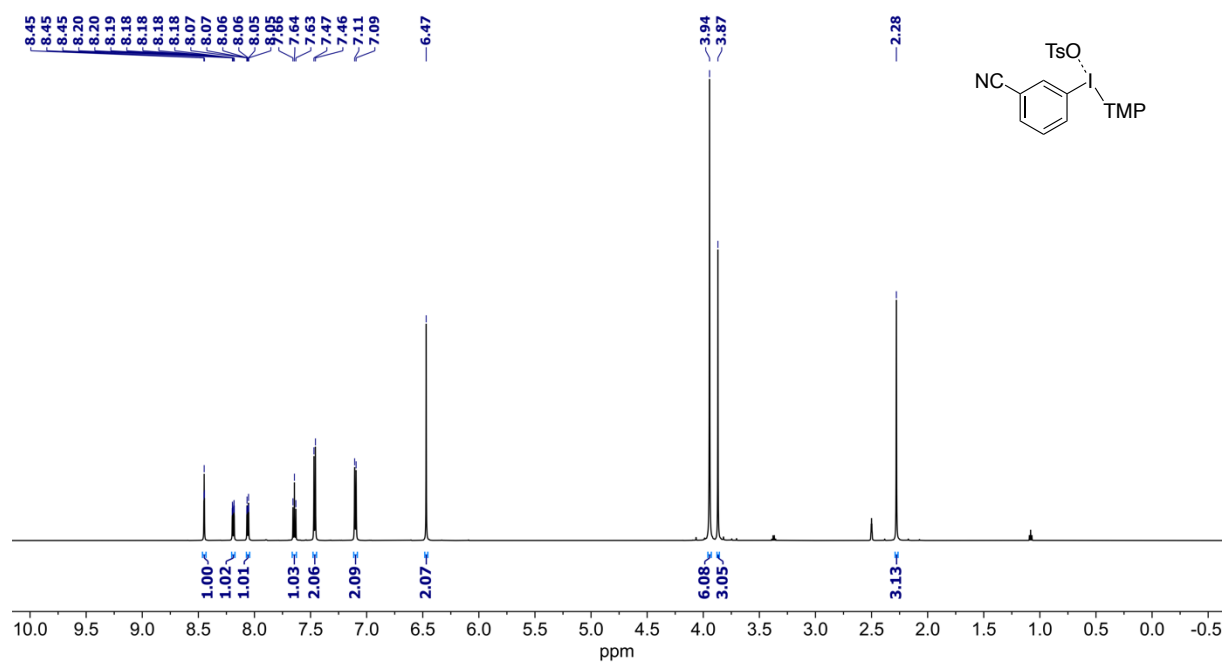


Figure 2.26. <sup>1</sup>H NMR (600 MHz, DMSO-*d*<sub>6</sub>) spectrum of **2f**.

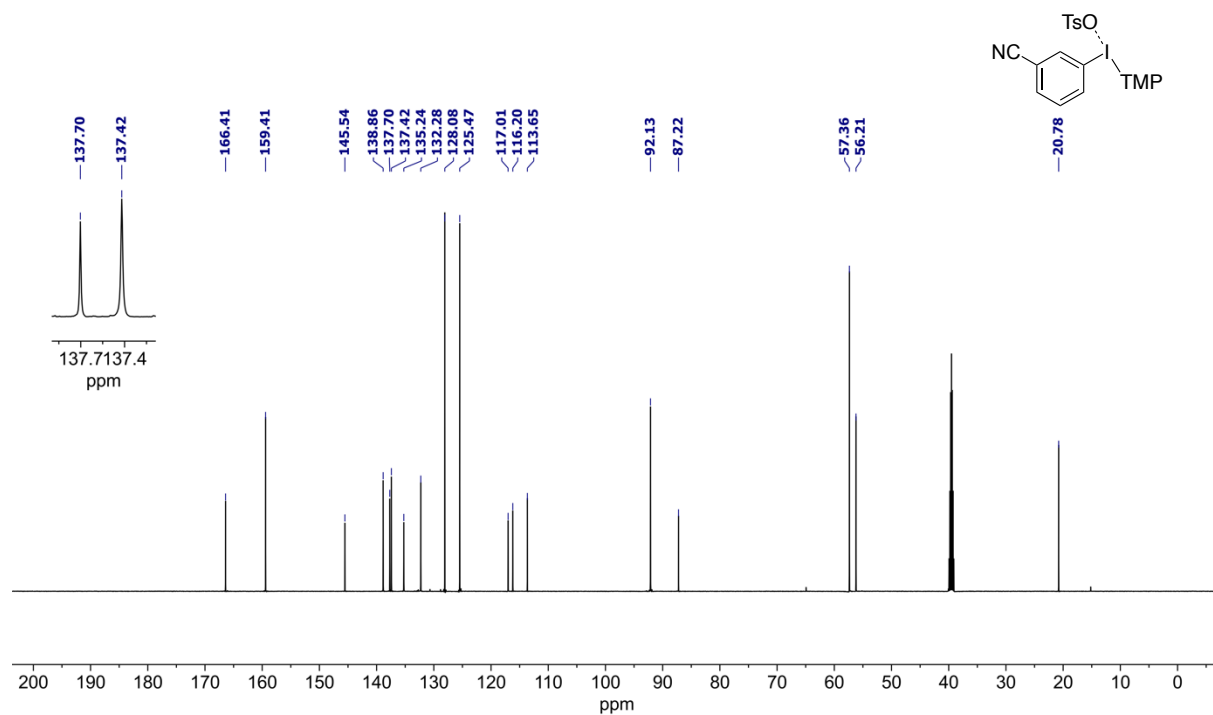


Figure 2.27. <sup>13</sup>C NMR (151 MHz, DMSO-*d*<sub>6</sub>) spectrum of **2f**.



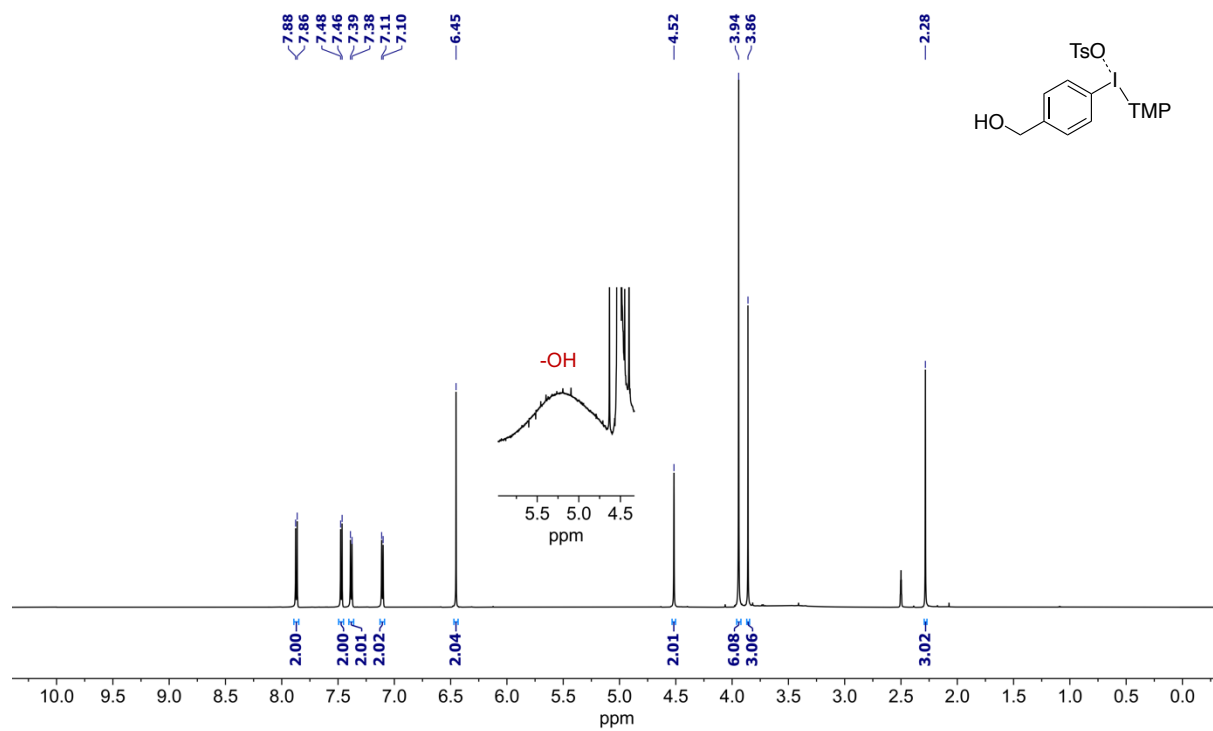


Figure 2.28.  $^1\text{H}$  NMR (600 MHz,  $\text{DMSO-}d_6$ ) spectrum of **2g**.

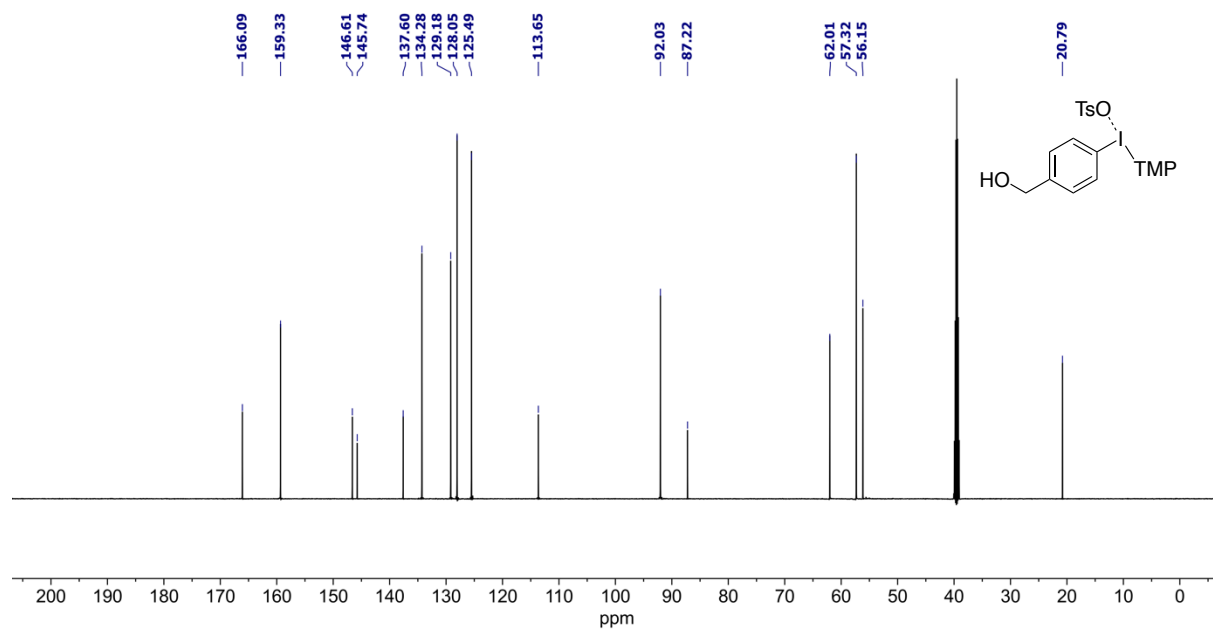


Figure 2.29.  $^{13}\text{C}$  NMR (151 MHz,  $\text{DMSO-}d_6$ ) spectrum of **2g**.

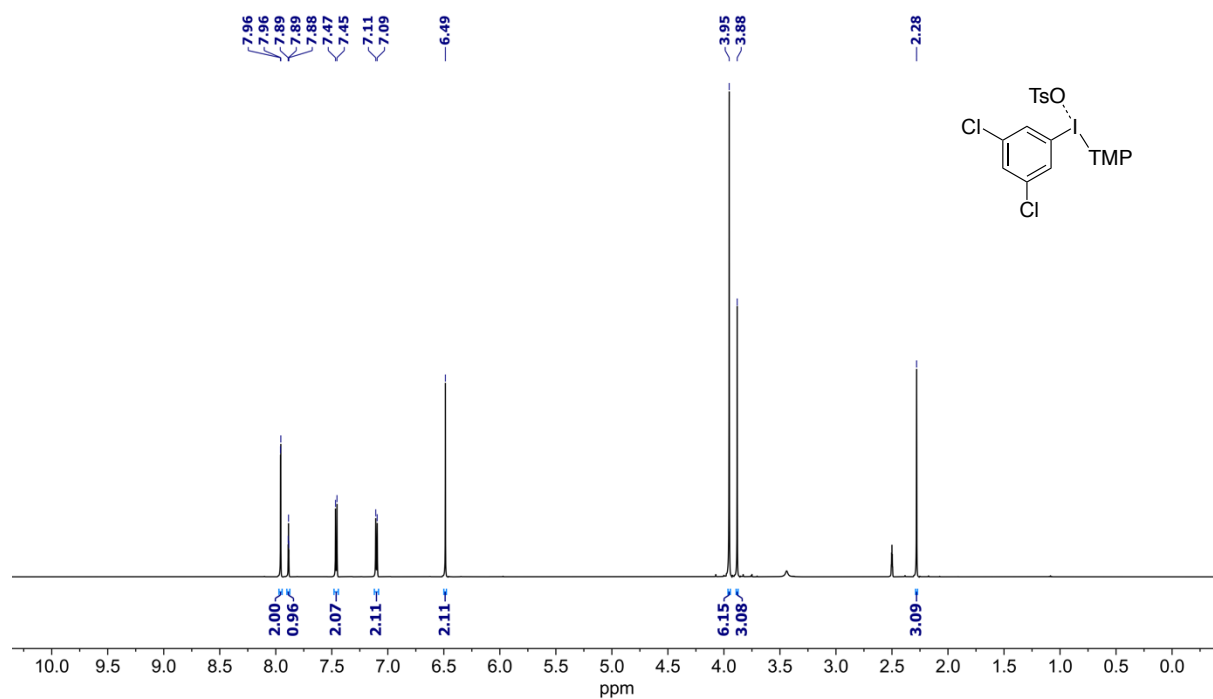


Figure 2.30.  $^1\text{H}$  NMR (600 MHz,  $\text{DMSO-}d_6$ ) spectrum of **2h**.

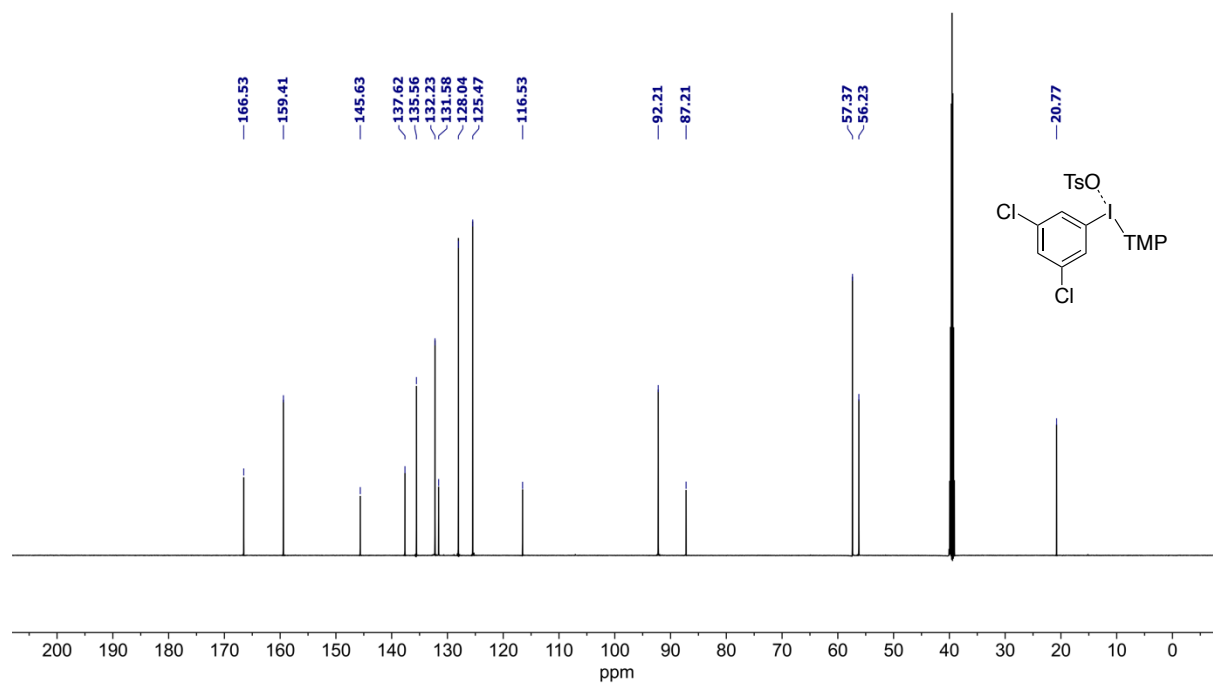
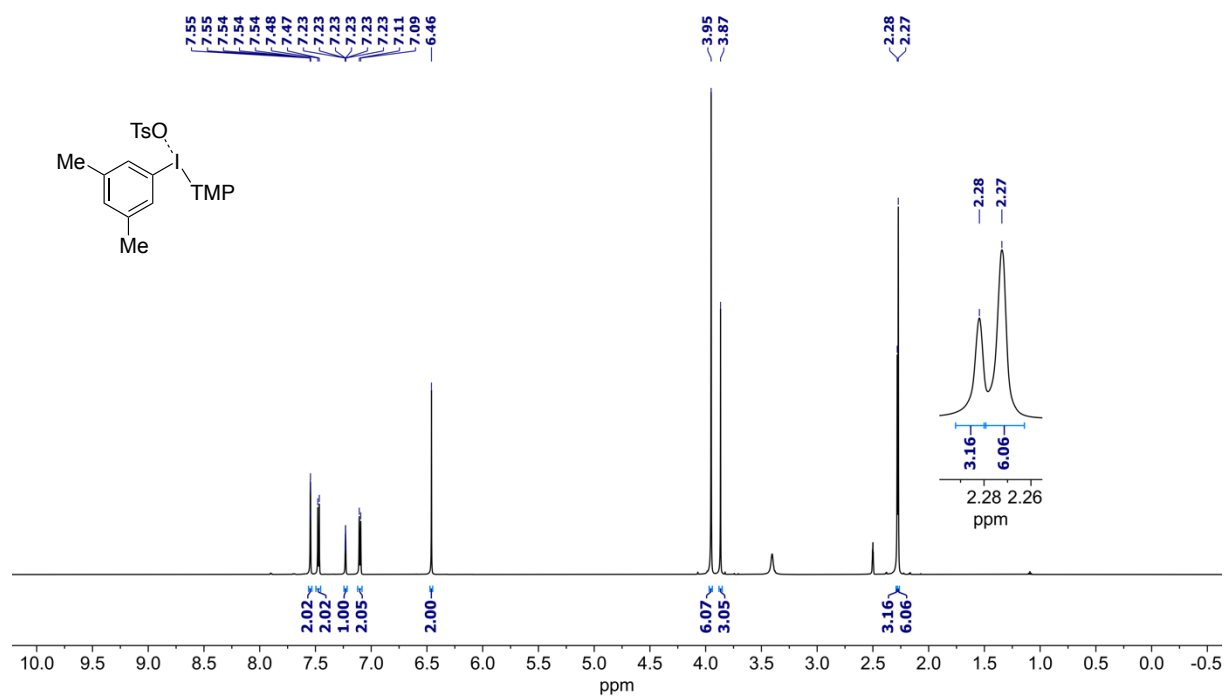
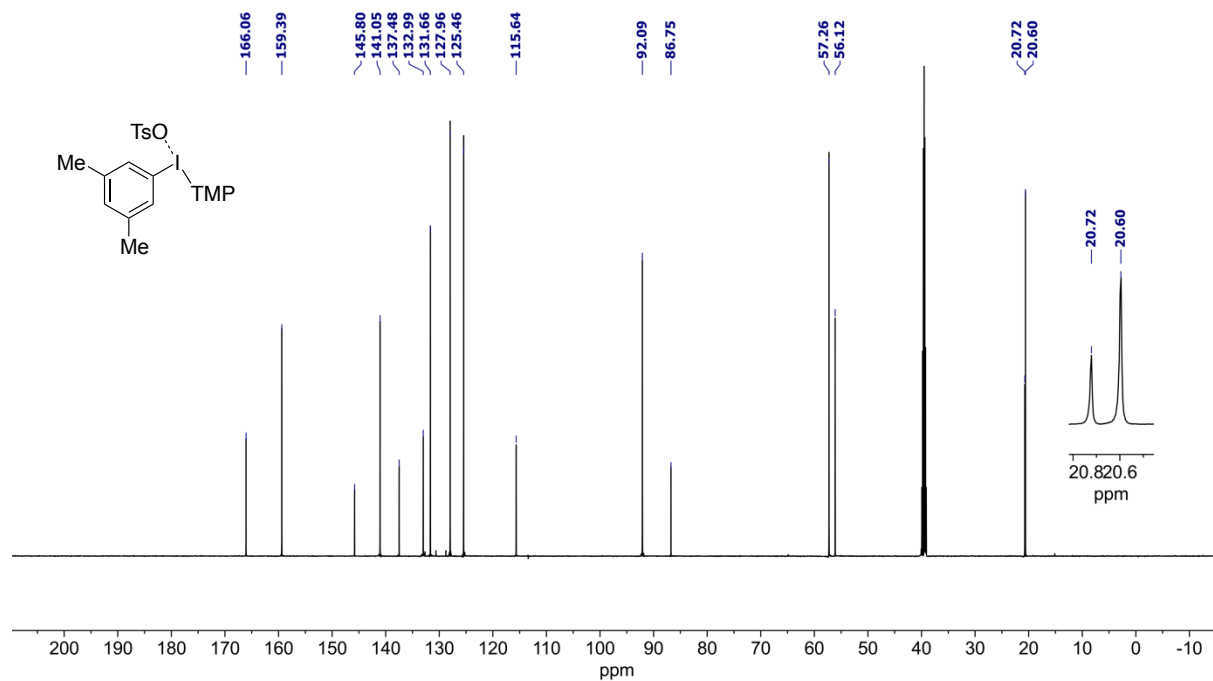


Figure 2.31.  $^{13}\text{C}$  NMR (151 MHz,  $\text{DMSO-}d_6$ ) spectrum of **2h**.



**Figure 2.32.** <sup>1</sup>H NMR (600 MHz, DMSO-*d*<sub>6</sub>) spectrum of **2i**.



**Figure 2.33.** <sup>13</sup>C NMR (151 MHz, DMSO-*d*<sub>6</sub>) spectrum of **2i**.

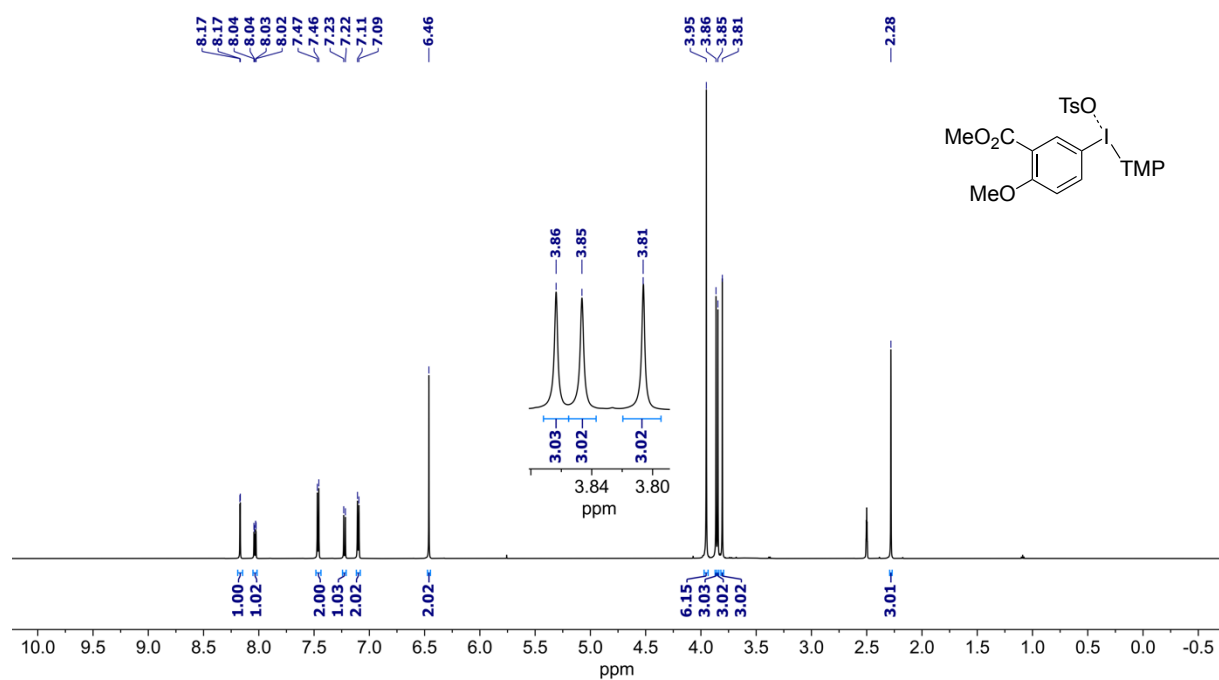


Figure 2.34. <sup>1</sup>H NMR (600 MHz, DMSO-*d*<sub>6</sub>) spectrum of **2j**.

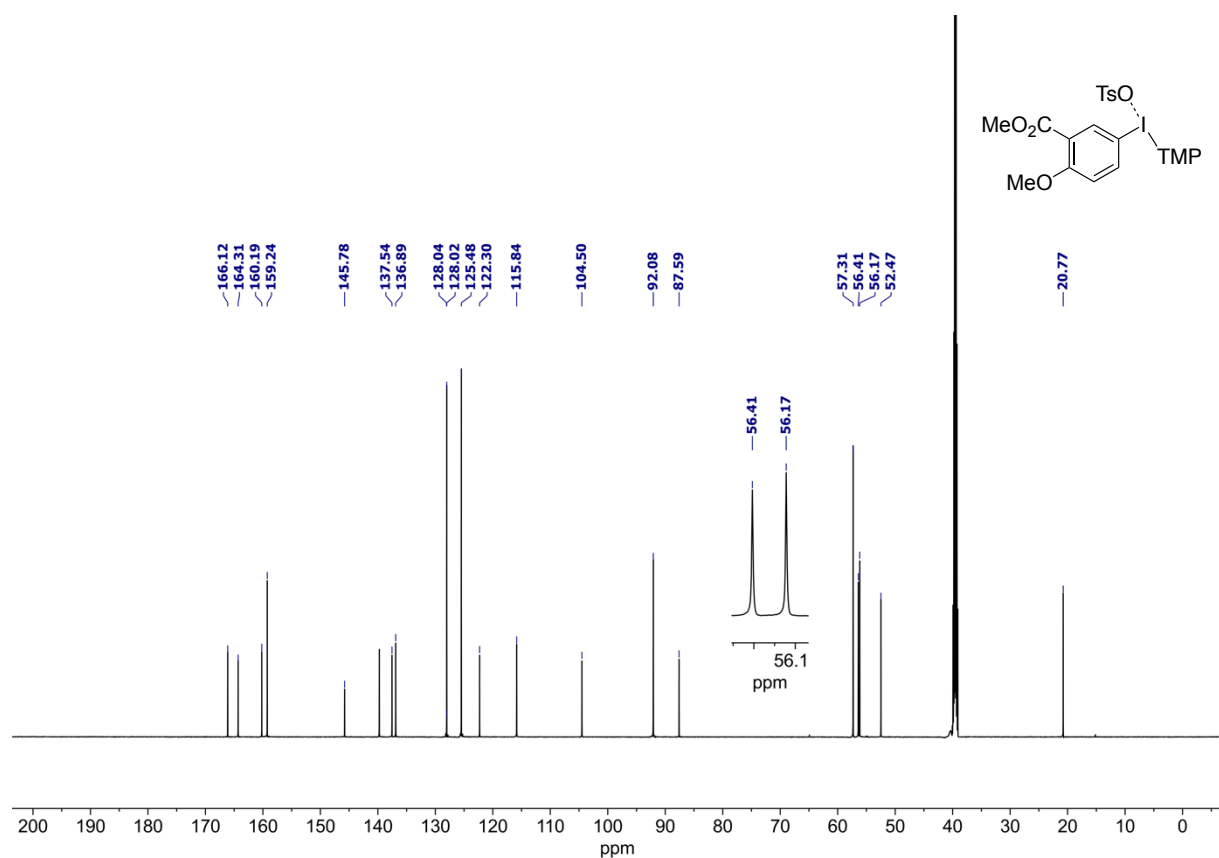


Figure 2.35. <sup>13</sup>C NMR (151 MHz, DMSO-*d*<sub>6</sub>) spectrum of **2j**.

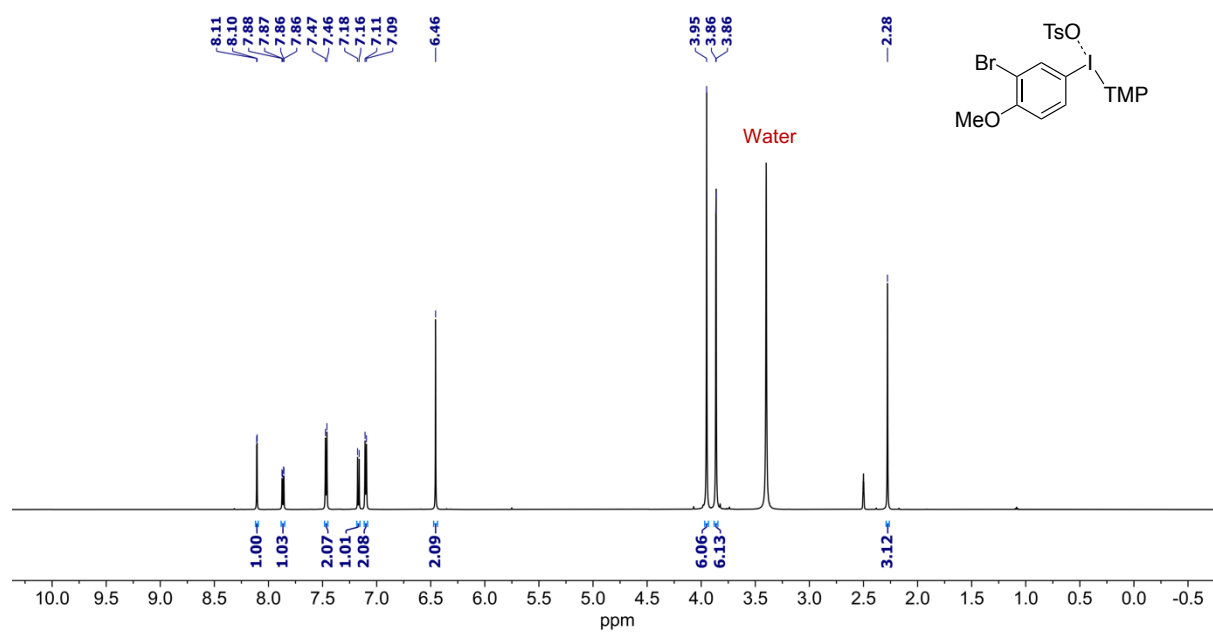


Figure 2.36.  $^1\text{H}$  NMR (600 MHz,  $\text{DMSO-}d_6$ ) spectrum of **2k**.

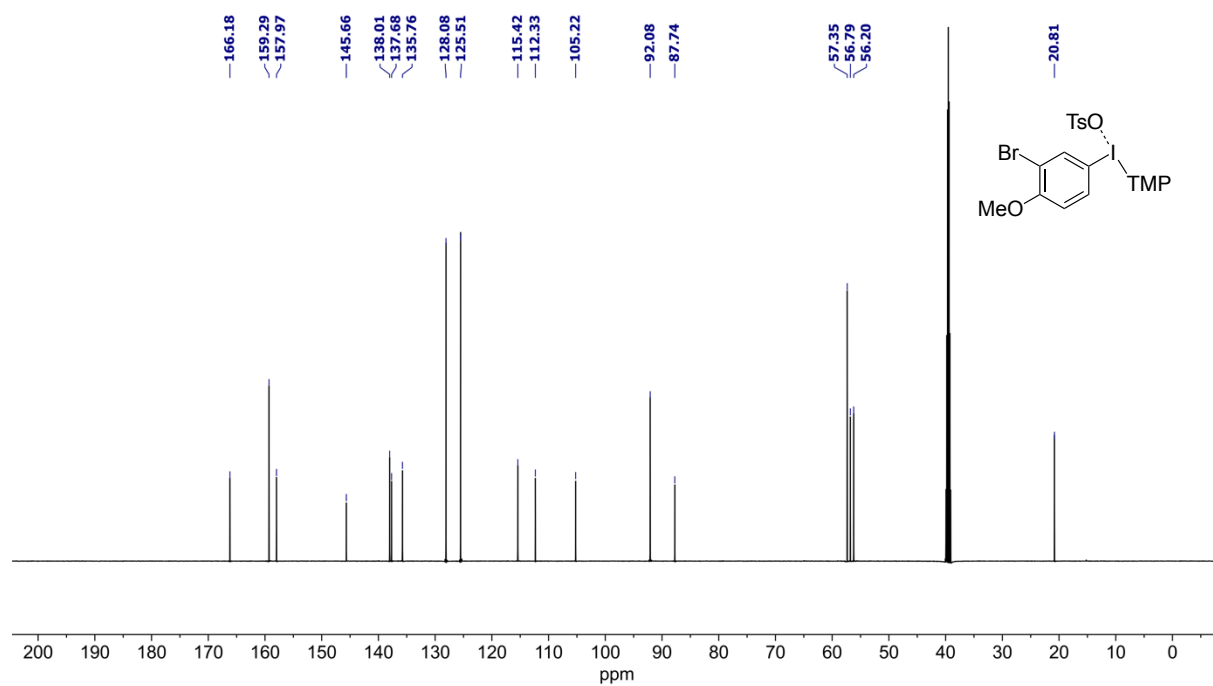
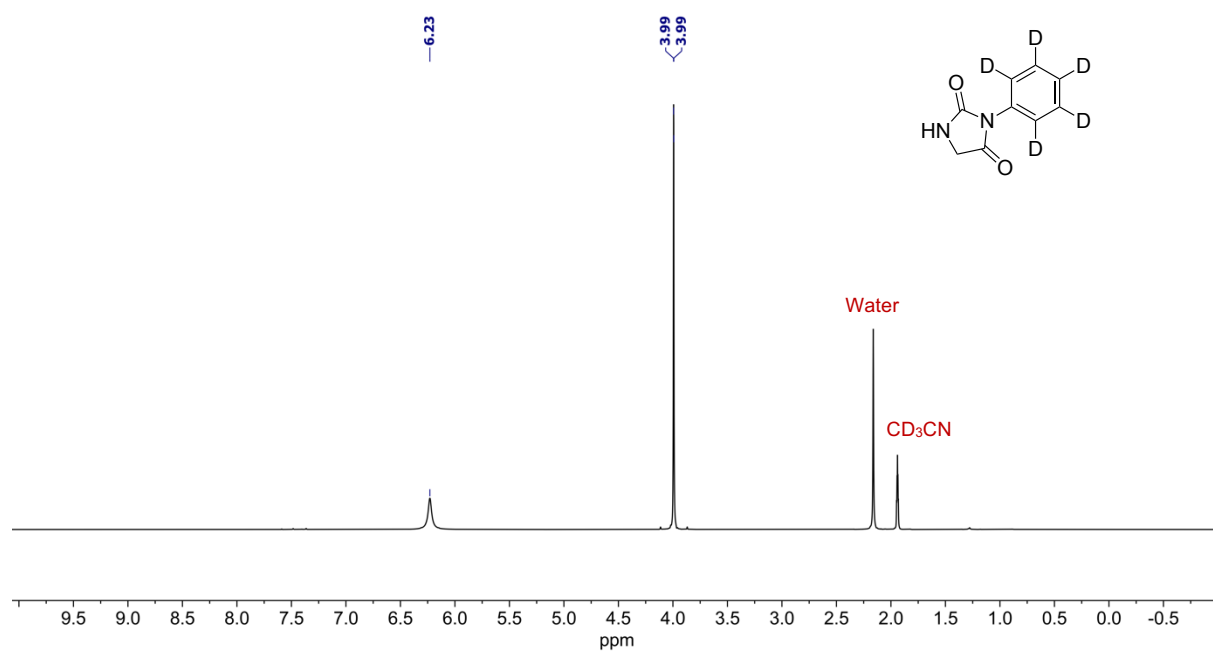
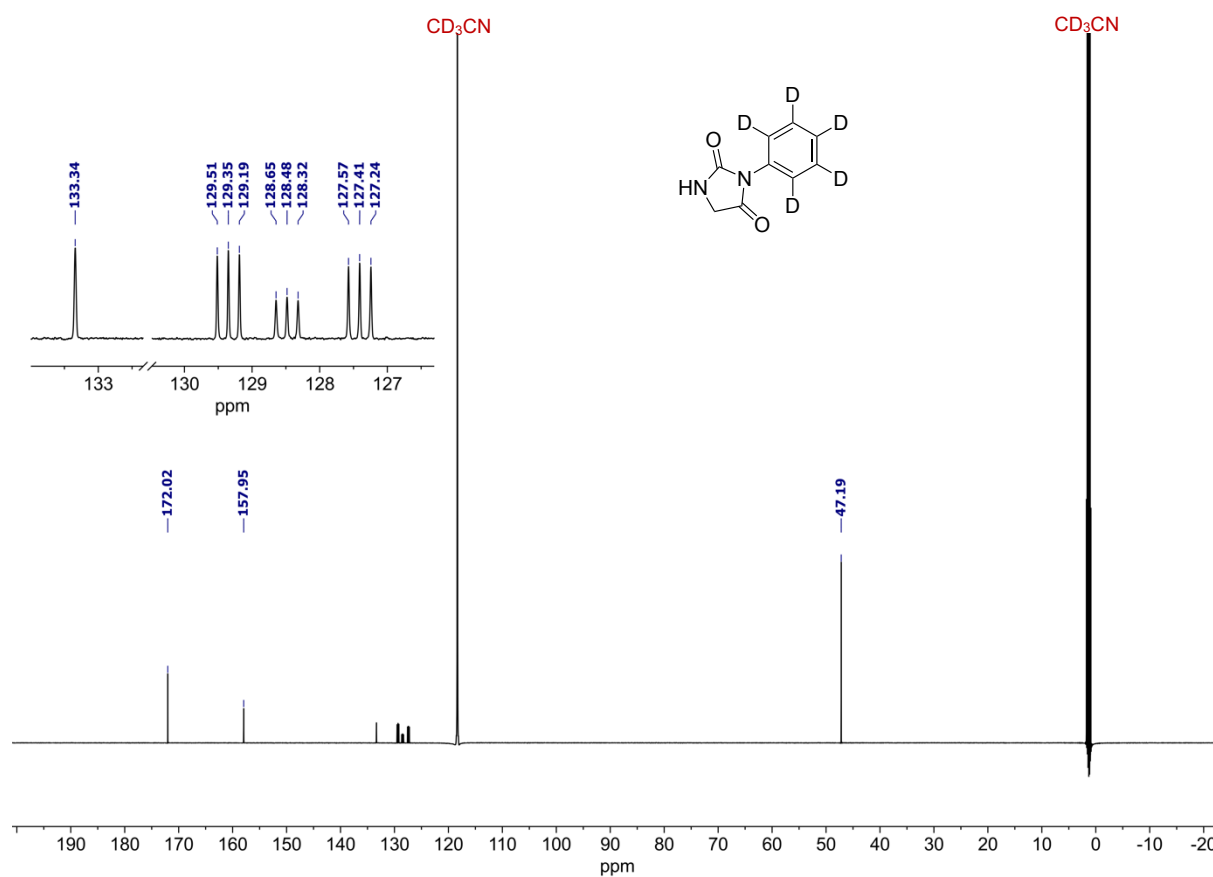


Figure 2.37.  $^{13}\text{C}$  NMR (151 MHz,  $\text{DMSO-}d_6$ ) spectrum of **2k**.



**Figure 2.38.** <sup>1</sup>H NMR (600 MHz, CD<sub>3</sub>CN) spectrum of **3a-d<sub>5</sub>**.



**Figure 2.39.** <sup>13</sup>C NMR (151 MHz, CD<sub>3</sub>CN) spectrum of **3a-d<sub>5</sub>**.

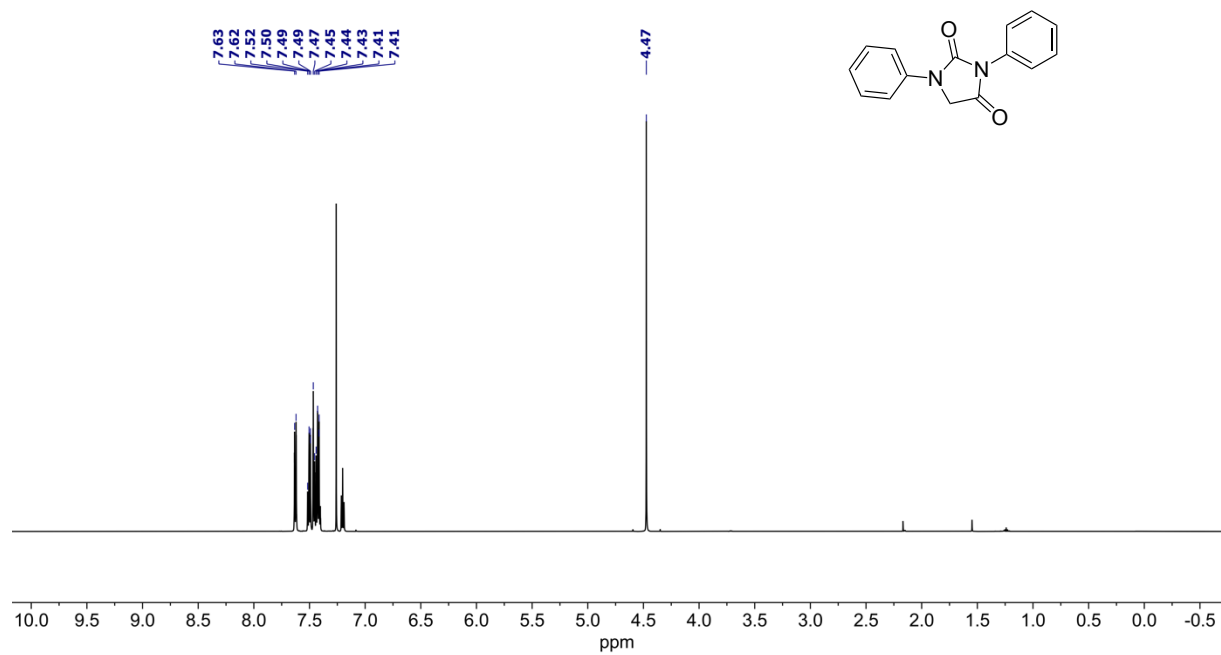


Figure 2.40. <sup>1</sup>H NMR (600 MHz, CDCl<sub>3</sub>) spectrum of 3c.

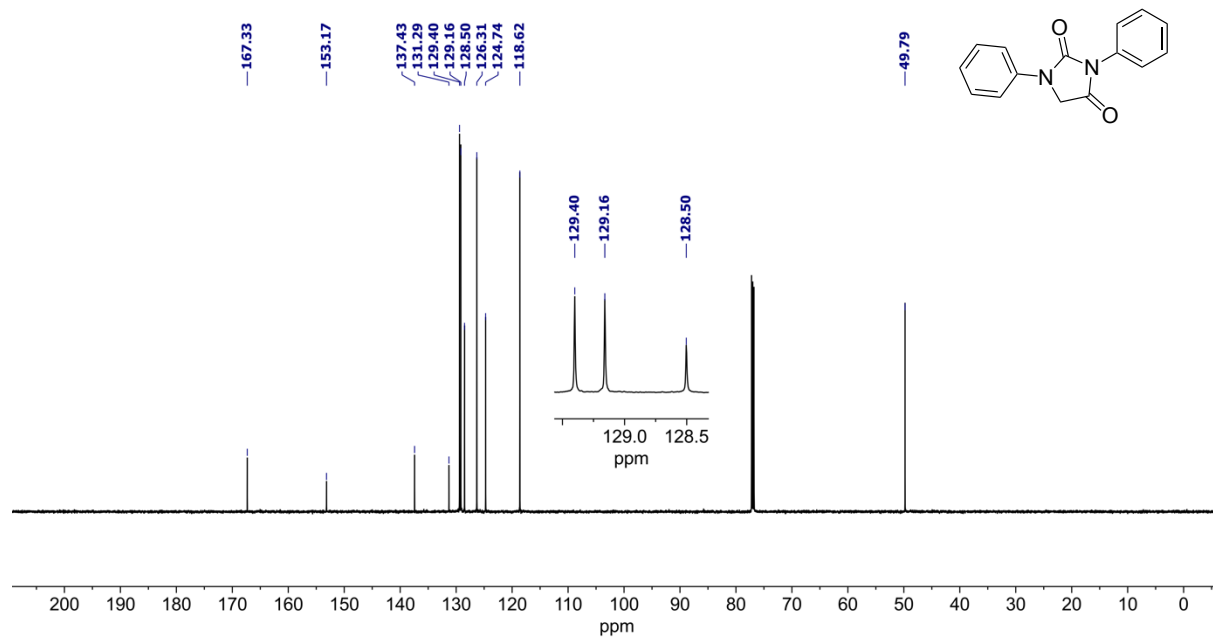
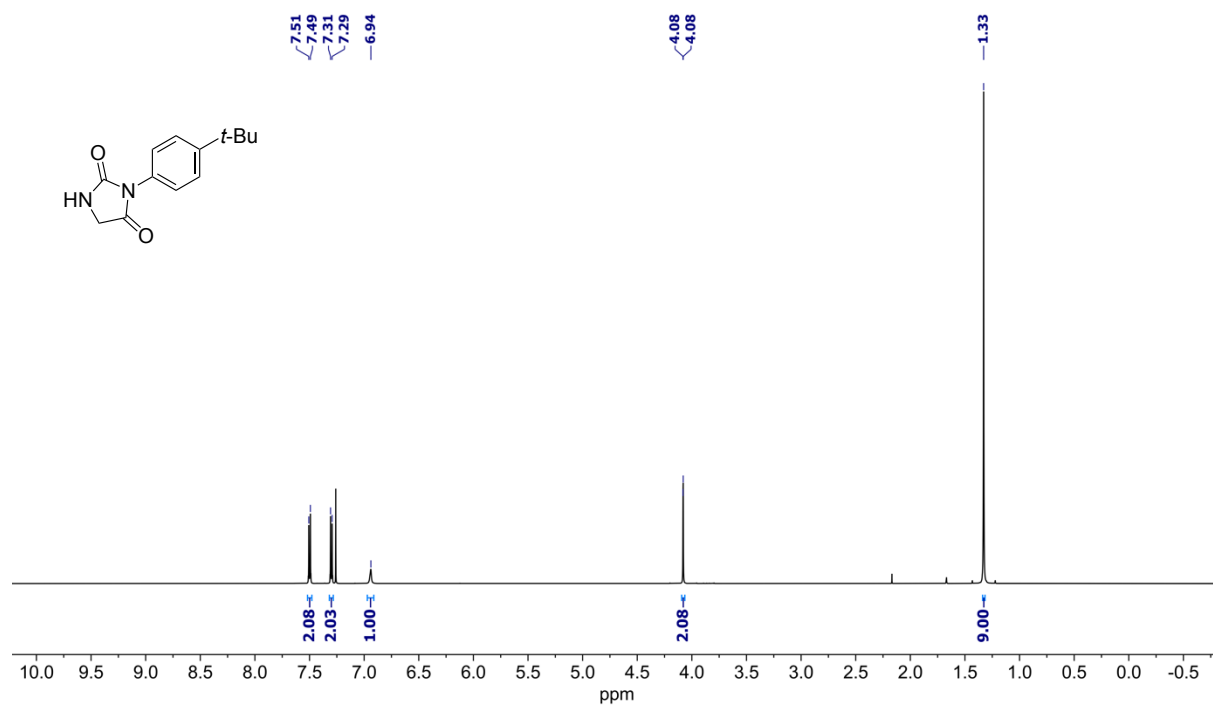
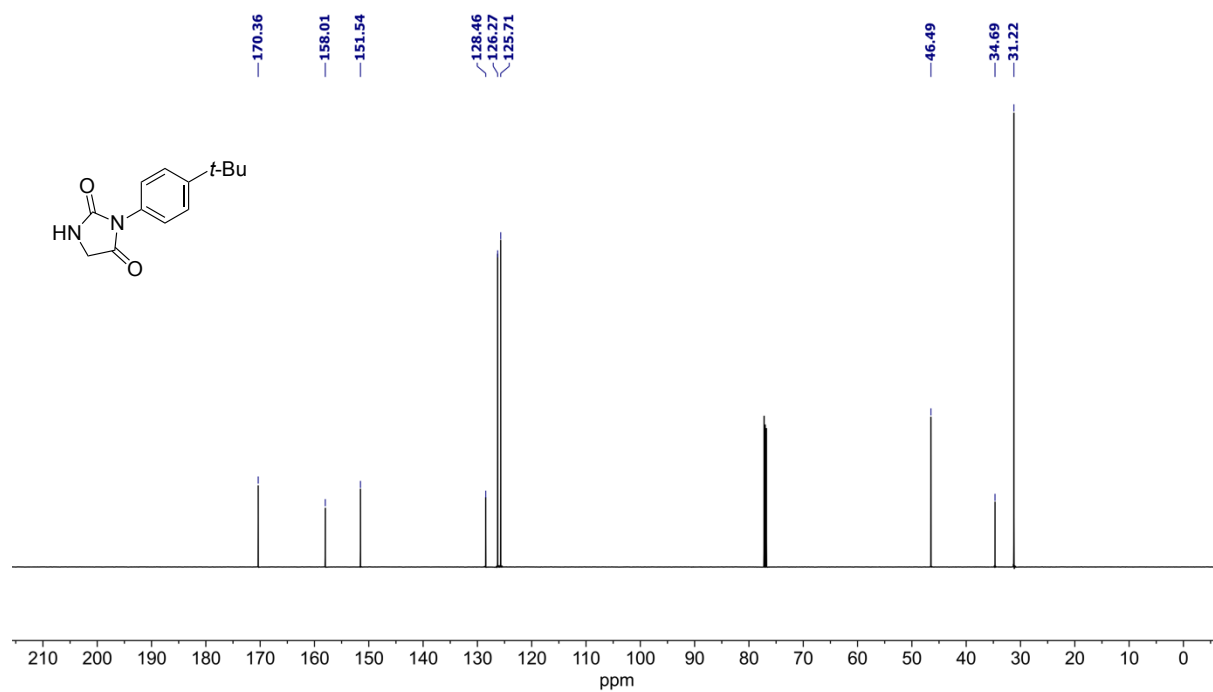


Figure 2.41. <sup>13</sup>C NMR (151 MHz, CDCl<sub>3</sub>) spectrum of 3c.



**Figure 2.42.**  $^1\text{H}$  NMR (600 MHz,  $\text{CDCl}_3$ ) spectrum of **3e**.



**Figure 2.43.**  $^{13}\text{C}$  NMR (151 MHz,  $\text{CDCl}_3$ ) spectrum of **3e**.



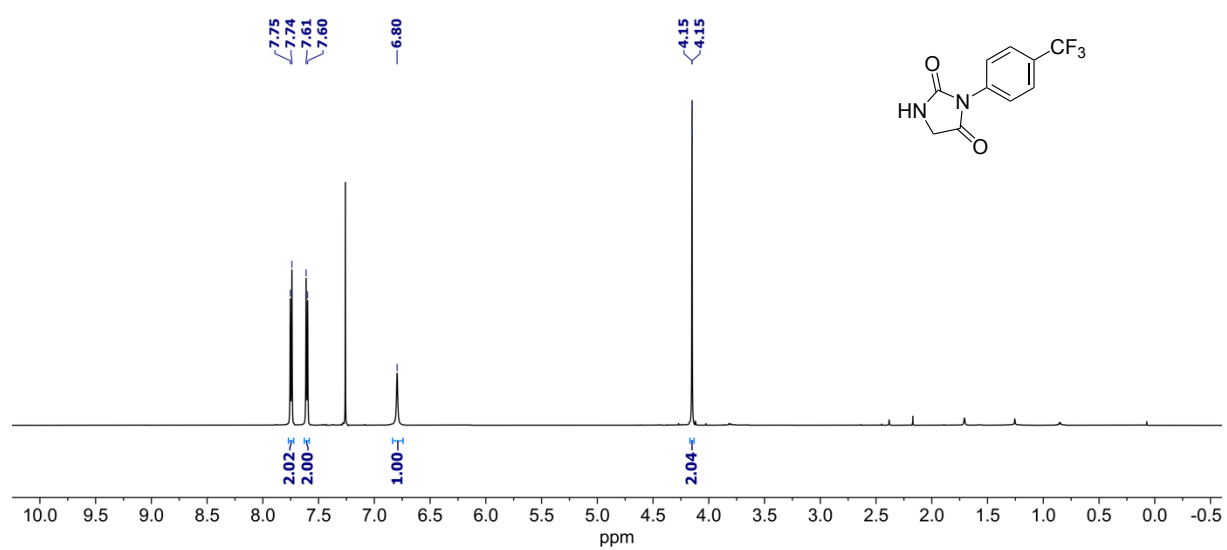


**Figure 2.44.** <sup>1</sup>H NMR (600 MHz, CDCl<sub>3</sub>) spectrum of **3i**.

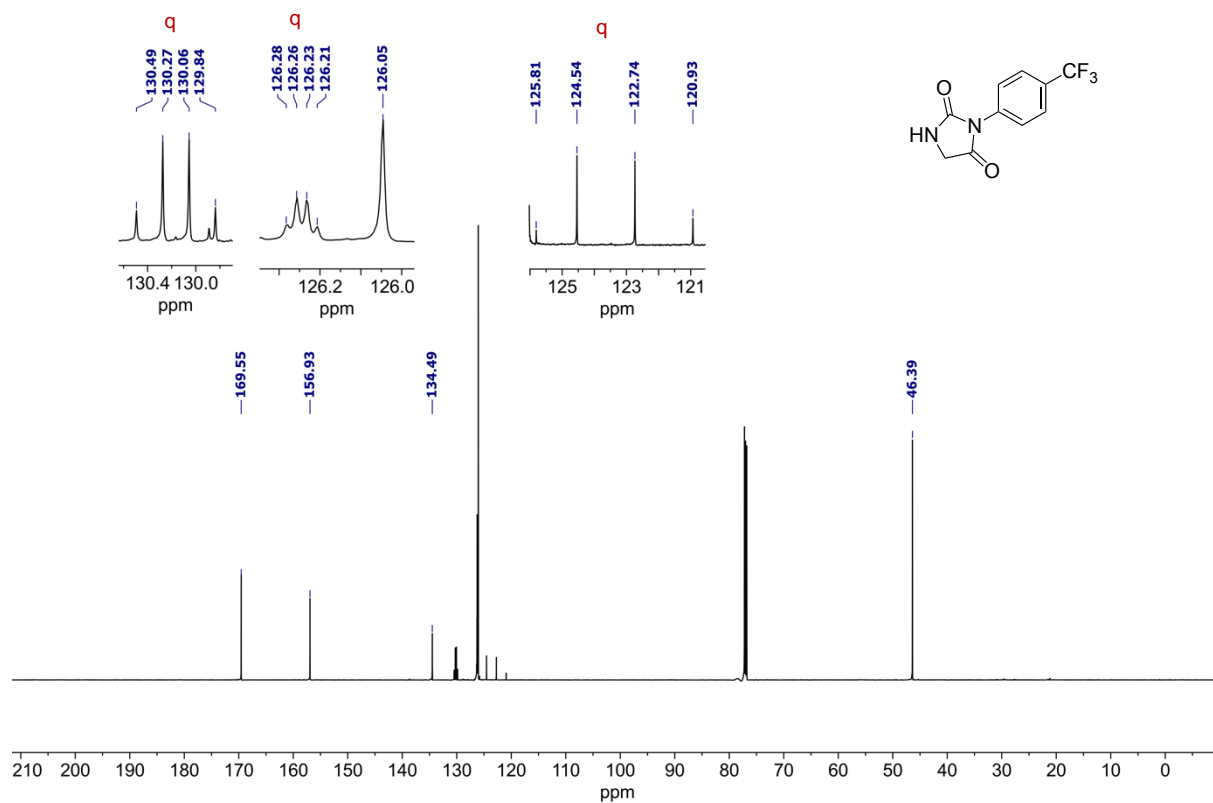


**Figure 2.45.** <sup>13</sup>C NMR (151 MHz, CDCl<sub>3</sub>) spectrum of **3i**. Quartets arising from  $J_{C-F}$  couplings are marked above the peaks.

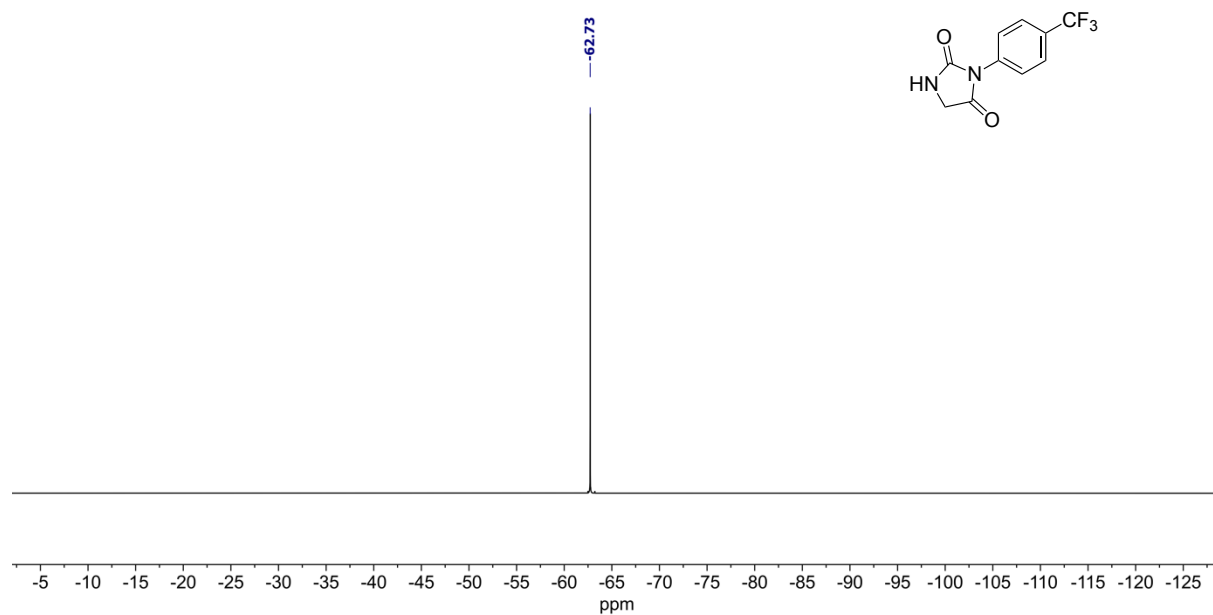


Figure 2.46.  $^{19}\text{F}$  NMR (376 MHz,  $\text{CDCl}_3$ ) spectrum of **3i**.

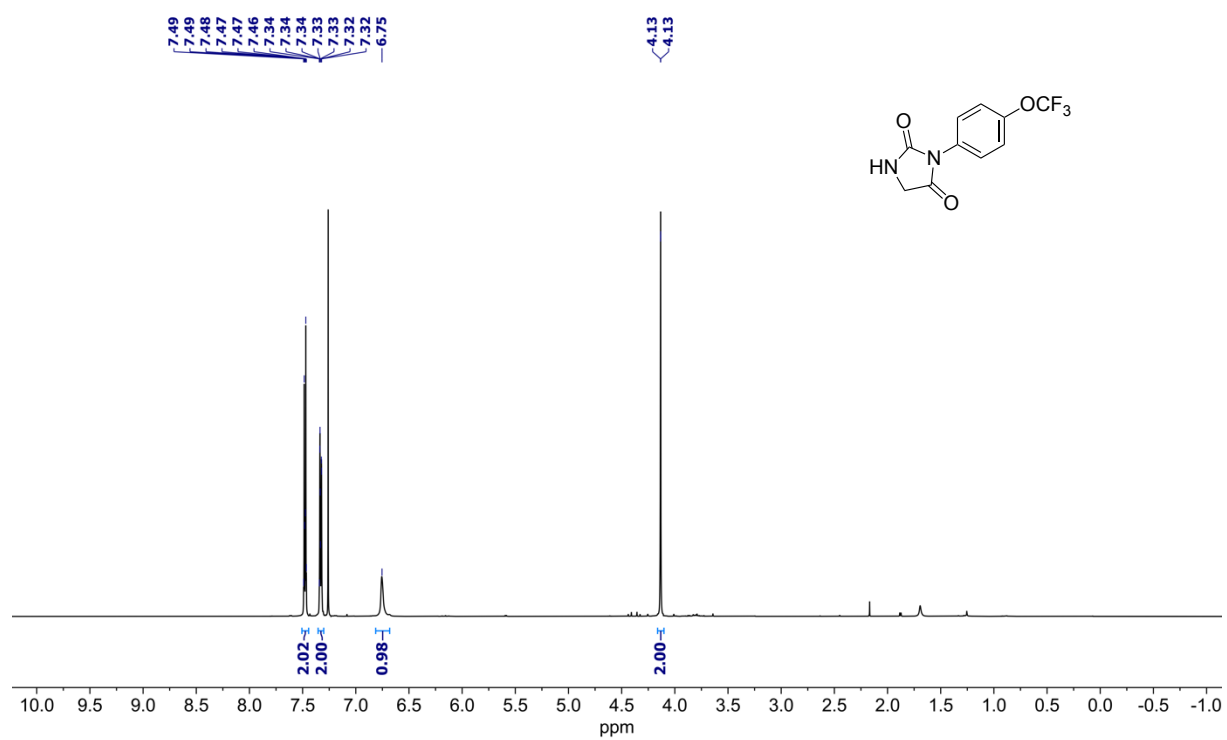
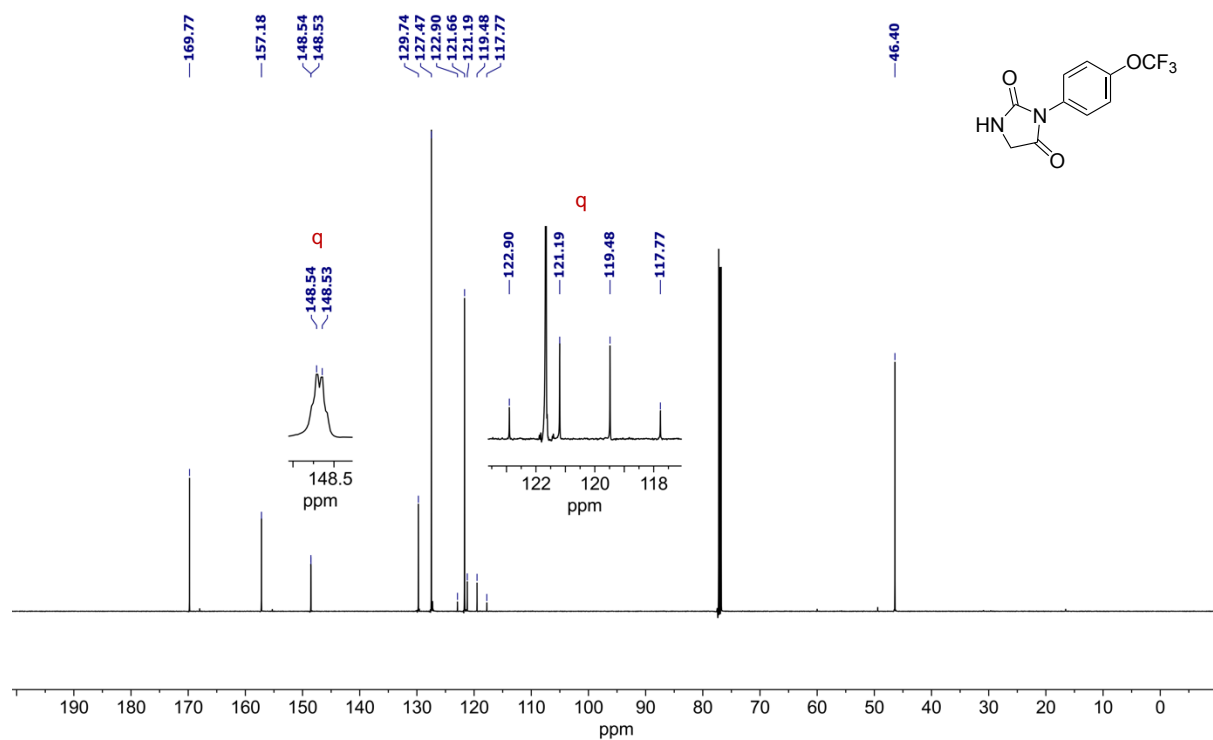
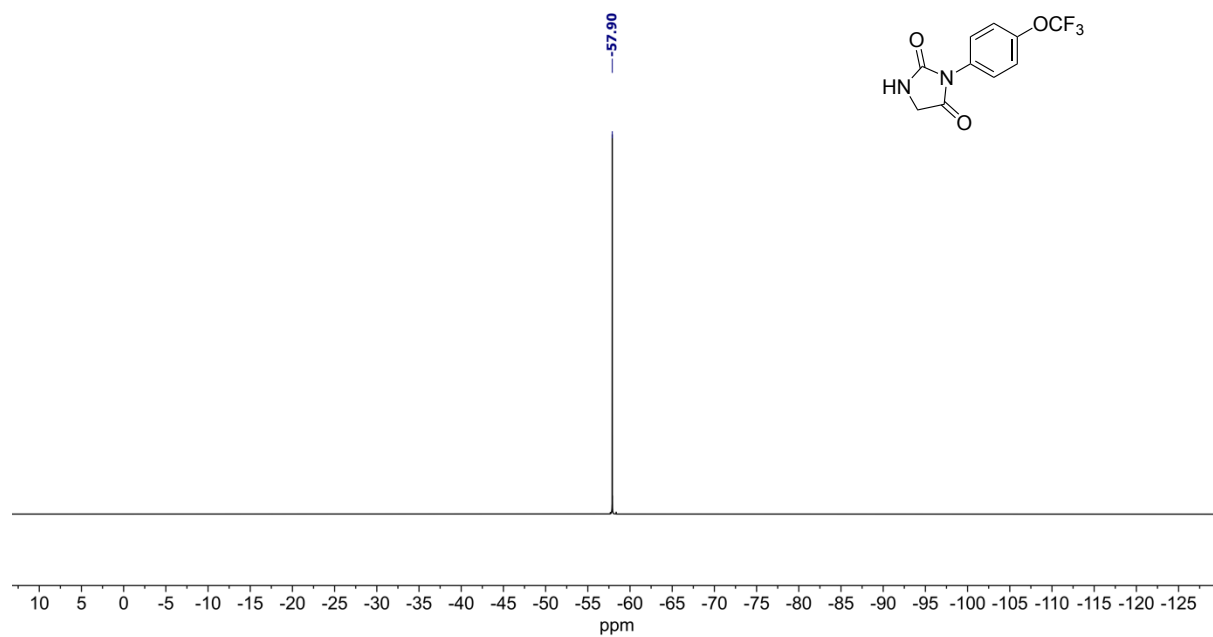


Figure 2.47.  $^1\text{H}$  NMR (600 MHz,  $\text{CDCl}_3$ ) spectrum of **3j**.



**Figure 2.48.** <sup>13</sup>C NMR (151 MHz, CDCl<sub>3</sub>) spectrum of **3j**. Quartets arising from  $J_{C-F}$  couplings are marked above the peaks.



**Figure 2.49.** <sup>19</sup>F NMR (376 MHz, CDCl<sub>3</sub>) spectrum of **3j**.

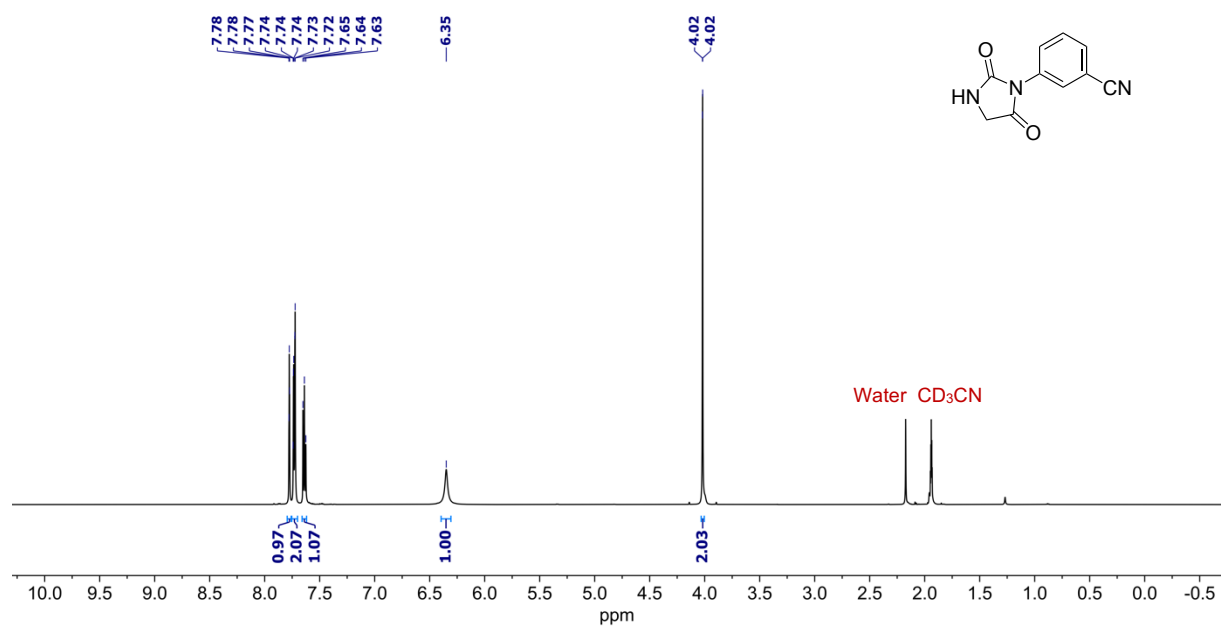


**Figure 2.50.** <sup>1</sup>H NMR (600 MHz, CD<sub>3</sub>CN) spectrum of **3p**.

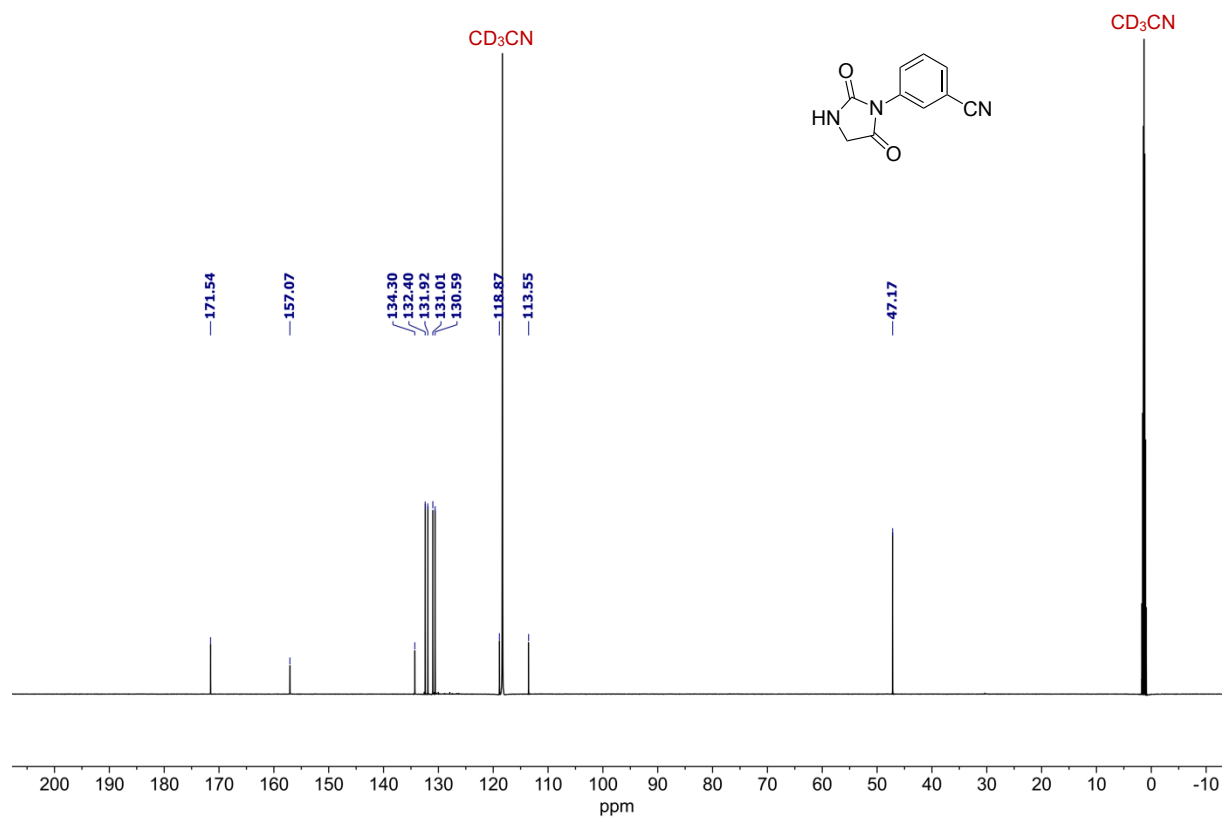


**Figure 2.51.** <sup>13</sup>C NMR (151 MHz, CD<sub>3</sub>CN) spectrum of **3p**.

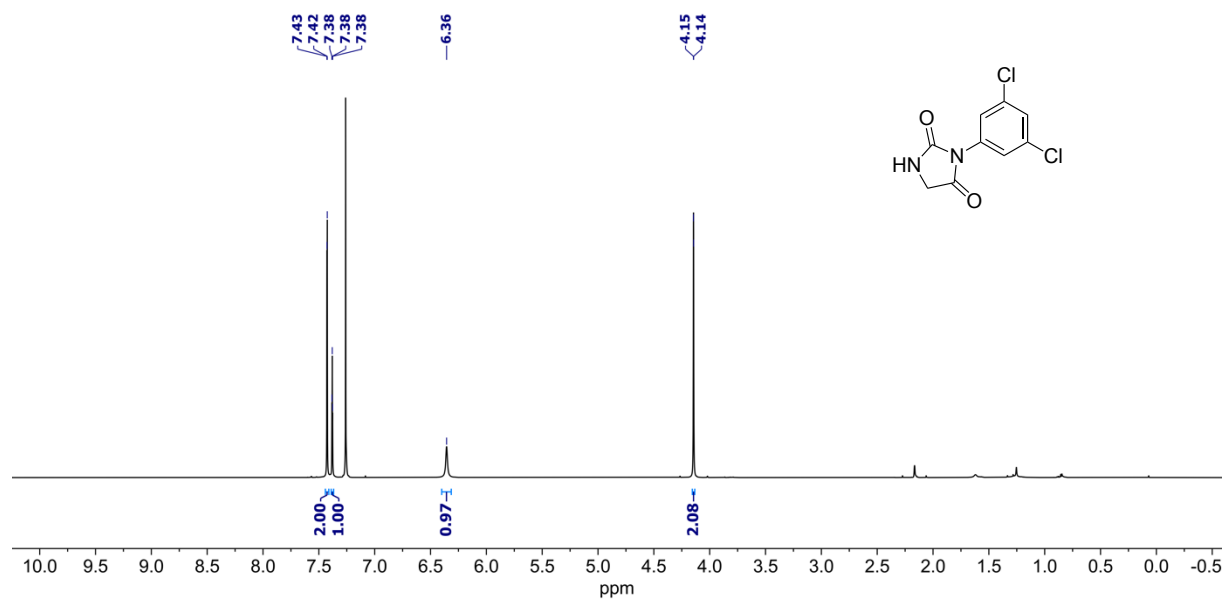


Figure 2.52.  $^1\text{H}$  NMR (600 MHz,  $\text{CDCl}_3$ ) spectrum of **3v**.

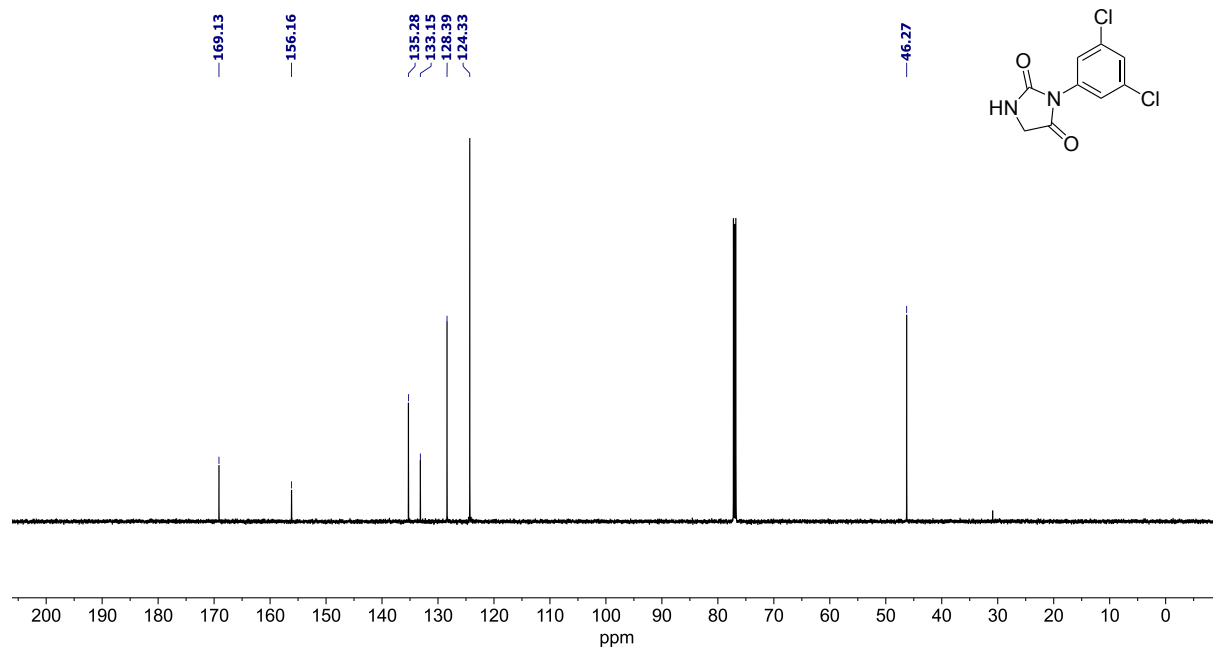


Figure 2.53.  $^{13}\text{C}$  NMR (151 MHz,  $\text{CDCl}_3$ ) spectrum of **3v**.

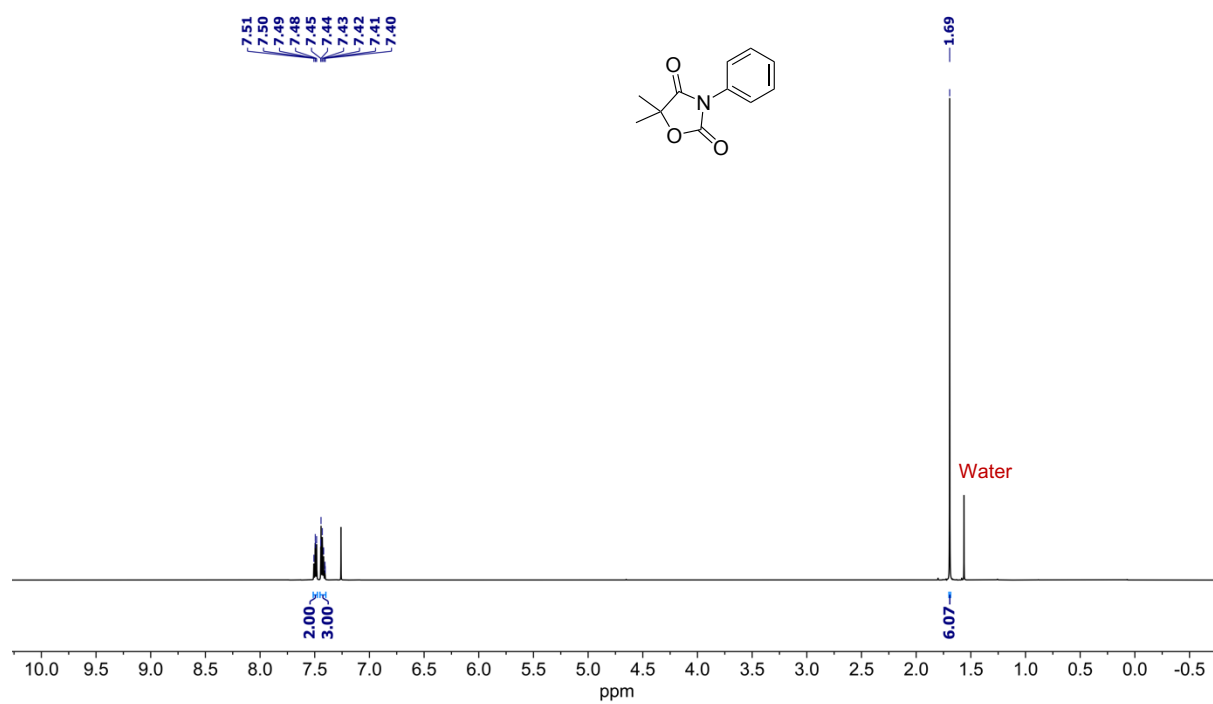


Figure 2.54.  $^1\text{H}$  NMR (600 MHz,  $\text{CDCl}_3$ ) spectrum of **6c**.

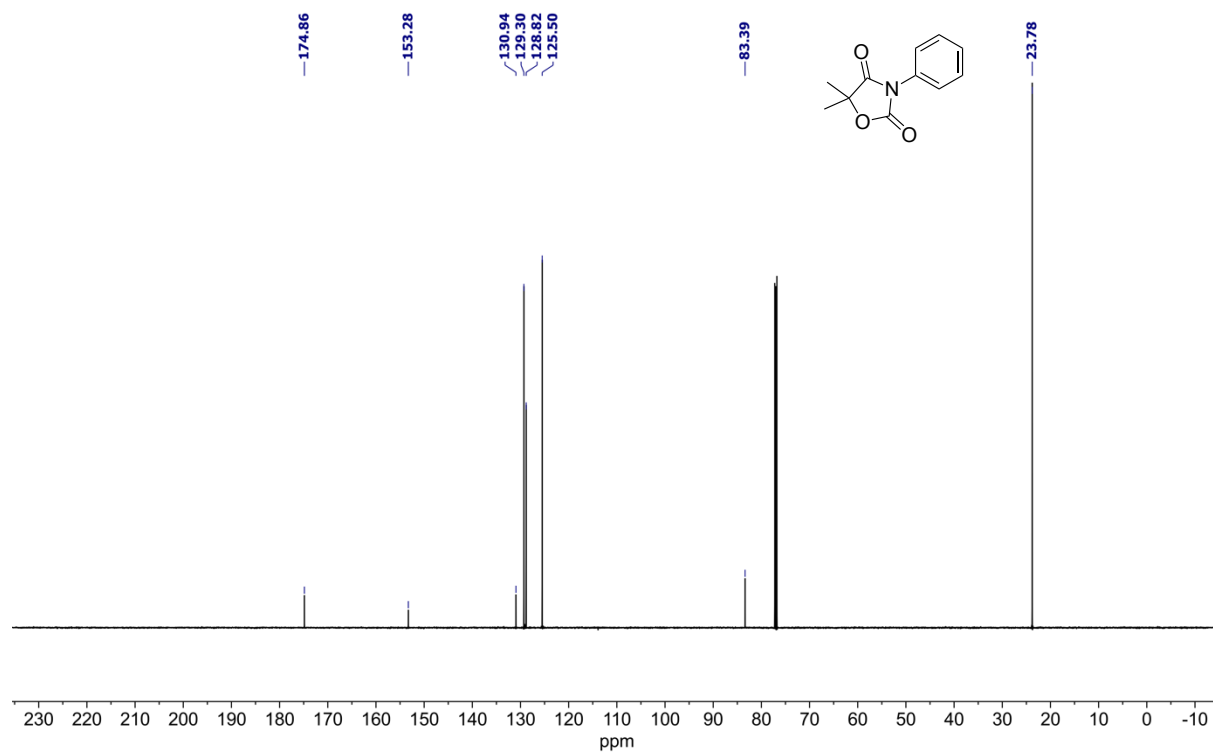


Figure 2.55.  $^{13}\text{C}$  NMR (151 MHz,  $\text{CDCl}_3$ ) spectrum of **6c**.

# Chapter 3: A mechanistic study of the Cu-catalyzed *N*-arylation of hydantoin using aryl(TMP)iodonium salts

## 3.1 Introduction

The experimental results from the *N*-3-arylation of hydantoins using unsymmetrical diaryliodonium salts described in Chapter 2 prompted us to investigate the reaction mechanism. This chapter covers the in-depth mechanistic study of said reaction using DFT calculations. The synergy between DFT calculations and experiments aid in the understanding of experimental reaction outcomes and can predict unexpected opportunities for reaction development.

The work presented in this chapter is covered in Paper II. Paper II will be published as a full article<sup>f</sup> covering all computational and experimental details. Therefore, this chapter will only comprise a summary of the most important findings. The manuscript and supporting information for Paper II can be found in the Appendix.

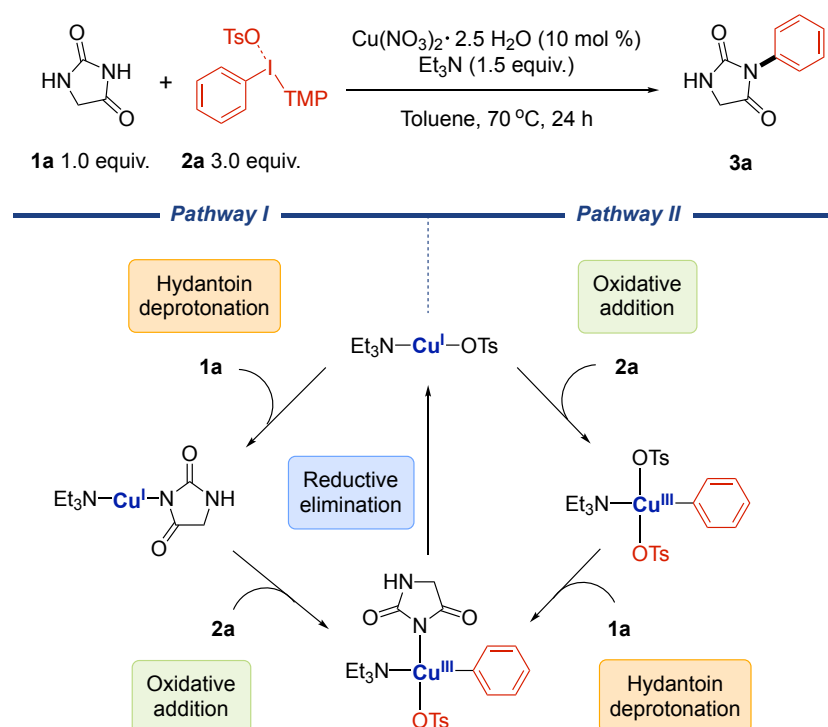
Symmetrical and unsymmetrical diaryliodonium salts were introduced in Chapter 2 as a source of arylating agents capable of transferring aryl groups to carbon- and heteroatom nucleophiles, both transition metal-free and transition metal-catalyzed. The use of copper as a transition metal-catalyst has proven to facilitate the transfer effectively, as also demonstrated in our work. However, the detailed mechanistic understanding of Cu-catalyzed couplings with diaryliodonium salts is modest and mostly limited to C-H-functionalization reactions with symmetrical salts.<sup>224-229</sup> A thorough investigation into the use of unsymmetrical aryl(Mes)iodonium salts in Cu-catalyzed fluorination reactions was reported by Sanford and co-workers.<sup>161, 230</sup> Based on DFT calculations and experimental results, they suggested a Cu<sup>I</sup>/Cu<sup>III</sup>-catalytic cycle, starting with the oxidative addition of aryl(Mes)iodonium. Oxidative addition as a first step is also suggested in the DFT studies of Cu-catalyzed C-H arylation reactions<sup>227-229</sup> with symmetrical salts. Closely related to the aryl(Mes)iodonium salts are the aryl(TMP)iodonium salts used in the work presented in Chapter 2. To the best

---

<sup>f</sup> Paper I and Paper III are communications and thus discussed in more details in their respective chapters.

of our knowledge, no mechanistic investigation of Cu-catalyzed arylation using ArI(TMP) salts have been reported. Regardless of the method, no detailed mechanistic investigation of *N*-3-hydantoin arylations have been reported.

As seen in the previous chapter, chemoselective aryl transfer from [ArI(TMP)]OTs to the N-3 position of hydantoins was facilitated by a Cu(II)nitrate salt in the presence of Et<sub>3</sub>N (TEA). I-TMP is generated as a byproduct in the process. The lack of previous mechanistic studies prompted us to propose two different reaction pathways, both based on Cu<sup>I</sup>/Cu<sup>III</sup>-catalytic cycles (Scheme 3.1).



**Scheme 3.1.** Proposed Cu<sup>I</sup>/Cu<sup>III</sup>-catalytic cycles for the *N*-3-arylation of hydantoins.

In pathway I, the imide NH (N-3 position) of the hydantoin is deprotonated by a Cu<sup>I</sup>-species prior to the oxidative addition of [ArI(TMP)]OTs. Deprotonation as a first step of the catalytic cycle has been proposed for Ullmann-type C-N coupling reactions using aryl iodides.<sup>124, 134</sup> In pathway II, oxidative addition to form a Cu<sup>III</sup>-species is the first step, followed by hydantoin deprotonation. Oxidative addition as a first step has been proposed for the C-H-arylations with diaryliodonium salts. The final product is formed by reductive elimination of a Cu<sup>III</sup>-species in both pathways.

The work presented in Paper II includes the exploration of the two mechanistic reaction pathways in Scheme 3.1 using DFT calculations. (PBE-D3/def2SVP/CPCM//PBE0-

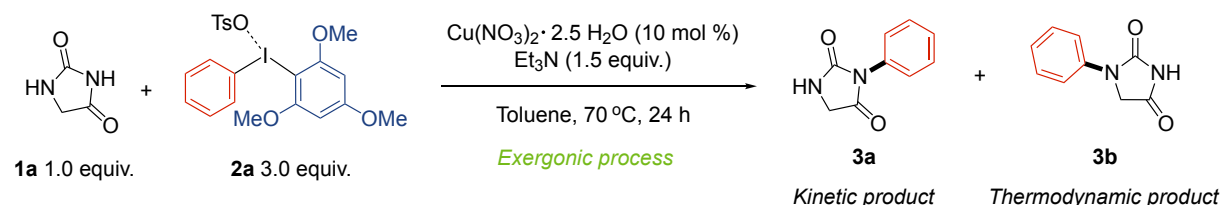


D3/def2TZVP/CPCM). Free energies were obtained considering standard state conditions. The reactants selected to study the full mechanism were hydantoin (**1a**) and [PhI(TMP)]OTs (**2a**). The questions we tried to answer during the study include:

- (1) Which substrate reacts with Cu first, **1a** or **2a**?
- (2) Is the observed regioselectivity in the arylation reaction due to thermodynamics or kinetics?
- (3) Does Cu participate in the deprotonation of hydantoin?
- (4) What is the role of TEA in the reaction?
- (5) What prevents TMP to be transferred in the arylation reaction?
- (6) Can we find a mechanism explaining the absence of linear trend in yields upon changing the steric and electronic properties of the aryl group being transferred (Chapter 2, Scheme 2.7)?

### 3.2 Summary of important findings in the mechanistic study

Prior to the study of the catalytic cycles, the thermodynamics of the reactions were investigated. We discovered that the arylation of hydantoin **1a** was highly exergonic in both N-3 (yielding **3a**) and N-1 position (yielding **3b**), with a slight preference for the latter. The observed experimental regioselectivity can therefore be attributed to kinetic preferences for the N-3 position. In the absence of TEA, the reactions were less exergonic, indicating the preferable presence of TEA.



**Scheme 3.2.** Thermodynamics of the N-1- and N-3-arylation of hydantoin under standard conditions. The slight thermodynamic preference (by 1.8 kcal/mol) for **3b** indicates that **3a** is formed due to kinetic preferences.

Investigation of the two pathways revealed that the highest energy barrier in pathway II is 4.9 kcal/mol higher than in pathway I. This pathway agrees with the obtained regio- and chemoselectivity of the arylation reaction, the observed KIE and the species detected during <sup>1</sup>H NMR spectroscopic reaction monitoring. Thus, based on

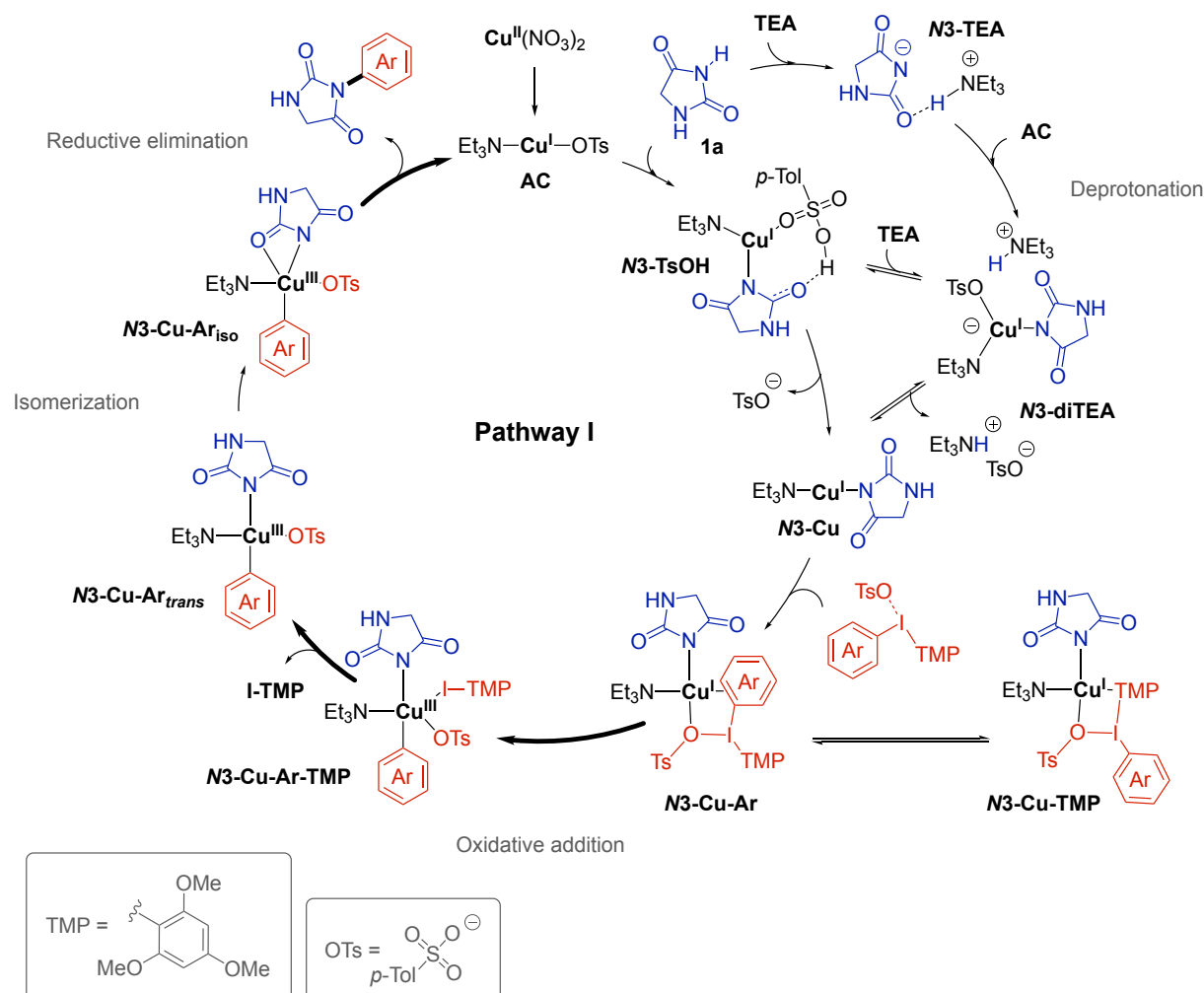
computational- and experimental results, we propose the catalytic cycle in Scheme 3.3, pathway I, as the preferred pathway for the *N*-3-arylation of hydantoins using aryl(TMP)iodonium salts.

The active catalytic Cu<sup>I</sup>-species (TEA)Cu(I)(OTs) (**AC**) is likely formed by TEA-assisted reduction<sup>231</sup> of Cu(II)(NO<sub>3</sub>)<sub>2</sub> (the employed catalyst). The first step of the cycle includes deprotonation of hydantoin in the kinetically preferred *N*-3 position and yields the Cu<sup>I</sup>-imido complex **N3-Cu**. **N3-Cu** is kinetically accessible *via* two pathways: (1) deprotonation by the base, TEA and (2) intramolecular Cu<sup>I</sup>-assisted deprotonation by the tosylate (OTs) anion. In both cases the proton abstraction is stabilized by the carbonyl groups (in 2-position) of hydantoin (**N3-TEA** and **N3-TsOH**). **N3-TEA** and **N3-TsOH** can further react with **AC** or TEA, respectively, to form the off-cycle ion-pair intermediate **N3-diTEA**. The low energy of **N3-diTEA** compared to the other reaction intermediates indicates that it can act as the catalysts resting state. Both deprotonation pathways lead to the formation of hydantoin-copper-complex **N3-Cu**. The simultaneous protonation of TEA to [TEAH]<sup>+</sup> can be monitored by <sup>1</sup>H NMR spectroscopy and is occurring before the I-TMP disassociation step.

The following step includes addition of the aryl(TMP)iodonium salt to **N3-Cu**. With Ph(TMP)iodonium tosylate (**2a**), the phenyl group interaction with the Cu-center provides the stable intermediate **N3-Cu-Ar**. During evaluation of the arene transfer chemoselectivity (Ph *vs.* TMP), we found that intermediate **N3-Cu-TMP** has a lower energy than **N3-Cu-Ar**. However, the transfer of TMP to Cu was found to be thermodynamically unfavored. **N3-Cu-TMP** is there considered to be an off-cycle intermediate in equilibrium with **N3-Cu-Ar** and has relevance since it might act as the catalysts resting state.

Cleavage of the C(Ar)-I bond in **N3-Cu-Ar** and the following oxidative addition of the Ar-fragment and I-TMP to the Cu-center yields the pentacoordinate Cu<sup>III</sup>-intermediate **N3-Cu-Ar-TMP**, in which the hydantoin and aryl-substituent are *trans* to each other. For arene-transfer to occur in the final step (reductive elimination), a rearrangement is necessary to put the two ligands in a *cis* configuration. This is a stepwise process in which the first step involves the disassociation of I-TMP (also visible in the <sup>1</sup>H NMR spectrum) from Cu. The formed square planar Cu<sup>III</sup>-complex **N3-Cu-Ar<sub>trans</sub>** undergoes an isomerization process where the carbonyl oxygen of hydantoin coordinates to Cu. The process yields the pentacoordinate Cu<sup>III</sup>-intermediate

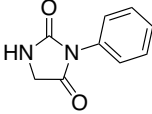
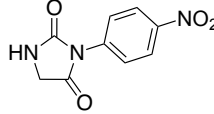
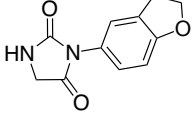
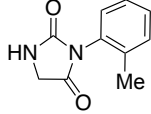
$N3$ -Cu-Ar<sub>iso</sub> which undergoes further reorientation during the reductive elimination transition state to provide the *cis* configuration, upon which the final product is released.



**Scheme 3.3.** Pathway I: Proposed catalytic cycle for the regio- and chemoselective  $N$ -3-arylation of hydantoins. Bold arrows indicate possible rate-determining transition states, which are dependent on the aryl group being transferred.

During the experimental work in Chapter 2, the stereoelectronic properties of  $[\text{ArI}(\text{TMP})]\text{OTs}$  and their influence on  $N$ -3-arylhydantoins yields were explored. The absence of a linear trend when using salts with different electronic properties (EDGs and EWGs) was seen. During the computational work, we discovered that three of the transition states (marked with bold arrows in Scheme 3.3) in pathway I are susceptible to be rate-determining: (1) the oxidative addition of the diaryliodonium salt (supported by the presence of a  $\beta$ -secondary KIE) (2) the disassociation of I-TMP and (3) the isomerization required for reductive elimination. Additionally, three species may behave as the catalyst resting states ( $N3$ -diTEA,  $N3$ -Cu-Ar and  $N3$ -Cu-TMP).

Both the rate-determining step and the resting state were found to be influenced by the electronic and steric properties of [ArI(TMP)]OTs in a different manner, which may explain why no linear trend is observed going from EWGs to EDGs. Indeed we found that the trends in the reaction energy span<sup>232</sup> (the overall reaction energy barrier) for the different substrates were in qualitative agreement with the obtained yields (Figure 3.1). Ultimately, these results highlight the need for fine-tuning of the non-transferred arene for increasing the efficiency in the arylation reaction.

				
	<b>3a</b>	<b>3g</b>	<b>3z</b>	<b>3q</b>
<b>Yield (%)</b>	78	59	30	0
<b><math>\Delta\Delta G</math> (kcal/mol)</b>	21.0	21.3	22.1	27.5

**Figure 3.1.** Comparison of product yields and reaction energy barriers for a selection of products with different stereoelectronic properties obtained from the *N*-3-arylation in Chapter 2.

### 3.3 Conclusion

Two pathways for the *N*-3-arylation of hydantoin were investigated, in which the pathway I, where **1a** reacts with Cu before **2a**, was found to be preferred. The observed preference for the N-3 over N-1 position can be attributed to a kinetic preference rather than a thermodynamic one. It was discovered that deprotonation of **1a** can be assisted by both a Cu-complex and TEA. TEA also partakes in the formation of the active Cu<sup>I</sup>-complex from the employed Cu<sup>II</sup>-catalyst. Further, a stable intermediate in which Cu and TMP interact was found, but the transfer of TMP to Cu was thermodynamically not favorable. Lastly, the change of the rate-determining step in the catalytic cycle explains the absence of a linear trend in product yields when changing the stereoelectronic properties of the arene being transferred.

# Chapter 4: Development of a methodology for Cu-catalyzed C(sp<sup>2</sup>)-N cross-coupling of cyclic imides and boronic acids

## 4.1 Introduction

This chapter covers the development of a method for C(sp<sup>2</sup>)-N-bond forming reactions (*N*-alkenylation and *N*-arylation of hydantoin and other cyclic imides with boronic acids). The work presented in this chapter is mainly covered in Paper III, but additional unpublished results are included as well. A brief introduction to *N*-alkenylation reactions and the use of boronic acids as coupling partner is given prior to the method development.

### 4.1.1 Access to enimides through *N*-alkenylation reactions

Structurally related to the more common enamines and enamides are the enimides (Figure 4.1, top left). Enimides are well established as key structures in various classes of biologically active compounds,<sup>233-238</sup> natural products<sup>48, 143, 239, 240</sup> and functional materials<sup>241, 242</sup> (Figure 4.1). Enimides can be considered versatile intermediates. As such they have been utilized as building blocks in the synthesis of more complex structures<sup>243-248</sup> and  $\beta$ -amino acid derivatives.<sup>249, 250</sup>

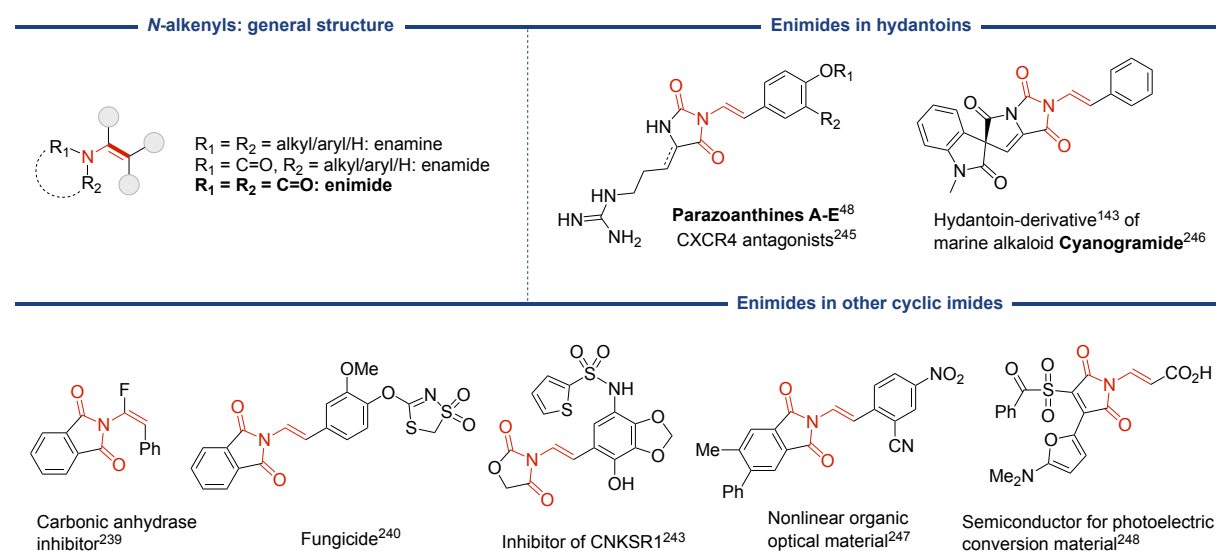
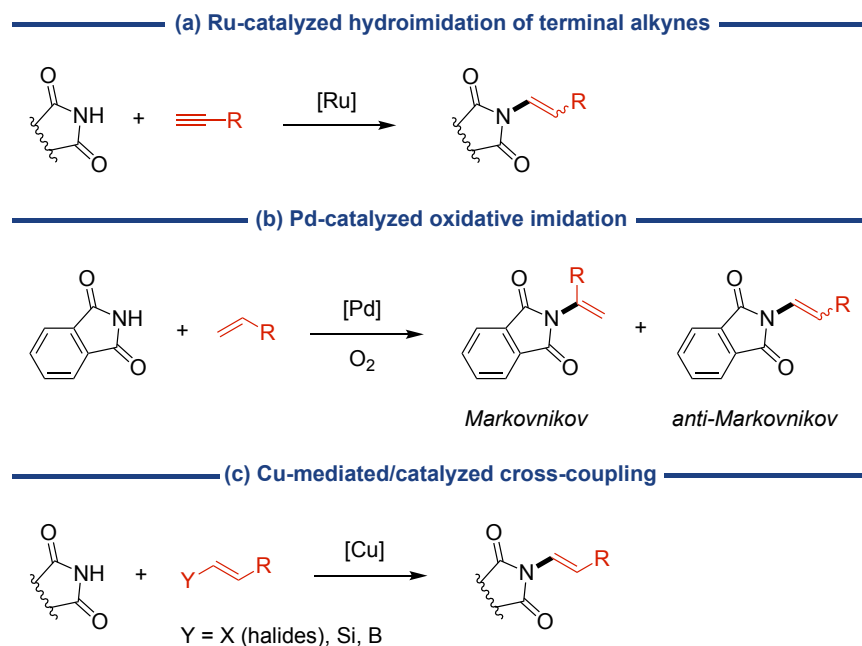


**Figure 4.1.** General structure of enimides and representative examples of cyclic enimides.

Regardless of the encounter of the cyclic enamide moiety in valuable structures, only a few strategies for the direct enimidic C-N bond construction are known. This bond construction, *N*-alkenylation, involves the direct installation of an alkene group onto a nitrogen atom. Alternative approaches to cyclic enamides is through cyclization<sup>251</sup> and/or elimination<sup>236, 239</sup> reactions which requires more steps, often leading to lower yields. For the direct *N*-alkenylation, both transition metal-free<sup>141, 142, 252-254</sup> and transition metal-catalyzed protocols have been reported, but the main strategies are based on metal-catalysis (Scheme 4.1).

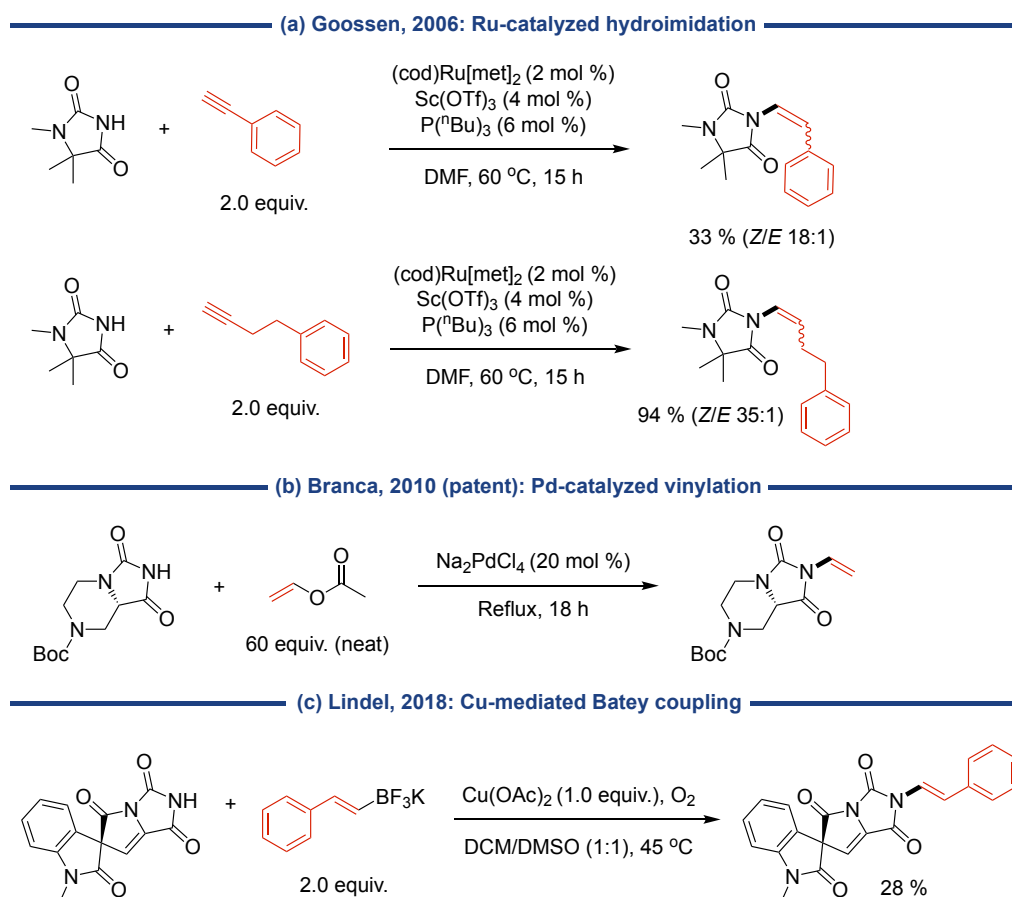
Ruthenium-catalyzed protocols have been developed where imides and alkynes are condensed in a hydroimidation reaction<sup>255-258</sup> (Scheme 4.1a). In general, these methods are well-developed and good yields are obtained, but *E/Z*-stereoselectivity remains a challenge. Additional drawbacks include structural limitations due to the use of terminal alkynes and the use of expensive Ru-catalysts.

A second approach include the palladium-catalyzed oxidative addition of alkenes to phthalimides<sup>259-262</sup> (Scheme 4.1b). This strategy has mainly been used to access *N*-vinylphthalimides (the Markovnikov product), but an *anti*-Markovnikov protocol has also been developed. The method is, however, only applicable for phthalimides, and therefore highly specialized.



**Scheme 4.1.** Main strategies for direct *N*-alkenylations of imides.

Another entry point to enamides is through copper-promoted cross-coupling reactions (Scheme 4.1c). Both vinyl-halides<sup>263, 264</sup> and vinyl-silanes<sup>265, 266</sup> have been used to access *N*-vinylimides. In particular, the use of vinyl-silanes demonstrated applicability to a wide range of imides. A significant addition to the Cu-protocol is the Chan-Lam<sup>g</sup> inspired methodology. The use of alkenylic boron coupling partners have proven to be an attractive route to enamides.<sup>143, 267-272</sup> This approach addresses some of the selectivity-issues with the other methods as it permits good control of *E/Z*-stereoselectivity. Compared to the Ru-based methods, the potential for larger structural diversity of enamides is conceivable using alkenylboronic reagents. These reagents are easily available, either commercially or by preparation.<sup>273</sup> Lastly, the use of an inexpensive Cu-catalyst is advantageous. Despite all the potential benefits the method provides, only highly substrate dependent examples have been reported.



**Scheme 4.2.** *N*-alkenylation of hydantoin derivatives using the main metal-promoted strategies.

<sup>g</sup> The Chan-Lam cross-coupling reaction was introduced in Chapter 1, Section 1.7

The main metal-promoted strategies (Scheme 4.1) have been utilized in *N*-3-alkenylation of hydantoins (Scheme 4.2). Goossen and co-workers reported a stereoselective Ru-catalyzed *anti*-Markovnikov addition of imides to alkynes (Scheme 4.2a).<sup>256</sup> Two examples of hydantoins were included in the substrate scope with varying yield and *E/Z*-selectivity. A vinylated bicyclic hydantoin was prepared in a series of reactions to obtain an anti-cancer compound (Scheme 4.2b).<sup>274</sup> A set of conditions from a reported Pd-catalyzed vinylation using vinyl acetate method was used.<sup>275</sup> The cyanogramide-hydantoin analog displayed in Figure 4.1 was *N*-alkenylated using modified Chan-Lam conditions (Scheme 4.2c).<sup>143</sup> The Cu-mediated process utilizes potassium alkenyltrifluoroborate salts as coupling partners and was first reported by Batey *et al.*<sup>268</sup> The coupling reaction failed using other conditions, but the target compound was obtained in 28 % using Batey conditions.

Two isolated examples of metal-free *N*-3-alkenylations of phenytoin have also been reported. One of the method utilizes trifluoropropenyliodonium salts for *E*-selective trifluoropropenylation.<sup>142</sup> The other method relies on *in situ* generated phosphorus ylides *via* multicomponent reactions for the *N*-alkenylations.<sup>141</sup>

Despite recent efforts in the development of protocols for *N*-alkenylation, some areas are still in the need for further development. Thus far, the lack of a general protocol for imide *N*-alkenylation is apparent, as only a few isolated examples for each method are reported. Moreover, a method that allows for better control over *E/Z*-selectivity while simultaneously allowing for the use of more structurally diverse alkenylboronic acids would be valuable.

#### 4.1.2 Boronic acids as coupling partners in cross-coupling reactions

The Chan-Lam cross-coupling reaction with arylboronic acids were introduced in Chapter 1. As displayed in Scheme 4.1, alkenylboronic acids can also serve as coupling partners under Chan-Lam conditions. Boronic acids are boron-containing organic compounds not found in nature. The first preparation and isolation of a boronic acid was reported in 1860 by Frankland.<sup>276-278</sup> Structurally, they are trivalent species containing one alkyl-, alkenyl- or aryl substituent and two hydroxyl groups (Figure 4.2a).<sup>273</sup> The sp<sup>2</sup>-hybridized boron-atom possess a vacant p-orbital which confers Lewis acidity. Consequently, the boron atom readily establishes reversible dative covalent bond with Lewis bases, *e.g.* oxygen- and nitrogen nucleophiles.<sup>279</sup> Most boronic acids exist as air-stable solids in a mixture of free boronic acid and dehydrated forms, most



often the cyclic boroxine (Figure 4.2b). Their chemical stability and ease of handling coupled with their unique reactivity make boronic acids highly attractive as reagents in organic synthesis. A supplementary trait is their low toxicity and ultimate degradation to boric acids ( $B(OH)_3$ ). As such, they can be considered “green” reagents. Several boronic acids are commercially available but can otherwise be prepared by synthesis. Numerous methods have been developed for the synthesis of boronic acids,<sup>273</sup> including borylation of aryl halides, which gives access to arylboronic acids, and hydroboration of alkynes to form alkenylboronic acids.

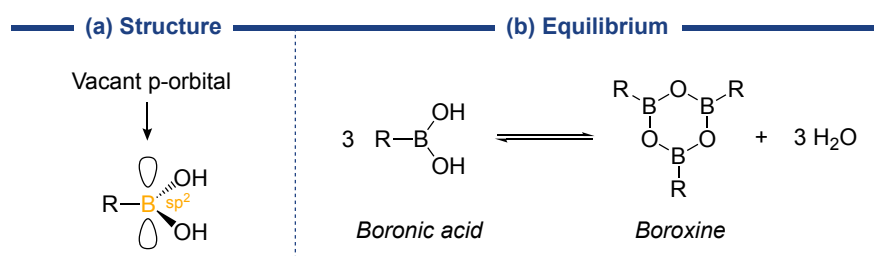
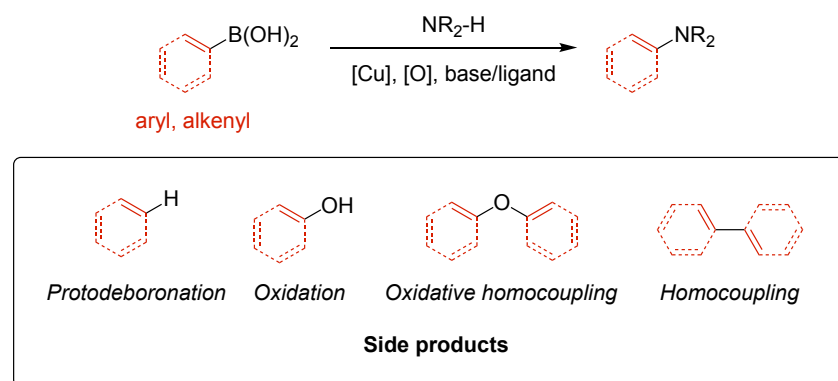


**Figure 4.2.** (a) Structure of boronic acids and (b) the dehydrative equilibrium between boronic acids and boroxines.

The Chan-Lam reaction can be hampered with competing side reactions (Scheme 4.3).<sup>135, 280</sup> The C-B bond in boronic acids is prone to undergo protolytic deboronation at higher temperatures<sup>273</sup> or in highly acidic- or basic aqueous solutions,<sup>281</sup> forming the protodeboronated product. They are also susceptible to oxidative damage by atmospheric oxidation. This process is, fortunately, kinetically slow for aryl- and alkenylboronic acids. The presence of stronger oxidants and metals can, however, increase the rate of the oxidation process.<sup>282, 283</sup> As a consequence of oxidation, and the propensity of boronic acids to couple with *O*-nucleophiles, the oxidative homocoupled product is an additional side product. Homocoupling of two boronic acids is another common side reaction.<sup>280, 284, 285</sup>



**Scheme 4.3.** Common products from side reactions in Chan-Lam coupling reactions.

Methods have been developed to mitigate these side reactions. One major method relies on “masking” the boronic acids, for example as their ester counterpart, to protect from degradation.<sup>286</sup> Hence, several boronic acid derivatives have been developed for this purpose. Some common boronic acid derivatives used in C(sp<sup>2</sup>)-N-coupling reactions<sup>132, 133, 135, 268, 269, 287-290</sup> and other cross-coupling reactions<sup>291, 292</sup> are shown in Figure 4.3.

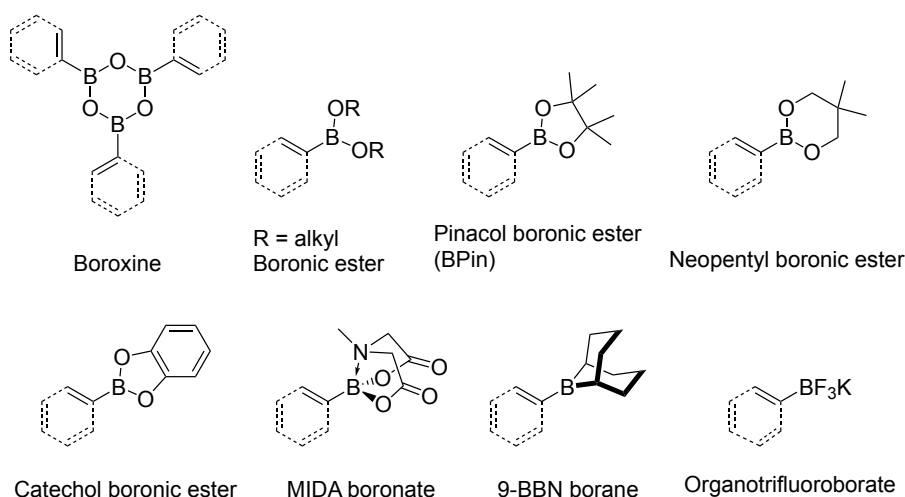


**Figure 4.3.** A selection of common boronic acid derivatives used in cross-coupling reactions.

## 4.2 Development of a method for *N*-alkenylation of imides

The lack of a more general protocol for *N*-alkenylation using the Chan-Lam methodology encouraged us to take upon the challenge to realize its full potential. The first part of this section includes the exploration, optimization and scope of the *N*-alkenylation reaction developed. Our previous work with *N*-arylation reactions (Chapter 2) prompted us to also try arylboronic acids under the conditions developed. Cu-catalyzed- or mediated *N*-arylation of hydantoins and related frameworks have been reported earlier, but sparingly.<sup>137, 289</sup> Thus, the second part of this section covers the *N*-arylation.

Most of the study is already included in Paper III. The following sections includes additional unpublished results. Due to the “*somewhat capricious nature of the reaction*”,<sup>293</sup> no general sets of conditions have been developed for the Chan-Lam reaction and careful optimization is required. Reaction parameters evaluated during the optimization include bases/ligands, catalysts, solvents and stoichiometry of the reagents. As this optimization process was considerably less demanding compared to the one in Chapter 2, the whole screening process is covered in one subsection.

### 4.2.1 Screening of reaction conditions

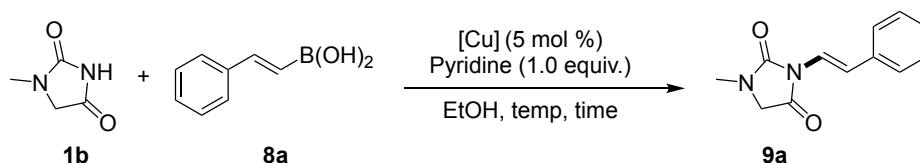
Reaction conditions were selected based on Chan-Lam type *N*-alkenylations previously reported,<sup>143, 267-272</sup> which comprise a Cu-salt, oxidant, often an amine-base and a suitable solvent. The optimization was initiated using 1-methylhydantoin **1b** as a model substrate and commercially available (*E*)-styrylboronic acid **8a** as coupling partner. Due to potential side product formation (see Scheme 4.3) an excess of boronic acid (3.0 equivalents) was used. The reaction was carried out in the presence of catalytic amounts of Cu(OTf)<sub>2</sub> using pyridine as ligand/base and ethanol as a solvent to ensure solubility, at slightly elevated temperature (40 °C). Access to air was paramount and ensured during all the reactions.

The reaction proceeded effectively and 98 % of the desired *N*-3-styrylated **9a** was afforded (Table 4.1, entry 1). Reducing the temperature to 25 °C was equally efficient as 97 % of **9a** was isolated, providing longer reaction times (Table 4.1, entry 2). The process was also effective using 2.0 equivalents of the boronic acid (Table 4.1, entry 3), so less reagent can be used if a slight reduction in yield is acceptable. A further reduction of the reagent equivalents was not favorable as a severe reduction in yield was seen (Table 4.1, entries 4-7). The stereochemistry of the alkene was retained in all reactions.

Less expensive Cu-salts were also evaluated. Cu(NO<sub>3</sub>)<sub>2</sub> · 2.5 H<sub>2</sub>O (Table 4.1, entry 8) was equally efficient as Cu(OTf)<sub>2</sub>, while CuCl<sub>2</sub> was less active and only 77 % of **9a** was obtained. Surprisingly, Cu(I)-catalyst CuCl (Table 4.1, entry 10) was just as effective as Cu(NO<sub>3</sub>)<sub>2</sub> · 2.5 H<sub>2</sub>O, while CuI failed to catalyze the reaction (Table 4.1, entry 11).

No correlation between effectiveness of the salt and its oxidation state is apparent from these results. The differences can rather be attributed to the counter anions. Studies suggest that the counter anions play an important role in formation of an active dinuclear copper-boron complexes during the catalytic cycle.<sup>280, 294, 295</sup> Control reactions (Table 4.1, entries 12-15) showed the dependence of the Cu-catalyst and base as the reaction did not proceed in the absence of either.

**Table 4.1.** Screening of reaction conditions



#	[Cu]	<b>8a</b> (equiv.)	Base/additive (equiv.)	Solvent	Temp (°C)	Time (h)	Yield (%) <sup>[a]</sup>
<b>Equivalents of styrylboronic acid</b>							
1	Cu(OTf) <sub>2</sub>	3.0	Pyridine (1.0)	EtOH	40	9	98
2	Cu(OTf) <sub>2</sub>	3.0	Pyridine (1.0)	EtOH	25	15	97 <sup>[b]</sup>
3	Cu(OTf) <sub>2</sub>	2.0	Pyridine (1.0)	EtOH	25	24	94
4	Cu(OTf) <sub>2</sub>	1.5	Pyridine (1.0)	EtOH	40	24	45
5	Cu(OTf) <sub>2</sub>	1.0	Pyridine (1.0)	EtOH	25	24	41
6	Cu(OTf) <sub>2</sub>	1.0	Pyridine (1.0)	EtOH	40	24	71
7	Cu(OTf) <sub>2</sub>	0.5	Pyridine (1.0)	EtOH	40	24	28
<b>Other Cu-catalysts</b>							
8	Cu(NO <sub>3</sub> ) <sub>2</sub> <sup>[c]</sup>	3.0	Pyridine (1.0)	EtOH	25	24	96
9	CuCl <sub>2</sub>	3.0	Pyridine (1.0)	EtOH	25	24	77
10	CuCl	3.0	Pyridine (1.0)	EtOH	25	24	95
11	CuI	3.0	Pyridine (1.0)	EtOH	25	24	0
<b>Control reactions</b>							
12	Cu(OTf) <sub>2</sub>	3.0	-	EtOH	40	23	8
13		3.0	Pyridine (1.0)	EtOH	40	24	0
14		3.0	Pyridine (1.0)	EtOH	80	24	0
15		3.0	-	EtOH	80	23	0

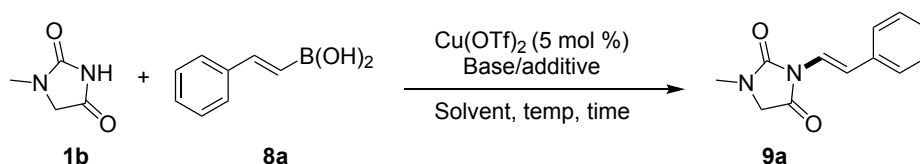
Conditions: 1-Methylhydantoin **1b** (0.20 mmol, 1.0 equiv.), boronic acid **8a** (as specified), catalyst (0.010 mmol, 0.050 equiv.), additive/base (as specified) in solvent EtOH (1 mL). [a] <sup>1</sup>H NMR yield using Mes as IS. [b] Isolated yield. [c] The (hemi)pentahydrate salt was used.

Equimolar amounts of pyridine and hydantoin ensured full conversion and near quantitative yield. Reducing the amount of pyridine to 0.2 equivalents (Table 4.2, entry 1) reduced the yield of **9a** to 47 %. The bulky 2,6-di-*tert*-butylpyridine (DTBP) did only provide 8 % of **9a** (Table 4.2, entry 2). These results are pointing towards deprotonation by a pyridine-copper complex (as is suggested during the

disproportionation step in the catalytic cycle, Scheme 4.10), rather than a direct deprotonation of the hydantoin. Other amine bases (Table 4.2, entries 3-5) and inorganic bases (Table 4.2, entries 6-10) suppressed the reaction to varying extents.

The strong solvent dependence<sup>296</sup> in Chan-Lam type coupling reactions was evident during a short screening of solvents. *i*-PrOH was less effective than EtOH, but 83 % of **9a** was obtained from the reaction (Table 4.2, entry 11). Aprotic solvents such as DMF (Table 4.2, entry 12) and toluene (Table 4.2, entry 13) were inefficient in the process, attesting to the need of a polar protic solvent.

**Table 4.2.** Screening of bases.



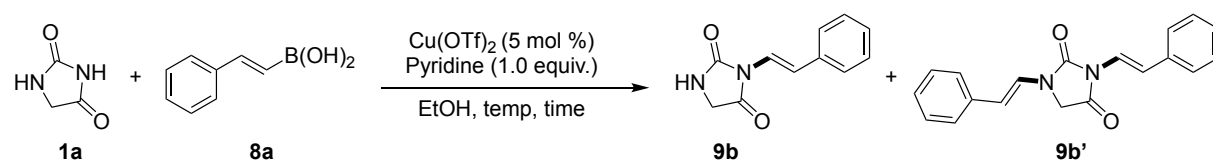
#	<b>8a</b> (equiv.)	Base/additive (equiv.)	Solvent	Temp (°C)	Time (h)	Yield (%) <sup>[a]</sup>
1	3.0	Pyridine (0.2)	EtOH	25	18	47
2	3.0	DTBP <sup>[b]</sup> (1.0)	EtOH	25	24	8
3	3.0	DIPEA (1.0)	EtOH	25	16	1
4	3.0	chxn <sup>[c]</sup> (1.0)	EtOH	25	16	0
5	3.0	Et <sub>3</sub> N (1.0)	EtOH	25	18	8
6	3.0	K <sub>2</sub> CO <sub>3</sub> (1.0)	EtOH	25	18	25
7	3.0	K <sub>2</sub> CO <sub>3</sub> (1.0)	EtOH	40	18	52
8	3.0	<i>t</i> -BuOK (1.0)	EtOH	25	18	22
9	3.0	LHMDS (1.0)	EtOH	25	18	3
10	3.0	LHMDS (1.0)	THF	25	24	0
11	3.0	Pyridine (1.0)	<i>i</i> -PrOH	25	24	83
12	3.0	Pyridine (1.0)	DMF	25	24	26
13	3.0	Pyridine (1.0)	Toluene	25	24	0

Conditions: *N*-Methylhydantoin **1b** (0.20 mmol, 1.0 equiv.), boronic acid **8a** (0.60 mmol, 3.0 equiv.), Cu(OTf)<sub>2</sub> (0.010 mmol, 0.050 equiv.), additive/base (as specified) in solvent (as specified, 1 mL). [a] <sup>1</sup>H NMR yield using Mes as IS. [b] DTBP = 2,6-di-*tert*-butylpyridine. [c] chxn = *trans*-1,2-diaminocyclohexane.

While the N-1 position of **1b** is substituted and blocked, the same site in **1a** is unsubstituted and thus a potential site for alkenylation. With the optimized conditions at hand for 1-methylated **1b**, we were interested to see if unsubstituted hydantoin **1a** could be regioselectively alkenylation in the N-3 position.

The first reaction was performed at 40 °C for 18 hours using 3 equivalents of the boronic acid (Table 4.3, entry 1). The crude reaction mixture was analyzed using <sup>1</sup>H NMR spectroscopy and revealed the possible formation of the bis-styrylated **9b'**. Only 58 % of the desired **9b** was isolated from this reaction. The reaction time was then reduced in an effort to obtain a more favorable **9b:9b'** ratio (Table 4.3, entry 2), working from the assumption that *N*-3-coupling occurs prior to *N*-1-coupling. Both products were isolated, and the identity of second product was confirmed as the bis-styrylated **9b'**. Further efforts to suppress formation of **9b'** included reduction of temperature and amount of coupling partner (Table 4.3, entries 3-5). The final set of optimized conditions (Table 4.3, entry 5) for unsubstituted hydantoin include 2 equivalents of **8a** and 25 °C, which afforded **9b** in 77 %.

**Table 4.3.** Optimization of reaction conditions for unsubstituted hydantoin.



#	<b>8a</b> (equiv.)	Temp (°C)	Time (h)	<b>9b:9b'</b> <sup>[a]</sup>	Yield <b>9b</b> (%) <sup>[b]</sup>	Yield <b>9b'</b> (%) <sup>[b]</sup>
1	3.0	40	18	2.5 : 1.0	58	-
2	3.0	40	6.5	2.5 : 1.0	68	30
3	2.0	40	8	4.4 : 1.0	-	-
4	3.0	25	8	6.5 : 1.0	70	-
5	2.0	25	19	4.8 : 1.0	77	-

Conditions: Hydantoin **1a** (0.4 mmol, 1.0 equiv.), *(E)*-styrylboronic acid **8a** (as specified), Cu(OTf)<sub>2</sub> (0.020 mmol, 0.050 equiv.), pyridine (0.40 mmol, 1.0 equiv.) and EtOH (2 mL). [a] <sup>1</sup>H NMR integral ratio of C-5 protons. [b] Isolated yield.

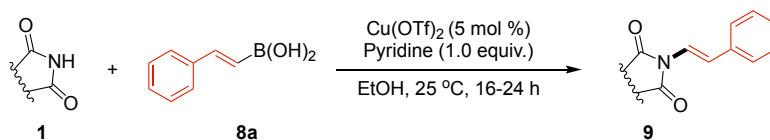
## 4.2.2 Scope and limitations of the developed reaction

With the optimized conditions for both substituted and unsubstituted hydantoins, the scope and limitations of the reaction was investigated. The following subsections will include *N*-alkenylation of various hydantoins and imides using a selection of alkenylboronic acids. Most of the structures are included in Paper III, but **9b'**, **9i**, **9n'**, and **15m** are additional structures included herein. Furthermore, discussion around side product formation, mechanism, and unexpected results, none of which were included in Paper III are also included. The pool of coupling partners was also expanded to include arylboronic acids and derivatives, which constitute the second part of this scope and limitations section. Non-commercial alkenylboronic acids and arylboroxines were prepared according to literature procedures.<sup>297-299</sup>

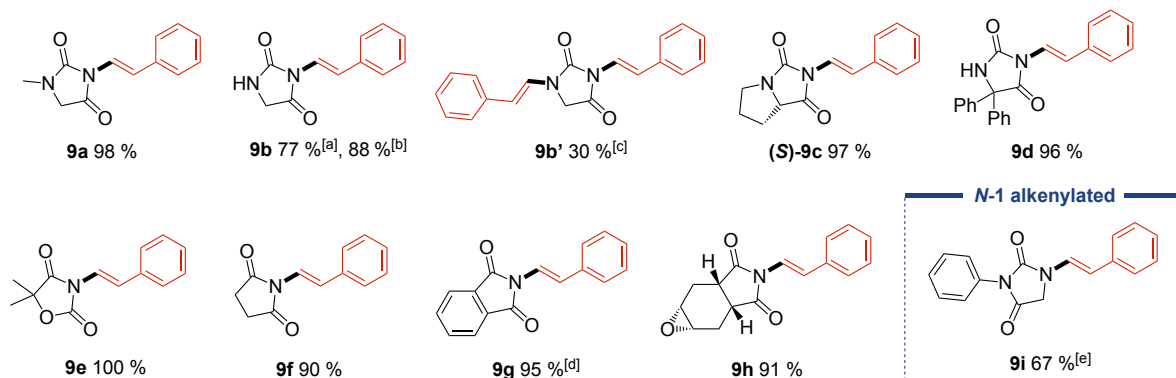
### 4.2.2.1 Substrate scope: Hydantoins and imides

We first sought to explore the styrylation with a wide range of imides (Scheme 4.4). As previously seen, 98 % of **9a**, 77 % of unsubstituted **9b** and 30 % of the bis-styrylated **9b'** was afforded during the optimization. Increasing the scale of the reaction (from 0.4 mmol to 1.5 mmol) had a positive outcome and 88 % of **9b** was isolated. *L*-proline-derived hydantoin (**S**)-**9c** was smoothly styrylated in 97 % yield with retention of the C-5 stereocenter. The structural similarities of the hydantoins suggest that our conditions could be a good alternative for the Batey-coupling of the hydantoin-cyanogranide (Scheme 4.2c). The anti-convulsant phenytoin was also pleasingly styrylated in excellent yields (**9d**, 96 %).

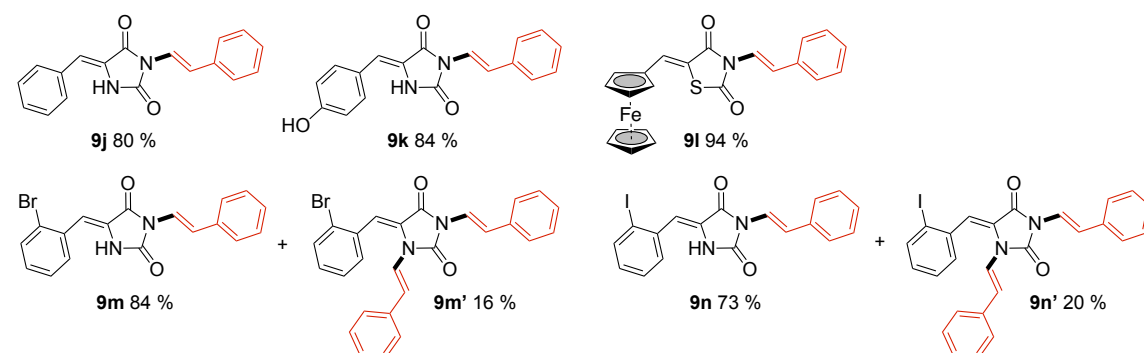
Other five-membered imides, including oxohydantoin, succinimide and phthalimide **9e-9g**, were also obtained in excellent yields (90-100 %). The mildness of the reaction was demonstrated with the epoxidated tetrahydrophthalimide. Ring-opening of epoxides in the presence of boronic acids have been reported,<sup>300, 301</sup> but fortunately, our reaction proceeded without ring-opening of the epoxide and **9h** was isolated in 91 % yield. 3-Phenylhydantoin **3a** was subjected to the conditions. Only 67 % of **9i** was isolated, yet again demonstrating the challenge of functionalizing the N-1 site.



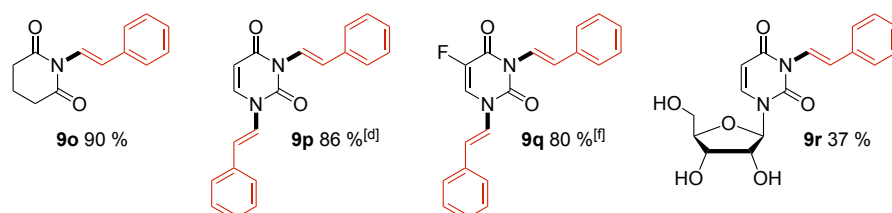
#### Hydantoin and 5-membered imides



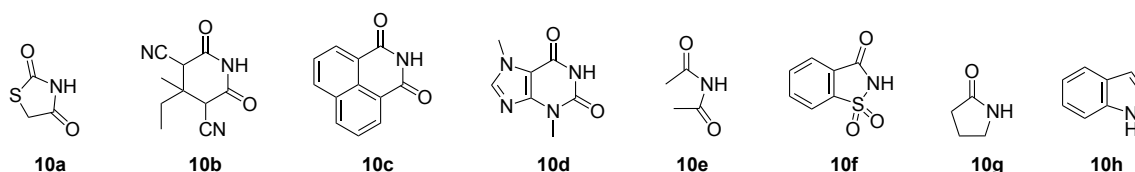
#### 5-arylidenehydantoin



#### Uracils and 6-membered imides



#### Unsuccessful



**Scheme 4.4.** Hydantoin- and imide scope. Conditions: imide **1** (0.40 mmol, 1.0 equiv.), boronic acid **8a** (1.2 mmol, 3.0 equiv.), Cu(OTf)<sub>2</sub> (0.020 mmol, 0.050 equiv.), pyridine (0.40 mmol, 1.0 equiv.) and EtOH (2 mL). [a] 2.0 equiv. boronic acid **8a** was used. [b] Reaction performed at 1.5 mmol scale. [c] Reaction performed at 40 °C for 6.5 h. [d] Reaction performed at 0.40 and 1.0 mmol scale. [e] Reaction performed at 0.2 mmol scale. [f] 4.0 equiv. boronic acid **8a** was used.

A series of 5-arylidenehydantoin were subjected to the conditions and alkenylated in excellent yields (**9j-9n'**). **9k** with a free hydroxy-group was pleasingly *N*-3-alkenylated



and not *O*-alkenylated. Expectedly, some *N*-1-alkenylation was observed in addition to the desired *N*-3-alkenylation, but only for the brominated- and iodinated substrate **9m** and **9n**. **9m'** and **9n'** were additionally isolated. Cu-catalyzed Suzuki-Miyaura cross-couplings with boronic acids/esters and aryl halides have been reported.<sup>302-305</sup> No aryl halide couplings were observed under our conditions. Inspired by recent *N*-arylations of ferrocenyl 2,4-thiazolidinedione (2,4-TZD) conjugates,<sup>306</sup> **9i** was alkenylated and successfully isolated in 94 %.

Our protocol was extended to include 6-membered imides. Glutarimide **9o** was efficiently alkenylated in 90 %. Uracils are privileged structures in drug development.<sup>307</sup> Bis-alkenylation of uracil and the chemotherapeutic agent 5-fluorouracil provided **9p** and **9q** in excellent yields. Mono-alkenylation was not possible under our conditions, even when reducing the amount of boronic acid. The nucleoside uridine **9r** was isolated in modest yields without any *O*-alkenylation. These results highlight the possibility of accessing drugs and nucleosides otherwise cumbersome to access.<sup>266, 308</sup>

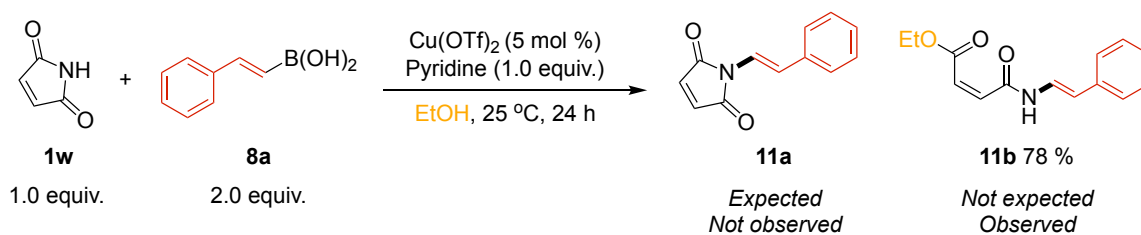
A range of *N*-nucleophiles (**10a-10h**) were not tolerated under our conditions. The successful alkenylation of ferrocenyl 2,4-TZD **9i** led us to believe 2,4-TZD **10a** could be alkenylated, but no reaction occurred. We theorize that the absence of a bulky ferrocenyl side-arm might have facilitated coordination of the sulfur atom to the Cu-center, preventing it from its catalytic function. Moreover, no reactions were observed with the 6-membered imides **10b**, **10c** and theobromine **10d**. Linear imide **10e** also failed to react, revealing the methods dependence on cyclic imides. As suggested by Wasielewski *et al.*<sup>309</sup> the carbonyl groups in imide **10e** can adopt a parallel, coplanar confirmation and chelate to the Cu<sup>II</sup>-center.<sup>310</sup> The chelation may attenuate the catalytic activity of copper and/or the reactivity of the imide. Cu-coordination was likely also the reason for saccharin **10f** to fail. A blue precipitate was formed during the reaction, indicating the possible formation of a stable Cu<sup>II</sup>-saccharin specie.<sup>311, 312</sup>

The alkenylation of the amidic position of hydantoin in **9i** suggested a possible successful alkenylation of cyclic amide **10g**. <sup>1</sup>H NMR analysis of the post-reaction mixture indicated formation of the product, but all isolation attempts failed for unknown reasons. Lastly, indole **10h** was not a suitable substrate for our conditions.

In all the successful alkenylations, complete retention of the (*E*)-alkene double bond was observed in all cases, highlighting control of the *E/Z*-stereoselectivity. Pleasingly, no isomerization of the (*Z*)-double bonds in 5-arylidenehydantoins were observed.

#### 4.2.2.2 Substrate scope: Maleimide

The unsaturated analog of succinimide **1i**, maleimide **1w** was also subjected to our conditions (Scheme 4.5). In accordance with the results in Scheme 4.4, the *N*-alkenylated maleimide **11a** was the expected product of the reaction. However, upon isolation and identification, **11a** was not seen. The product of the reaction was identified as the ring-opened and *N*-alkenylated maleimide ethyl ester **11b**. The formation of the unexpected product gave rise to a new project which is further described in Chapter 5.

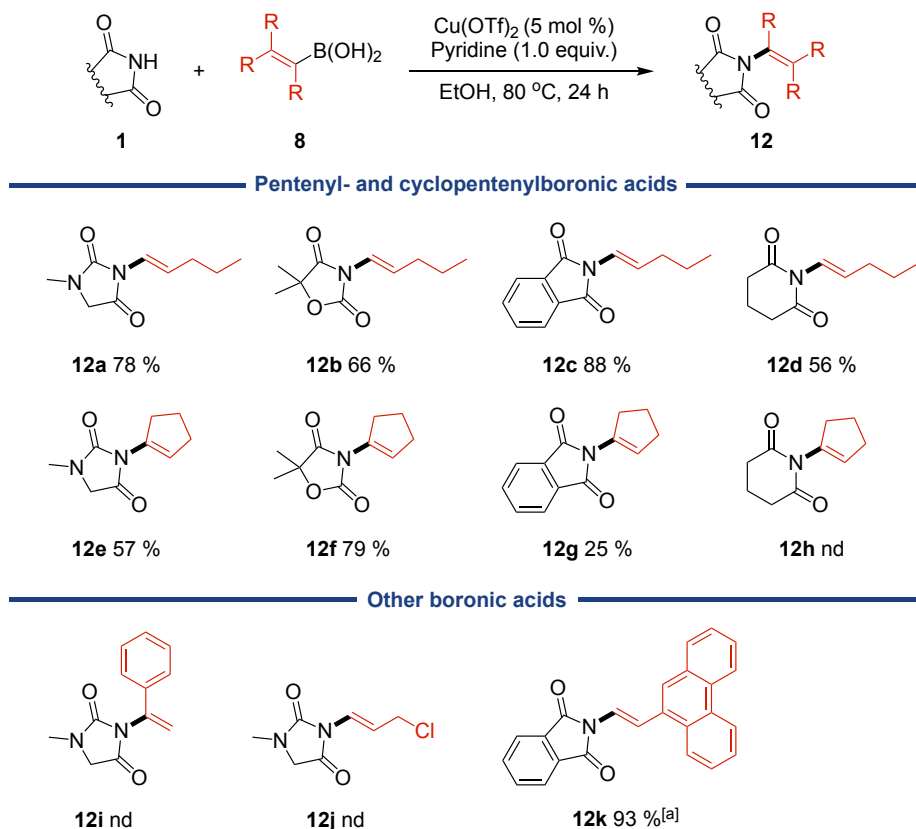


**Scheme 4.5.** *N*-alkenylation of maleimide **1w** and formation of the unexpected ring-opened product **11b**.

#### 4.2.2.3 Substrate scope: Alkenylboronic acids

A selection of alkenylboronic acids were investigated with some imides (Scheme 4.6). The use of pentenyl- and cyclopentenylboronic acids required higher reaction temperatures (80 °C) as they were less reactive than their styryl counterparts.

Overall, the yields were lower for the pentenyl- and cyclopentenylboronic acids **8b** and **8c** than for the styrylboronic acid **8a**. By comparing the  $^1\text{H}$  NMR chemical shifts of the alkene protons belonging to pentenyl- and styrylboronic acid, higher shifts are found for the styryl protons. An upfield shift change of 0.85 ppm can be seen in the pentenylboronic acid, indicating a higher electron density around the pentenyl double bond compared to the styryl double bond. Consequently, electrons are more easily donated towards the vacant p-orbital of boron, which in turn increases the double bond character of the C-B bond. With higher double bond character, more energy is required for bond breaking to occur. Alternatively, a higher energy barrier is seen in the Lewis pairing step in the catalytic cycle (see Scheme 4.10). We believe these are the reasons for the inferior performance and requirement for higher temperatures for the **8b** and **8c** compared to **8a**.



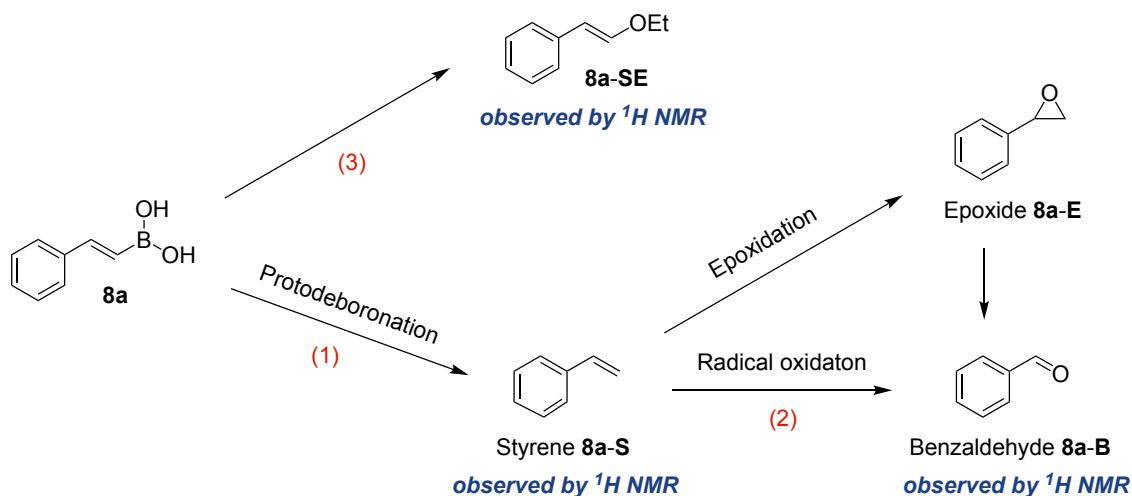
**Scheme 4.6.** Alkenylboronic acid scope. Conditions: imide **1** (0.40 mmol, 1.0 equiv.), boronic acid **8b-8f** (1.2 mmol, 3.0 equiv.), Cu(OTf)<sub>2</sub> (0.020 mmol, 0.050 equiv.), pyridine (0.40 mmol, 1.0 equiv.) and EtOH (2 mL). [a] Reaction was performed at 0.18 mmol scale at 25 °C.

The performance of the coupling varied within the boronic acids and the imide substrates. Pentenylboronic acid **8b** was transferred in good yields to hydantoin and oxohydantoin, affording **12a** and **12b** in 78 % and 66 %, respectively. Phthalimide **12c** was isolated in very good yields (88 %), while a significant reduction in yield was seen with glutarimide **12d**. The cyclopentenylboronic acid **8c** was more challenging, likely due to its more sterically demanding arrangement around the Cu-center. **12e** and **12f** were obtained in average to good yields, while phthalimide **12g** was only isolated in 25 %. For reasons unknown, transfer of cyclopentenylboronic **8c** to glutarimide was not detected. Thus, no **12h** was isolated. Despite the moderate results, access to 1,1,2-trisubstituted alkenes can be obtained, previously inaccessible with the Ru-based methods mention in Section 4.1.1. 1-Phenylvinylboronic acid **8d** and the chlorinated boronic acid **8e** failed to react. Based on the lasting green color of the reaction solution, a stable Cu-complex was likely formed with **8d**. The result was, however, not surprising with **8d** being more sterically demanding than the cyclopentenylboronic acid **8c**. Boronic acid **8e** failed to react due to decomposition. In contrast to the previous boronic acids, phenanthreneboronic acid **8f** was effective and **12k** was obtained in 93 % yield.

#### 4.2.2.4 Side product formation in the *N*-alkenylation reactions

Boronic acids propensity to partake in competitive side reactions was briefly discussed in Section 4.1.2. Although not detrimental, side reactions were observed under our conditions. As demonstrated during the optimization, 2.0-3.0 equivalents of the boronic acid were essential for reaction completion and optimal yields. A reduction to 1.5 equivalents had a negative impact on both conversion of the starting material and the obtained yields (see Table 4.1). These side reactions might contribute to the need for > 1.5 equivalents of **8a**.

Scheme 4.7 presents observed side products from various reactions and plausible pathways from styrylboronic acid **8a**. (1): Styrene **8a-S** was observed in the commercially obtained **8a** (experimental section, Figure 4.13). Likely due to being exposed to the atmosphere and stored over time without any precautions. In fresh, “homemade” batches of **8a**,<sup>313, 314</sup> no styrene was visible, but protodeboronation can be Cu-induced.<sup>135</sup> No styrene was seen in the <sup>1</sup>H NMR analysis of the post-reaction mixtures, likely due to its reactive nature.



**Scheme 4.7.** Proposed pathways to observed side products.

(2): Regardless of the reaction outcome, benzaldehyde **8a-B** was always detected in the <sup>1</sup>H NMR analysis of the post-reaction mixture (experimental section, Figure 4.10). Formation of **8a-B** might take place directly from the styrene *via* a radical oxidation mechanism, or *via* the epoxide **8a-E**. No epoxide was, however, detected in the <sup>1</sup>H NMR analysis of the post-reaction mixture. (3): A product observed in all the post-reaction mixtures was identified as the styrylether **8a-SE** (experimental section, Figure 4.12). We expected to observe the ethoxyboronic ester, as esterification of boronic acids

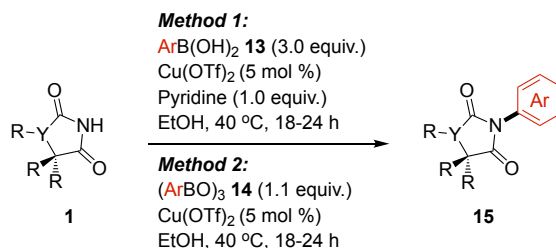
in the presence of alcohols is common.<sup>273</sup> However, they often require harsher conditions.<sup>315, 316</sup> Formation of **8a-SE** directly from (*E*)-styrylboronates have been reported under very similar conditions (Cu-catalyst, amine base and EtOH at 25 °C).<sup>317</sup>

#### 4.2.2.5 Substrate scope: Arylboronic acids

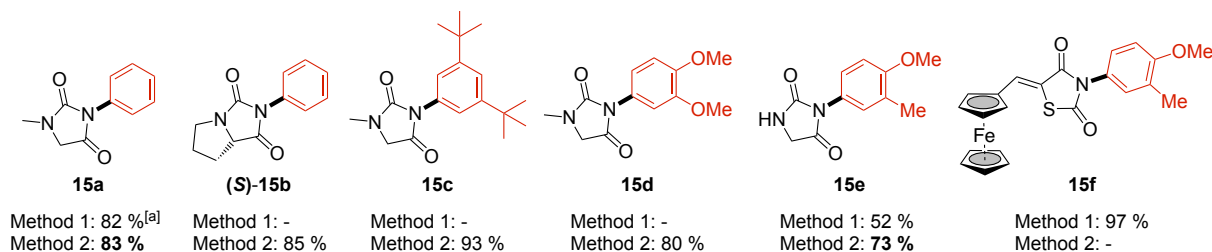
After the alkenylation study, we proceeded to expand the scope to include arylboronic acids. Additionally, we also explored arylboroxines as coupling partners, which can be prepared by simple dehydration of the arylboronic acids. The use of boroxines as coupling partners is well documented. Studies have compared boroxines and their parent boronic acids in cross-coupling reactions and found the boroxines to be of superior reactivity.<sup>267, 289, 318, 319</sup>

Method 1 relied on the combination of boronic acids and pyridine to furnish the desired products, while no pyridine was required when using boroxines (method 2). Our method was overall high yielding and tolerable to diverse aryl groups, including heterocycles (Scheme 4.8). 1-Methylhydantoin **1b** was phenylated using both methods in equal yields, while (*S*)-**15b** was obtained using phenylboroxine. Electron-rich aryl groups were smoothly transferred by boroxines to give hydantoins **15c-15e** in very good to excellent yields **15e** was also arylated using the boronic acid, but a reduction in yield from 73 % to 52 % was observed. Ferrocenyl 2,4-TZD was only arylated with boronic acid and the electron-rich **15f** was successfully isolated in 97 % yield.

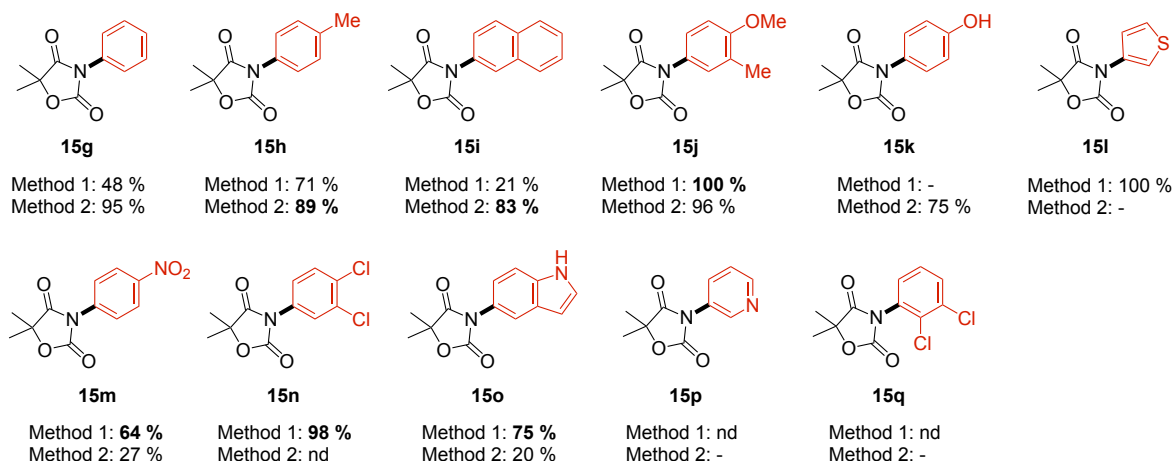
Phenylation of oxohydantoin **15g** was significantly impacted by choice of method. The boroxine was again the superior arylating agent, and 95 % (against 48 % from the boronic acid) of **15g** was afforded. The electron-neutral- and rich **15h-15l** were isolated in very good yields using boroxines as aryl source, while the electron-poor **15m** and **15n** were isolated in good yields using the boronic acids. Indole **15o** was also successfully arylated with the boronic acid without arylation of the indole nitrogen atom. Pyridyl- and *ortho*-substituted aryl groups were not suitable under our conditions as no **15p** nor **15q** were formed.



#### Hydantoins and 2,4-TZD



#### Oxohydantoins<sup>[b]</sup>



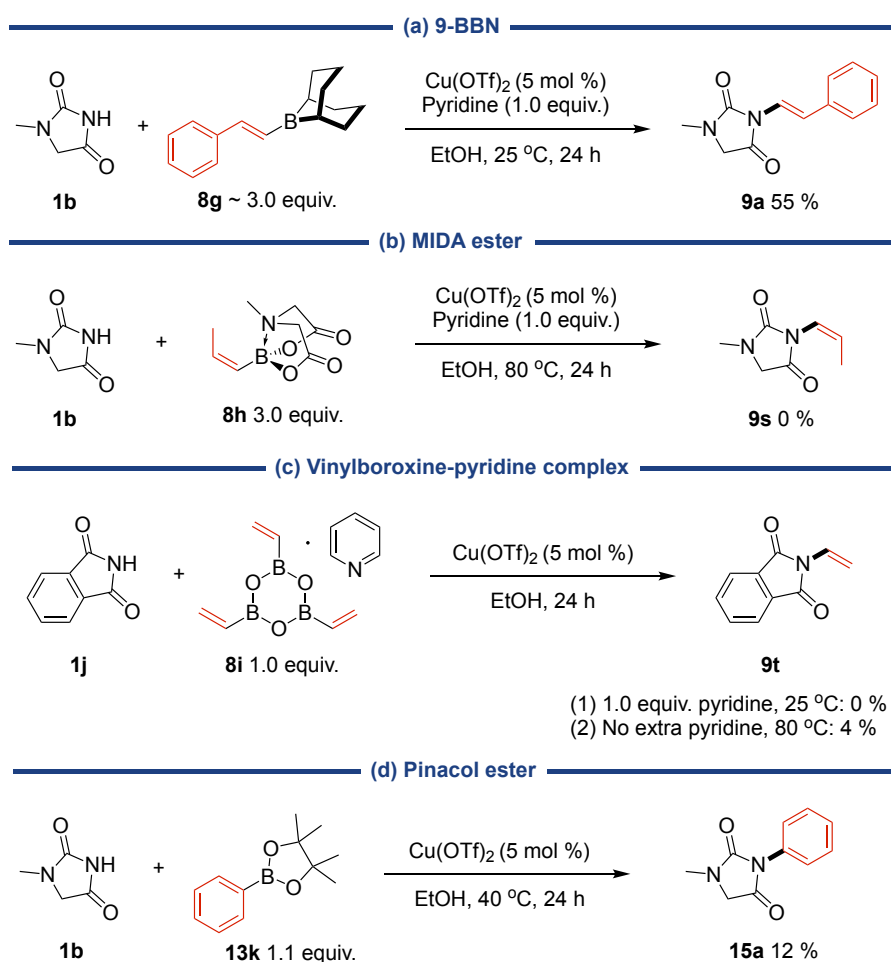
**Scheme 4.8.** Arylboronic acid scope. **Method 1:** imide **1** (0.40 mmol, 1.0 equiv.), boronic acid **13a-13j** (1.2 mmol, 3.0 equiv.), Cu(OTf)<sub>2</sub> (0.020 mmol, 0.050 equiv.), pyridine (0.40 mmol, 1.0 equiv.). **Method 2:** imide **1** (0.40 mmol, 1.0 equiv.), boroxine **14a-14i'** (0.44 mmol, 1.1 equiv.), Cu(OTf)<sub>2</sub> (0.020 mmol, 0.050 equiv.). [a] No pyridine was used. [b] Reactions were performed on a 0.14 mmol scale. nd: reaction was attempted, but the product was not detected. -: reaction not attempted.

Based on these results, it is hard to draw any conclusion as to which method operates best with which substrate. The dynamic behavior of boronic acids must be taken into consideration. Depending on the substituents of the aryl groups, the equilibrium constant varies. A study<sup>320</sup> has shown that EDGs supports boroxine formation while EWGs destabilizes the boroxine relative to its parent boronic acid. Additionally, pyridine can partake in ligand-facilitated formation of boroxines.<sup>321</sup> Without any measurements taken during our reactions, it is impossible to imply whether the active arylating agent is in fact the free acid or the anhydride. Nevertheless, the protocol developed give access to a range of arylated hydantoins, including very electron-rich

ones, which was challenging with our previous diaryliodonium salt-based method (Chapter 2). Additionally, oxohydantoin could be arylated with both electron-rich and electron-poor arenes in very good to excellent yields. Only one such protocol regarding the arylation of oxohydantoin has been previously reported.<sup>322</sup>

### 4.2.3 C(sp<sup>2</sup>)-N coupling reactions with other boronic acid derivatives

Other boronic acid derivatives were evaluated as coupling partners (Scheme 4.9). Alkylborane reagent (*E*)-styryl-9-BBN **8g** have been utilized as alkenylation agent in C-C bond-forming reactions,<sup>323-326</sup> but no C-N bond-formation has been reported. **8g** was prepared<sup>299</sup> in a THF-solution and used as such (Scheme 4.9a). **8g** was less effective than the boronic acid and only 55 % of **9a** was isolated.



**Scheme 4.9.** *N*-Alkenylation- and arylation of imides with boronic acid derivatives. All reactions were performed on a 0.2 mmol scale using 1 mL of EtOH.

The MIDA-protected *cis*-propenyl boronate ester **8h** (Scheme 4.9b) have only been used as coupling partner in Suzuki-Miyaura C-C cross-couplings.<sup>327-329</sup> **8h** failed to furnish the desired product **9s** under our conditions.

We desired to expand the alkenylation scope to include the vinyl group (Scheme 4.9c). The instability of vinylboronic acid<sup>330, 331</sup> and our previous success using arylboroxines as coupling partners encouraged us to utilize trivinylboroxine **8i** as vinyl source. Two reactions were carried out, but only 4 % of the desired **9t** was obtained at best. Phthalimide **1j** has been successfully vinylylated with **8i**, but under another set of conditions.<sup>267</sup>

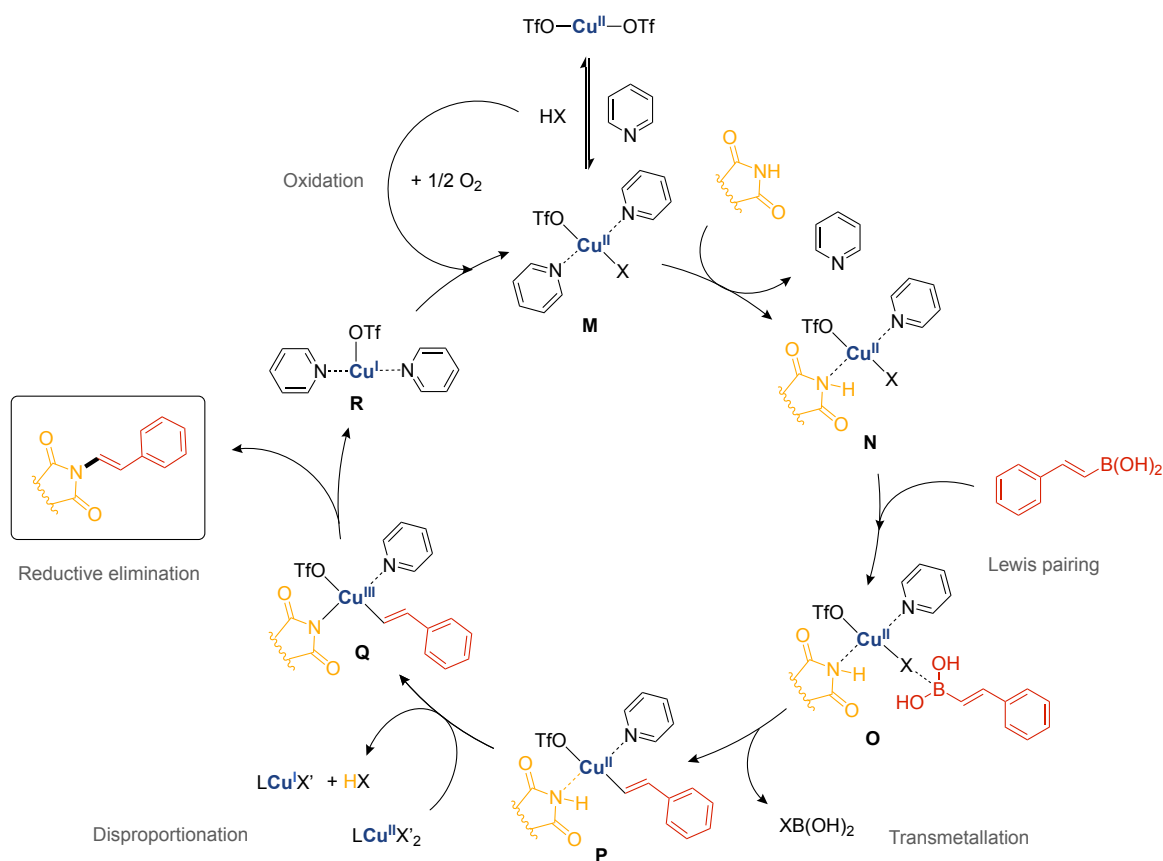
Aryl pinacol boronic (BPin) esters are frequently used as aryl sources.<sup>130, 135, 288, 332, 333</sup> The performance of **13k** under our conditions (Scheme 4.9d) was inferior and only 12 % of **15a** was isolated. Reactivity issues with BPin compounds due to catalyst inhibition by pinacol (generated by hydrolysis of the starting material) have been reported<sup>135</sup> and might be the cause of the inefficiency.

#### 4.2.4 Reaction mechanism: Proposal of a catalytic cycle

No extensive investigation for the reaction mechanism was done in this work. Regardless, a proposed mechanism based on previous reports and observations during the optimization study is given in Scheme 4.10. The mechanism of the arylation reactions will not be covered as they are only secondary to the alkenylation reactions.

A brief study was conducted to investigate the role of pyridine in the reaction. Pyridine is known to partake in ligand-facilitated formation of the boroxines.<sup>321</sup> Clear indication of pyridine-boron coordination of vinylboronic acid (and hence boroxine formation) has been reported.<sup>331</sup> <sup>1</sup>H NMR spectroscopic analysis of boronic acid-pyridine mixture showed significant downfield chemical shift changes of the pyridine protons upon coordination. Our <sup>1</sup>H NMR spectra (experimental section, Figure 4.14-4.16) revealed only slight upfield changes ( $\Delta\delta$  0.1–0.2 ppm) in the mixture of styrylboronic acid **8a** and pyridine. Broadening of the  $\alpha$ -alkene proton of the styrylboronic acid (and boroxine) was seen, indicating a dynamic process. Ultimately, the lack of strong evidence of pyridine-facilitated boroxine formation is likely favoring the boronic acid as the reacting specie. Additionally, no consideration was taken to ensure dry conditions in any of our reactions. The presence of water pushes the equilibrium towards formation of the boronic acid.





**Scheme 4.10.** Proposed catalytic cycle for the *N*-alkenylation of imides using boronic acids. X and X' = OTf, OH or OEt, L = unknown ligand as the ligation state of the  $\text{Cu}^{\text{II}}$ -oxidant in the disproportionation step remains unknown.<sup>130</sup>

Studies suggest displacement of the anion, most likely by the solvent, for the formation of the active catalyst.<sup>135, 280, 334</sup> Whether one or both triflate anions ( $^-\text{OTf}$ ) are displaced, and whether it is by the solvent or water is in this case not known. However, the choice of solvent was paramount in this reaction, as a polar protic solvent was required (see Table 4.2). Addition of pyridine to the solution induced a rapid color change from blue to dark green. As previous mechanistic studies suggest the active catalyst to possess a square planar geometry, we suggest the active  $\text{Cu}^{\text{II}}$ -species **M**. Subsequent replacement of one pyridine unit with the nucleophile gives intermediate **N**.

Lewis pairing include the coordination of one of the anionic ligands (either OTf or X) to the empty p-orbital of the boron atom in the boronic acid/boroxine. **O** can then undergo transmetalation to obtain **P**. During the disproportionation step, the substrate is deprotonated and an acid (HX) is generated. A base, presumably pyridine, is required to mitigate re-protonation of the substrate. The  $\text{Cu}^{\text{II}} \rightarrow \text{Cu}^{\text{III}}$  oxidation generates  $\text{Cu}^{\text{III}}$ -species **Q** which upon reductive elimination delivers the desired product and  $\text{Cu}^{\text{I}}$ -species **R** that is oxidized **M** for completion of the catalytic cycle.

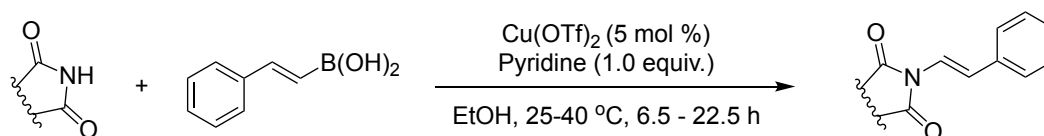
### 4.3 Conclusion

A general and highly efficient Cu-catalyzed strategy for C(sp<sup>2</sup>)-N bond forming with cyclic imides has been developed. The method enables the preparation of (*E*)-enimides, using (*E*)-alkenylboronic acids, in excellent yields under mild and practical conditions. A broad range of cyclic 5- and 6-membered imides are well accepted and di- and tri-substituted alkenylboronic acids can be utilized. Retention of alkene double bond configurations were seen in all cases. The method also enables the preparation of *N*-arylimides using arylboronic acids as coupling partners. High functional group tolerance is displayed as both halogen-, hydroxy-, epoxide- and iron containing compounds and a selection of heterocycles are well tolerated. The usefulness of the strategy is exemplified by diversification of the nucleoside uridine and pharmaceutically relevant agents such as phenytoin and 5-fluorouracil.

### 4.4 Experimental

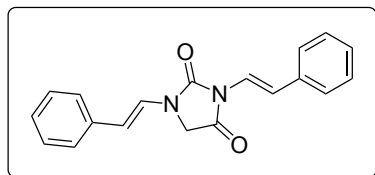
Experimental details and data for compounds not included in Paper III are described herein. Information about reagents, solvents and instrumentation are covered in the supporting information to Paper III.

#### Synthesis and characterization of *N*-alkenylhydantoin



Hydantoin (0.40 mmol, 1.0 equiv.), (*E*)-styrylboronic acid (0.60 mmol, 3.0 equiv.), Cu(OTf)<sub>2</sub> (7.2 mg, 0.020 mmol, 0.050 equiv.) and ethanol (2 mL) were added to a 5 mL round-bottom flask equipped with a magnetic stir bar. Pyridine (32  $\mu$ L, 0.40 mmol, 1.0 equiv.) was added via a syringe, a cooler was connected to the flask and the mixture was stirred with access to air at the indicated temperature (25-40 °C) and time (6.5 - 22.5 h) The crude mixture was either purified by filtration followed by washing, column chromatography (using silica gel and eluent system as specified) or both as specified. The desired product was dried under high vacuum.

### (*E,E*)-1,3-distyrylhydantoin (**9b'**)



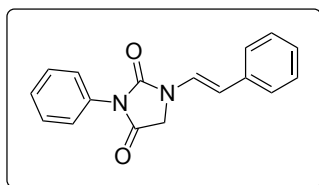
Following the general procedure at 40 °C for 6.5 h, **9b'** was obtained after filtration and washing with ethanol (3 x 1 mL) of the crude reaction mixture and column chromatography (chloroform:hexane [2:1]) as a colorless solid (36.2 mg, 30 %).

<sup>1</sup>H NMR (600 MHz, CDCl<sub>3</sub>): δ 7.62 (d, *J* = 15.1 Hz, 1H), 7.57 (d, *J* = 14.7 Hz, 1H), 7.46 – 7.42 (m, 2H), 7.38 – 7.31 (m, 6H), 7.29 – 7.26 (m, 1H), 7.25 – 7.21 (m, 1H), 7.16 (d, *J* = 15.1 Hz, 1H), 5.87 (d, *J* = 14.7 Hz, 1H), 4.16 (s, 2H).

<sup>13</sup>C NMR (151 MHz, CDCl<sub>3</sub>): δ 166.3, 152.1, 135.3, 135.2, 128.8, 128.7, 127.9, 127.1, 126.3, 125.6, 121.4, 121.0, 117.4, 112.0, 47.1.

HRMS (ESI) *m/z* [M + Na]<sup>+</sup>: Calcd. for C<sub>19</sub>H<sub>16</sub>N<sub>2</sub>NaO<sub>2</sub><sup>+</sup>: 327.1104, found: 327.1103.

### 3-Phenyl-(*E*)-1-styrylhydantoin (**9i**)



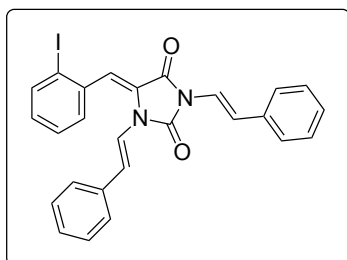
Following the general procedure at 0.2 mmol scale at 25 °C for 22.5 h, **9i** was obtained after filtration of the crude reaction mixture and washing with ethanol (3 x 0.5 mL) as a colorless solid (37.2 mg, 67 %).

<sup>1</sup>H NMR (600 MHz, CDCl<sub>3</sub>): δ 7.62 (d, *J* = 14.8 Hz, 1H), 7.52 – 7.48 (m, 2H), 7.46 – 7.40 (m, 3H), 7.39 – 7.36 (m, 2H), 7.35 – 7.31 (m, 2H), 7.25 – 7.21 (m, 1H), 5.91 (d, *J* = 14.8 Hz, 1H), 4.29 (s, 2H).

<sup>13</sup>C NMR (151 MHz, CDCl<sub>3</sub>): δ 167.4, 153.0, 135.4, 131.1, 129.2, 128.8, 128.6, 127.0, 126.0, 125.7, 121.7, 111.6, 47.7.

HRMS (ESI) *m/z* [M + Na]<sup>+</sup>: Calcd. for C<sub>17</sub>H<sub>14</sub>N<sub>2</sub>NaO<sub>2</sub><sup>+</sup>: 301.0947, found: 301.0947.

**(Z)-(5-(2-iodobenzylidene))-(*E,E*)-1,3-distyrylhydantoin (**9n'**)**



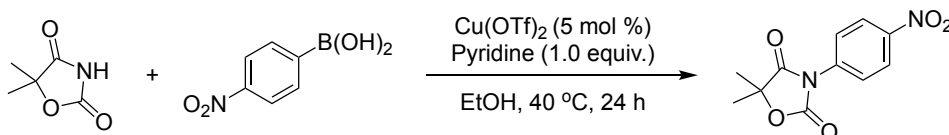
Following the general procedure at 25° C for 20 h, **9n'** was obtained after filtration and washing with ethanol (3 x 0.5 mL) of the crude reaction mixture and column chromatography (chloroform:hexane:acetone [7:2:1]) as a yellow solid (41.0 mg, 20 %).

<sup>1</sup>H NMR (600 MHz, CDCl<sub>3</sub>): δ 7.93 (dd, *J* = 8.0, 1.2 Hz, 1H), 7.70 (d, *J* = 15.1 Hz, 1H), 7.50 – 7.46 (m, 2H), 7.37 (t, *J* = 7.7 Hz, 2H), 7.31 – 7.24 (m, 3H), 7.23 – 7.17 (m, 4H), 7.06 (s, 1H), 7.02 (td, *J* = 7.7, 1.7 Hz, 1H), 6.90 (dd, *J* = 7.8, 1.7 Hz, 2H), 6.57 (d, *J* = 14.7 Hz, 1H), 6.47 (d, *J* = 14.7 Hz, 1H).

<sup>13</sup>C NMR (151 MHz, CDCl<sub>3</sub>): δ 160.5, 151.4, 139.1, 136.6, 135.4, 134.7, 131.0, 130.2, 128.8, 128.5, 127.9, 127.8, 127.7, 126.6, 126.4, 125.9, 123.8, 121.5, 119.6, 117.6, 117.2, 99.9.

HRMS (ESI) *m/z* [M + Na]<sup>+</sup>: Calcd. for C<sub>26</sub>H<sub>19</sub>IN<sub>2</sub>NaO<sub>2</sub><sup>+</sup>: 541.0383, found: 541.0383.

**5,5-dimethyl-3-(4-nitrophenyl) oxazolidine-2,4-dione (**15m**)<sup>335</sup>**



Oxohydantoin (20.7 mg, 0.160 mmol, 1.00 equiv.), 4-nitrophenylboronic acid (77.2 mg, 0.462 mmol, 2.90 equiv.), Cu(OTf)<sub>2</sub> (2.9 mg, 0.0080 mmol, 0.050 equiv.) and EtOH (1 mL) were added to a 5 mL round-bottom flask equipped with a magnetic stir bar. Pyridine (12 μL, 0.16 mmol, 1.0 equiv.) was added via a syringe, a cooler was connected to the flask and the mixture was stirred with access to air at 40 °C for 24 h. Purification by flash column chromatography (chloroform:hexane:acetone [8:1:1]) gave a mixture of **15m** and 4-nitrophenol. The mixture was dissolved in DCM and extracted using aqueous NaHCO<sub>3</sub> (sat.) until the aqueous layer stopped taking on a yellow color. The organic layer was dried under reduced pressure to give **15m** as a pale yellow solid (25.0 mg, 64 %).

<sup>1</sup>H NMR (600 MHz, CDCl<sub>3</sub>): δ 8.38 – 8.34 (m, 2H), 7.82 – 7.78 (m, 2H), 1.72 (s, 6H).

<sup>13</sup>C NMR (151 MHz, CDCl<sub>3</sub>): δ 174.1, 152.1, 146.9, 136.6, 125.4, 124.5, 83.7, 23.8.

HRMS (ESI) *m/z* [M + Na]<sup>+</sup>: Calcd. for C<sub>11</sub>H<sub>10</sub>N<sub>2</sub>NaO<sub>5</sub><sup>+</sup>: 273.0482, found: 273.0482.

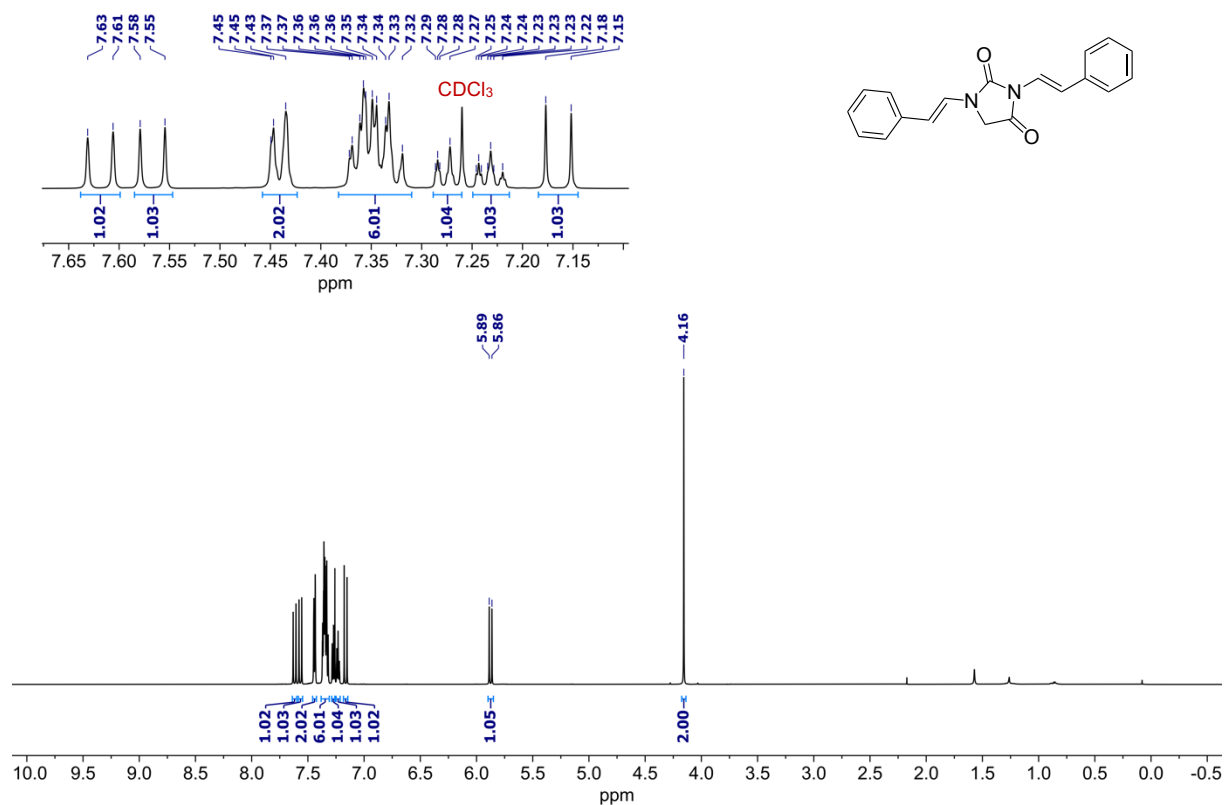


Figure 4.4. <sup>1</sup>H NMR (600 MHz, CDCl<sub>3</sub>) spectrum of 9b'.

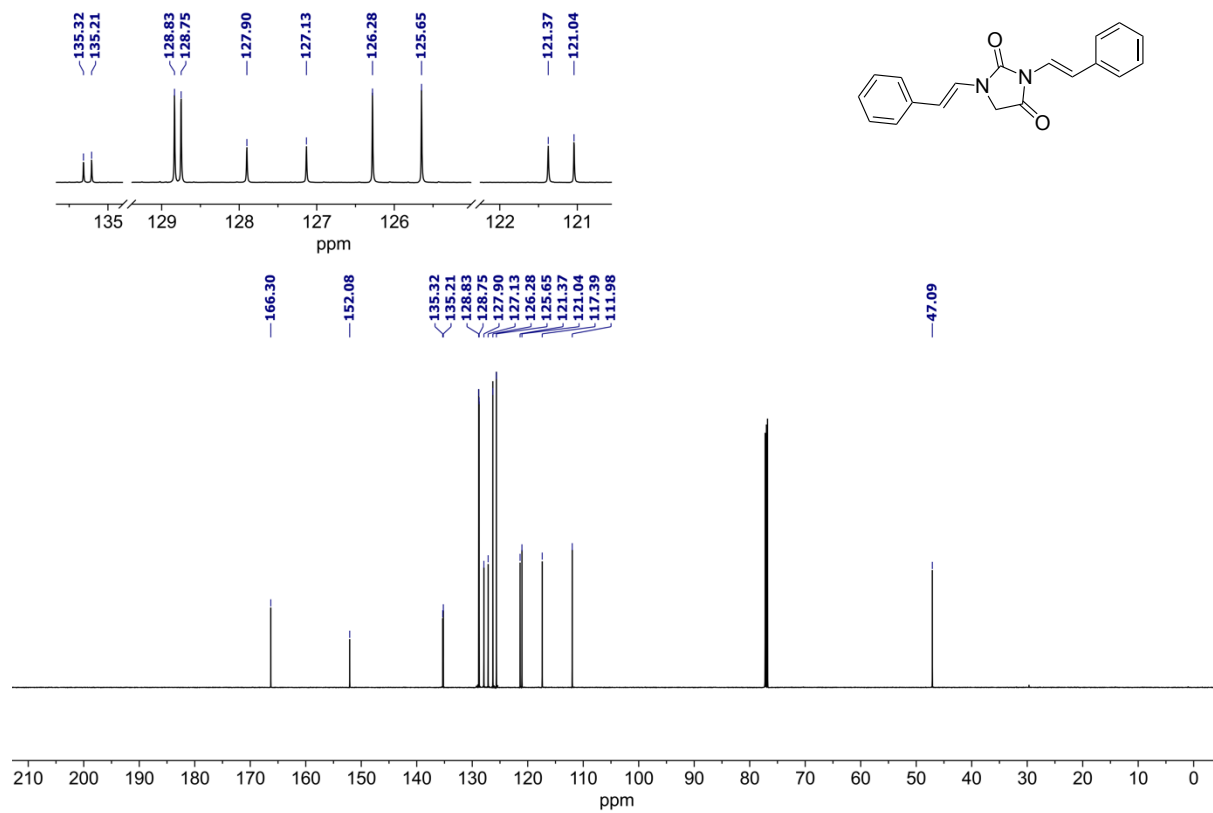
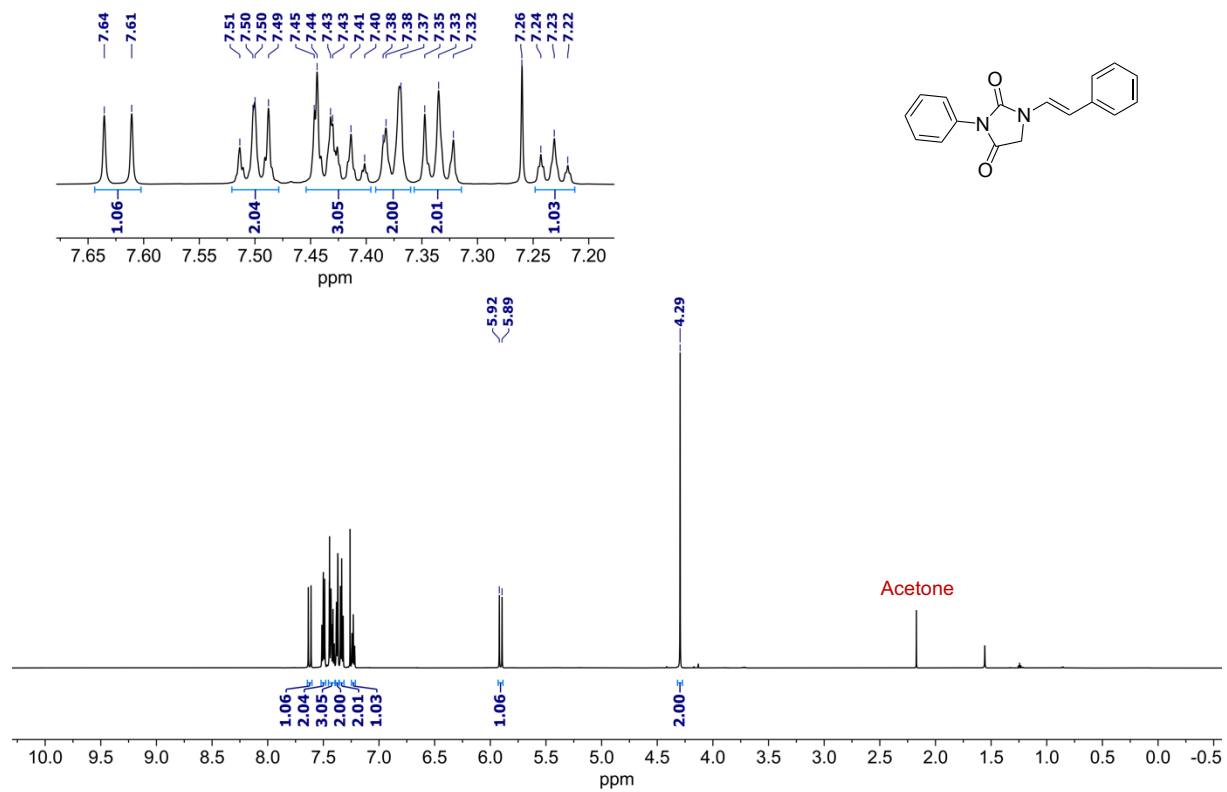
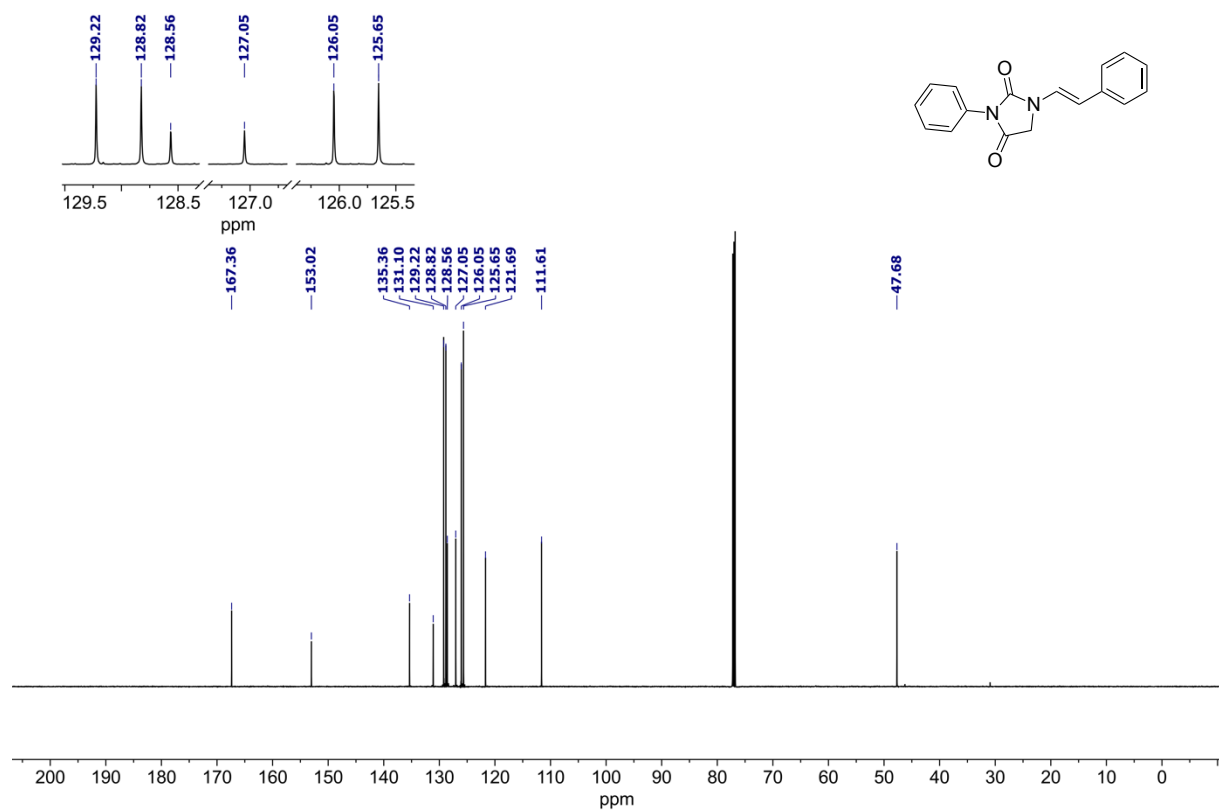


Figure 4.5. <sup>13</sup>C NMR (151 MHz, CDCl<sub>3</sub>) spectrum of 9b'.



**Figure 4.6.**  $^1\text{H}$  NMR (600 MHz,  $\text{CDCl}_3$ ) spectrum of **9i**.



**Figure 4.7.**  $^{13}\text{C}$  NMR (151 MHz,  $\text{CDCl}_3$ ) spectrum of **9i**.

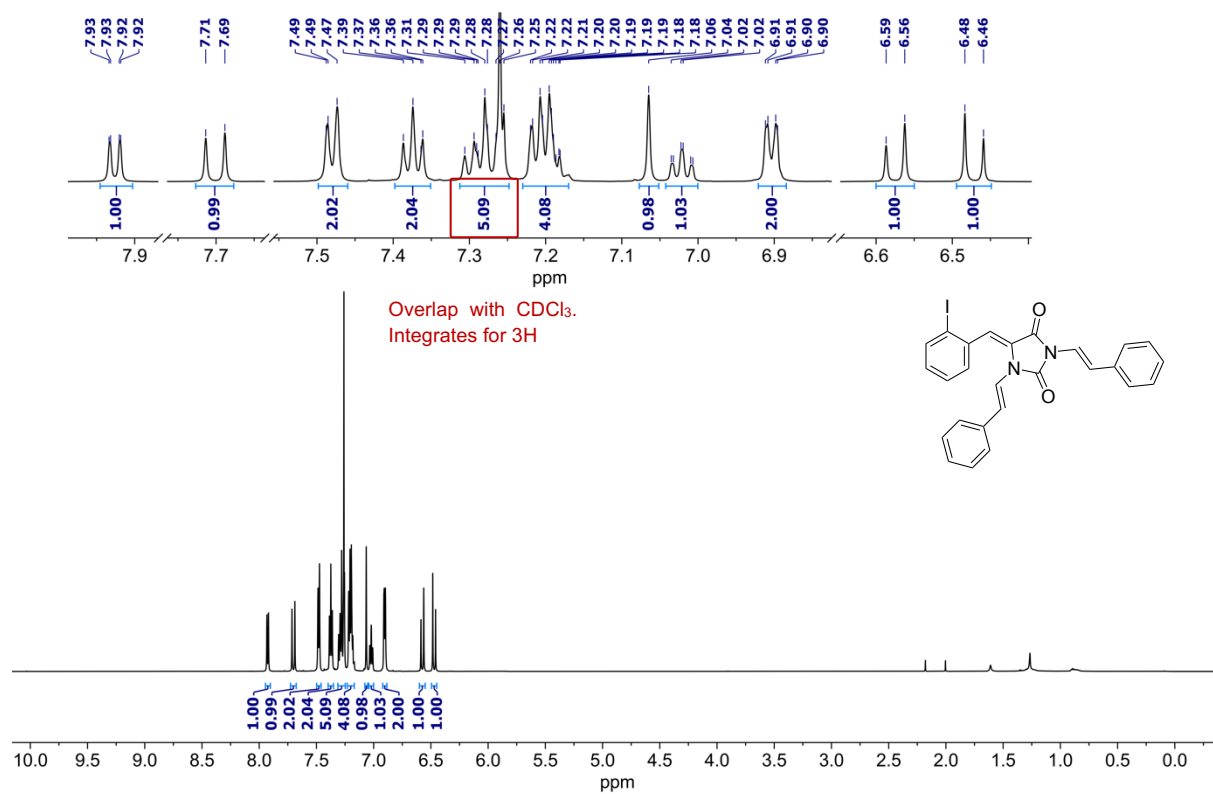


Figure 4.8.  $^1\text{H}$  NMR (600 MHz,  $\text{CDCl}_3$ ) spectrum of **9n'**.

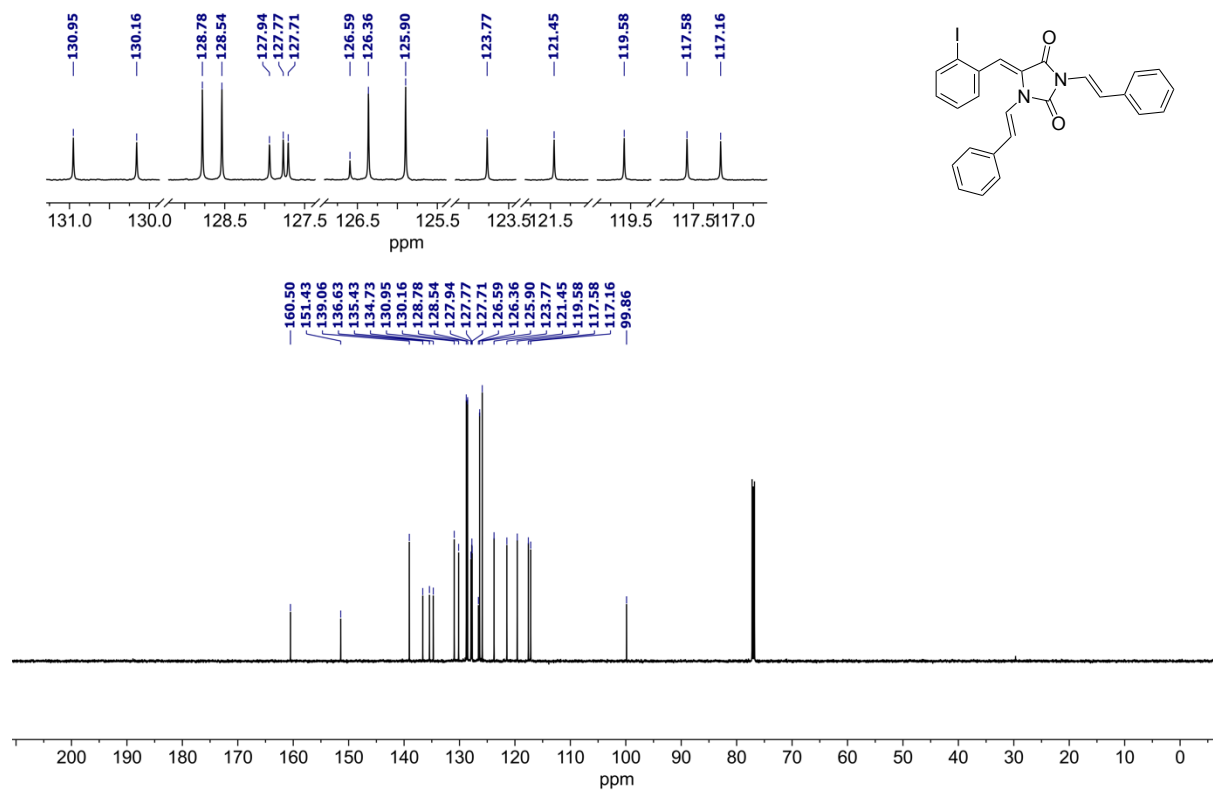
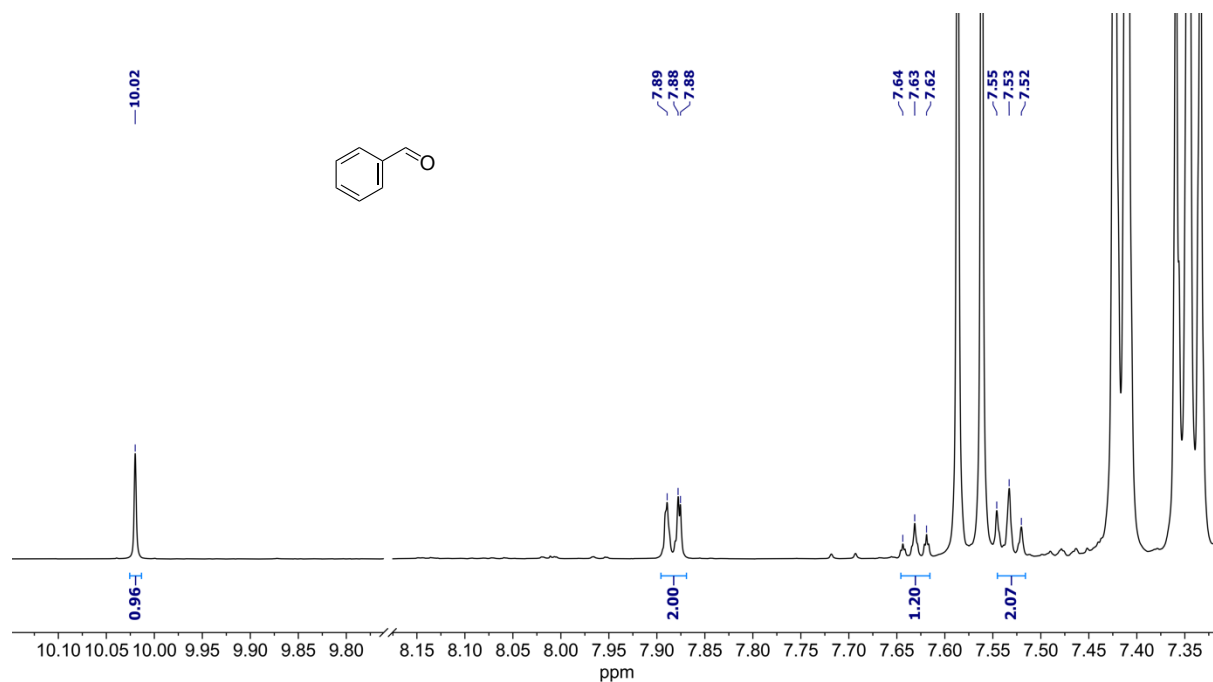
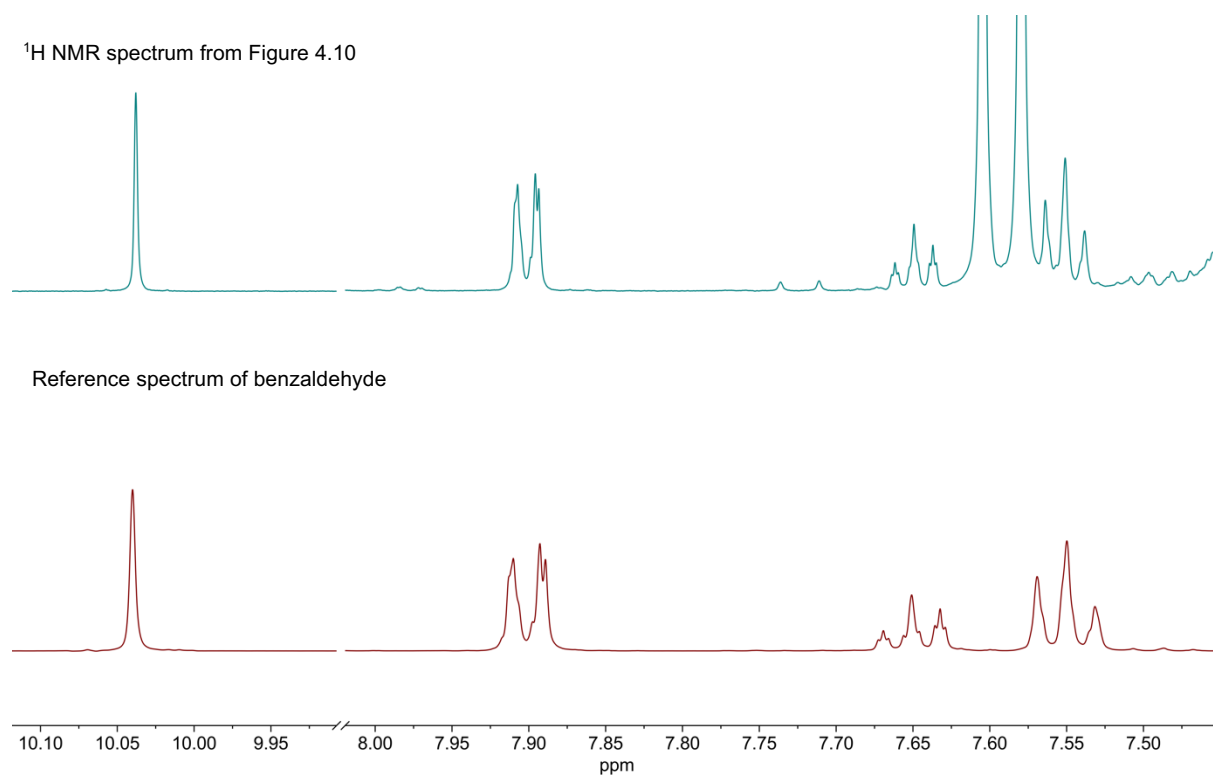


Figure 4.9.  $^{13}\text{C}$  NMR (151 MHz,  $\text{CDCl}_3$ ) spectrum of **9n'**.

## <sup>1</sup>H NMR spectra of observed side products and mechanistic investigation into boroxine formation



**Figure 4.10.** <sup>1</sup>H NMR (600 MHz, CDCl<sub>3</sub>) spectrum. The marked peaks were identified as benzaldehyde **8a-B** (see spectrum in Figure 4.11) and were present in all reactions.



**Figure 4.11.** <sup>1</sup>H NMR (600 MHz, CDCl<sub>3</sub>) spectrum. Comparison of spectrum in Figure 4.10 (top) and pure benzaldehyde (bottom).



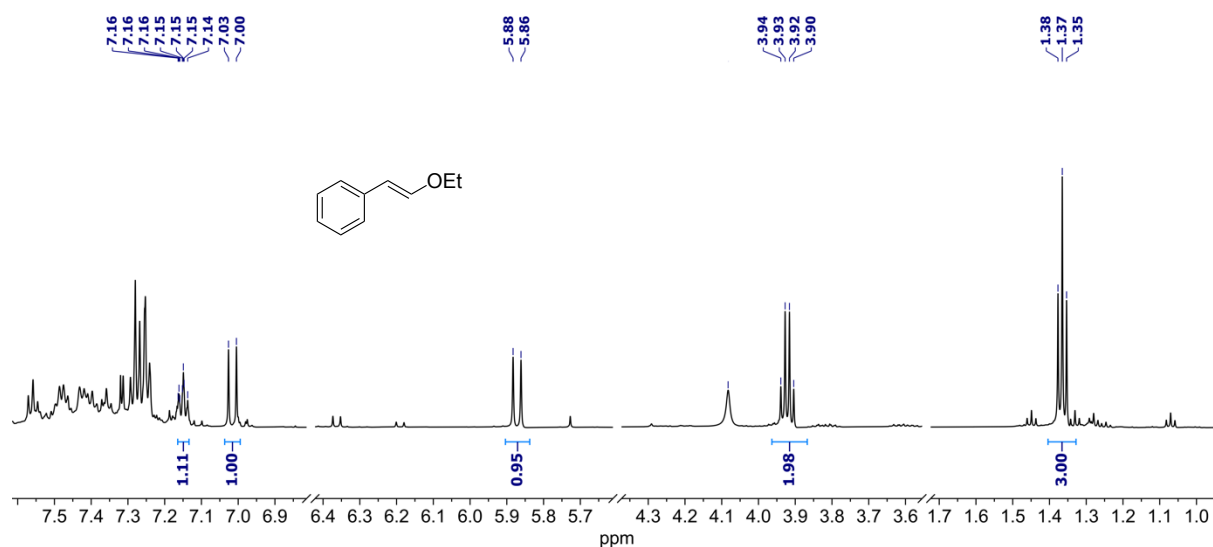


**Figure 4.12.**  $^1\text{H}$  NMR (600 MHz,  $\text{CDCl}_3$ ) spectrum of (*E*)-(2-ethoxyvinyl)benzene **8a-SE** present in a crude reaction mixture. The remaining unmarked protons are located in the overlapping, aromatic region.

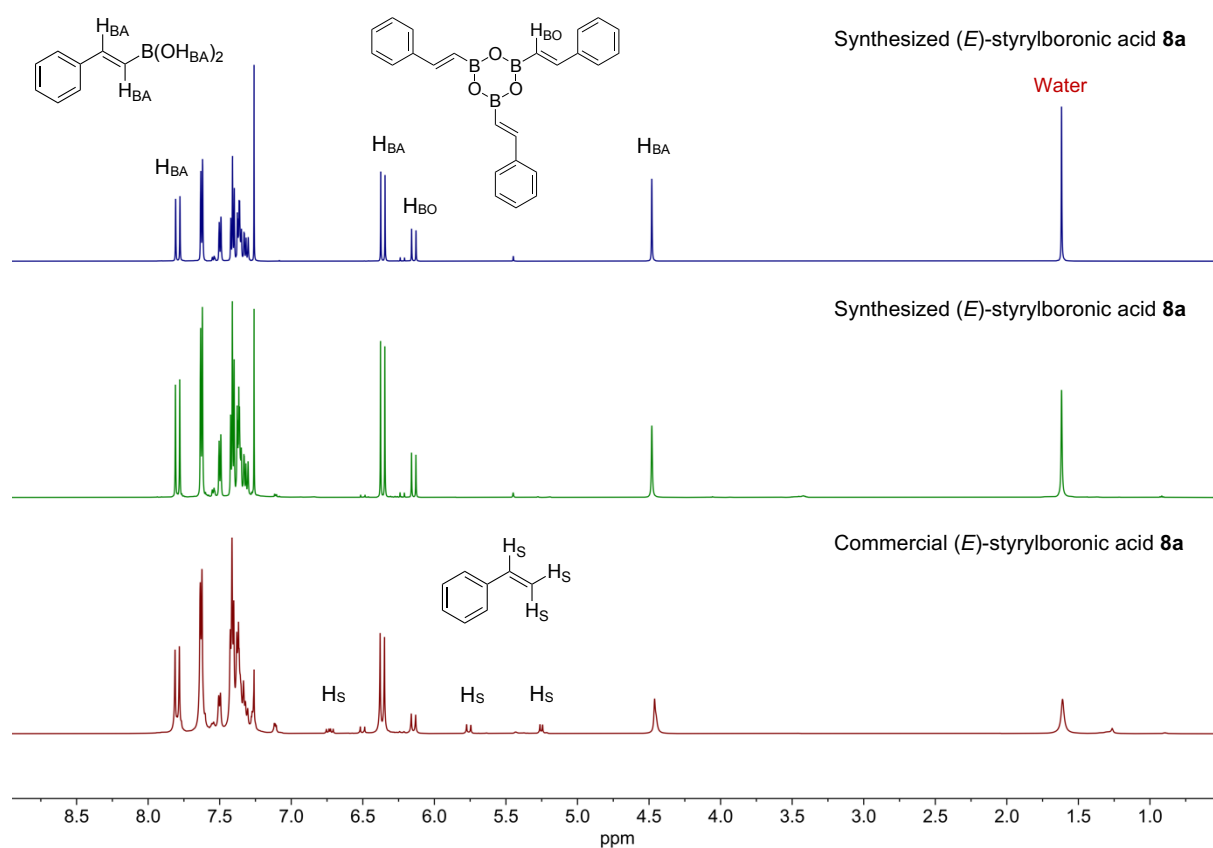


**Figure 4.13.**  $^1\text{H}$  NMR (600 MHz,  $\text{CDCl}_3$ ) spectra of (*E*)-styrylboronic acid **8a**. Commercially obtained **8a** (bottom) with traces of styrene ( $\text{H}_s$ ). Synthesized **8a** (top and middle) without styrene. The presence of the boroxine **8a'** ( $\text{H}_{\text{Bo}}$ ) can be seen in all spectra, but in various ratios to the boronic acid ( $\text{H}_{\text{BA}}$ ).

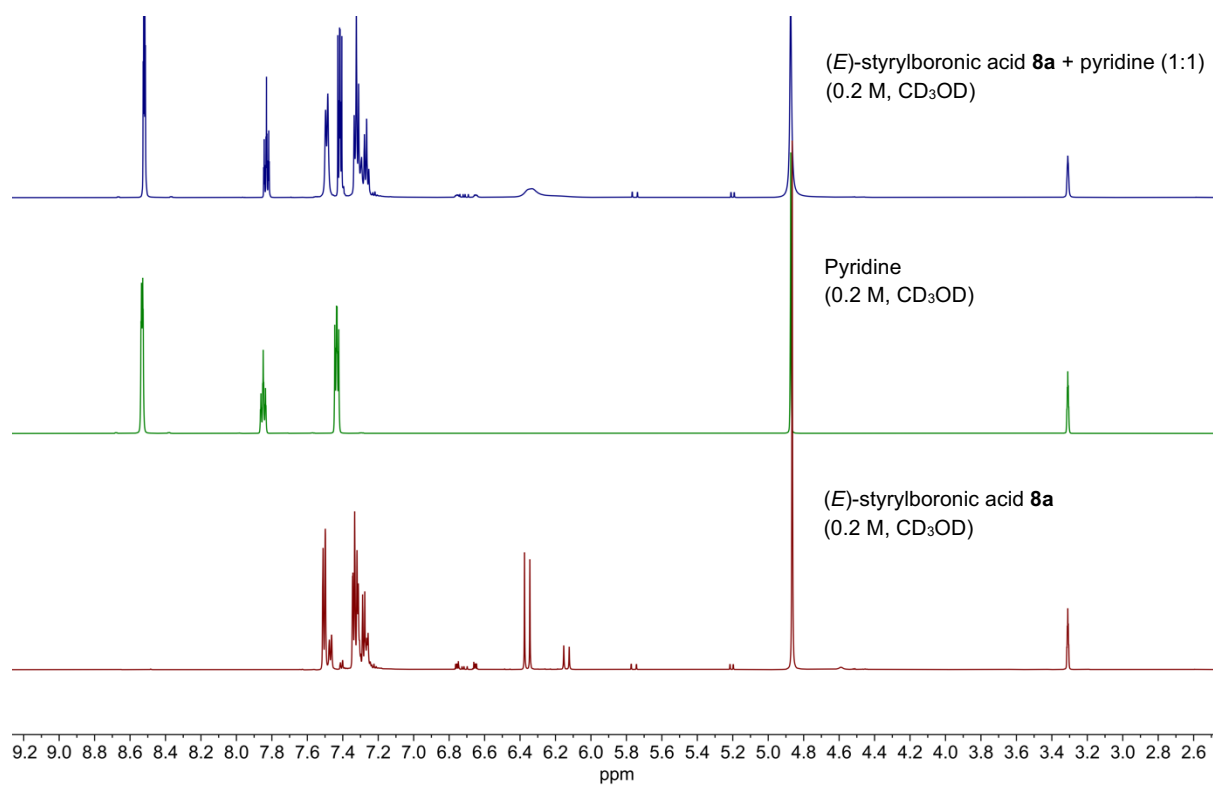


**Figure 4.14.** <sup>1</sup>H NMR (600 MHz, CD<sub>3</sub>OD) spectrum. Bottom: boronic acid **8a**, middle: pyridine, top: 1:1 mixture of **8a** and pyridine.

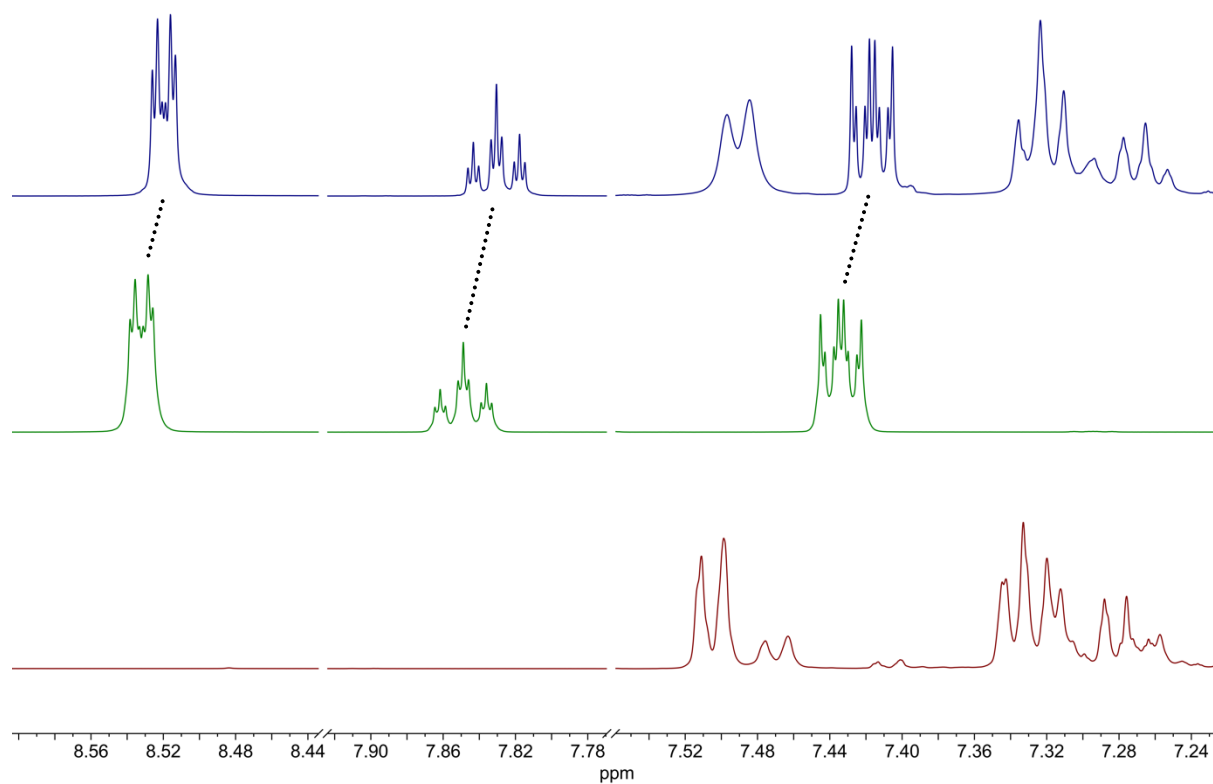


**Figure 4.15.** <sup>1</sup>H NMR (600 MHz, CD<sub>3</sub>OD) spectrum. Bottom: boronic acid **8a**, middle: pyridine, top: 1:1 mixture of **8a** and pyridine. The upfield chemical shift change of pyridine in the mixture is indicated with black dots.

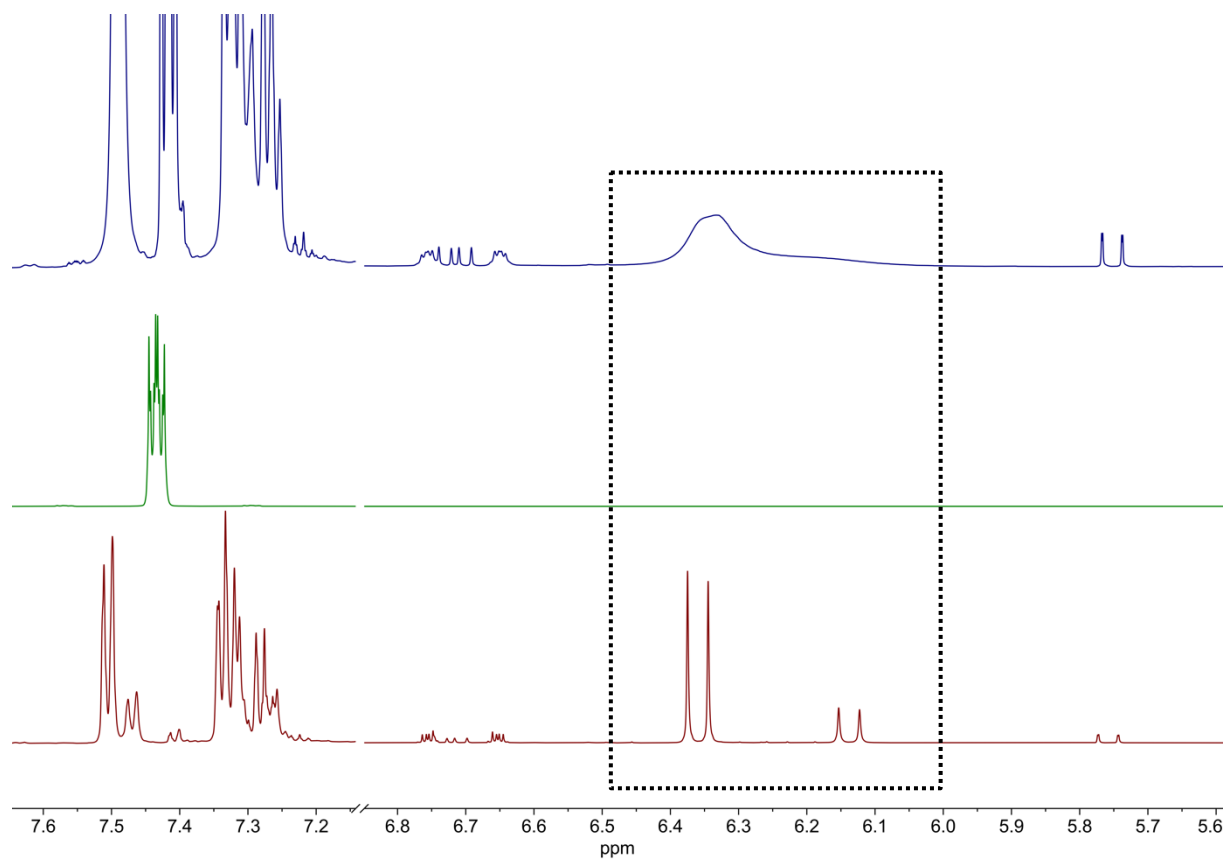


**Figure 4.16.**  $^1\text{H}$  NMR (600 MHz,  $\text{CD}_3\text{OD}$ ) spectrum Bottom: boronic acid **8a**, middle: pyridine, top: 1:1 mixture of **8a** and pyridine. The broadening of the boronic acid/boroxine peaks (framed) in the mixture indicate a dynamic process, likely due to interaction between pyridine and the empty boron p-orbital.



# Chapter 5: Simple access to *N*-substituted maleamates *via* one-pot C(sp<sup>2</sup>)-N cross-coupling and ring-opening of maleimides

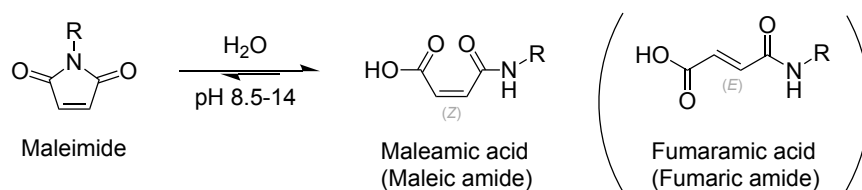
## 5.1 Introduction

During the reaction between maleimide **1w** and (*E*)-styrylboronic acid **8a** (Chapter 4, Scheme 4.5), we discovered the formation of the unexpected *N*-alkenylated and ring-opened maleamate **11b**. This chapter covers further exploration of **11b**, including a short (attempted) optimization of reaction conditions and the reactivity of **11b** in various transformations. A brief introduction to maleimides, maleamic acids and esters (maleamates) is given prior to further investigation of compound **11b**. The results presented in this section does not represent a full study as future work is needed.

## 5.2 Formation of maleamic acids and esters from maleimides

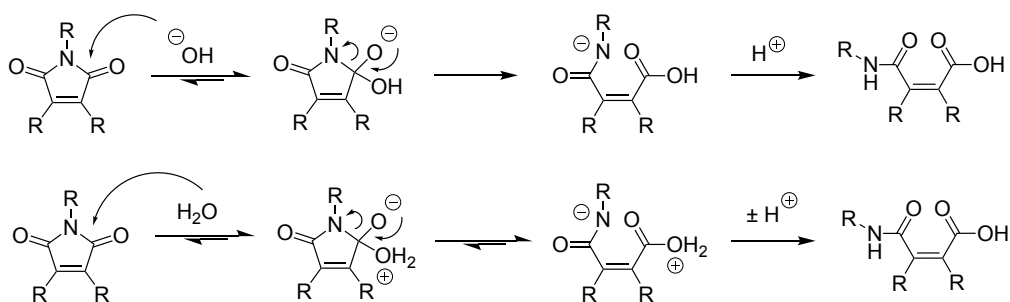
Maleimides are frequently used as building blocks in organic synthesis due to their dense functionality. Besides substitutions at the nitrogen atom,<sup>309, 336</sup> they partake in C-C cross coupling reactions.<sup>337, 338</sup> Furthermore, they are susceptible to reactions across the double bond including cycloaddition reactions<sup>339-343</sup> and conjugate additions.<sup>344-346</sup> The latter is commonly used in bio-conjugation reactions to modify cysteine residues, proteins and peptides.<sup>347, 348</sup>

Compared to its saturated counterpart (succinimide), maleimide and *N*-substituted maleimides are more inclined to undergo hydrolytic cleavage under basic conditions (Scheme 5.1).<sup>349, 350</sup> Ring-opening produces the linear (*Z*)-alkene maleamic acid. The (*E*)-analog, fumaramic acid, is not observed as a direct hydrolysis product.



**Scheme 5.1.** Hydrolytic cleavage of maleimide under basic conditions to produce maleamic acid (also referred to maleic amide).

The ring-opening mechanism<sup>349-351</sup> (Scheme 5.2) involves a nucleophilic attack from H<sub>2</sub>O/OH<sup>-</sup> on the maleimide carbonyl groups followed by a cleavage of the carbonyl-nitrogen bond, then a protonation process to furnish the maleamic acid. Besides concentration-, pH- and temperature-dependence, the rate of the hydrolysis is affected by the substituents of the maleimide. Introduction of electron withdrawing groups on either C=C<sup>352, 353</sup> or the nitrogen<sup>350, 354</sup> accelerates the rate of hydrolysis, due to higher electrophilicity of the carbonyl groups.

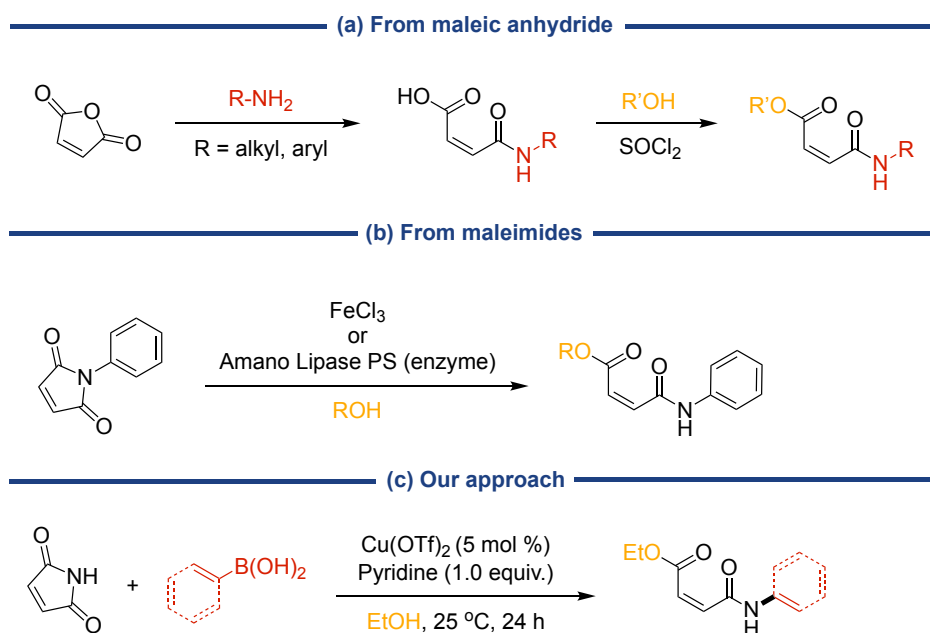


**Scheme 5.2.** Mechanism of maleimide hydrolysis. Top: nucleophilic attack by hydroxide. Bottom: nucleophilic attack by water.

### 5.2.1 Strategies to access *N*-substituted maleamic acids and esters

Since **11b** is the *N*-substituted maleamic ester produced directly from maleimide, we were naturally interested to see how these structures are accessed in the literature. Also, whether our method can provide a complimentary entry point to such structures.

Maleamic acids and their ester derivatives have found application in biologically active compounds,<sup>355-357</sup> in drug delivery systems,<sup>358-360</sup> and as ligands in metal-complexes.<sup>361-363</sup> As their ring-closed analog, the maleamic acids and their derivatives can undergo numerous transformations. A few of them include MCRs to prepare more complex molecules,<sup>364, 365</sup> isomerization to form the fumaramic analog,<sup>366</sup> esterification,<sup>367</sup> hydrolysis<sup>368</sup> and peptide-coupling reactions.<sup>369</sup> *N*-substituted maleamic acids are usually prepared from maleic anhydride and aryl- or alkylamines (Scheme 5.3a).<sup>343, 356, 370-375</sup> Access to the ester is usually granted through esterification with the appropriate alcohol, which requires the presence of thionyl chloride. Only two examples have been reported obtaining the ester directly from the maleimide (Scheme 5.3b), where the presence of either a metal-catalyst<sup>376</sup> or an enzyme<sup>377</sup> was required. The methods are also limited to aryl and alkyl substituents. As far as we are concerned, no one-pot sequence involving *N*-functionalization and subsequent ring-opening/hydrolysis and esterification of maleimide (Scheme 5.3c) has been reported.



**Scheme 5.3.** Strategies to access *N*-functionalized maleamic acids and esters.

## 5.3 Exploration of the formation and reactivity of (*E*)-*N*-styryl ethyl maleamate

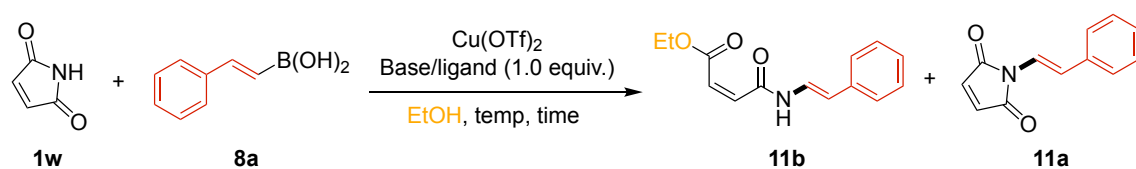
Further exploration of **11b** was motivated by several factors: (1) the lack of a method where *N*-functionalized maleamates are obtained directly from maleimides, (2) the scarcity of *N*-alkenylated maleamates reported<sup>378-381</sup> and (3) the potential use of **11b** as a building block in further synthetic manipulations. We believe the several functional sites of **11b** allows for access to new, complex molecules hard to obtain by other methods. As the reaction in question was serendipitously discovered, optimization of the reaction conditions performed before further exploration. As none of this work is published at the time of writing this dissertation, all experimental details are covered in the experimental section.

### 5.3.1 Optimization of reaction conditions for the one-pot C-(sp<sup>2</sup>)-*N* coupling and ring-opening reaction

The conditions shortly investigated herein are based directly on the results obtained in the formation of **11b** from the previous chapter. Upon exploration of the reaction, the presence of the ring-closed product **11a** in addition to the ring-opened product **11b**, was discovered (Table 5.1). **11a** was likely not discovered in the initial reaction (Table 5.1, entry 1) due to the small amounts produced. Based on the results described in Chapter 4, **11a** is likely the initial product formed. In the scope of *N*-alkenylation,

only cyclic imides were allowed under our conditions, while linear substrates were not reactive. After formation of **11a**, the presence of copper<sup>376, 382</sup> and a base may instigate the hydrolysis and esterification to form **11b**. Alternatively, the ester is formed directly by attack from EtOH. Scaling down the reaction from 0.40 mmol to 0.20 mmol using the same conditions (Table 5.1, entry 2) affected the reaction negatively as only 64 % of **11b** was formed. Unconverted starting material prompted further attempts of optimization including varying the equivalents of boronic acid **8a**, catalyst loading, base, time and temperature (Table 5.1, entries 3-7), none of which improved the outcome of **11b**. As such, the original conditions from entry 1 (Table 5.1) were used further.

**Table 5.1.** Screening of reaction conditions.



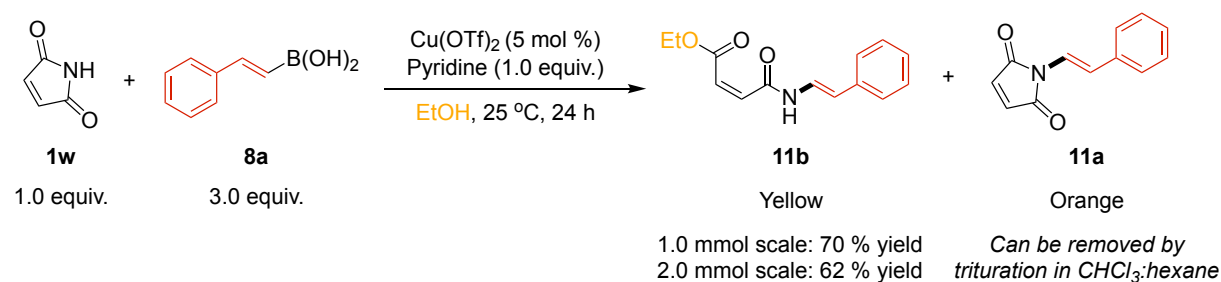
#	<b>8a</b> (equiv.)	Cu(OTf) <sub>2</sub> (mol %)	Base (1.0 equiv)	Temp (°C)	Time (h)	Yield <b>11b</b> (%) <sup>[a]</sup>	Yield <b>11a</b> (%) <sup>[a]</sup>
1 <sup>[b]</sup>	2.0	5	Pyridine	25	24	78 <sup>[c]</sup>	nd
2	2.0	5	Pyridine	25	24	64	7
3	2.0	5	Pyridine	40	48	40	5
4	2.0	5	Pyridine	60	4.5	39	8
5	2.0	10	Pyridine	60	19	28	nd*
6	2.0	5	Pyridine	60	48	34	nd*
7	3.0	5	DMAP	25	24	0	0

Conditions: Maleimide **1w** (0.2 mmol, 1.0 equiv.), I-styrylboronic acid **8a** (as specified), Cu(OTf)<sub>2</sub> (as specified), base (0.20 mmol, 1.0 equiv.) and EtOH (1 mL). [a] <sup>1</sup>H NMR yield using Mes as IS. [b] Reaction performed on a 0.40 mmol scale [c] Isolated yield. \* Not detected due to overlapping peaks in the <sup>1</sup>H NMR spectrum.

As larger quantities of **11b** were needed for further reactions, we looked into scaling up the process (Scheme 5.4). Upon purification by column chromatography on SiO<sub>2</sub>, **11b** was seen as a yellow band. An additional orange, less polar band was also discovered. The band containing this product was identified as the *N*-styrylmaleimide **11a**, which is likely in equilibrium with **11b**. Unfortunately, the tailing of **11a** could not be avoided in any of the eluents used, and further purification by trituration was



necessary. Ultimately, the yield was affected in the upscaling process due to the need of a second purification. Nevertheless, 62-70 % yield of **11b** was obtained depending on the reaction scale.

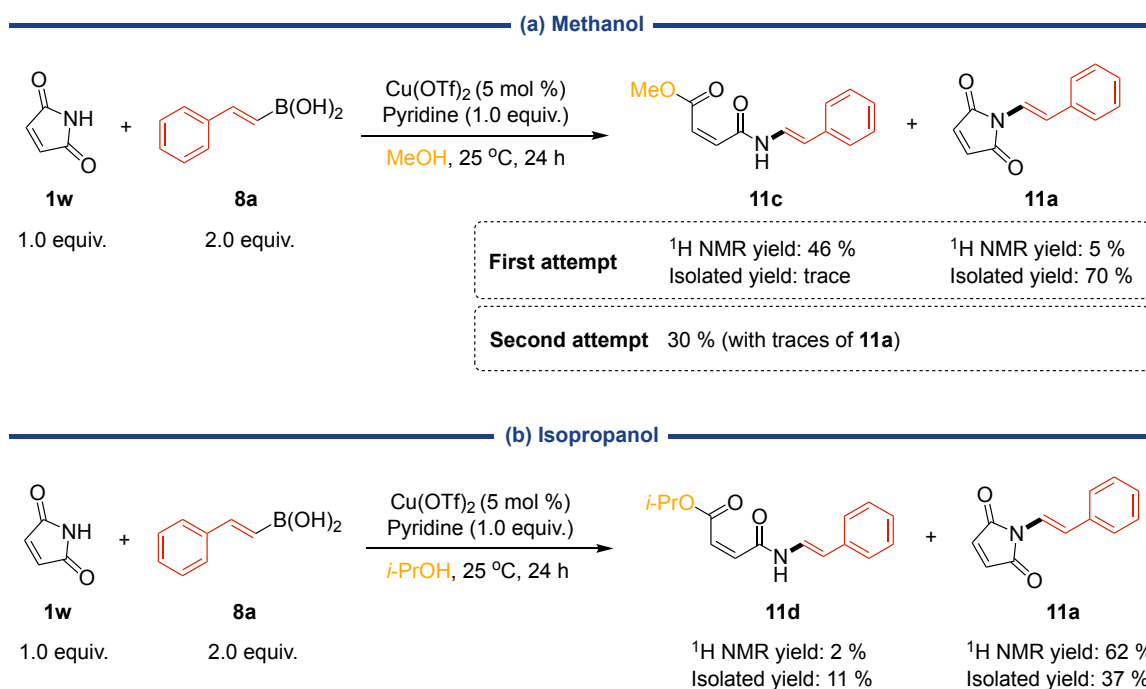


**Scheme 5.4.** Scale up of the reaction to 1.0 and 2.0 mmol scale.

### 5.3.2 Can we produce other esters by changing the solvent?

As previously mentioned, the exact details on the ethyl ester formation (**11b**) are unclear and likely involves either a direct ethanolysis or hydrolysis and subsequent esterification of the acid. Regardless, ethanol is paramount for product formation. Based on this, we theorized that other alcohol-based solvents would furnish the corresponding ester. Ethanol was replaced by methanol (MeOH) in an attempt to prepare the methyl ester **11c** (Scheme 5.5a) and isopropanol (*i*-PrOH) to prepare the isopropyl ester **11d** (Scheme 5.5b).

Yields were measured in the post-reaction mixture using  $^1\text{H}$  NMR spectroscopic analysis, which revealed 46 % of the ring-opened methyl ester **11c** and only 5 % of **11a**. The starting material (maleimide **1w**) was not fully converted. However, upon isolation, only trace amounts of **11c** were obtained while 70 % of **11a** was isolated. We believe the dynamic equilibrium between **1w**, **11a** and **11c** shifted upon a lengthy isolation process. The increase from the total 51 % to 70 % yield points to further reaction after the 24 hours reaction time. At the time the reaction was performed, the possibility for further reaction was not taken into consideration and the methanol was not immediately removed from the post-reaction mixture.



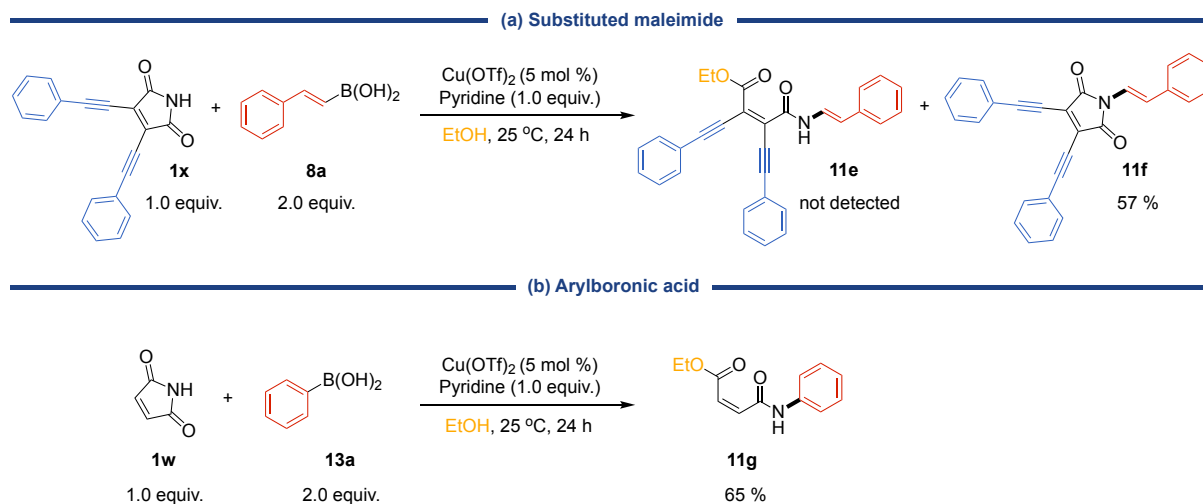
**Scheme 5.5.** Preparation of the (a) methyl and (b) isopropyl ester of **11b** by replacing EtOH with MeOH and *i*-PrOH.

The results clearly demonstrate low tolerance towards a solvent change, likely for two reasons: (1) the *N*-alkenylation process is highly influenced by the choice of solvent as earlier discussed and demonstrated in Chapter 4 (Table 4.2). Ethanol was the superior solvent, isopropanol yielded the *N*-alkenylated product in lower yields and methanol was not tested. (2) The ring-opening step is influenced by the nucleophilicity of the solvent (MeOH > EtOH > *i*-PrOH) as this step involves a nucleophilic addition. Thus, low yields obtained using methanol is likely due to its ineffectiveness in the C-N coupling reaction as around 50 % of the starting material remained unconverted.

### 5.3.3 Changing the maleimide or the coupling partner: how will it affect the reaction?

Next, we redirected the focus to substituted maleimides and phenylboronic acid (Scheme 5.6) to evaluate if they were suitable substrates for the reaction. 2,3-bis(phenylethynyl)maleimide (PEM) **1x** was prepared from the dibromomaleimide precursor *via* a Sonogashira cross-coupling reaction according to literature.<sup>383</sup> In the reaction with the boronic acid, **11e** was isolated in 57 % yield. Ring-opened **11f** was not detected in the reaction. We attribute the observed results to the lesser electrophilicity of **1x**. Based on <sup>13</sup>C NMR chemical shifts of the unsubstituted maleimide **1w** and PEM **1x**, the maleimide carbons in **1x** have lower chemical shifts

(170.4 and 135.1 ppm *vs.* 166.3 and 128.5 ppm), and hence less electrophilic and less susceptible for nucleophilic attack of the carbonyls. Replacing styrylboronic acid with arylboronic under our conditions was proven successful in Chapter 4. **8a** was replaced with phenylboronic acid **13a** (Scheme 5.6b), and the arylated **11g** was isolated in 65 % yield.

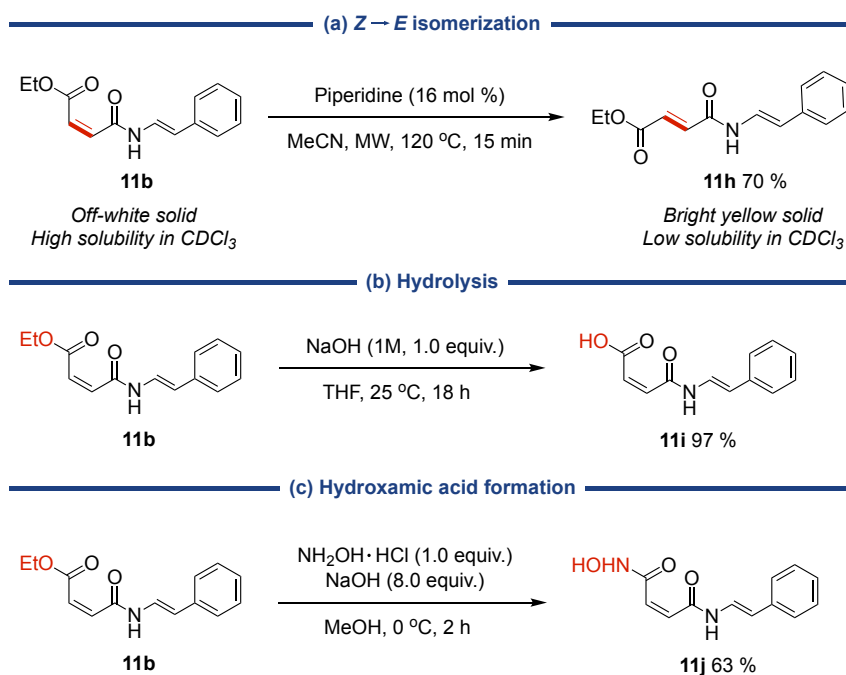


**Scheme 5.6.** *N*-functionalization and ring-opening of (a) substituted maleimide and (b) using arylboronic acid as coupling partner.

### 5.3.4 (*E*)-*N*-styryl ethyl maleamate (**11b**) as synthon in synthetic transformations

Next, we wanted to explore the reactivity of **11b**. Containing multiple reactive sites, **11b** carries the potential as a useful building block in synthetic transformations. This section covers the exploratory studies using **11b** as a synthon in a range of reactions. The purpose of the chosen transformations was to gain access to new compounds with similar structural features to the ones found in bioactive molecules.<sup>368, 384-387</sup>

We started with some well-established reactions in which substrates similar to **11b** have been subjected (Scheme 5.7). The selective *Z* → *E* isomerization<sup>366</sup> reaction (Scheme 5.7a) was successful, providing the fumaramate **11h** in 70 % yield. Hydrolysis<sup>368</sup> (Scheme 5.7b) proceeded smoothly without cyclization, and the carboxylic acid **11i** was obtained in 97 % yield. Formation of the hydroxamic acid<sup>368</sup> (Scheme 5.7c) **11j** was less efficient, but **11j** was obtained in 63 % yield.



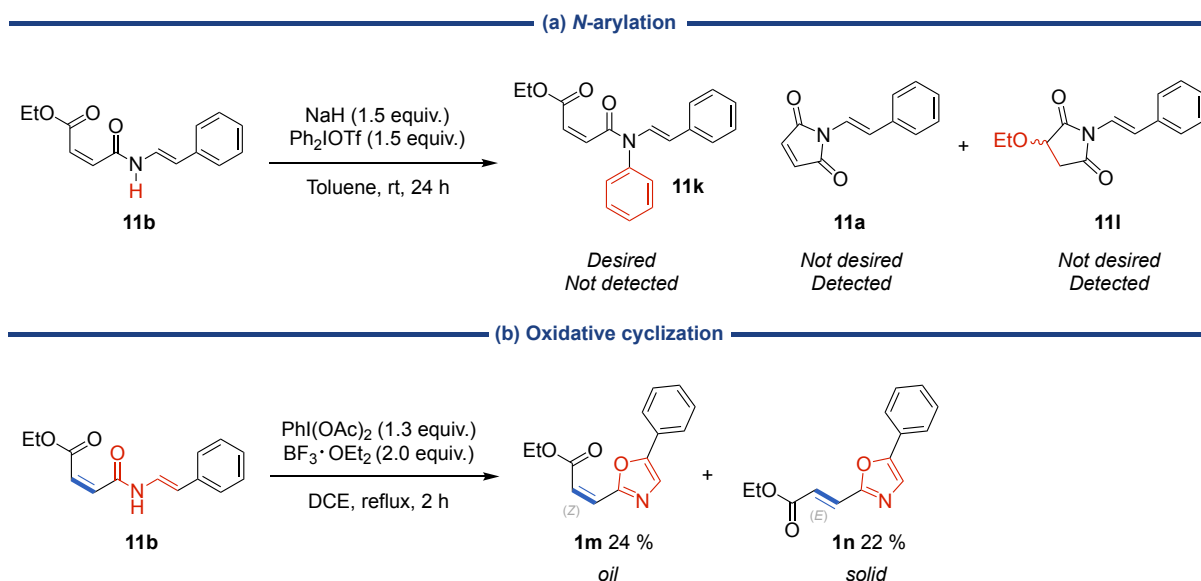
**Scheme 5.7.** Exploration of the reactivity of **11b**: (a) *Z* → *E* isomerization, (b) hydrolysis and (c) formation of hydroxamic acid.

In line with our previous work, *N*-arylation of the linear amide was naturally attempted (Scheme 5.8a). A reported metal-free protocol<sup>388</sup> was used where symmetrical diaryliodonium salts were utilized. **11b** was clearly not a good substrate for the reaction as the desired **11k** was not detected. Not surprisingly, the ring-opened **11a** was present. Additionally, the ethoxy-conjugated **11l** was detected in the isolated<sup>h</sup> mixture with **11a**. Maleimides have been used as Michael/conjugate acceptors. The presence of NaH is likely responsible for both the ring-closing and the conjugate addition of the ethoxy group to the maleimide double bond.

Containing an enamide moiety (Scheme 5.8b, marked in red), **11b** was subjected to phenyliodine<sup>III</sup>-diacetate (PIDA)-mediated intramolecular cyclization to form oxazoles.<sup>389</sup> No double bond (Scheme 5.8b, marked in blue) isomerization was anticipated, and only the oxazole **11m** was expected. However, prior to isolation, two fluorescent spots were seen during TLC analysis. The two products were isolated and confirmed as the (*Z*)- and (*E*)-substituted oxazoles **11m** and **11n**. Only 24 % and 22 % of **11m** and **11n**, respectively, were obtained as the separation of the isomers was challenging. Upon addition of the oxidizing agent, PIDA, to the enamide, acetic acid is generated.<sup>389</sup> Acidic catalyzed isomerization of maleic acid to fumaric acid at higher

<sup>h</sup> Bachelor student Robin Mikael Hallin performed both the synthesis and isolation of the mixture.

temperatures is well known<sup>390</sup> and likely the cause for the partial isomerization seen here.



**Scheme 5.8.** Exploration of the reactivity of **11b**: (a) *N*-arylation and (b) oxazole formation.

## 5.4 Conclusion

A one-pot protocol to access new *N*-substituted maleamates directly from maleimides have been developed. The method relies on a Cu-catalyzed strategy for the direct C(sp<sup>2</sup>)-N bond formation of maleimide and a subsequent ring-opening of the *N*-substituted maleimide. The details of the ring-opening process were not explored in detail but likely involves a direct solvolysis or a two-step hydrolysis and esterification.

The method utilizes (*E*)-styrylboronic acid as coupling partner and gives access to new *N*-alkenylated maleamates. Arylboronic acids were also allowed under the conditions. The maleamates obtained can be further utilized as synthons in synthetic transformations including hydrolysis, isomerization and oxazole-formation. The results obtained are only preliminary and requires further investigation. Suggestions for further investigations are included in the “future prospects” chapter.

## 5.5 Experimental

### General considerations

All reactions were performed with open access to air unless otherwise stated. Commercially available reagents and solvents were purchased from Sigma-Aldrich, TCI, and Alfa Aesar were used without further purification unless stated otherwise. Hexanes were distilled prior to use. Thin layer chromatography was performed on 60 F<sub>254</sub> silica coated aluminum plates from Merck and visualized using UV-light. Flash chromatography was performed on silica gel from Merck (Silicagel 60, 40-63  $\mu\text{m}$ ) using fritted glass columns.

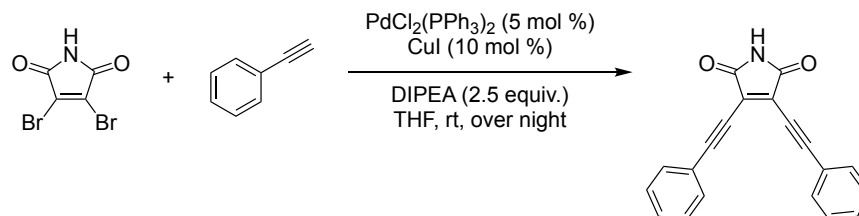
<sup>1</sup>H and <sup>13</sup>C NMR spectra were recorded using Bruker AVIIIHD400, AVI600 and AVII600 spectrometers. Spectra were calibrated using the residual solvent peaks for CDCl<sub>3</sub> (<sup>1</sup>H: 7.26 ppm; <sup>13</sup>C: 77.00 ppm) and DMSO-*d*<sub>6</sub> (<sup>1</sup>H: 2.50 ppm; <sup>13</sup>C: 39.52 ppm).

Microwave experiments were carried out in sealed vessels in a synthesis reactor (Monowave 300, Anton Paar GmbH) equipped with an internal IR probe calibrated with a Ruby thermometer.

High-resolution mass spectra (HRMS) were obtained by electron spray ionization (ESI) on Bruker Daltonik GmbH MAXIS II ETD spectrometer.

## Synthesis and characterization of starting materials

### 2,3-bis(phenylethynyl)maleimide (**1x**)<sup>383</sup>



**1x** was prepared according to a literature procedure<sup>383</sup> with slight modifications.

2,3-Dibromomaleimide (381 mg, 1.50 mmol, 1.00 equiv.) and dry THF (10 mL) were added to a 50 mL Schlenk-flask equipped with a stir bar. The flask was evacuated and refilled with argon, then phenylacetylene (412  $\mu$ L, 3.75 mmol, 2.50 equiv.), CuI (28.7 mg, 0.150 mmol, 0.100 equiv.), PdCl<sub>2</sub>(PPh<sub>3</sub>)<sub>2</sub> (52.5 mg, 0.0750 mmol, 0.0500 equiv.) and DIPEA (653  $\mu$ L, 3.75 mmol, 2.50 equiv.) were successively added to the solution under a stream of argon. The mixture was stirred at room temperature for 23 h, upon which several color changes occurred. The final red-orange solution was treated with H<sub>2</sub>O (20 mL) and EtOAc (20 mL) to induce phase separation. The organic layer was isolated and washed with saturated solution of NH<sub>4</sub>Cl (20 mL). The aqueous phases were combined and extracted with EtOAc (50 mL). The combined organic layers were dried over anhydrous MgSO<sub>4</sub>, filtered and concentrated under reduced pressure. The crude product was isolated by column chromatography (SiO<sub>2</sub>, hexane:EtOAc [4:1]). All fractions containing **1x** were collected and recrystallized by hot recrystallization from CHCl<sub>3</sub> to give pure **1x** as yellow-orange needles (170 mg, 38 %).

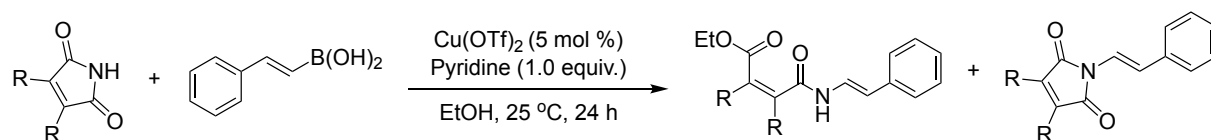
<sup>1</sup>H NMR (600 MHz, CDCl<sub>3</sub>):  $\delta$  7.66 – 7.63 (m, 4H), 7.50 (br s, 1H), 7.48 – 7.44 (m, 2H), 7.44 – 7.40 (m, 4H).

<sup>13</sup>C NMR (151 MHz, CDCl<sub>3</sub>):  $\delta$  166.4, 132.5, 130.5, 128.6, 128.5, 121.4, 110.2, 80.2.

HRMS (ESI)  $m/z$  [M + Na]<sup>+</sup>: Calcd. for C<sub>20</sub>H<sub>11</sub>NNaO<sub>2</sub><sup>+</sup>: 320.0682, found: 320.0681.

# Synthesis and characterization of (*E*)-*N*-styrylmalesamates, (*E*)-*N*-styrylmalesimides and *N*-arylmalesamates

## General procedure



Maleimide (0.40 mmol, 1.0 equiv.), boronic acid (0.80 mmol, 2.0 equiv.), Cu(OTf)<sub>2</sub> (7.2 mg, 0.020 mmol, 0.050 equiv.) and ethanol (2 mL) were added to a 5 mL round-bottom flask equipped with a magnetic stir bar. Pyridine (32  $\mu$ L, 0.40 mmol, 1.0 equiv.) was added via a syringe, a cooler was connected to the flask and the mixture was stirred with access to air at 25 °C for 24 hours. The crude mixture was purified by column chromatography using silica gel and eluent system as specified. The desired product was dried under high vacuum.

## Scale-up and purification of **11b**

**1.0 mmol scale:** Maleimide (97.1 mg, 1.00 mmol, 1.00 equiv.), (*E*)-styrylboronic acid (438 mg, 3.00 mmol, 3.00 equiv.), Cu(OTf)<sub>2</sub> (18.1 mg, 0.0500 mmol, 0.0500 equiv.) and ethanol (5 mL) were added to a 25 mL round-bottom flask equipped with a magnetic stir bar. Pyridine (81  $\mu$ L, 1.0 mmol, 1.0 equiv.) was added via a syringe, a cooler was connected to the flask and the mixture was stirred at 25 °C for 24-30 hours. The crude product was purified by column chromatography (chloroform:hexane:acetone [6:4:1]). All the fractions containing the desired product was collected, solvents were removed under reduced pressure and then re-dissolved in a small amount of chloroform (~5 mL). Hexane (~15 mL) was added and the precipitate was isolated by filtration and washed with hexane (3 x ~5 mL). The precipitation process was repeated, and the desired product **11b** was obtained as an off-white solid (172 mg, 70 %).

**2.0 mmol scale:** Procedure and purification is the same as in the 1.0 mmol reaction. Maleimide (194 mg, 2.00 mmol, 1.00 equiv.), (*E*)-styrylboronic acid (747 mg, 5.05 mmol, 2.52 equiv.), Cu(OTf)<sub>2</sub> (36.1 mg, 0.100 mmol, 0.0500 equiv.), ethanol (10 mL) and pyridine (161  $\mu$ L, 2.00 mmol, 1.00 equiv.) was used. The desired product **11b** was obtained as an off-white solid (306 mg, 62 %).



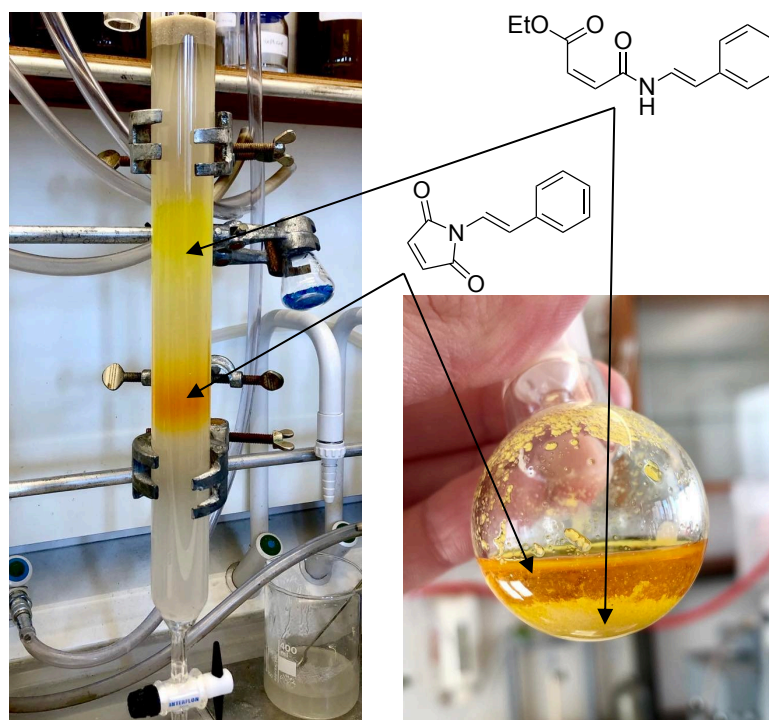
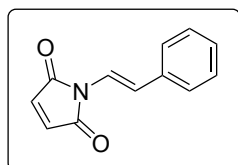


**Figure 5.1.** Purification of **11b**. Column chromatography (left) displays **11b** as a yellow band and **11a** as an orange band. Despite the seemingly good separation, **11a** is tailing into the fractions of **11b**. Trituration of the product mixture induces precipitation of **11b** and leaves **11a** in solution.

### *(E)*-*N*-styrylmaleimide (**11a**)



Following the general procedure and replacing EtOH with MeOH, **11a** was obtained as the major product in the attempted formation of **11c** after column chromatography (chloroform:hexane:acetone [6:3:1]) as a bright, orange solid (55.7 mg, 70 %).

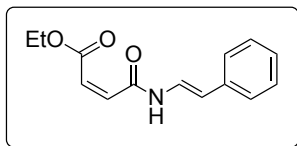
$^1\text{H}$  NMR (600 MHz,  $\text{CDCl}_3$ ):  $\delta$  7.43 – 7.39 (m, 3H), 7.33 (t,  $J = 7.7$  Hz, 2H), 7.27 – 7.23 (m, 2H), 7.13 (d,  $J = 15.2$  Hz, 1H), 6.78 (s, 2H)

$^{13}\text{C}$  NMR (151 MHz,  $\text{CDCl}_3$ ):  $\delta$  168.5, 135.7, 134.5, 128.7, 127.5, 126.0, 119.2, 116.8.

HRMS (APPI, MeCN)<sup>i</sup>  $m/z$   $[\text{M}]^+$ : Calcd. for  $\text{C}_{12}\text{H}_9\text{NO}_2^+$ : 199.0628, found: 199.0626.

<sup>i</sup> It was necessary to use MeCN as solvent rather than MeOH to prevent hydrolysis.

**(*E*)-*N*-styryl ethyl maleamate (11b)**



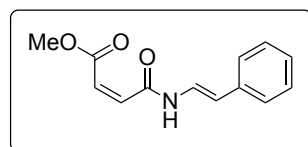
Following the general procedure, **11b** was obtained after column chromatography (chloroform:hexane:acetone [6:3:1]) as an off-white solid (76.5 mg, 78 %).

$^1\text{H}$  NMR (600 MHz,  $\text{CDCl}_3$ ):  $\delta$  11.08 (d,  $J = 9.5$  Hz, 1H), 7.57 (dd,  $J = 14.7, 10.4$  Hz, 1H), 7.38 – 7.34 (m, 2H), 7.32 – 7.27 (m, 2H), 7.22 – 7.16 (m, 1H), 6.40 (d,  $J = 13.4$  Hz, 1H), 6.31 (d,  $J = 14.7$  Hz, 1H), 6.23 (d,  $J = 13.4$  Hz, 1H), 4.31 (q,  $J = 7.2$  Hz, 2H), 1.36 (t,  $J = 7.1$  Hz, 3H).

$^{13}\text{C}$  NMR (151 MHz,  $\text{CDCl}_3$ ):  $\delta$  166.6, 160.8, 138.0, 136.0, 128.5, 126.7, 126.3, 125.6, 122.4, 114.9, 62.0, 13.9.

HRMS (ESI)  $m/z$   $[\text{M} + \text{Na}]^+$ : Calcd. for  $\text{C}_{14}\text{H}_{15}\text{NNaO}_3^+$ : 268.0944, found: 268.0943.

**(*E*)-*N*-styryl methyl maleamate (11c)**



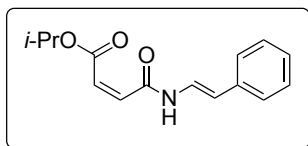
Following the general procedure and replacing EtOH with MeOH, **11c** was obtained after column chromatography (hexane:EtOAc [1:1]) as a yellow-orange oil (27.4 mg, 30 %).

$^1\text{H}$  NMR (600 MHz,  $\text{CDCl}_3$ ):  $\delta$  10.95 (d,  $J = 10.4$  Hz, 1H), 7.57 (dd,  $J = 14.7, 10.4$  Hz, 1H), 7.37 – 7.34 (m, 2H), 7.31 – 7.27 (m, 2H), 7.20 – 7.17 (m, 1H), 6.40 (d,  $J = 13.3$  Hz, 1H), 6.31 (d,  $J = 14.7$  Hz, 1H), 6.24 (d,  $J = 13.3$  Hz, 1H), 3.86 (s, 3H).

$^{13}\text{C}$  NMR (151 MHz,  $\text{CDCl}_3$ ):  $\delta$  167.2, 160.6, 139.0, 136.1, 128.6, 126.8, 125.7, 125.6, 122.4, 115.1, 52.9.

HRMS (ESI)  $m/z$   $[\text{M} + \text{Na}]^+$ : Calcd. for  $\text{C}_{13}\text{H}_{13}\text{NNaO}_3^+$ : 254.0788, found: 254.0787.

**(E)-N-styryl isopropyl maleamate (11d)**



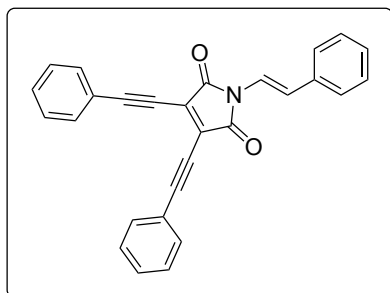
Following the general procedure on a 0.2 mmol scale and replacing EtOH with *i*-PrOH, **11d** was obtained after column chromatography (hexane:EtOAc [2:1]) as a pale yellow oil that solidified upon drying under high vacuum (11.8 mg, 11 %).

<sup>1</sup>H NMR (600 MHz, CDCl<sub>3</sub>): δ 11.15 (d, *J* = 10.2 Hz, 1H), 7.57 (dd, *J* = 14.7, 10.4 Hz, 1H), 7.38 – 7.35 (m, 2H), 7.29 (t, *J* = 7.8 Hz, 2H), 7.20 – 7.17 (m, 1H), 6.38 (d, *J* = 13.4 Hz, 1H), 6.31 (d, *J* = 14.7 Hz, 1H), 6.19 (d, *J* = 13.4 Hz, 1H), 5.15 (hept, *J* = 6.3 Hz, 1H), 1.34 (d, *J* = 6.3 Hz, 6H).

<sup>13</sup>C NMR (151 MHz, CDCl<sub>3</sub>): δ 166.3, 160.8, 138.8, 136.2, 128.6, 126.8, 126.5, 125.7, 122.5, 115.0, 70.1, 21.6.

HRMS (ESI) *m/z* [M + Na]<sup>+</sup>: Calcd. for C<sub>15</sub>H<sub>17</sub>NNaO<sub>3</sub><sup>+</sup>: 282.1101, found: 282.1099.

**(E)-N-styryl-bis(phenylethynyl)maleimide (11f)**



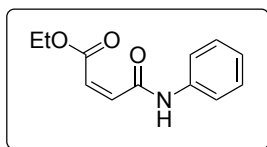
Following the general procedure on a 0.2 mmol scale, **11f** was obtained after column chromatography (hexane:EtOAc [4:1]) and a short silica plug (toluene) as a dark red solid (44.9 mg, 57 %)

<sup>1</sup>H NMR (600 MHz, CDCl<sub>3</sub>): δ 7.69 – 7.65 (m, 4H), 7.52 (d, *J* = 15.1 Hz, 1H), 7.49 – 7.41 (m, 8H), 7.35 (t, *J* = 7.7 Hz, 2H), 7.29 – 7.25 (m, 1H), 7.19 (d, *J* = 15.1 Hz, 1H).

<sup>13</sup>C NMR (151 MHz, CDCl<sub>3</sub>): δ 165.0, 135.6, 132.6, 130.6, 128.7, 128.7, 127.8, 127.7, 126.2, 121.4, 119.9, 117.0, 110.9, 80.4.

HRMS (ESI) *m/z* [M + Na]<sup>+</sup>: Calcd. for C<sub>28</sub>H<sub>17</sub>NNaO<sub>2</sub><sup>+</sup>: 422.1151, found: 422.1145.

***N*-phenyl ethyl maleamate (11g)**<sup>370</sup>



Following the general procedure replacing (*E*)-styrylboronic acid **8a** with phenylboronic acid **13a**, **11g** was obtained after column chromatography (chloroform:hexane:acetone [6:3:1]) as a yellow oil (56.6 mg, 65 %).

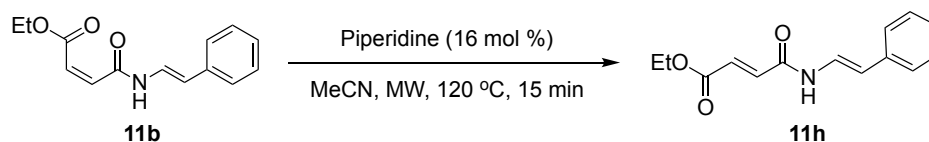
<sup>1</sup>H NMR (600 MHz, CDCl<sub>3</sub>): δ 10.86 (br s, 1H), 7.66 (dd, *J* = 8.6, 1.2 Hz, 2H), 7.33 (dd, *J* = 8.6, 7.4 Hz, 2H), 7.12 (tt, *J* = 7.4, 1.2 Hz, 1H), 6.42 (d, *J* = 13.4 Hz, 1H), 6.19 (d, *J* = 13.2 Hz, 1H), 4.29 (q, *J* = 7.2 Hz, 2H), 1.33 (t, *J* = 7.2 Hz, 3H).

<sup>13</sup>C NMR (151 MHz, CDCl<sub>3</sub>): δ 166.7, 161.6, 139.9, 137.8, 128.9, 125.5, 124.5, 120.0, 62.0, 13.9.

HRMS (ESI) *m/z* [M + Na]<sup>+</sup>: Calcd. for C<sub>12</sub>H<sub>13</sub>NNaO<sub>3</sub><sup>+</sup>: 242.0788, found: 242.0787.

## Synthesis and characterization of compounds obtained from reactions with **11b**

### (*E*)-*N*-styryl ethyl fumaramate (**11h**)



**11h** was prepared according to a literature procedure<sup>366</sup> with slight modifications.

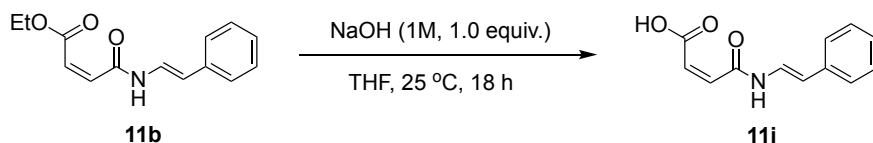
In a 10 mL MW reaction vial (Anton-Paar G10), (*E*)-*N*-styryl ethyl maleamate (**11b**, 61.4 mg, 0.250 mmol, 1.00 equiv.), piperidine (4.0  $\mu$ L, 0.040 mmol, 0.16 equiv.), CH<sub>3</sub>CN (0.25 mL) and a magnetic stirring bar was added. The vial was sealed, the reaction mixture pre-stirred for 1 min and then heated under microwave irradiation for 15 min at 120 °C. The reaction mixture was allowed to cool to room temperature, the resulting precipitate was filtered, washed with a small amount of MeCN (3 x 0.2 mL) and dried under high vacuum. **11h** was afforded as a bright, yellow solid (43.0 mg, 70 %)

<sup>1</sup>H NMR (600 MHz, CDCl<sub>3</sub>):  $\delta$  7.86 (d,  $J$  = 10.8 Hz, 1H), 7.60 (dd,  $J$  = 14.6, 10.8 Hz, 1H), 7.36 – 7.32 (m, 2H), 7.30 (t,  $J$  = 7.7 Hz, 2H), 7.23 – 7.18 (m, 1H), 7.02 (d,  $J$  = 15.3 Hz, 1H), 6.96 (d,  $J$  = 15.3 Hz, 1H), 6.25 (d,  $J$  = 14.6 Hz, 1H), 4.29 (q,  $J$  = 7.1 Hz, 2H), 1.34 (t,  $J$  = 7.1 Hz, 3H).

<sup>13</sup>C NMR (151 MHz, CDCl<sub>3</sub>):  $\delta$  165.5, 160.6, 135.5, 135.1, 131.8, 128.8, 127.2, 125.8, 122.1, 115.1, 61.4, 14.1.

HRMS (ESI)  $m/z$  [M + Na]<sup>+</sup>: Calcd. for C<sub>14</sub>H<sub>15</sub>NNaO<sub>3</sub><sup>+</sup>: 268.0944, found: 268.0943.

**(*E*)-*N*-styryl maleamic acid (**11i**)**



**11i** was prepared according to a literature procedure<sup>368</sup> with slight modifications.

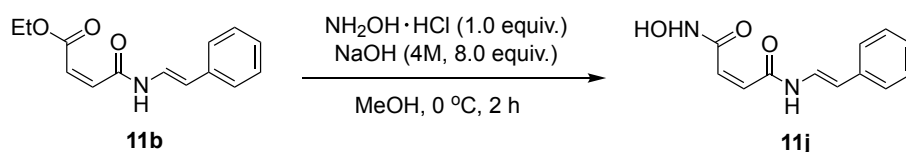
In a 4 mL screw cap vial, (*E*)-*N*-styryl ethyl maleamate (**11b**, 61.4 mg, 0.250 mmol, 1.00 equiv.) was dissolved in THF (0.5 mL). A solution of NaOH (1.0 M, 0.25 mmol, 0.25 mL, 1.0 equiv.) was added, in which a color change from yellow to red was observed. The reaction mixture was allowed to stir at 25 °C for 18 h, then washed with Et<sub>2</sub>O (1 mL). The top, ethereal layer was removed from the vial with a pipette. The remaining aqueous phase was acidified with HCl (2.0 M, 10 drops), the precipitate was filtered and washed with de-ionized water (3 x 0.3 mL) and dried under high vacuum. **11i** was afforded as a bright, yellow solid (52.8 mg, 97 %)

<sup>1</sup>H NMR (600 MHz, DMSO-*d*<sub>6</sub>): δ 13.37 (br s, 1H), 10.76 (d, *J* = 10.1 Hz, 1H), 7.44 (dd, *J* = 14.7, 10.1 Hz, 1H), 7.40 – 7.34 (m, 2H), 7.30 (t, *J* = 7.7 Hz, 2H), 7.20 – 7.14 (m, 1H), 6.39 (d, *J* = 12.1 Hz, 1H), 6.34 (d, *J* = 12.1 Hz, 1H), 6.29 (d, *J* = 14.7 Hz, 1H).

<sup>13</sup>C NMR (151 MHz, DMSO-*d*<sub>6</sub>): δ 166.7, 162.3, 136.1, 131.8, 130.1, 128.8, 126.6, 125.5, 122.9, 113.9.

HRMS (ESI) *m/z* [M - H]<sup>+</sup>: Calcd. for C<sub>12</sub>H<sub>10</sub>NO<sub>3</sub><sup>+</sup>: 216.0666, found: 216.0659.

### *N*<sup>1</sup>-hydroxy-*N*<sup>4</sup>-((*E*)-styryl)maleamide (**11j**)



**11j** was prepared according to a literature procedure<sup>368</sup> with slight modifications.

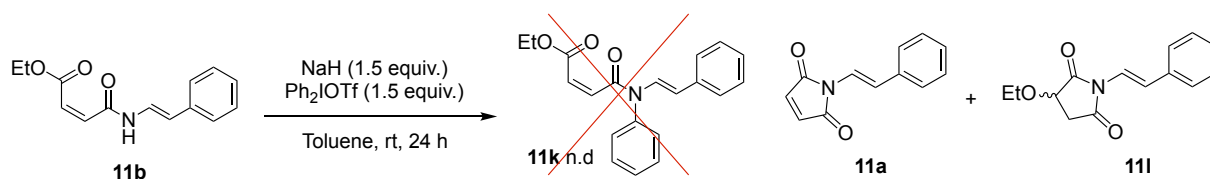
In a 4 mL screw cap vial, (*E*)-*N*-styryl ethyl maleamate (**11b**, 61.2 mg, 0.250 mmol, 1.00 equiv.) was dissolved in MeOH (0.56 mL). Hydroxylamine hydrochloride (17.8 mg, 0.256 mmol, 1.02 equiv.) was added and the heterogenous solution was cooled to 0 °C. A solution of NaOH (4.0 M, 2.0 mmol, 0.5 mL, 8.0 equiv.) was added and the mixture was stirred at 0 °C for 2 h. HCl (2M, 40 drops) was added to the solution, the precipitate was filtered, washed with de-ionized water (3 x 0.3 mL) and acetone (3 x 0.5 mL) and dried under high vacuum. **11j** was afforded as a bright, yellow solid (36.4 mg, 63 %).

<sup>1</sup>H NMR (600 MHz, DMSO-*d*<sub>6</sub>):  $\delta$  11.52 (d,  $J = 10.1$  Hz, 1H), 9.88 – 8.73 (br s, 1H), 7.52 – 7.13 (m, 6H), 6.30 – 6.14 (m, 3H).

<sup>13</sup>C NMR (151 MHz, DMSO-*d*<sub>6</sub>):  $\delta$  162.1, 161.9, 136.4, 131.9, 129.0, 128.8, 126.4, 125.3, 123.2, 112.9.

HRMS (ESI)  $m/z$   $[\text{M} + \text{Na}]^+$ : Calcd. for  $\text{C}_{12}\text{H}_{12}\text{N}_2\text{NaO}_3^+$ : 255.0740, found: 255.0740.

### Attempted synthesis of (*N*-phenyl)-(*E*)-*N*-styryl ethyl maleamate (**11k**)



Preparation of **11k** was attempted using a literature procedure.<sup>388</sup>

To an oven-dried 25-ml round-bottomed flask, flushed with argon, (*E*)-*N*-styryl ethyl maleamate (**11b**, 61.5 mg, 0.250 mmol, 1.00 equiv.), diaryliodonium triflate (161 mg, 0.370 mmol, 1.50 equiv.) and NaH (60 % in mineral oil) (15 mg, 0.38 mmol, 1.5 equiv.) were added. The flask was fitted with a condenser, stir bar, rubber septum, argon-balloon and a needle outlet. Through the septum, dry toluene (5 mL) was added, and when the bubbling had stopped, the outlet was removed. The reaction mixture was stirred under argon, at room temperature for 24 h, changing from dark red to orange. Solvent was removed under reduced pressure, and product was isolated using column chromatography (chloroform:hexane:acetone [6:3:1]), giving an orange, oily substance, identified as a mix of **11a** and **11l**.

**11a** is characterized above.

Characterization of **11l** from the mixture:

<sup>1</sup>H NMR (400 MHz, CDCl<sub>3</sub>): δ 7.60 (d, *J* = 15.2 Hz, 1H), [7.45 – 7.39 (m, 2H), 7.37 – 7.30 (m, 2H), 7.29 – 7.22 (m, 1H)]<sup>j</sup>, 7.17 (d, *J* = 15.2 Hz, 1H), 4.34 (dd, *J* = 8.3, 4.3 Hz, 1H), 4.05 (dq, *J* = 9.2, 7.0 Hz, 1H), 3.71 (dq, *J* = 9.1, 7.0 Hz, 1H), 3.09 (dd, *J* = 18.4, 8.2 Hz, 1H), 2.73 (dd, *J* = 18.4, 4.3 Hz, 1H), 1.27 (t, *J* = 7.0 Hz, 3H).

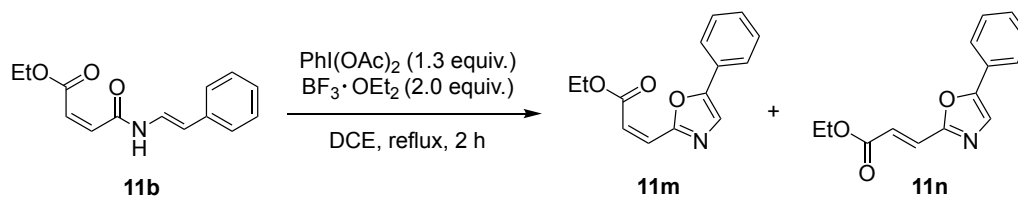
<sup>13</sup>C NMR (101 MHz, CDCl<sub>3</sub>): δ 174.0, 172.3, 135.7, 135.3, 128.7, 128.1, 126.4, 122.8, 117.3, 72.6, 67.1, 36.0, 15.1.

HRMS (APPI, MeCN) *m/z* [M]<sup>+</sup>: Calcd. for C<sub>14</sub>H<sub>15</sub>NO<sub>3</sub><sup>+</sup>: 245.1046, found: 245.1045.

<sup>j</sup> Exact determination of chemical shifts in this region was impossible due to overlapping protons from **11a**.



**Ethyl (*Z*)-3-(5-phenyloxazol-2-yl) acrylate (**11m**) and  
Ethyl (*E*)-3-(5-phenyloxazol-2-yl) acrylate (**11n**)**



**11m** and **11n** were prepared according to a literature procedure.<sup>389</sup>

To a solution of (*E*)-*N*-styryl ethyl maleamate (**11b**, 98.1 mg, 0.400 mmol, 1.00 equiv.) in anhydrous DCE (4 mL) was added BF<sub>3</sub>·OEt<sub>2</sub> (99  $\mu$ L, 0.80 mmol, 2.0 equiv.). The reaction mixture was heated to reflux, then PhI(OAc)<sub>2</sub> (167 mg, 0.520 mmol, 1.30 equiv.) was added in one portion. After stirring under reflux for 2 h, the reaction mixture was cooled down to room temperature, quenched with sat. aq. NaHCO<sub>3</sub> (5 mL) and then extracted with DCM (3 x 5 mL). The combined organic layers were washed with brine (5 mL), drier over anhydrous Na<sub>2</sub>SO<sub>4</sub> and concentrated under reduced pressure. The crude product was purified by flash chromatography (SiO<sub>2</sub>, hexane:EtOAc [2:1], *R<sub>F</sub>* = 0.25 (*Z*-isomer), 0.38 (*E*-isomer)) to give the *Z*-isomer **11m** as a pale yellow oil (23.4 mg, 24 %) and the *E*-isomer **11n** as a pale yellow solid (21.3 mg, 22 %).

<sup>1</sup>H NMR (600 MHz, CDCl<sub>3</sub>):  $\delta$  **Z-isomer**: 7.68 – 7.64 (m, 2H), 7.45 – 7.40 (m, 3H), 7.37 – 7.33 (m, 1H), 6.67 (d, *J* = 12.7 Hz, 1H), 6.23 (d, *J* = 12.7 Hz, 1H), 4.33 (q, *J* = 7.1 Hz, 2H), 1.31 (t, *J* = 7.2 Hz, 3H). **E-isomer**: 7.70 – 7.66 (m, 2H), 7.48 (s, 1H), 7.48 (d, *J* = 16.0 Hz, 1H), 7.46 – 7.42 (m, 2H), 7.39 – 7.35 (m, 1H), 6.80 (d, *J* = 16.0 Hz, 1H), 4.30 (q, *J* = 7.2 Hz, 2H), 1.35 (t, *J* = 7.1 Hz, 3H).

<sup>13</sup>C NMR (151 MHz, CDCl<sub>3</sub>):  $\delta$  **Z-isomer**: 165.7, 157.8, 152.1, 128.95, 128.92, 127.5, 125.0, 124.5, 123.8, 122.6, 61.2, 14.1. **E-isomer**: 165.8, 158.6, 152.6, 129.2, 129.0, 128.5, 127.2, 124.60, 124.59, 124.5, 61.0, 14.2.

HRMS (ESI) *m/z* [M + Na]<sup>+</sup>: Calcd. for C<sub>14</sub>H<sub>13</sub>NNaO<sub>3</sub><sup>+</sup>: 266.0793, found: 266.0788 (for both isomers).

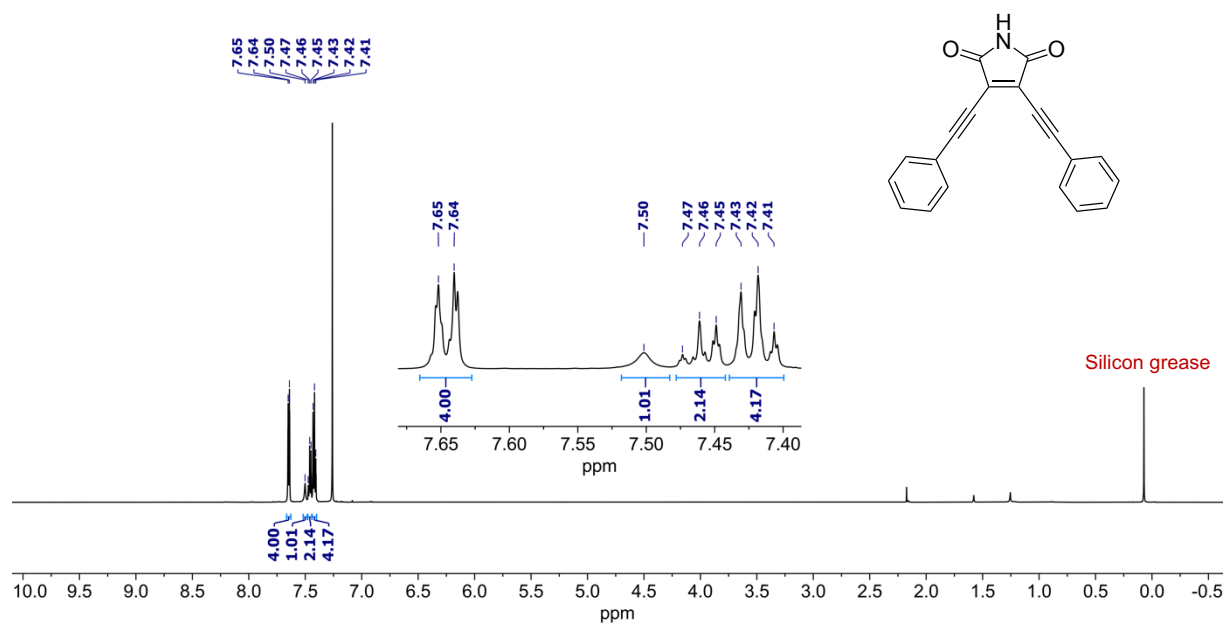


Figure 5.2. <sup>1</sup>H NMR (600 MHz, CDCl<sub>3</sub>) spectrum of **1x**.

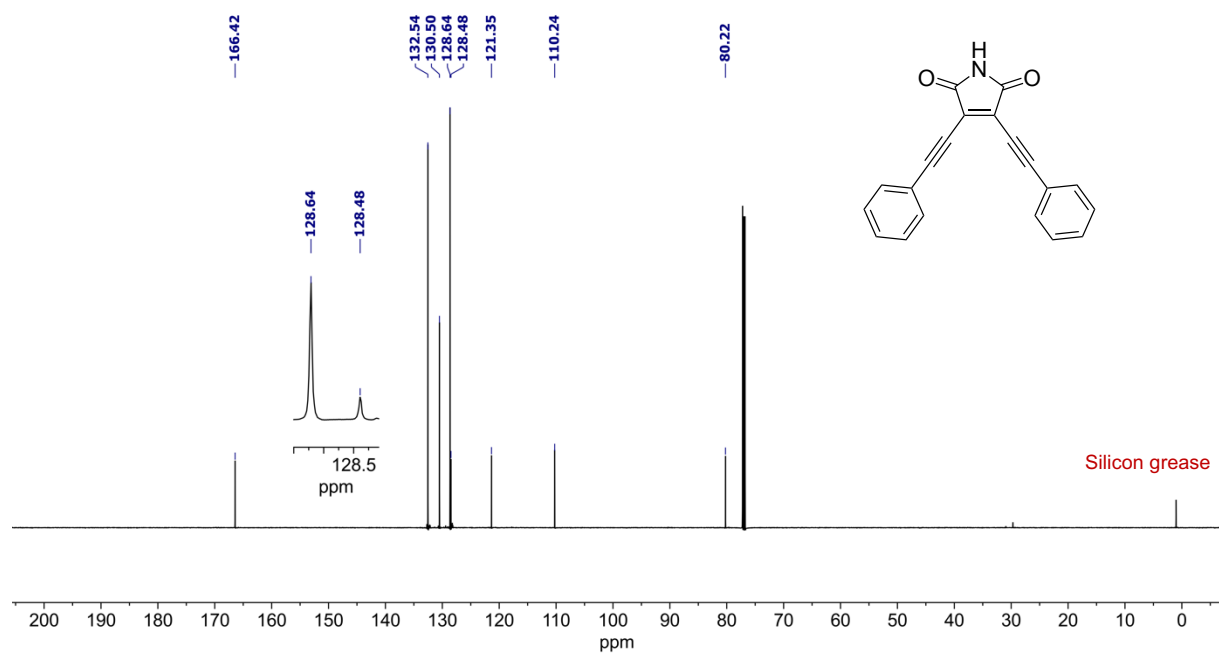
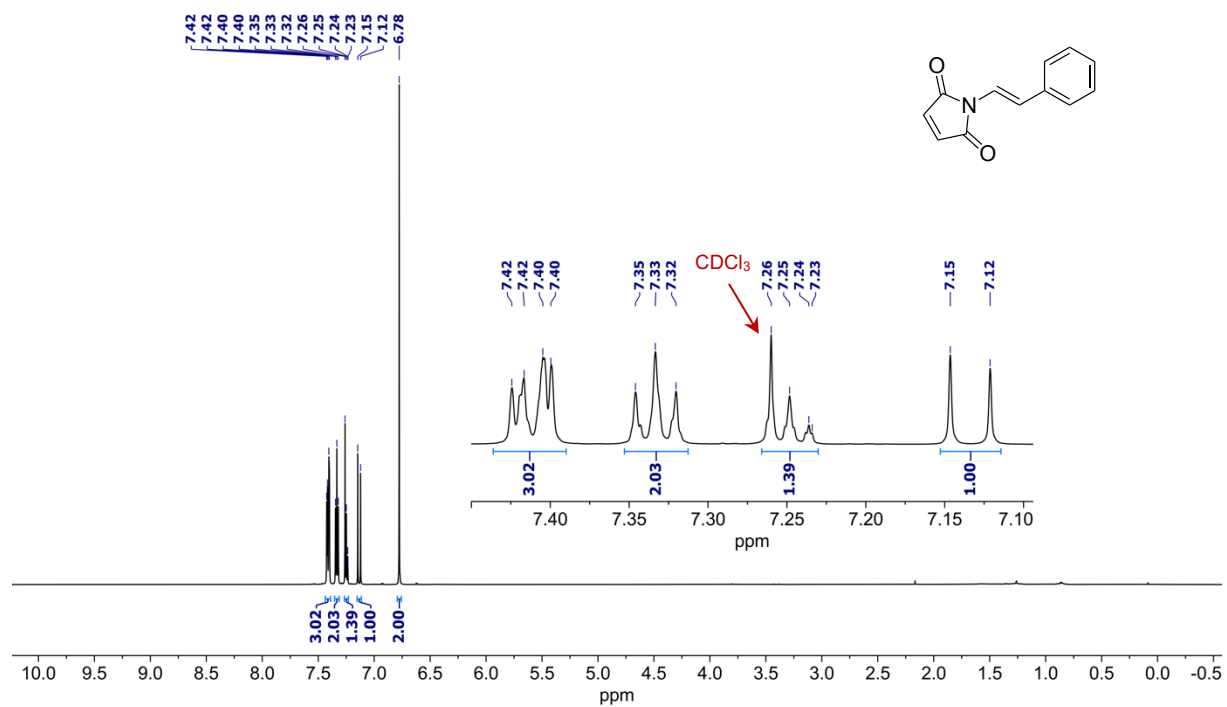
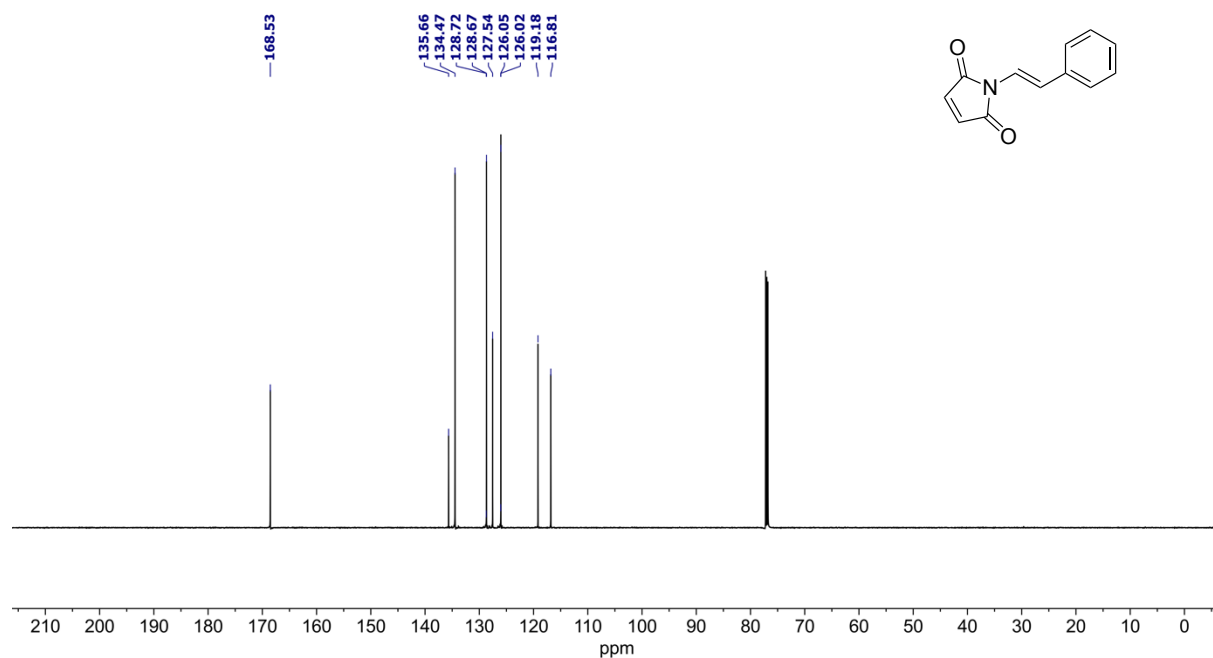


Figure 5.3. <sup>13</sup>C NMR (151 MHz, CDCl<sub>3</sub>) spectrum of **1x**.



**Figure 5.4.** <sup>1</sup>H NMR (600 MHz, CDCl<sub>3</sub>) spectrum of 11a.



**Figure 5.5.** <sup>13</sup>C NMR (151 MHz, CDCl<sub>3</sub>) spectrum of 11a.

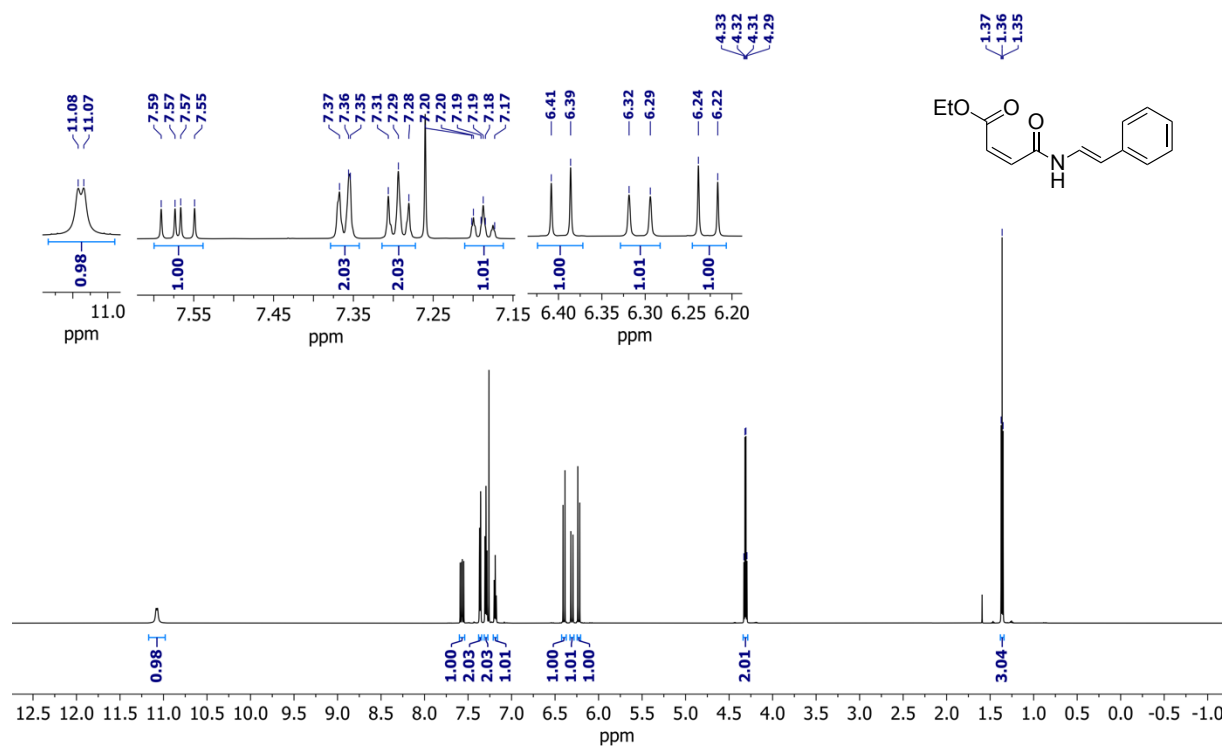


Figure 5.6.  $^1\text{H}$  NMR (600 MHz,  $\text{CDCl}_3$ ) spectrum of 11b.

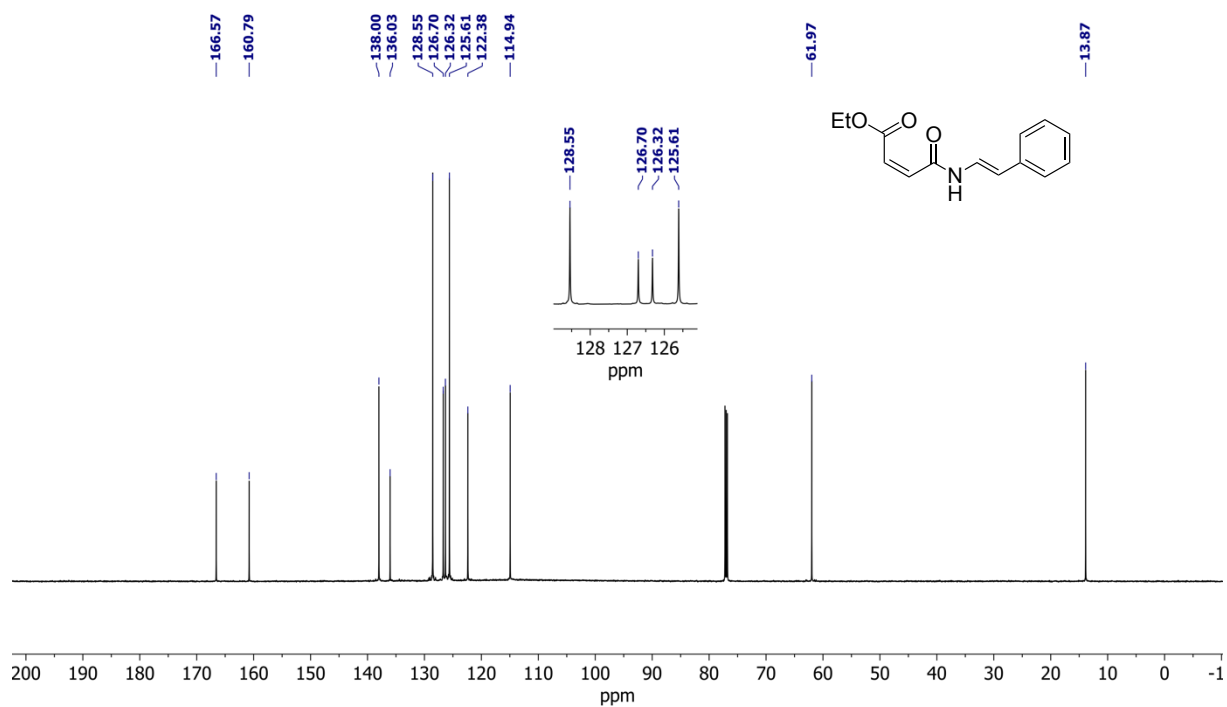
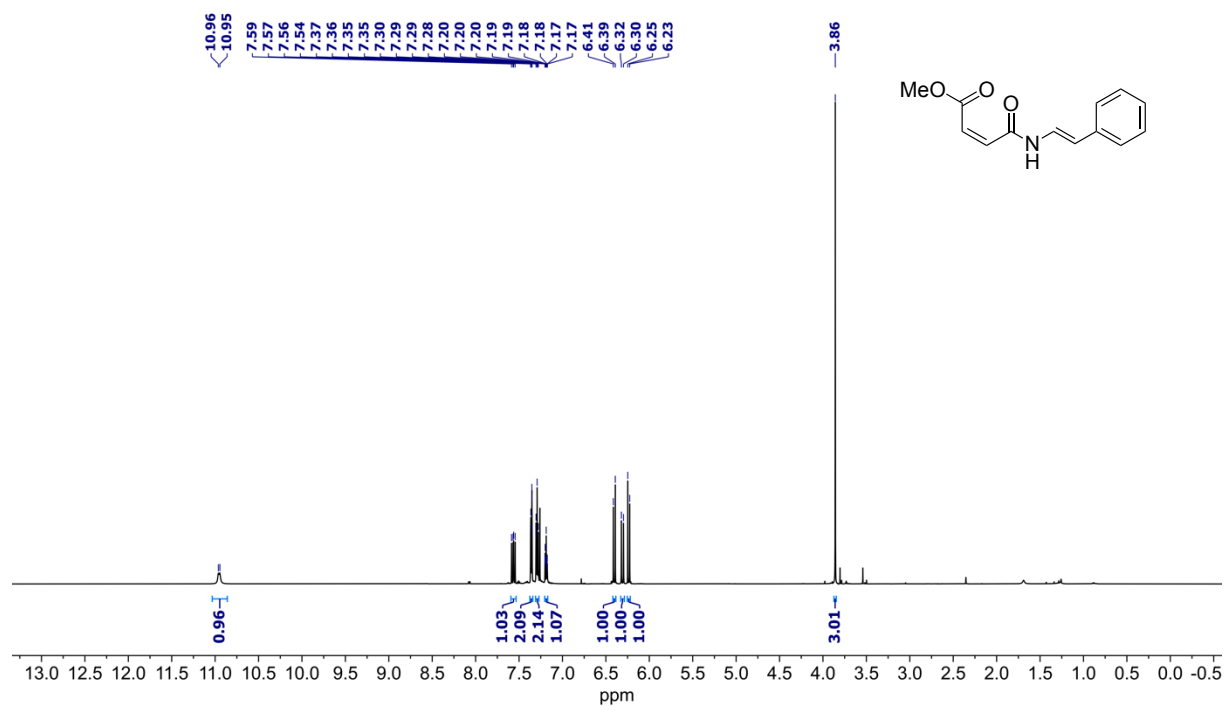
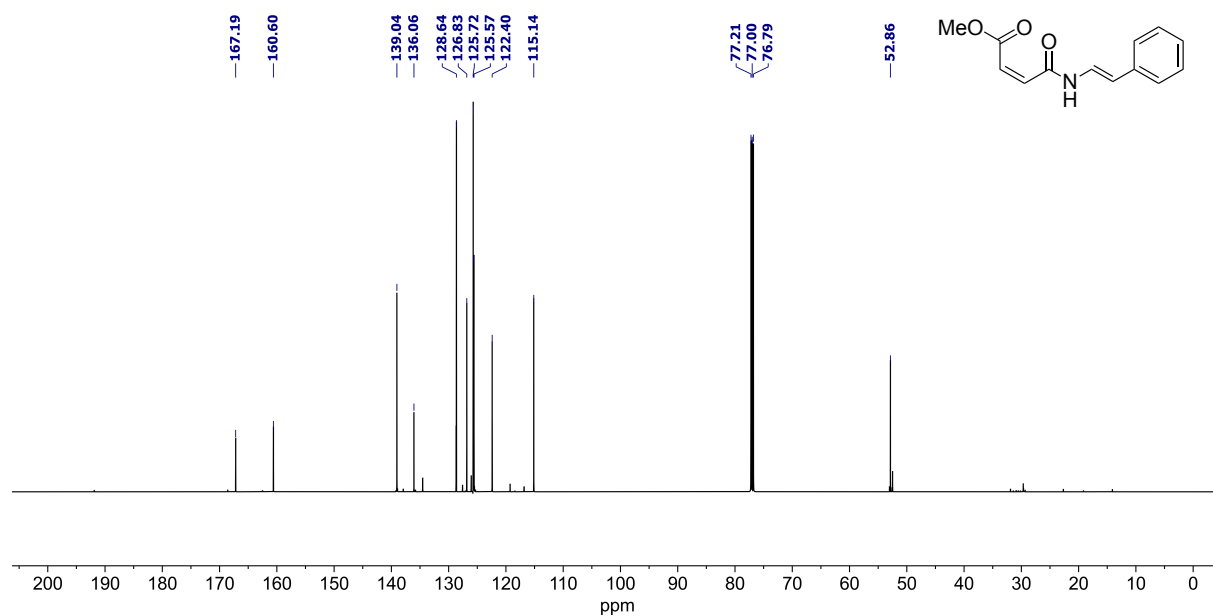


Figure 5.7.  $^{13}\text{C}$  NMR (151 MHz,  $\text{CDCl}_3$ ) spectrum of 11b.



**Figure 5.8.**  $^1\text{H}$  NMR (600 MHz,  $\text{CDCl}_3$ ) spectrum of **11c**.



**Figure 5.9.**  $^{13}\text{C}$  NMR (151 MHz,  $\text{CDCl}_3$ ) spectrum of **11c**. The small peaks in the aromatic region belongs to **11a**.

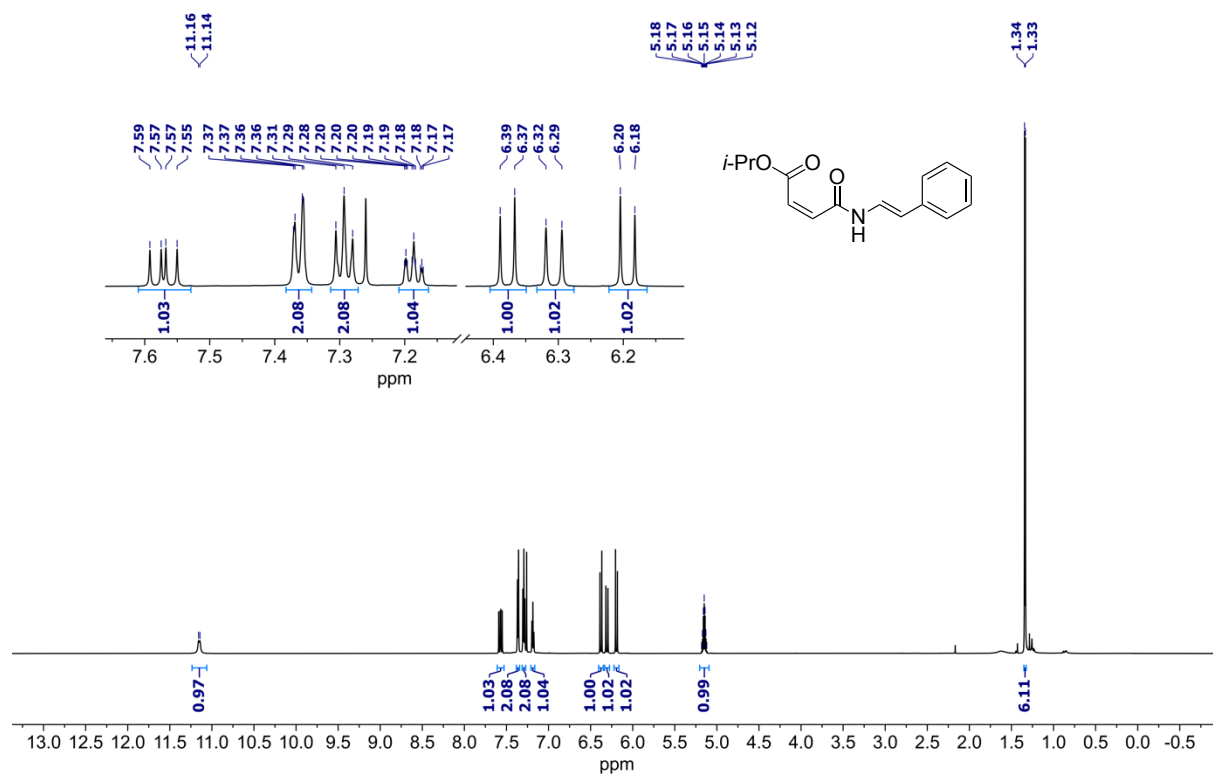


Figure 5.10. <sup>1</sup>H NMR (600 MHz, CDCl<sub>3</sub>) spectrum of 11d.

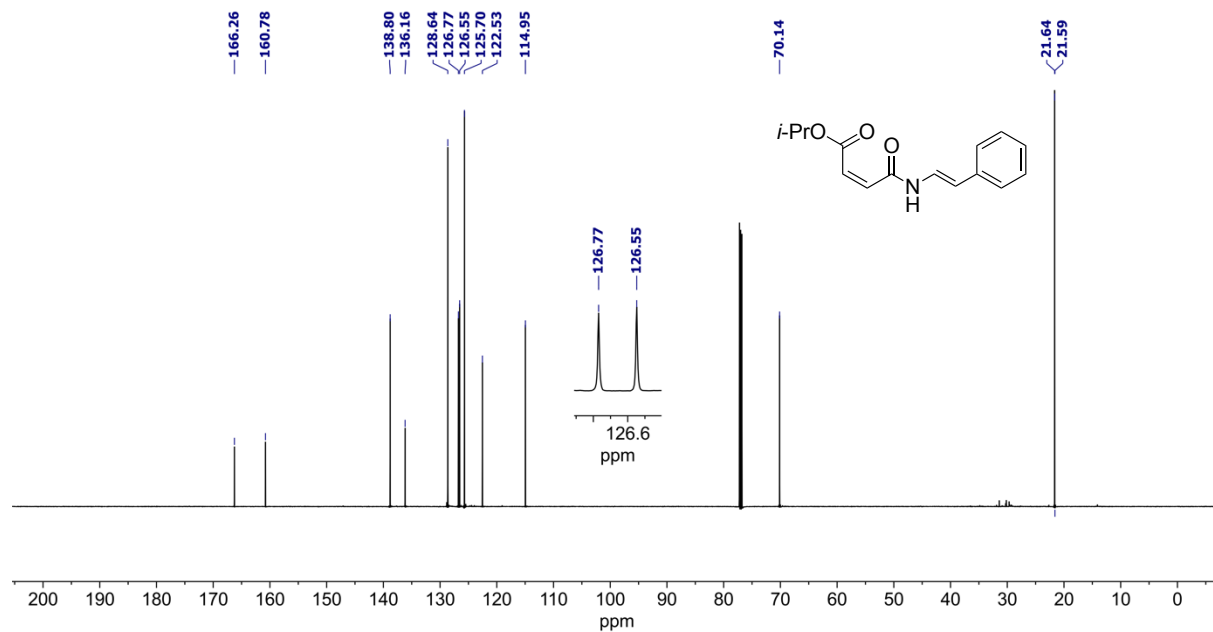
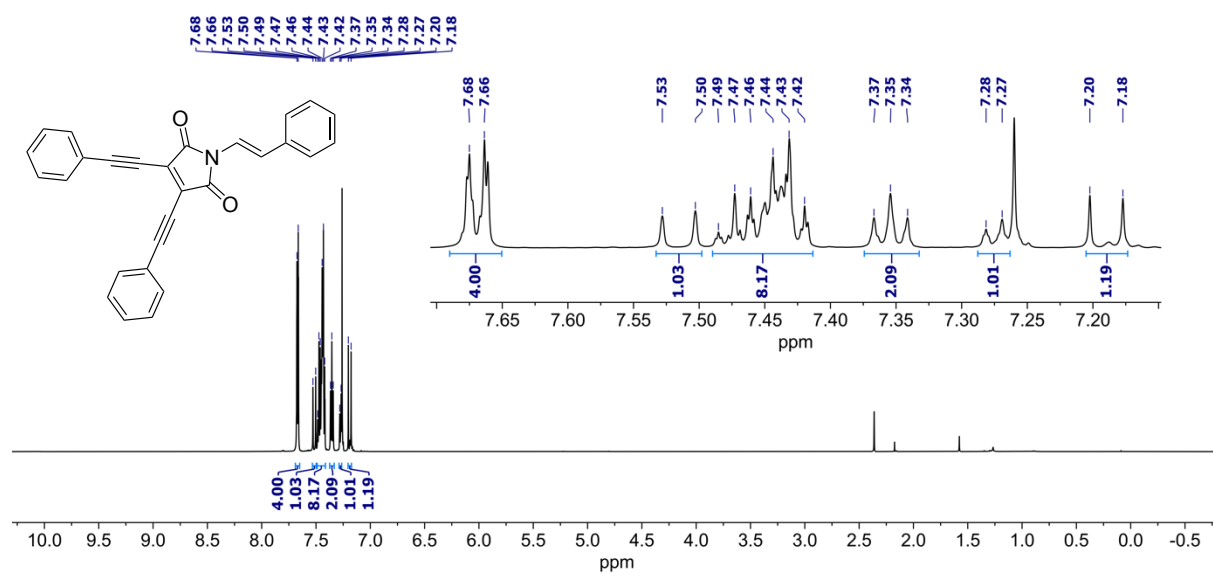
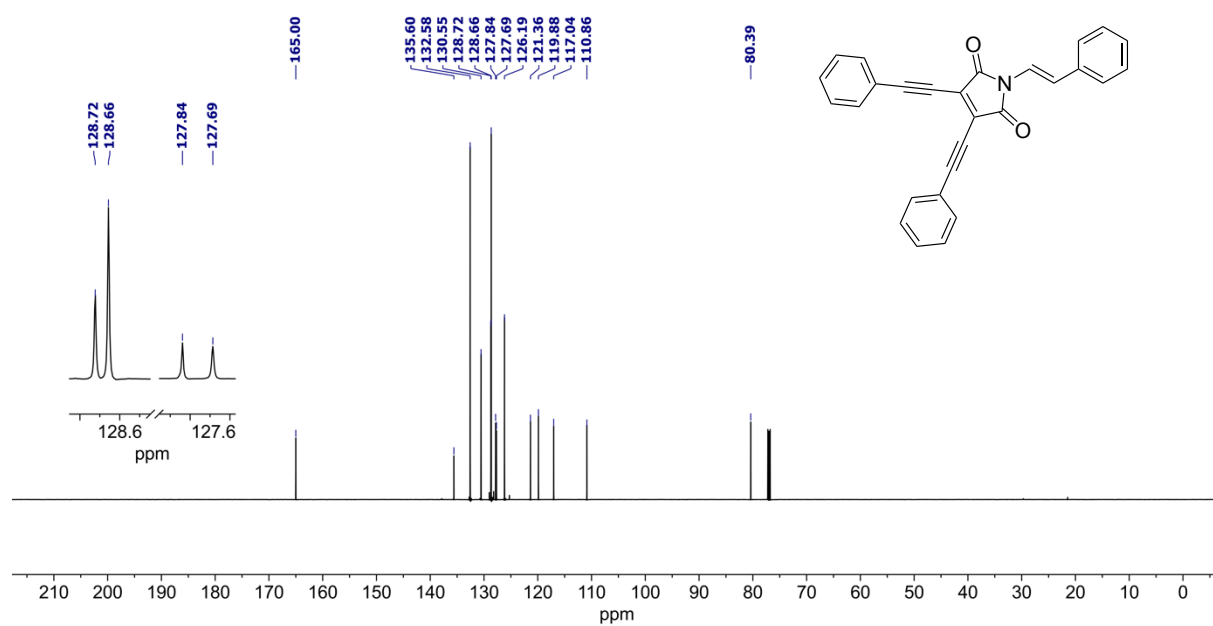


Figure 5.11. <sup>13</sup>C NMR (151 MHz, CDCl<sub>3</sub>) spectrum of 11d.



**Figure 5.12.** <sup>1</sup>H NMR (600 MHz, CDCl<sub>3</sub>) spectrum of **11f**.



**Figure 5.13.** <sup>13</sup>C NMR (151 MHz, CDCl<sub>3</sub>) spectrum of **11f**.

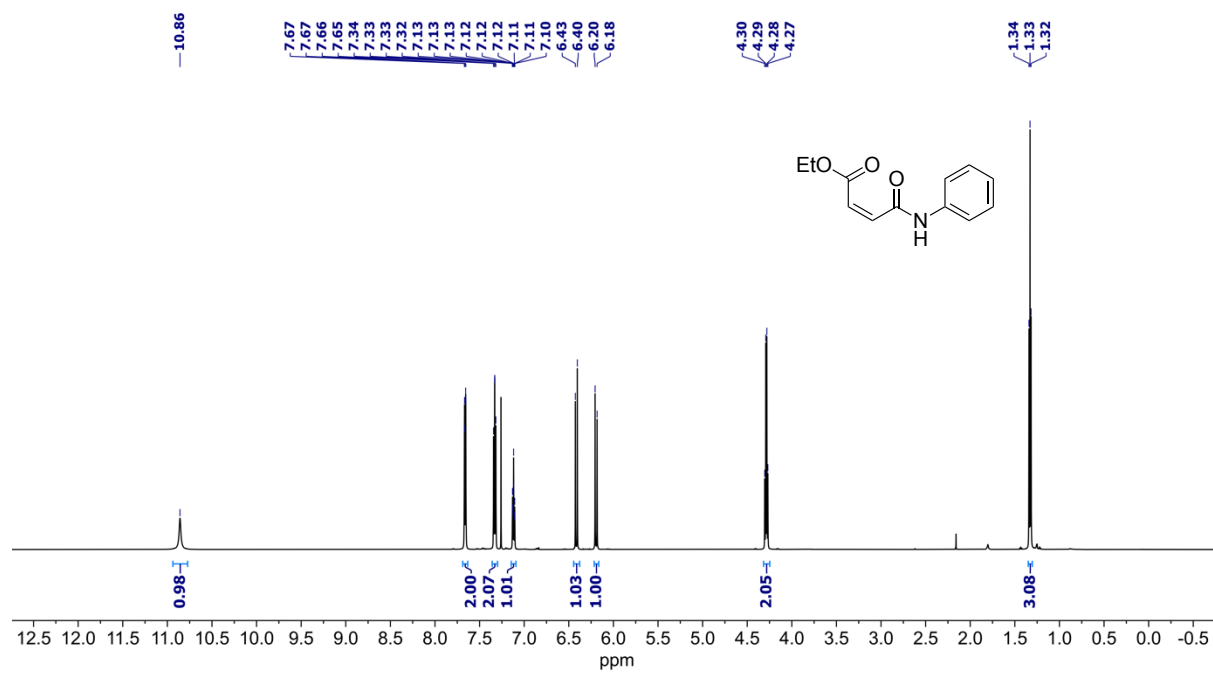


Figure 5.14.  $^1\text{H}$  NMR (600 MHz,  $\text{CDCl}_3$ ) spectrum of **11g**.

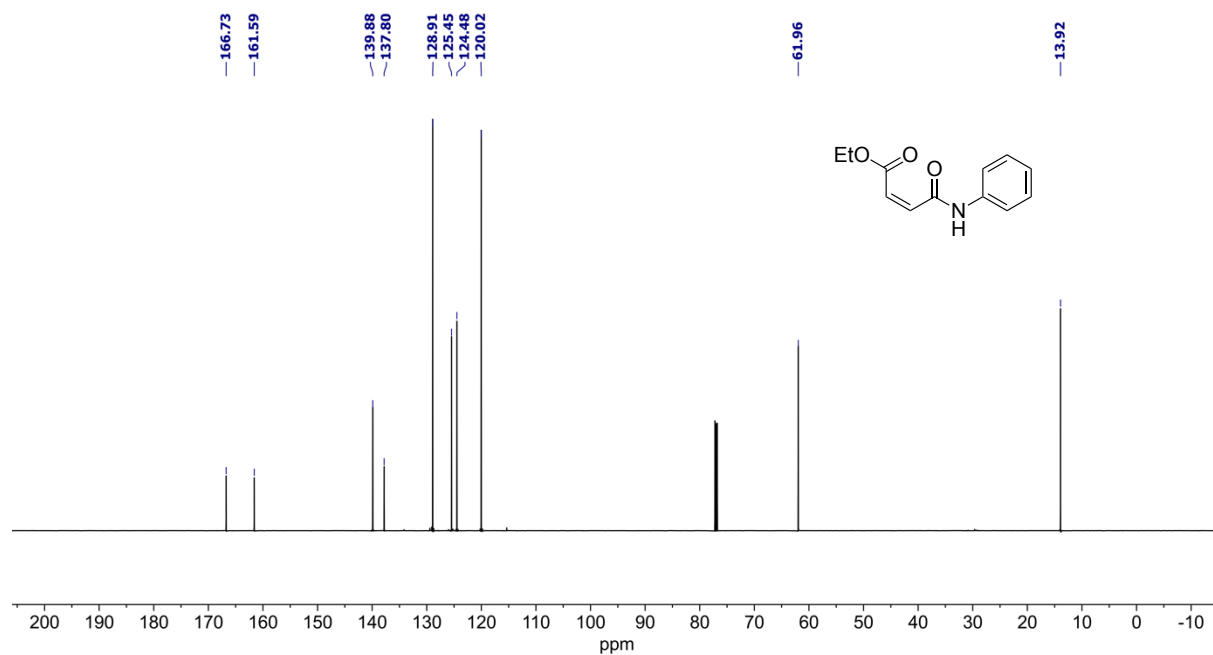


Figure 5.15.  $^{13}\text{C}$  NMR (151 MHz,  $\text{CDCl}_3$ ) spectrum of **11g**.



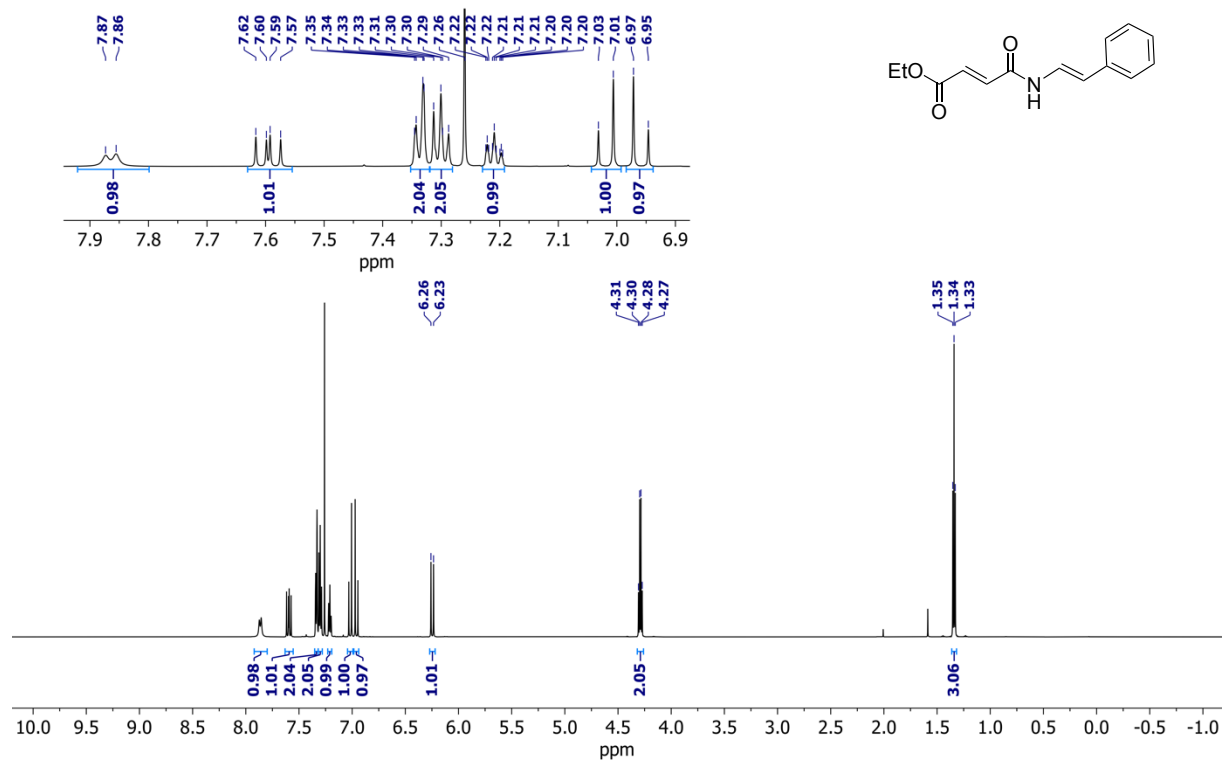


Figure 5.16. <sup>1</sup>H NMR (600 MHz, CDCl<sub>3</sub>) spectrum of 11h.

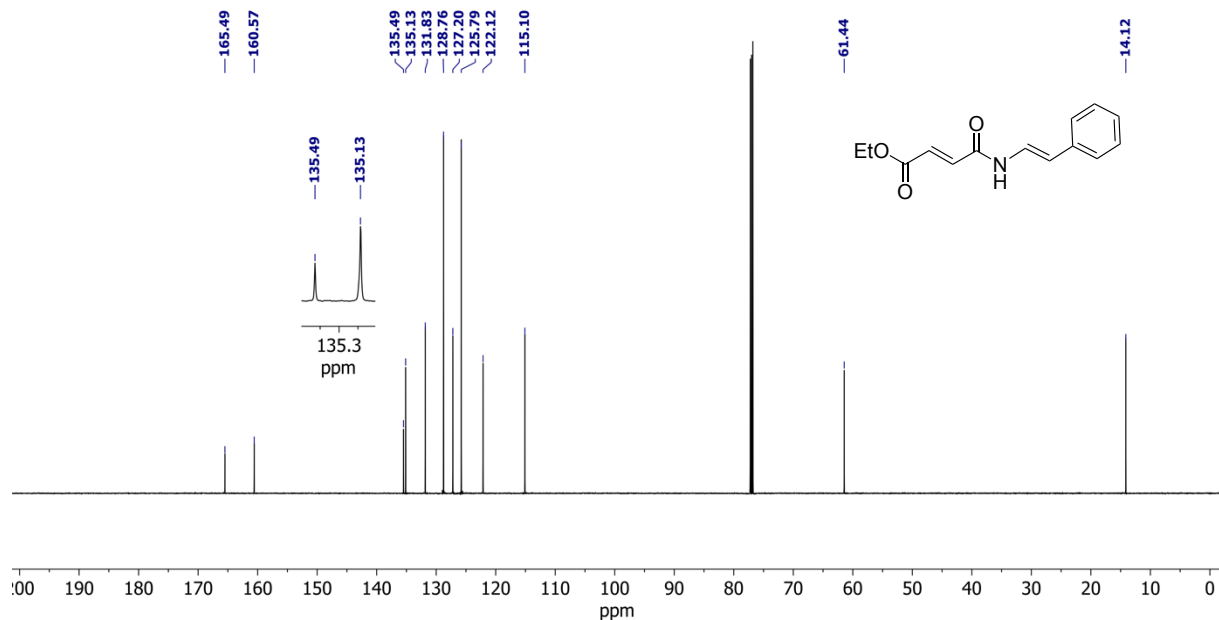
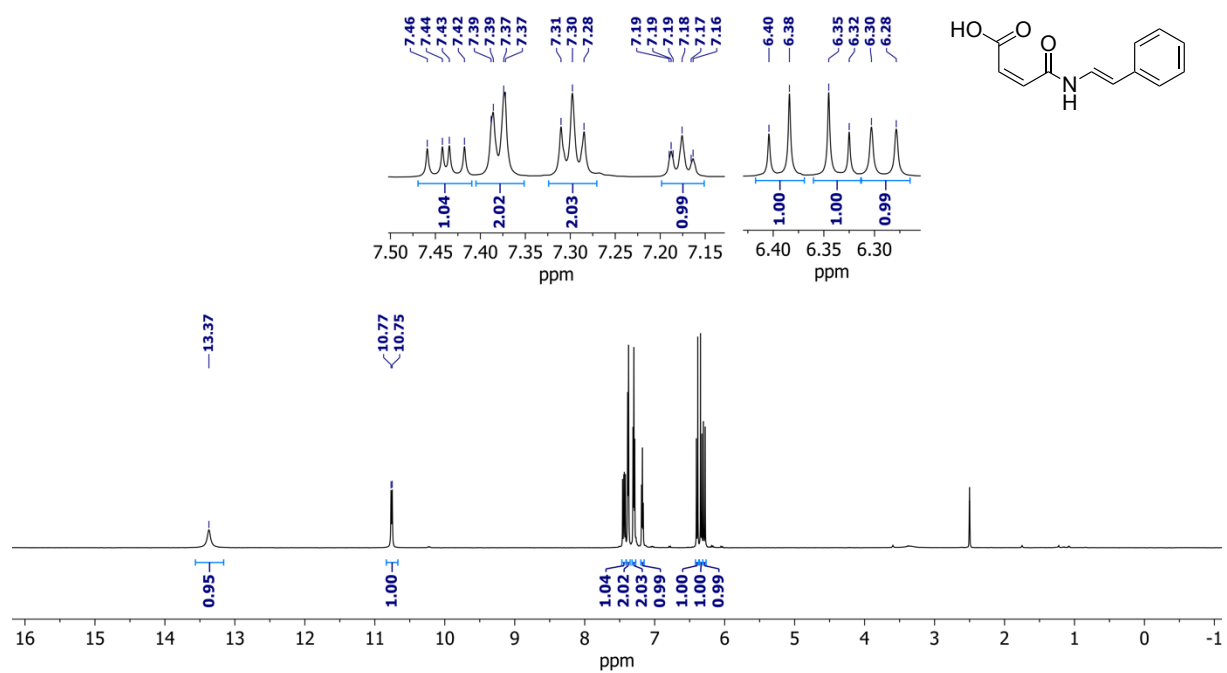
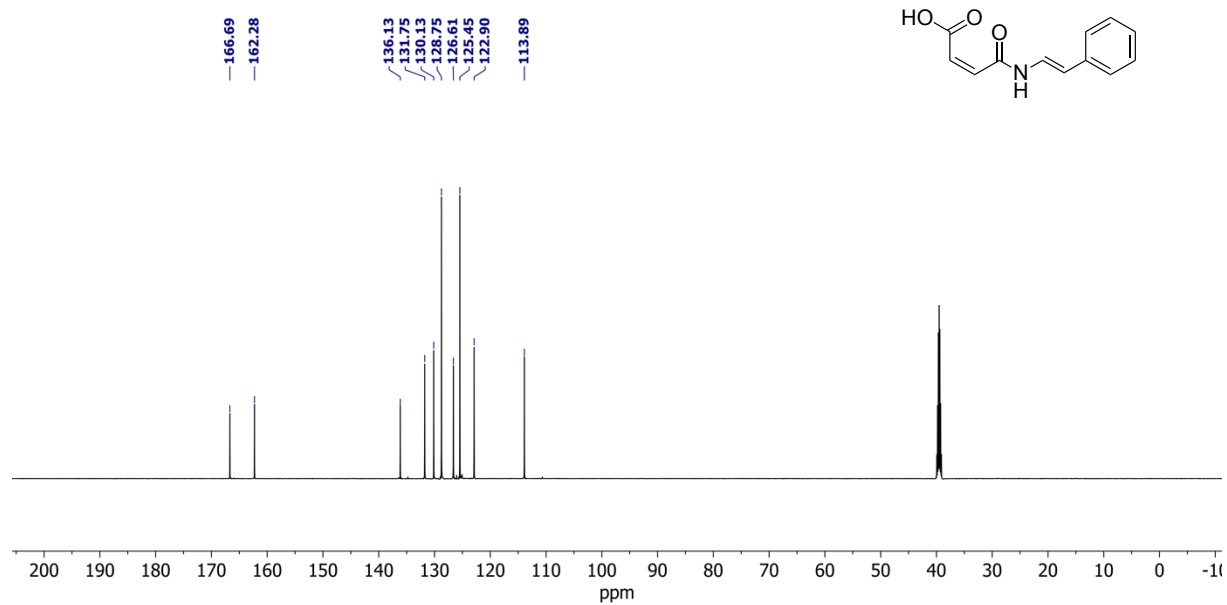


Figure 5.17. <sup>13</sup>C NMR (151 MHz, CDCl<sub>3</sub>) spectrum of 11h.



**Figure 5.18.** <sup>1</sup>H NMR (600 MHz, DMSO-*d*<sub>6</sub>) spectrum of 11i.



**Figure 5.19.** <sup>13</sup>C NMR (151 MHz, DMSO-*d*<sub>6</sub>) spectrum of 11i.

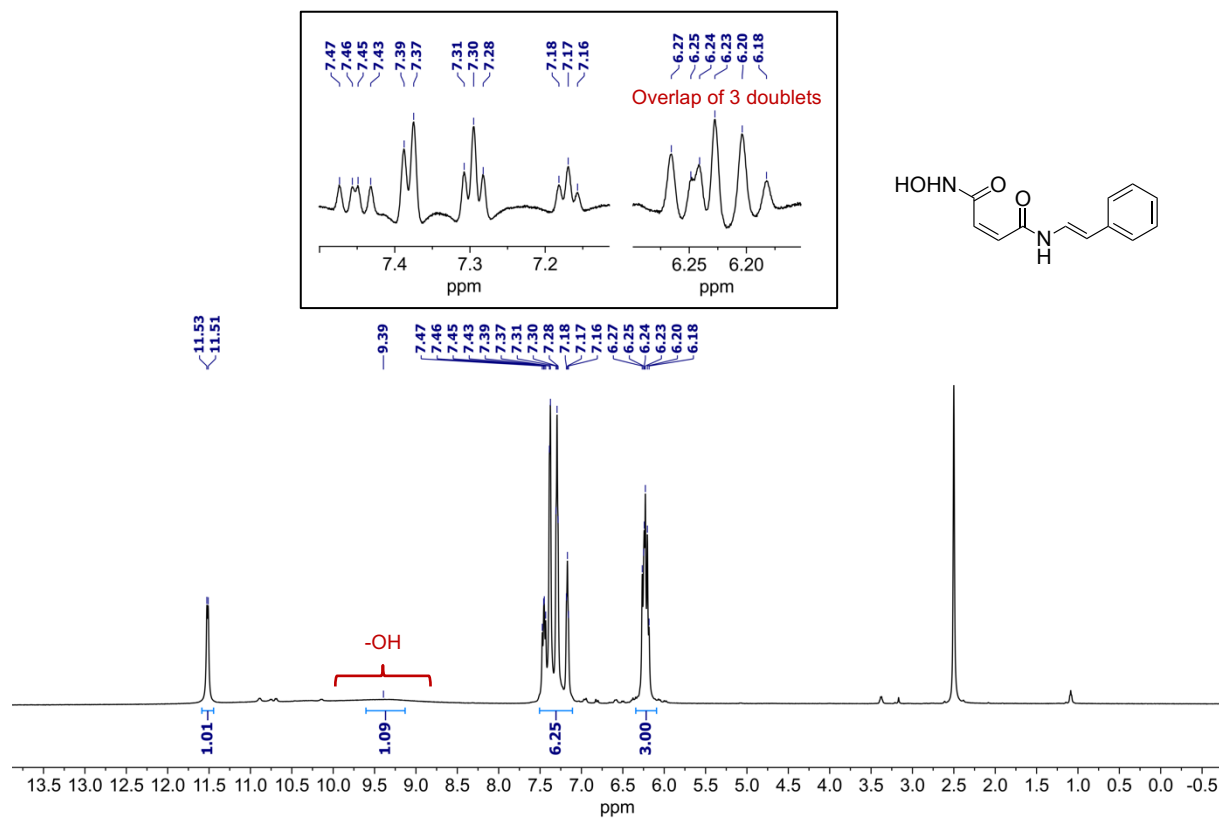


**Figure 5.20.**  $^1\text{H}$  NMR (600 MHz,  $\text{DMSO}-d_6$ ) spectrum of **11j**. Framed region: A sine bell II (70 %) window function was applied to the peaks in the aromatic region to reveal the splitting patterns.

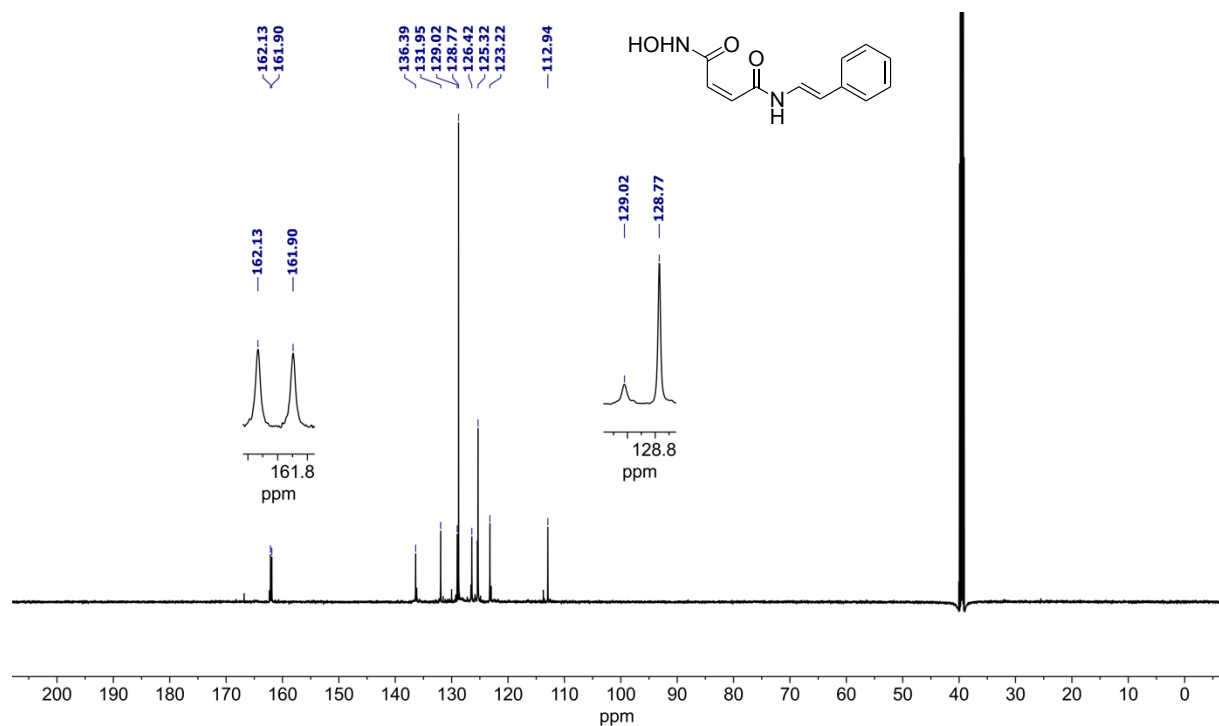


**Figure 5.21.**  $^{13}\text{C}$  NMR (151 MHz,  $\text{DMSO}-d_6$ ) spectrum of **11j**.

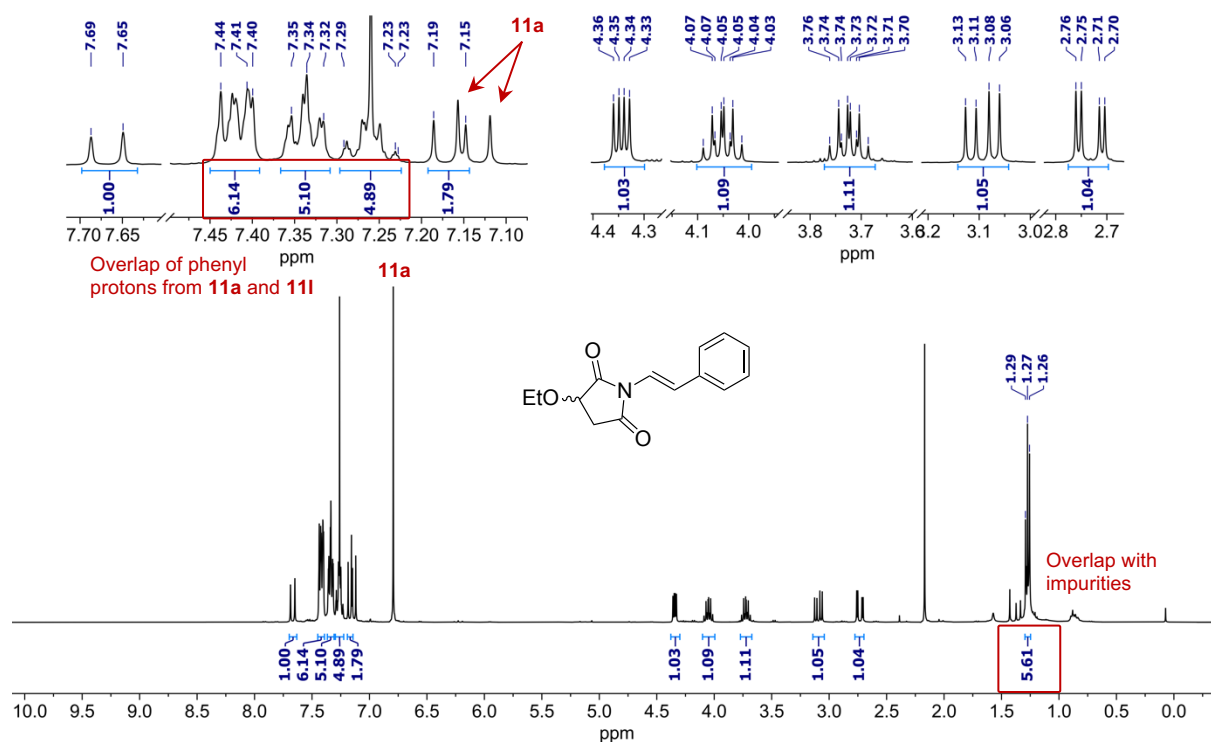


**Figure 5.22.**  $^1\text{H}$  NMR (400 MHz,  $\text{CDCl}_3$ ) spectrum of **11l** and **11a**. The integrated peaks belong to **11l**. Peaks belonging to **11a** is marked in red (the  $^1\text{H}$  NMR spectrum of **11a** is shown in Figure 5.2).

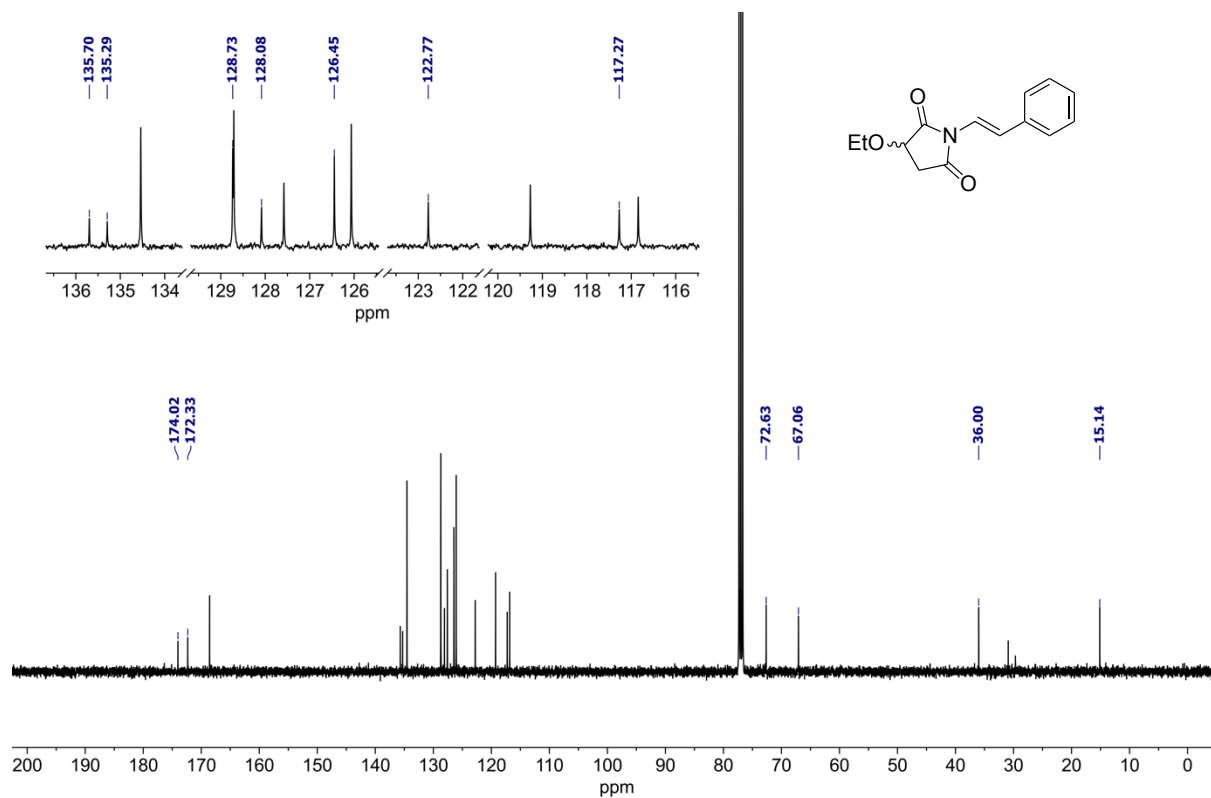


**Figure 5.23.**  $^{13}\text{C}$  NMR (101 MHz,  $\text{CDCl}_3$ ) spectrum of **11l** and **11a**. The marked peaks belong to **11l**. Peaks belonging to **11a** are not marked (the  $^{13}\text{C}$  NMR spectrum of **11a** is shown in Figure 5.3).

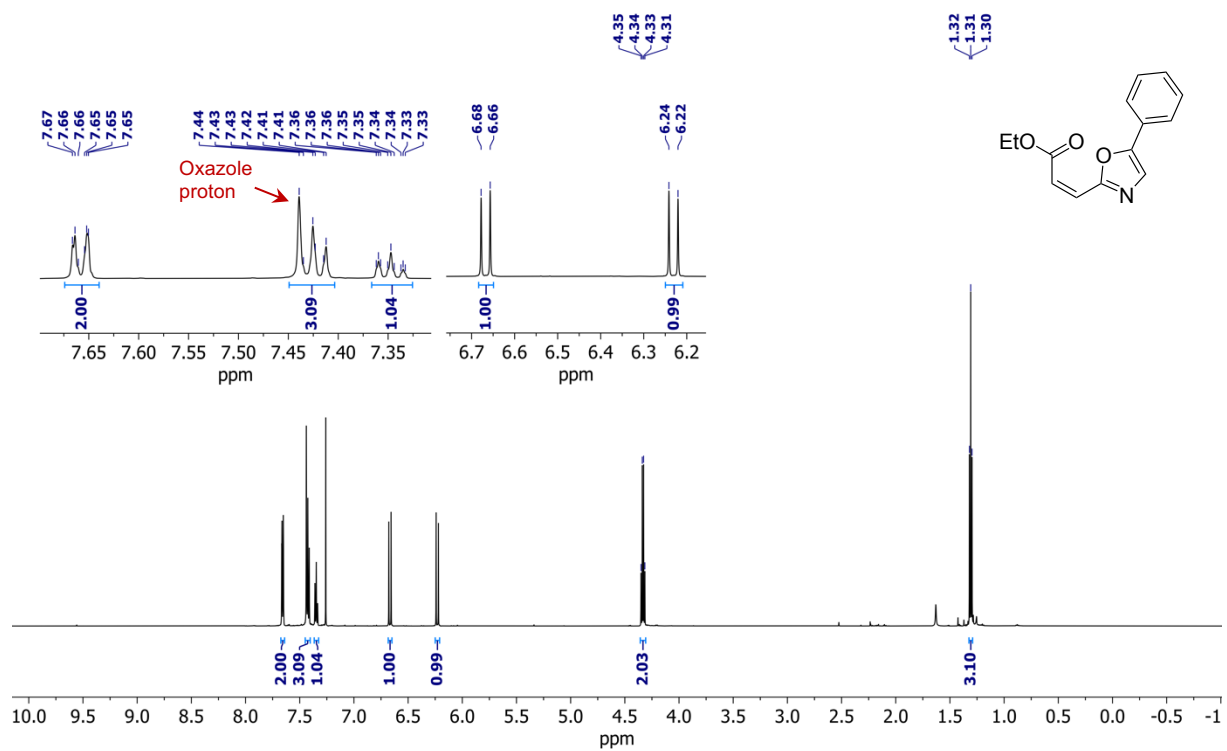


Figure 5.24. <sup>1</sup>H NMR (600 MHz, CDCl<sub>3</sub>) spectrum of **11m**.

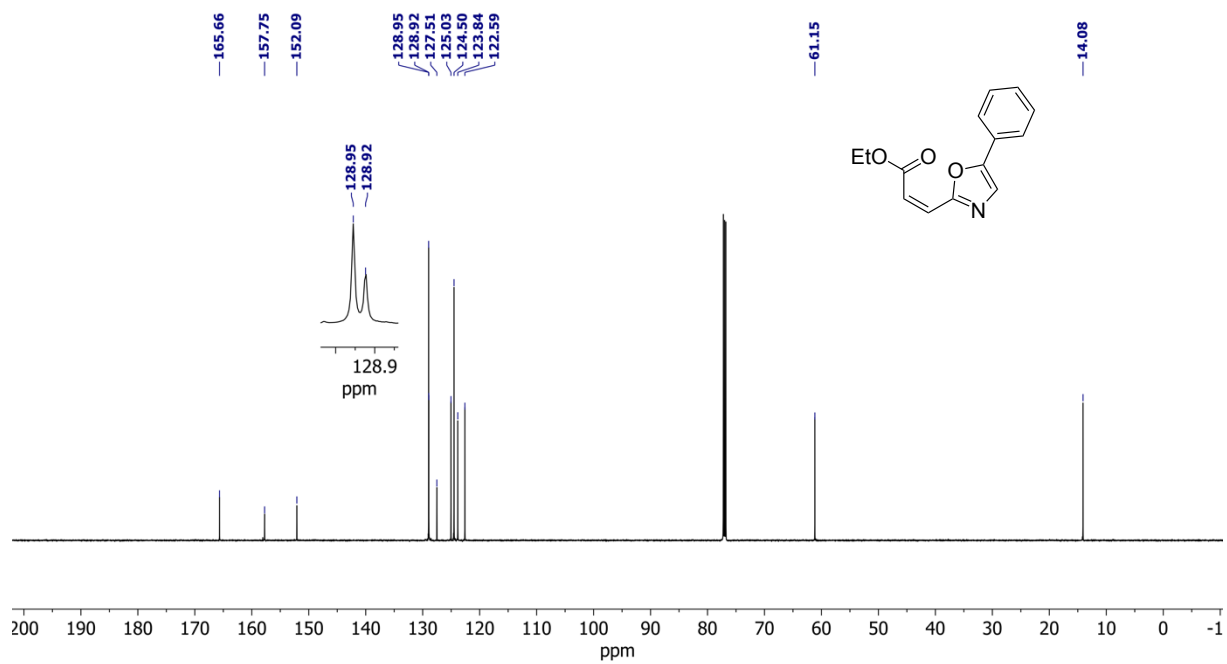


Figure 5.25. <sup>13</sup>C NMR (151 MHz, CDCl<sub>3</sub>) spectrum of **11m**.

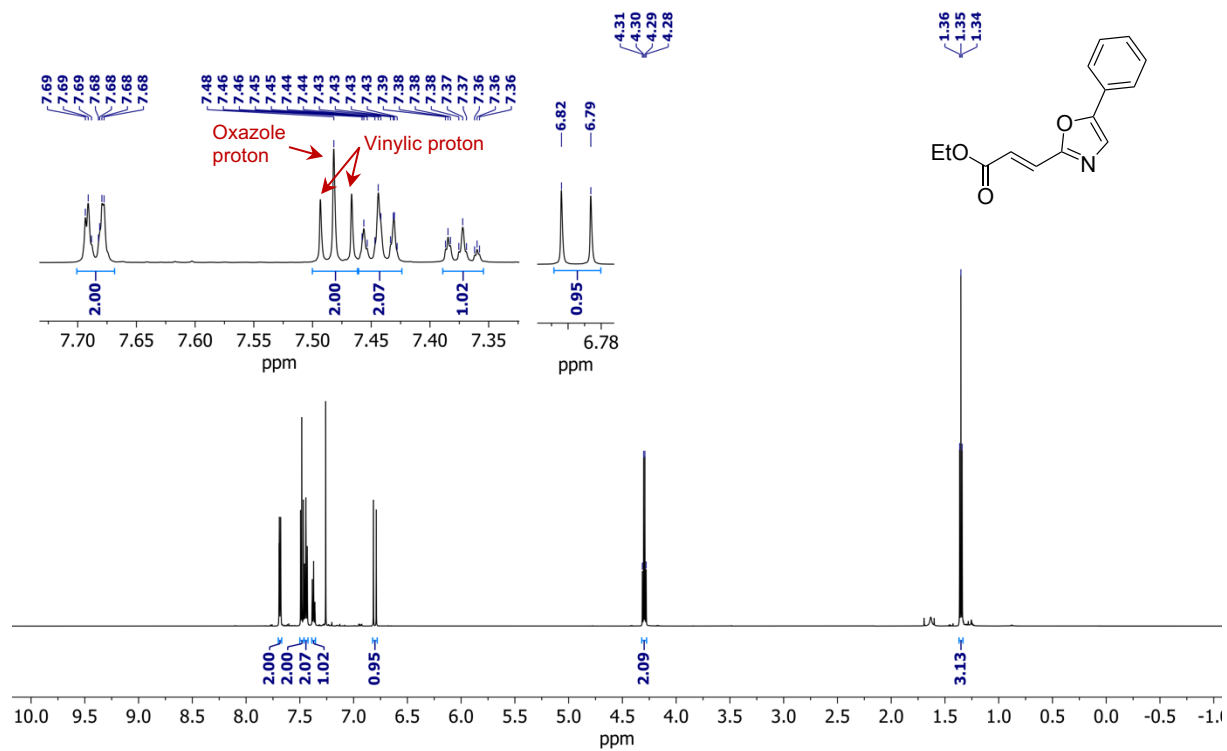


Figure 5.26. <sup>1</sup>H NMR (600 MHz, CDCl<sub>3</sub>) spectrum of 11n.

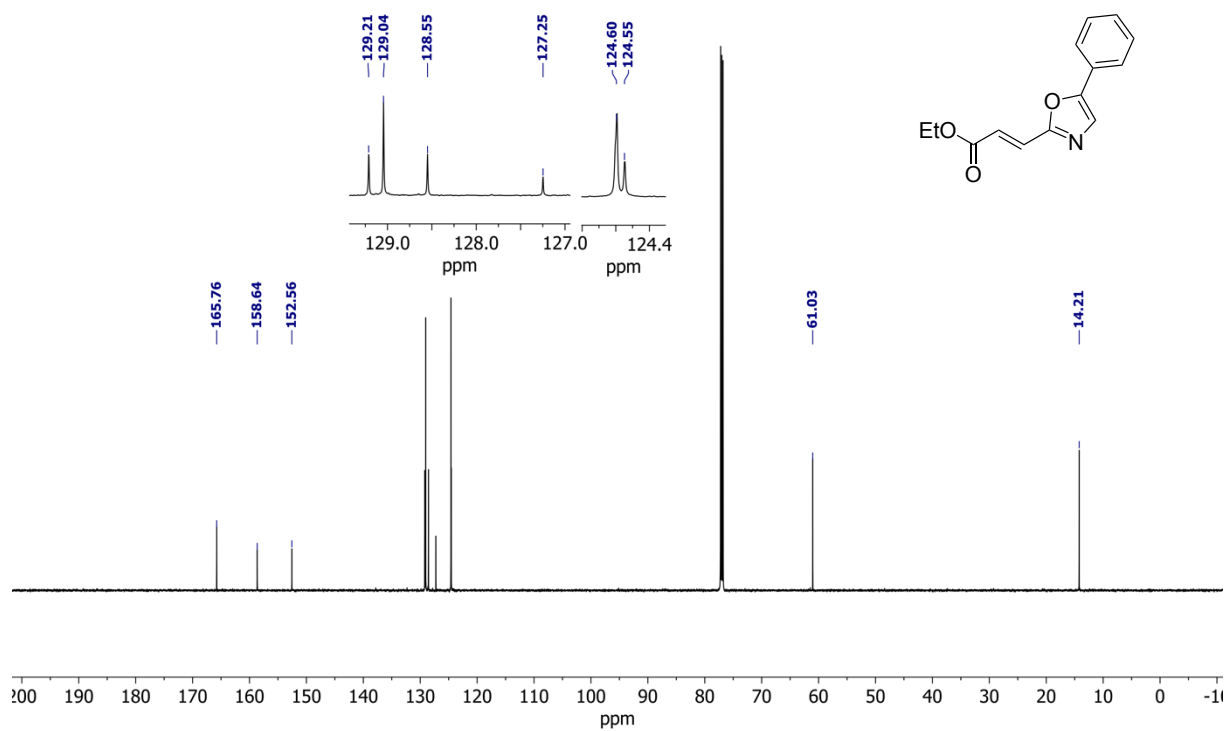
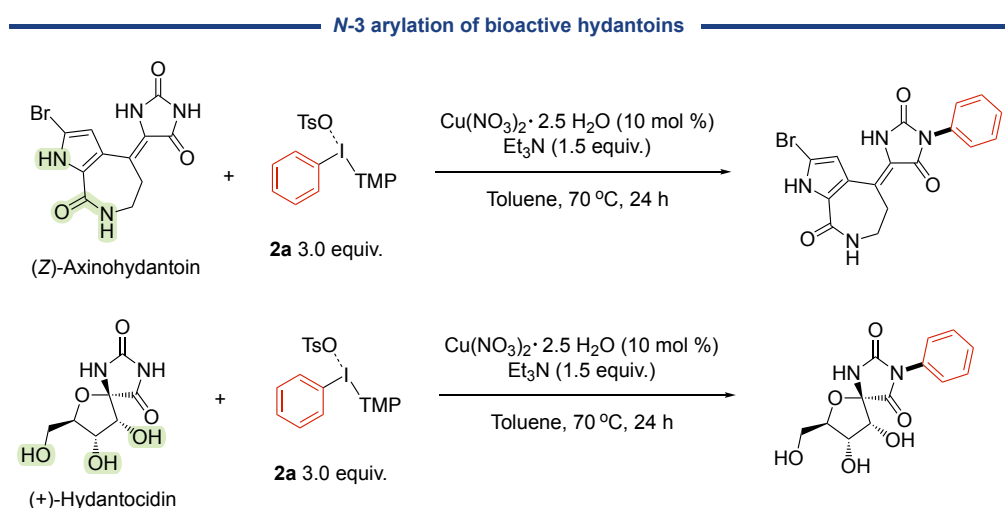


Figure 5.27. <sup>13</sup>C NMR (151 MHz, CDCl<sub>3</sub>) spectrum of 11n.

# Chapter 6: Future prospects

## 6.1 Chapter 2 and 3: *N*-3-arylation of hydantoins

During the development of a method for *N*-3-arylation of hydantoins with diaryliodonium salt, we discovered a “sweet spot” in the tolerance of both aryl groups and hydantoins/imides. Transfer of neutral arenes, or arenes bearing weak EDGs and EWGs were well tolerated, while the strong EDGs and EWGs were less tolerated. Most hydantoins and imides were well tolerated. One natural continuation of this work is therefore to exploit the strengths of the methods. Considering the successful derivatization of pharmaceutically relevant hydantoins, more challenging substrates can potentially be arylated, starting with (*Z*)-Axinohydantoin<sup>391, 392</sup> and (±)-Hydantocidin<sup>49, 109</sup> (Figure 6.1).



**Figure 6.1.** Suggestions for *N*-3-arylation of bioactive hydantoins including (*Z*)-Axinohydantoin and (±)-Hydantocidin. These substrates are especially challenging considering the potential reactive sites for arylation (marked in green).

By utilizing aryl substituents with neutral character, hydantoins with more structurally complex *N*-3 positions can be accessed. A natural starting point would include the use of aryl(TMP)iodonium tosylates already reported (Figure 6.1a).<sup>172</sup> and salts similar to previously reported ones (Figure 6.2b). The benzylic phthalimide salt used for the synthesis of **3f** have the potential for small, structure modifications (marked in blue) which can survive the oxidative conditions used in the salt syntheses. These can be prepared by alkylation of potassium phthalimide with the respective iodobenzyl bromides according to literature methods,<sup>393</sup> followed by iodonium salt synthesis.<sup>172, 394</sup>

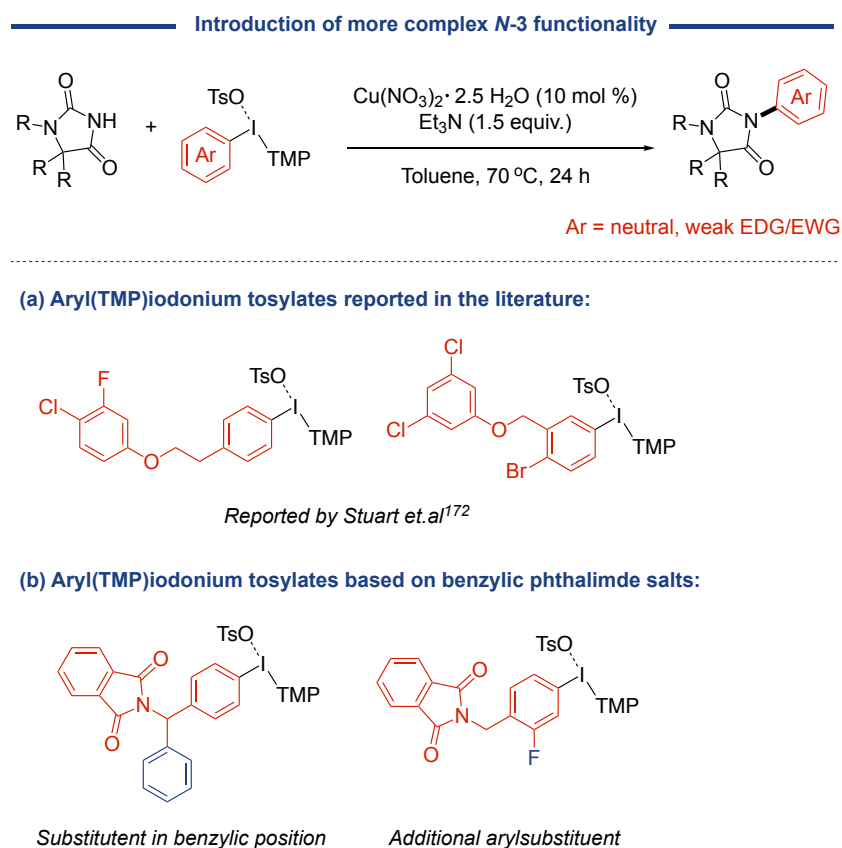


**Figure 6.2.** Potential coupling partners with neutral or weakly electron-donating- or withdrawing groups that can be used to build more complex N-3-arylated hydantoins.

After the recent finalization of the computational study, a way for the N-3-arylation protocol to improve is by exploiting the synergy between computations and experiments. The mechanistic understanding gained can help with modifications of the reaction conditions to include the transfer of arenes outside the mentioned “sweet spot”, *i.e.* going to the stereoelectronic extremes (Figure 6.3). For the electron-poor and sterically congested substrates this can be achieved by adjusting the auxiliary (*i.e.* the TMP) since the TMP group is responsible for the stabilization of the catalyst resting state for these substrates (and hence the size of the energy barriers). For the electron-rich substrates, changing the anion of the diaryliodonium salt can be an option since the anion is involved in both the resting state and the highest transition state. A counter anion effect was experimentally observed (Chapter 2) and should be included in future computational work regardless to study their effect on the reaction. A second option involves exploring ligand design by replacement of TEA with other ligands.



### Can we extend the green zones?

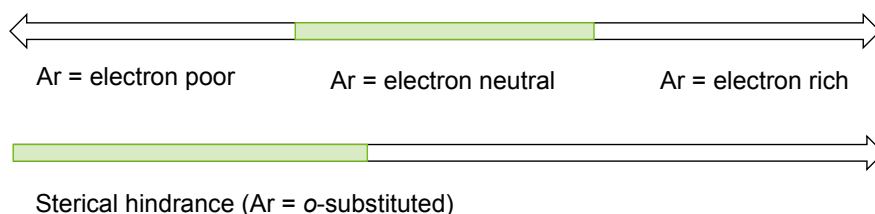


**Figure 6.3.** Utilization of DFT calculations to modify and improve experimental conditions.

Hydantoin/imides besides **1a** were not studied by DFT calculations and should thus be included in further studies. Additional extensions could include the investigation into favorable conditions for bis-arylation and ultimately for the challenging regioselective *N*-1-arylation. In both cases, calculation of the energy barrier for the second deprotonation (in the *N*-1 position after *N*-3 is arylated) is a suggested first step, followed by calculations where other, stronger bases are included in addition to TEA/other ligand(s). For direct *N*-1-arylation of unsubstituted hydantoin, we theorize that a directing group (DG) may be necessary. DG-design can be done computationally to see if the selectivity can be directed to the *N*-1 position prior to experimental trials.

## 6.2 Chapter 4: *N*-alkenylation of cyclic imides with boronic acids

While investigating the scope and limitations for the *N*-alkenylation of imides using alkenylboronic acids, we discovered that the method is mostly limited to cyclic imides and that (*E*)-styrylboronic acid was the superior boronic acid for alkenylation. Pentenyl- and cyclopentenylboronic acid were, however, moderately efficient, while the boronic acid with a phenyl group in 1-position failed under our conditions. As the imide scope was rather comprehensive, continuation of the work presented in this chapter involves expansion of the alkenylboronic acid scope. Naturally, (*E*)-styrylboronic acids with various substituents in *ortho*-, *meta* and *para*-positions of the phenyl ring should be included (Figure 6.4a). Although with poorer performance, 1,2,2-trisubstituted (*E*)-alkenylboronic could be further explored (Figure 6.4b) as the method allows for such substitution pattern. Restrictions in the size of the 1-substituent must, however, be taken into consideration as coupling with 1-phenylvinylboronic acid failed.

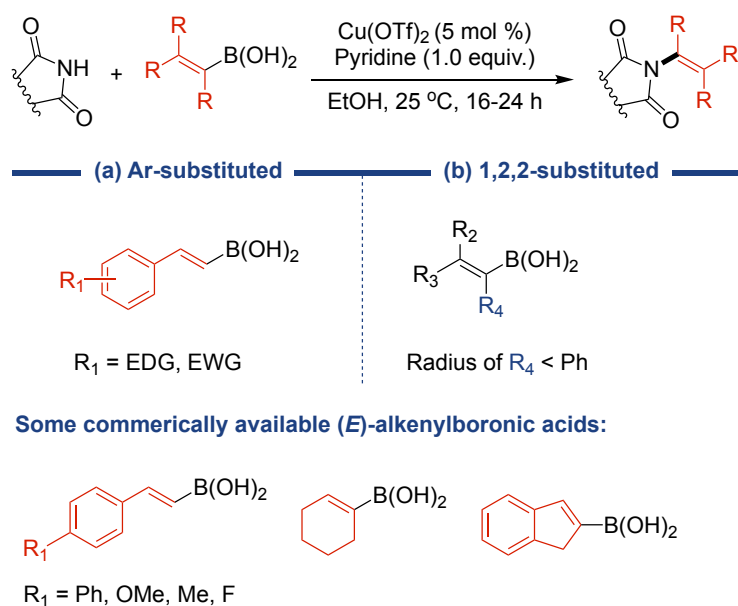


**Figure 6.4.** Potential coupling partners (commercially available) for future work including (a) aryl-substituted (*E*)-styrylboronic acids, (b) 1,1,2-trisubstituted (*E*)-alkenylboronic acids.

### 6.3 Chapter 5: *N*-alkenylation and ring-opening of maleimides

The work described in Chapter 5, *N*-alkenylation and ring-opening of maleimide is far from complete, and naturally warrants further studying. A starting point could include getting better control of the *N*-substituted maleimide-maleamate equilibrium and induce a shift in the desired direction (Figure 6.5). A standard synthesis of *N*-arylmaleimides from *N*-arylmaleamic acids is dehydration in acetic anhydride in the presence of sodium acetate,<sup>372, 395</sup> and may be used to exclusively obtain *N*-styrylmaleimides (Figure 6.4, left). The opposite reaction may require a stronger nucleophile (<sup>-</sup>OEt under our conditions) for the ring-opening to proceed to a full extent, which can be formed by the presence of a stronger base (Figure 6.5, right).

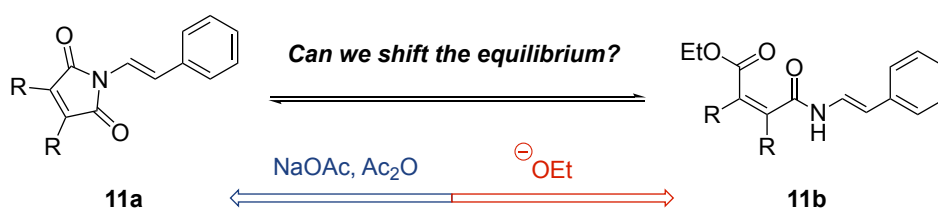


**Figure 6.5.** Controlling the formation of either **11a** or **11b** by pushing the equilibrium with the addition of sodium acetate and acetic anhydride (left) or by creating a stronger nucleophile (right), respectively.

Further work with exploring **11b** as a synthon is a reasonable next step as it still has unrealized potential (Figure 6.6). The enamide moiety offers a plethora of synthetic transformations,<sup>396</sup> including cross-coupling reactions, heterocycle synthesis and *N*-functionalization reactions. The alkenes can undergo *E* → *Z* isomerization, epoxidations, reductions, nucleophilic additions and pericyclic reactions. Since the *in situ* formation of other esters than the ethyl ester was only partially successful, transesterification reactions might also be explored. Additionally, it can be worth investigating the fumaramate **11h** as a synthon, especially in reactions where ring-closing of **11b** presents as a problem.

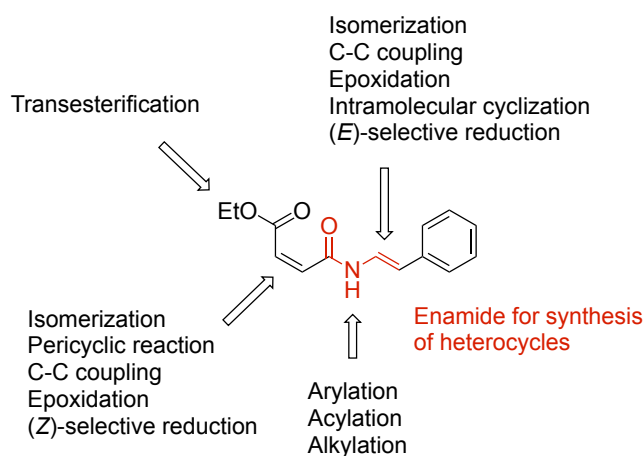


**Figure 6.6.** Exploration of **11b** as a synthon in a few, selected transformations.



## References

- [1] Baeyer, A. *Justus Liebigs Ann. Chem.* **1861**, *117* (2), 178-180.
- [2] Strecker, A. *Justus Liebigs Ann. Chem.* **1870**, *155* (2), 177-185.
- [3] Ware, E. *Chem. Rev.* **1950**, *46* (3), 403-470.
- [4] Gawas, P. P.; Ramakrishna, B.; Veeraiah, N.; Nutalapati, V. *J. Mater. Chem. C* **2021**, *9* (46), 16341-16377.
- [5] Konnert, L.; Lamaty, F.; Martinez, J.; Colacino, E. *Chem. Rev.* **2017**, *117* (23), 13757-13809.
- [6] López, C. A.; Trigo, G. G. The Chemistry of Hydantoins. In *Advances in Heterocyclic Chemistry*, Katritzky, A. R. Ed.; Vol. 38; Academic Press: Orlando, Florida, 1985, pp 177-228.
- [7] Bausch, M.; Selmarten, D.; Gostowski, R.; Dobrowolski, P. *J. Phys. Org. Chem.* **1991**, *4* (1), 67-69.
- [8] Pickett, L. W.; McLean, M. *J. Am. Chem. Soc.* **1939**, *61* (2), 423-425.
- [9] Bausch, M. J.; David, B.; Dobrowolski, P.; Prasad, V. *J. Org. Chem.* **1990**, *55* (23), 5806-5808.
- [10] Zhang, L.; Zhou, F.; Li, Z.; Liu, B.; Yan, R.; Li, J.; Hu, Y.; Zhang, C.; Luo, Z.; Guo, K. *Polym. Chem.* **2020**, *11* (35), 5669-5680.
- [11] Reich, H. *Equilibrium pKa Table (DMSO Solvent and Reference)*. ACS Division of Organic Chemistry, 2021. [https://organicchemistrydata.org/hansreich/resources/pka/pka\\_data/pka-compilation-reich-bordwell.pdf](https://organicchemistrydata.org/hansreich/resources/pka/pka_data/pka-compilation-reich-bordwell.pdf) (accessed January 8th, 2023).
- [12] Kleinpeter, E. *Struct. Chem.* **1997**, *8* (2), 161-173.
- [13] Bhikharee, D.; Elzagheid, M. I.; Rhyman, L.; Ramasami, P. *J. Mol. Liq.* **2022**, *347*, 117942.
- [14] Safi, Z. S.; Faris, W. M. *Orient. J. Chem.* **2014**, *30* (3), 1045-1054.
- [15] Ingold, C. K.; Sako, S.; Thorpe, J. F. *J. Chem. Soc., Trans.* **1922**, *121* (0), 1177-1198.
- [16] Zhao, H.; Yu, R.; Qiao, H.; Liu, C. *ACS Omega* **2020**, *5* (23), 13463-13472.
- [17] Burton, S. G.; Dorrington, R. A. *Tetrahedron: Asymmetry* **2004**, *15* (18), 2737-2741.
- [18] Matcher, G. F.; Dorrington, R. A.; Burton, S. G. Enzymatic Production of Enantiopure Amino Acids from Mono-substituted Hydantoin Substrates. In *Unnatural Amino Acids: Methods and Protocols*, Pollegioni, L., Servi, S. Eds.; Humana Press: Totowa, NJ, 2012, pp 37-54.

- [19] May, O.; Verseck, S.; Bommarius, A.; Drauz, K. *Org. Process Res. Dev.* **2002**, *6* (4), 452-457.
- [20] Zamora, W. J.; Curutchet, C.; Campanera, J. M.; Luque, F. J. *J. Phys. Chem. B* **2017**, *121* (42), 9868-9880.
- [21] Prevet, H.; Flipo, M.; Roussel, P.; Deprez, B.; Willand, N. *Tetrahedron Lett.* **2016**, *57* (26), 2888-2894.
- [22] Colacino, E.; Porcheddu, A.; Charnay, C.; Delogu, F. *React. Chem. Eng.* **2019**, *4* (7), 1179-1188.
- [23] Martínez-López, D.; Yu, M.-L.; García-Iriepa, C.; Campos, P. J.; Frutos, L. M.; Golen, J. A.; Rasapalli, S.; Sampedro, D. *J. Org. Chem.* **2015**, *80* (8), 3929-3939.
- [24] Marazzi, M.; García-Iriepa, C.; Benitez-Martin, C.; Najera, F.; Monari, A.; Sampedro, D. *Molecules* **2021**, *26* (23), 7379.
- [25] Luo, H.; Zhang, D.; Jiang, C.; Yuan, X.; Chen, C.; Zhou, K. *ACS Appl. Mater. Interfaces* **2015**, *7* (15), 8061-8069.
- [26] Wang, F.; Ren, F.; Ma, D.; Mu, P.; Wei, H.; Xiao, C.; Zhu, Z.; Sun, H.; Liang, W.; Chen, J.; Chen, L.; Li, A. *J. Mater. Chem. A* **2018**, *6* (1), 266-274.
- [27] Wang, N.; Feng, X.; Pei, J.; Cui, Q.; Li, Y.; Liu, H.; Zhang, X. *ACS Sustain. Chem. Eng.* **2022**, *10* (11), 3604-3613.
- [28] Liu, W.; Zhang, S.; Xiao, L.; Wan, Y.; He, L.; Wang, K.; Qi, Z.; Li, X. *Pest Manag. Sci.* **2022**, *78* (4), 1438-1447.
- [29] Lehmann, S. V.; Hoeck, U.; Breinholdt, J.; Olsen, C. E.; Kreilgaard, B. *Contact Derm.* **2006**, *54* (1), 50-58.
- [30] Luo, Z.; Liu, T.; Guo, W.; Wang, Z.; Huang, J.; Zhu, Y.; Zeng, Z. *Org. Process Res. Dev.* **2018**, *22* (9), 1188-1199.
- [31] Leitch, J. A.; Cook, H. P.; Bhonoah, Y.; Frost, C. G. *J. Org. Chem.* **2016**, *81* (20), 10081-10087.
- [32] Li, X.-R.; Lu, C.-F.; Chen, Z.-X.; Li, Y.; Yang, G.-C. *Tetrahedron: Asymmetry* **2012**, *23* (18), 1380-1384.
- [33] Orazi, O. O.; Corral, R. A.; Bertorello, H. E. *J. Org. Chem.* **1965**, *30* (4), 1101-1104.
- [34] Hernández-Torres, G.; Tan, B.; Barbas III, C. F. *Org. Lett.* **2012**, *14* (7), 1858-1861.
- [35] Ángel, A. Y. B.; Bragança, E. F.; Alberto, E. E. *ChemistrySelect* **2019**, *4* (39), 11548-11552.
- [36] Ahmedova, A.; Marinova, P.; Marinov, M.; Stoyanov, N. *J. Mol. Struct.* **2016**, *1108*, 602-610.

- [37] Puszyńska-Tuszkano, M.; Grabowski, T.; Daszkiewicz, M.; Wietrzyk, J.; Filip, B.; Maciejewska, G.; Cieślak-Golonka, M. *J. Inorg. Biochem.* **2011**, *105* (1), 17-22.
- [38] Hu, X.; Xu, X.; Wang, D.; Zhang, Y. *Acta Crystallogr. E* **2009**, *65* (11), m1426.
- [39] Vatannavaz, L.; Sabounchei, S. J.; Sedghi, A.; Karamian, R.; Farida, S. H. M.; Rahmani, N. *Polyhedron* **2020**, *181*, 114478.
- [40] Puszyńska-Tuszkano, M.; Daszkiewicz, M.; Maciejewska, G.; Adach, A.; Cieślak-Golonka, M. *Struct. Chem.* **2010**, *21* (2), 315-321.
- [41] Pavlovich, G. Z.; Luthy, R. G. *Water Res.* **1988**, *22* (3), 327-336.
- [42] Hajiahmadi, Z.; Tavangar, Z. *Mol. Simul.* **2021**, *47* (8), 619-627.
- [43] Liu, A.; Ren, X.; An, M.; Zhang, J.; Yang, P.; Wang, B.; Zhu, Y.; Wang, C. *Sci. Rep.* **2014**, *4* (1), 3837.
- [44] Patching, S. G. *J. diagn. imaging ther.* **2017**, *4* (1), 3-26.
- [45] Bow, J.-P. J.; Adami, V.; Marasco, A.; Grønnevik, G.; Rivers, D. A.; Alvaro, G.; Riss, P. J. *Chem. Commun.* **2022**, *58* (54), 7546-7549.
- [46] Bauman, A.; Piel, M.; Höhnemann, S.; Krauss, A.; Jansen, M.; Solbach, C.; Dannhardt, G.; Rösch, F. *J. Labelled Compd. Radiopharm.* **2011**, *54* (10), 645-656.
- [47] Tomohara, K.; Ito, T.; Hasegawa, N.; Kato, A.; Adachi, I. *Tetrahedron Lett.* **2016**, *57* (8), 924-927.
- [48] Cachet, N.; Genta-Jouve, G.; Regalado, E. L.; Mokrini, R.; Amade, P.; Culioli, G.; Thomas, O. P. *J. Nat. Prod.* **2009**, *72* (9), 1612-1615.
- [49] Nakajima, M.; Itoi, K.; Takamatsu, Y.; Kinoshita, T.; Okazaki, T.; Kawakubo, K.; Shindo, M.; Honma, T.; Tohjigamori, M.; Haneishi, T. *J. Antibiot (Tokyo)* **1991**, *44* (3), 293-300.
- [50] Lee, T. H.; Khan, Z.; Kim, S. Y.; Lee, K. R. *J. Nat. Prod.* **2019**, *82* (11), 3020-3024.
- [51] Flosi, W. J.; DeGoey, D. A.; Grampovnik, D. J.; Chen, H.-j.; Klein, L. L.; Dekhtyar, T.; Masse, S.; Marsh, K. C.; Mo, H. M.; Kempf, D. *Biorg. Med. Chem.* **2006**, *14* (19), 6695-6712.
- [52] Bichard, C. J. F.; Mitchell, E. P.; Wormald, M. R.; Watson, K. A.; Johnson, L. N.; Zographos, S. E.; Koutra, D. D.; Oikonomakos, N. G.; Fleet, G. W. J. *Tetrahedron Lett.* **1995**, *36* (12), 2145-2148.
- [53] Cortes, S.; Liao, Z.-K.; Watson, D.; Kohn, H. *J. Med. Chem.* **1985**, *28* (5), 601-606.
- [54] Su, M.; Xia, D.; Teng, P.; Nimmagadda, A.; Zhang, C.; Odom, T.; Cao, A.; Hu, Y.; Cai, J. *J. Med. Chem.* **2017**, *60* (20), 8456-8465.

- [55] Lin, X.; Tago, K.; Okazaki, N.; So, T.; Takahashi, K.; Mashino, T.; Tamura, H.; Funakoshi-Tago, M. *Int. Immunopharmacol.* **2021**, *100*, 108092.
- [56] Czopek, A.; Byrtus, H.; Zagórska, A.; Siwek, A.; Kazek, G.; Bednarski, M.; Sapa, J.; Pawłowski, M. *Pharmacol. Rep.* **2016**, *68* (5), 886-893.
- [57] Pinder, R. M.; Brogden, R. N.; Speight, T. M.; Avery, G. S. *Drugs* **1977**, *13* (1), 3-23.
- [58] Edmunds, J. J.; Klutchko, S.; Hamby, J. M.; Bunker, A. M.; Connolly, C. J. C.; Winters, R. T.; Quin III, J.; Sircar, I.; Hodges, J. C. *J. Med. Chem.* **1995**, *38* (19), 3759-3771.
- [59] Carmi, C.; Cavazzoni, A.; Zuliani, V.; Lodola, A.; Bordi, F.; Plazzi, P. V.; Alfieri, R. R.; Petronini, P. G.; Mor, M. *Bioorg. Med. Chem. Lett.* **2006**, *16* (15), 4021-4025.
- [60] Cho, S.; Kim, S.-H.; Shin, D. *Eur. J. Med. Chem.* **2019**, *164*, 517-545.
- [61] Taylor, R. D.; MacCoss, M.; Lawson, A. D. G. *J. Med. Chem.* **2014**, *57* (14), 5845-5859.
- [62] Cozzoli, A.; Capogrosso, R. F.; Sblendorio, V. T.; Dinardo, M. M.; Jagerschmidt, C.; Namour, F.; Camerino, G. M.; De Luca, A. *Pharmacol. Res.* **2013**, *72*, 9-24.
- [63] Ostrowski, J.; Kuhns, J. E.; Lupisella, J. A.; Manfredi, M. C.; Beehler, B. C.; Krystek, S. R., Jr.; Bi, Y.; Sun, C.; Seethala, R.; Golla, R.; Slep, P. G.; Fura, A.; An, Y.; Kish, K. F.; Sack, J. S.; Mookhtiar, K. A.; Grover, G. J.; Hamann, L. G. *Endocrinology* **2007**, *148* (1), 4-12.
- [64] Potin, D.; Launay, M.; Monatlik, F.; Malabre, P.; Fabreguettes, M.; Fouquet, A.; Maillet, M.; Nicolai, E.; Dorgeret, L.; Chevallier, F.; Besse, D.; Dufort, M.; Caussade, F.; Ahmad, S. Z.; Stetsko, D. K.; Skala, S.; Davis, P. M.; Balimane, P.; Patel, K.; Yang, Z.; Marathe, P.; Postelneck, J.; Townsend, R. M.; Goldfarb, V.; Sheriff, S.; Einspahr, H.; Kish, K.; Malley, M. F.; DiMarco, J. D.; Gougoutas, J. Z.; Kadiyala, P.; Cheney, D. L.; Tejwani, R. W.; Murphy, D. K.; McIntyre, K. W.; Yang, X.; Chao, S.; Leith, L.; Xiao, Z.; Mathur, A.; Chen, B.-C.; Wu, D.-R.; Traeger, S. C.; McKinnon, M.; Barrish, J. C.; Robl, J. A.; Iwanowicz, E. J.; Suchard, S. J.; Dhar, T. G. M. *J. Med. Chem.* **2006**, *49* (24), 6946-6949.
- [65] Kelly, T. A.; Jeanfavre, D. D.; McNeil, D. W.; Woska, J. R., Jr.; Reilly, P. L.; Mainolfi, E. A.; Kishimoto, K. M.; Nabozny, G. H.; Zinter, R.; Bormann, B.-J.; Rothlein, R. *J. Immunol.* **1999**, *163* (10), 5173-5177.
- [66] Meusel, M.; Gütschow, M. *Org. Prep. Proced. Int.* **2004**, *36* (5), 391-443.
- [67] Kumar, V. *Synlett* **2021**, *32* (19), 1897-1910.
- [68] Urech, F. *Justus Liebigs Ann. Chem.* **1873**, *165* (1), 99-103.
- [69] Read, W. T. *J. Am. Chem. Soc.* **1922**, *44* (8), 1746-1755.



- [70] Bucherer, H. T.; Lieb, V. A. *J. Prakt. Chem.* **1934**, *141* (1-2), 5-43.
- [71] Biltz, H. *Ber. Dtsch. Chem. Ges.* **1908**, *41* (1), 1379-1393.
- [72] Vincent-Rocan, J.-F.; Ivanovich, R. A.; Clavette, C.; Leckett, K.; Bejjani, J.; Beauchemin, A. M. *Chem. Sci.* **2016**, *7* (1), 315-328.
- [73] Nique, F.; Hebbe, S.; Triballeau, N.; Peixoto, C.; Lefrançois, J.-M.; Jary, H.; Alvey, L.; Manioc, M.; Housseman, C.; Klaassen, H.; Van Beeck, K.; Guédin, D.; Namour, F.; Minet, D.; Van der Aar, E.; Feyen, J.; Fletcher, S.; Blanqué, R.; Robin-Jagerschmidt, C.; Deprez, P. *J. Med. Chem.* **2012**, *55* (19), 8236-8247.
- [74] Declas, N.; Le Vaillant, F.; Waser, J. *Org. Lett.* **2019**, *21* (2), 524-528.
- [75] Konnert, L.; Dimassi, M.; Gonnet, L.; Lamaty, F.; Martinez, J.; Colacino, E. *RSC Adv.* **2016**, *6* (43), 36978-36986.
- [76] Li, K.; Shi, D.-Q. *J. Heterocycl. Chem.* **2009**, *46* (3), 544-547.
- [77] Broeren, M. A. C.; de Waal, B. F. M.; van Genderen, M. H. P.; Sanders, H. M. H. F.; Fytas, G.; Meijer, E. W. *J. Am. Chem. Soc.* **2005**, *127* (29), 10334-10343.
- [78] Dieltiens, N.; Claeys, D. D.; Zhdankin, V. V.; Nemykin, V. N.; Allaert, B.; Verpoort, F.; Stevens, C. V. *Eur. J. Org. Chem.* **2006**, *2006* (11), 2649-2660.
- [79] Burkett, D. J.; Wyatt, B. N.; Mews, M.; Bautista, A.; Engel, R.; Dockendorff, C.; Donaldson, W. A.; St. Maurice, M. *Biorg. Med. Chem.* **2019**, *27* (18), 4041-4047.
- [80] Muccioli, G. G.; Wouters, J.; Charlier, C.; Scriba, G. K. E.; Pizza, T.; Di Pace, P.; De Martino, P.; Poppitz, W.; Poupaert, J. H.; Lambert, D. M. *J. Med. Chem.* **2006**, *49* (3), 872-882.
- [81] Joshi, K. C.; Pathak, V. N.; Goyal, M. K. *J. Heterocycl. Chem.* **1981**, *18* (8), 1651-1653.
- [82] Muccioli, G. G.; Poupaert, J. H.; Wouters, J.; Norberg, B.; Poppitz, W.; Scriba, G. K. E.; Lambert, D. M. *Tetrahedron* **2003**, *59* (8), 1301-1307.
- [83] Muccioli, G. G.; Wouters, J.; Poupaert, J. H.; Norberg, B.; Poppitz, W.; Scriba, G. K. E.; Lambert, D. M. *Org. Lett.* **2003**, *5* (20), 3599-3602.
- [84] Hashmi, I. A.; Aslam, A.; Ali, S. K.; Ahmed, V.-u.; Ali, F. I. *Synth. Commun.* **2010**, *40* (19), 2869-2874.
- [85] Hulme, C.; Ma, L.; Romano, J. J.; Morton, G.; Tang, S.-Y.; Cherrier, M.-P.; Choi, S.; Salvino, J.; Labaudiniere, R. *Tetrahedron Lett.* **2000**, *41* (12), 1889-1893.
- [86] Marcaccini, S.; Ignacio, J. M.; Macho, S.; Pepino, R.; Torroba, T. *Synlett* **2005**, (20), 3051-3054.
- [87] Xu, C.; Chen, Z.-Z.; Xu, Z.-G.; Ding, Y.; Meng, J.-P.; Tang, D.-Y.; Li, Y.; Lei, J. *Synlett* **2018**, *29* (16), 2199-2202.

- [88] Sañudo, M.; García-Valverde, M.; Marcaccini, S.; Torroba, T. *Tetrahedron* **2012**, *68* (12), 2621-2629.
- [89] Huang, A.; Wo, K.; Pierson, A.; Lee, S. Y. C.; Yang, E.; Johnson, C. *J. Heterocycl. Chem.* **2016**, *53* (5), 1499-1504.
- [90] Trišović, N.; Božić, B.; Obradović, A.; Stefanović, O.; Marković, S.; Čomić, L.; Božić, B.; Ušćumlić, G. *J. Serb. Chem. Soc.* **2011**, *76* (12), 1597-1606.
- [91] Trišović, N.; Valentić, N.; Ušćumlić, G. *Chem. Cent. J.* **2011**, *5* (1), 62.
- [92] Hmuda, S.; Trišović, N.; Rogan, J.; Poleti, D.; Vitnik, Ž.; Vitnik, V.; Valentić, N.; Božić, B.; Ušćumlić, G. *Monatsh. Chem.* **2014**, *145* (5), 821-833.
- [93] Tzvetkov, N. T.; Euler, H.; Müller, C. E. *Beilstein J. Org. Chem.* **2012**, *8*, 1584-1593.
- [94] Yung, D. K.; Forrest, T. P.; Gilroy, M. L.; Vohra, M. M. *J. Pharm. Sci.* **1973**, *62* (11), 1764-1768.
- [95] Czopek, A.; Kołaczkowski, M.; Bucki, A.; Byrtus, H.; Pawłowski, M.; Kazek, G.; Bojarski, A. J.; Piaskowska, A.; Kalinowska-Thućsik, J.; Partyka, A.; Wesołowska, A. *Biorg. Med. Chem.* **2015**, *23* (13), 3436-3447.
- [96] Hassanin, M. A.; Mustafa, M.; Abourehab, M. A. S.; Hassan, H. A.; Aly, O. M.; Beshr, E. A. M. *Pharmaceuticals* **2022**, *15* (7), 857.
- [97] Luo, G.; Xi, G.; Wang, X.; Qin, D.; Zhang, Y.; Fu, F.; Liu, X. *J. Appl. Polym. Sci.* **2017**, *134* (22), 44897.
- [98] Gak Simić, K.; Đorđević, I.; Lazić, A.; Radovanović, L.; Petković-Benazzouz, M.; Rogan, J.; Trišović, N.; Janjić, G. *CrystEngComm* **2021**, *23* (13), 2606-2622.
- [99] Talamas, F. X.; Ao-Ieong, G.; Brameld, K. A.; Chin, E.; de Vicente, J.; Dunn, J. P.; Ghate, M.; Giannetti, A. M.; Harris, S. F.; Labadie, S. S.; Leveque, V.; Li, J.; Lui, A. S. T.; McCaleb, K. L.; Nájera, I.; Schoenfeld, R. C.; Wang, B.; Wong, A. *J. Med. Chem.* **2013**, *56* (7), 3115-3119.
- [100] Hernández-López, H.; Sánchez-Miranda, G.; Araujo-Huitrado, J. G.; Granados-López, A. J.; López, J. A.; Leyva-Ramos, S.; Chacón-García, L. *J. Chem.* **2019**, *2019*, 5608652.
- [101] Mahmoud, M.; Abed, A. Y.; Al-Nuzal, S. *J. Pharm. Sci.* **2018**, *10* (11), 2836-2840.
- [102] Payen, O.; Top, S.; Vessières, A.; Brulé, E.; Plamont, M.-A.; J. McGlinchey, M.; Müller-Bunz, H.; Jaouen, G. *J. Med. Chem.* **2008**, *51* (6), 1791-1799.
- [103] Cogan, P. S.; Koch, T. H. *J. Med. Chem.* **2003**, *46* (24), 5258-5270.
- [104] Dreaden, E. C.; Gryder, B. E.; Austin, L. A.; Tene Defo, B. A.; Hayden, S. C.; Pi, M.; Quarles, L. D.; Oyelere, A. K.; El-Sayed, M. A. *Bioconjugate Chem.* **2012**, *23* (8), 1507-1512.

- [105] Crosignani, S.; Jorand-Lebrun, C.; Page, P.; Campbell, G.; Colovray, V.; Missotten, M.; Humbert, Y.; Cleva, C.; Arrighi, J.-F.; Gaudet, M.; Johnson, Z.; Ferro, P.; Chollet, A. *ACS Med. Chem. Lett.* **2011**, *2* (8), 644-649.
- [106] Shintani, Y.; Kato, K.; Kawami, M.; Takano, M.; Kumamoto, T. *Chem Pharm Bull (Tokyo)* **2021**, *69* (4), 407-410.
- [107] Biltz, H.; Slotta, K. *J. Prakt. Chem.* **1926**, *113* (1), 233-267.
- [108] Salmon, M. R.; Kozlowski, A. Z. *J. Am. Chem. Soc.* **1945**, *67* (12), 2270-2271.
- [109] Pham, T. Q.; Pyne, S. G.; Skelton, B. W.; White, A. H. *J. Org. Chem.* **2005**, *70* (16), 6369-6377.
- [110] Šmit, B. M.; Pavlović, R. Z. *Tetrahedron* **2015**, *71* (7), 1101-1108.
- [111] Han, J.-T.; Wang, J.-M.; Chen, S.-C.; Qiu, L.-H.; Wang, M.-A. *Chinese J. Org. Chem.* **2010**, *30* (5), 691-697.
- [112] Kruger, H. G.; Mdluli, P.; Power, T. D.; Raasch, T.; Singh, A. *J. Mol. Struct. (Theochem.)* **2006**, *771* (1), 165-170.
- [113] Kruger, H. G.; Mdluli, P. S. *Struct. Chem.* **2006**, *17* (1), 121-125.
- [114] Handzlik, J.; Szymańska, E.; Alibert, S.; Chevalier, J.; Otrębska, E.; Pękala, E.; Pagès, J.-M.; Kieć-Kononowicz, K. *Biorg. Med. Chem.* **2013**, *21* (1), 135-145.
- [115] Lamiri, M.; Bougrin, K.; Daou, B.; Soufiaoui, M.; Nicolas, E.; Giralt, E. *Synth. Commun.* **2006**, *36* (11), 1575-1584.
- [116] Mudit, M.; Khanfar, M.; Muralidharan, A.; Thomas, S.; Shah, G. V.; van Soest, R. W. M.; El Sayed, K. A. *Biorg. Med. Chem.* **2009**, *17* (4), 1731-1738.
- [117] Thirupathi Reddy, Y.; Narsimha Reddy, P.; Koduru, S.; Damodaran, C.; Crooks, P. A. *Biorg. Med. Chem.* **2010**, *18* (10), 3570-3574.
- [118] Tshiluka, N. R.; Bvumbi, M. V.; Tshishonga, U.; Mnyakeni-Moleele, S. S. *J. Chem. Res.* **2022**, *46* (4), 17475198221104183.
- [119] Keenan, T.; Jean, A.; Arseniyadis, S. *ACS Organic & Inorganic Au* **2022**, *2* (4), 312-317.
- [120] Fernández-Nieto, F.; Mas Roselló, J.; Lenoir, S.; Hardy, S.; Clayden, J. *Org. Lett.* **2015**, *17* (15), 3838-3841.
- [121] López-Alvarado, F.; Avendaño, C.; Carlos Menéndez, J. *Tetrahedron Lett.* **1992**, *33* (45), 6875-6878.
- [122] Chemler, S. R. *Beilstein J. Org. Chem.* **2015**, *11*, 2252-2253.
- [123] Allen, S. E.; Walvoord, R. R.; Padilla-Salinas, R.; Kozlowski, M. C. *Chem. Rev.* **2013**, *113* (8), 6234-6458.
- [124] Yang, Q.; Zhao, Y.; Ma, D. *Org. Process Res. Dev.* **2022**, *26* (6), 1690-1750.
- [125] Ullmann, F.; Bielecki, J. *Ber. Dtsch. Chem. Ges.* **1901**, *34* (2), 2174-2185.
- [126] Ullmann, F. *Ber. Dtsch. Chem. Ges.* **1903**, *36* (2), 2382-2384.

- [127] Goldberg, I. *Ber. Dtsch. Chem. Ges.* **1906**, *39* (2), 1691-1692.
- [128] Chan, D. M. T.; Monaco, K. L.; Wang, R.-P.; Winters, M. P. *Tetrahedron Lett.* **1998**, *39* (19), 2933-2936.
- [129] Lam, P. Y. S.; Clark, C. G.; Saubern, S.; Adams, J.; Winters, M. P.; Chan, D. M. T.; Combs, A. *Tetrahedron Lett.* **1998**, *39* (19), 2941-2944.
- [130] West, M. J.; Fyfe, J. W. B.; Vantourout, J. C.; Watson, A. J. B. *Chem. Rev.* **2019**, *119* (24), 12491-12523.
- [131] Evano, G.; Blanchard, N.; Toumi, M. *Chem. Rev.* **2008**, *108* (8), 3054-3131.
- [132] Qiao, J. X.; Lam, P. Y. S. Recent Advances in Chan–Lam Coupling Reaction: Copper-Promoted C–Heteroatom Bond Cross-Coupling Reactions with Boronic Acids and Derivatives. In *Boronic Acids*, Hall, D. G. Ed.; Wiley-VCH Verlag & Co. KGaA: Weinheim, 2011, pp 315-361.
- [133] Chen, J.-Q.; Li, J.-H.; Dong, Z.-B. *Adv. Synth. Catal.* **2020**, *362* (16), 3311-3331.
- [134] Bhunia, S.; Pawar, G. G.; Kumar, S. V.; Jiang, Y.; Ma, D. *Angew. Chem. Int. Ed.* **2017**, *56* (51), 16136-16179.
- [135] Vantourout, J. C.; Miras, H. N.; Isidro-Llobet, A.; Sproules, S.; Watson, A. J. B. *J. Am. Chem. Soc.* **2017**, *139* (13), 4769-4779.
- [136] López-Alvarado, P.; Avendaño, C.; Menéndez, J. C. *J. Org. Chem.* **1996**, *61* (17), 5865-5870.
- [137] Hügel, H.; Rix, C.; Fleck, K. *Synlett* **2006**, *2006* (14), 2290-2292.
- [138] Wang, C.; Zhao, Q.; Vargas, M.; Jones, J. O.; White, K. L.; Shackelford, D. M.; Chen, G.; Saunders, J.; Ng, A. C. F.; Chiu, F. C. K.; Dong, Y.; Charman, S. A.; Keiser, J.; Vennerstrom, J. L. *J. Med. Chem.* **2016**, *59* (23), 10705-10718.
- [139] Thilmany, P.; Gérard, P.; Vanoost, A.; Deldaele, C.; Petit, L.; Evano, G. *J. Org. Chem.* **2019**, *84* (1), 392-400.
- [140] Abha Saikia, R.; Barman, D.; Dutta, A.; Jyoti Thakur, A. *Eur. J. Org. Chem.* **2021**, *2021* (3), 400-410.
- [141] Bahrami, M.; Ramazani, A.; Hanifehpour, Y.; Fattahi, N.; Taghavi Fardood, S.; Azimzadeh Asiabi, P.; Joo, S. W. *Phosphorus Sulfur Silicon Relat. Elem.* **2016**, *191* (10), 1368-1374.
- [142] Csenki, J. T.; Mészáros, Á.; Gonda, Z.; Novák, Z. *Chem. Eur. J.* **2021**, *27* (63), 15638-15643.
- [143] Monecke, M.; Lindel, T. *Org. Lett.* **2018**, *20* (24), 7969-7972.
- [144] Hartmann, C.; Meyer, V. *Ber. Dtsch. Chem. Ges.* **1894**, *27* (1), 426-432.

- [145] Ochiai, M. Reactivities, Properties and Structures. In *Hypervalent Iodine Chemistry: Modern Developments in Organic Synthesis*, Wirth, T. Ed.; Springer: Berlin, Heidelberg, 2003, pp 5-68.
- [146] Karandikar, S. S.; Bhattacharjee, A.; Metze, B. E.; Javalay, N.; Valente, E. J.; McCormick, T. M.; Stuart, D. R. *Chem. Sci.* **2022**, *13* (22), 6532-6540.
- [147] Merritt, E. A.; Olofsson, B. *Angew. Chem. Int. Ed.* **2009**, *48* (48), 9052-9070.
- [148] Olofsson, B. Arylation with Diaryliodonium Salts. In *Hypervalent Iodine Chemistry*, Wirth, T. Ed.; Springer: Cham, 2016, pp 135-166.
- [149] Wang, Y.; An, G.; Wang, L.; Han, J. *Curr. Org. Chem.* **2020**, *24* (18), 2070-2105.
- [150] Yusubov, M. S.; MaskaeV, A. V.; Zhdankin, V. V. *ARKIVOC* **2011**, *2011* (1), 370-409.
- [151] Novák, Z.; Aradi, K.; Tóth, B.; Tolnai, G. *Synlett* **2016**, *27* (10), 1456-1485.
- [152] Basu, S.; Sandtorv, A. H.; Stuart, D. R. *Beilstein J. Org. Chem.* **2018**, *14*, 1034-1038.
- [153] Jalalian, N.; Ishikawa, E. E.; Silva, L. F.; Olofsson, B. *Org. Lett.* **2011**, *13* (6), 1552-1555.
- [154] Kervefors, G.; Kersting, L.; Olofsson, B. *Chem. Eur. J.* **2021**, *27* (18), 5790-5795.
- [155] Stuart, D. R. *Chem. Eur. J.* **2017**, *23* (63), 15852-15863.
- [156] Deprez, N. R.; Sanford, M. S. *Inorg. Chem.* **2007**, *46* (6), 1924-1935.
- [157] Pacheco-Benichou, A.; Besson, T.; Fruit, C. *Catalysts* **2020**, *10* (5).
- [158] Iyanaga, M.; Aihara, Y.; Chatani, N. *J. Org. Chem.* **2014**, *79* (24), 11933-11939.
- [159] Fañanás-Mastral, M. *Synthesis* **2017**, *49*.
- [160] Ichiishi, N.; Brooks, A. F.; Topczewski, J. J.; Rodnick, M. E.; Sanford, M. S.; Scott, P. J. H. *Org. Lett.* **2014**, *16* (12), 3224-3227.
- [161] Ichiishi, N.; Canty, A. J.; Yates, B. F.; Sanford, M. S. *Org. Lett.* **2013**, *15* (19), 5134-5137.
- [162] Villo, P.; Kervefors, G.; Olofsson, B. *Chem. Commun.* **2018**, *54* (64), 8810-8813.
- [163] Malmgren, J.; Santoro, S.; Jalalian, N.; Himo, F.; Olofsson, B. *Chem. Eur. J.* **2013**, *19* (31), 10334-10342.
- [164] Beringer, F. M.; Dehn, J. W., Jr.; Winicov, M. *J. Am. Chem. Soc.* **1960**, *82* (11), 2948-2952.
- [165] Koser, G. F.; Wettach, R. H.; Smith, C. S. *J. Org. Chem.* **1980**, *45* (8), 1543-1544.
- [166] Lindstedt, E.; Reitti, M.; Olofsson, B. *J. Org. Chem.* **2017**, *82* (22), 11909-11914.

- [167] Zhu, M.; Jalalian, N.; Olofsson, B. *Synlett* **2008**, *2008* (04), 592-596.
- [168] Bielawski, M.; Aili, D.; Olofsson, B. *J. Org. Chem.* **2008**, *73* (12), 4602-4607.
- [169] Bielawski, M.; Zhu, M.; Olofsson, B. *Adv. Synth. Catal.* **2007**, *349* (17-18), 2610-2618.
- [170] Bielawski, M.; Olofsson, B. *Chem. Commun.* **2007**, (24), 2521-2523.
- [171] Merritt, E. A.; Malmgren, J.; Klinke, F. J.; Olofsson, B. *Synlett* **2009**, *2009* (14), 2277-2280.
- [172] Seidl, T. L.; Sundalam, S. K.; McCullough, B.; Stuart, D. R. *J. Org. Chem.* **2016**, *81* (5), 1998-2009.
- [173] Carreras, V.; Sandtorv, A. H.; Stuart, D. R. *J. Org. Chem.* **2017**, *82* (2), 1279-1284.
- [174] Soldatova, N.; Postnikov, P.; Kukurina, O.; Zhdankin, V. V.; Yoshimura, A.; Wirth, T.; Yusubov, M. S. *ChemistryOpen* **2017**, *6* (1), 18-20.
- [175] Soldatova, N.; Postnikov, P.; Kukurina, O.; Zhdankin, V. V.; Yoshimura, A.; Wirth, T.; Yusubov, M. S. *Beilstein J. Org. Chem.* **2018**, *14*, 849-855.
- [176] Hossain, M. D.; Kitamura, T. *Tetrahedron* **2006**, *62* (29), 6955-6960.
- [177] Iwama, T.; Birman, V. B.; Kozmin, S. A.; Rawal, V. H. *Org. Lett.* **1999**, *1* (4), 673-676.
- [178] Gallagher, R. T.; Basu, S.; Stuart, D. R. *Adv. Synth. Catal.* **2020**, *362* (2), 320-325.
- [179] Koseki, D.; Aoto, E.; Shoji, T.; Watanabe, K.; In, Y.; Kita, Y.; Dohi, T. *Tetrahedron Lett.* **2019**, *60* (18), 1281-1286.
- [180] Sun, D.; Yin, K.; Zhang, R. *Chem. Commun.* **2018**, *54* (11), 1335-1338.
- [181] Nilova, A.; Metzke, B.; Stuart, D. R. *Org. Lett.* **2021**, *23* (12), 4813-4817.
- [182] Geng, X.; Mao, S.; Chen, L.; Yu, J.; Han, J.; Hua, J.; Wang, L. *Tetrahedron Lett.* **2014**, *55* (29), 3856-3859.
- [183] Jung, S.-H.; Sung, D.-B.; Park, C.-H.; Kim, W.-S. *J. Org. Chem.* **2016**, *81* (17), 7717-7724.
- [184] Moon, S.-Y.; Koh, M.; Rathwell, K.; Jung, S.-H.; Kim, W.-S. *Tetrahedron* **2015**, *71* (10), 1566-1573.
- [185] Soldatova, N. S.; Semenov, A. V.; Geyl, K. K.; Baykov, S. V.; Shetnev, A. A.; Konstantinova, A. S.; Korsakov, M. M.; Yusubov, M. S.; Postnikov, P. S. *Adv. Synth. Catal.* **2021**, *363* (14), 3566-3576.
- [186] Zhang, R.; Liu, Z.; Peng, Q.; Zhou, Y.; Xu, L.; Pan, X. *Org. Biomol. Chem.* **2018**, *16* (11), 1816-1822.
- [187] Sheng, J.; He, R.; Xue, J.; Wu, C.; Qiao, J.; Chen, C. *Org. Lett.* **2018**, *20* (15), 4458-4461.

- [188] Ma, C.; Wu, X.; Zeng, Q.; Zhou, L.; Huang, Y. *New J. Chem.* **2017**, *41* (8), 2873-2877.
- [189] Aradi, K.; Mészáros, Á.; Tóth, B. L.; Vincze, Z.; Novák, Z. *J. Org. Chem.* **2017**, *82* (22), 11752-11764.
- [190] Wu, Y.; Izquierdo, S.; Vidossich, P.; Lledós, A.; Shafir, A. *Angew. Chem. Int. Ed.* **2016**, *55* (25), 7152-7156.
- [191] Beletskaya, I. P.; Davydov, D. V.; Moreno-Mañas, M. *Tetrahedron Lett.* **1998**, *39* (31), 5621-5622.
- [192] Beletskaya, I. P.; Davydov, D. V.; Gorovoy, M. S. *Tetrahedron Lett.* **2002**, *43* (35), 6221-6223.
- [193] Saikia, R. A.; Talukdar, K.; Pathak, D.; Sarma, B.; Thakur, A. J. *J. Org. Chem.* **2023**, *88* (6), 3567-3581.
- [194] Hall Jr., H. K. *J. Am. Chem. Soc.* **1957**, *79* (20), 5441-5444.
- [195] Haynes, W. M. *CRC Handbook of Chemistry and Physics*; 95th ed.; CRC Press: Boca Raton, FL, 2014.
- [196] Williams, R. *pKa Data Compiled by R. Williams*. [https://organicchemistrydata.org/hansreich/resources/pka/pka\\_data/pka-compilation-williams.pdf](https://organicchemistrydata.org/hansreich/resources/pka/pka_data/pka-compilation-williams.pdf) (accessed December 26th, 2022).
- [197] Seidl, T. L.; Stuart, D. R. *J. Org. Chem.* **2017**, *82* (22), 11765-11771.
- [198] Chan, L.; McNally, A.; Toh, Q. Y.; Mendoza, A.; Gaunt, M. J. *Chem. Sci.* **2015**, *6* (2), 1277-1281.
- [199] Ross, T. L.; Ermert, J.; Hocke, C.; Coenen, H. H. *J. Am. Chem. Soc.* **2007**, *129* (25), 8018-8025.
- [200] Xiao, Z. Arylation Reactions Using Diaryliodonium Salts. PhD dissertation, Newcastle University, 2020.
- [201] Bouquin, M.; Jaroschik, F.; Taillefer, M. *Tetrahedron Lett.* **2021**, *75*, 153208.
- [202] Sundalam, S. K.; Stuart, D. R. *J. Org. Chem.* **2015**, *80* (12), 6456-6466.
- [203] Matsuzaki, K.; Okuyama, K.; Tokunaga, E.; Saito, N.; Shiro, M.; Shibata, N. *Org. Lett.* **2015**, *17* (12), 3038-3041.
- [204] Wang, W.; Zhou, J.; Wang, C.; Zhang, C.; Zhang, X.-Q.; Wang, Y. *Commun. Chem.* **2022**, *5* (1), 145.
- [205] Bigot, A.; Williamson, A. E.; Gaunt, M. J. *J. Am. Chem. Soc.* **2011**, *133* (35), 13778-13781.
- [206] Cahard, E.; Male, H. P. J.; Tissot, M.; Gaunt, M. J. *J. Am. Chem. Soc.* **2015**, *137* (25), 7986-7989.
- [207] Besset, T.; Jubault, P.; Pannecoucke, X.; Poisson, T. *Org. Chem. Front.* **2016**, *3* (8), 1004-1010.

- [208] Altomonte, S.; Zanda, M. *J. Fluorine Chem.* **2012**, *143*, 57-93.
- [209] Yuan, H.; Guo, L.; Liu, F.; Miao, Z.; Feng, L.; Gao, H. *ACS Catal.* **2019**, *9* (5), 3906-3912.
- [210] Xie, Q.; Zhang, X.; Liu, H.; Zhang, F.; Luo, X.; Luo, H. *Asian J. Org. Chem.* **2022**, *11* (3), e202100792.
- [211] Peterson, M. J.; Sarges, R.; Aldinger, C. E.; MacDonald, D. P. *Metabolism* **1979**, *28* (4, Supplement 1), 456-461.
- [212] Allegretti, P. E.; de las Mercedes Schiavoni, M.; Guzmán, C.; Ponzinibbio, A.; Furlong, J. J. P. *Eur. J. Mass Spectrom.* **2007**, *13* (4), 291-306.
- [213] Puszynska-Tuszkanow, M.; Daszkiewicz, M.; Maciejewska, G.; Cieslak-Golonka, M. *Inorg. Chem. Commun.* **2009**, *12* (6), 484-486.
- [214] Yamaoka, N.; Sumida, K.; Itani, I.; Kubo, H.; Ohnishi, Y.; Sekiguchi, S.; Dohi, T.; Kita, Y. *Chem. Eur. J.* **2013**, *19* (44), 15004-15011.
- [215] Oh, C. H.; Kim, J. S.; Jung, H. H. *J. Org. Chem.* **1999**, *64* (4), 1338-1340.
- [216] Dohi, T.; Ito, M.; Morimoto, K.; Minamitsuji, Y.; Takenaga, N.; Kita, Y. *Chem. Commun.* **2007**, (40), 4152-4154.
- [217] Pou, S.; Dodean, R. A.; Frueh, L.; Liebman, K. M.; Gallagher, R. T.; Jin, H.; Jacobs, R. T.; Nilsen, A.; Stuart, D. R.; Doggett, J. S.; Riscoe, M. K.; Winter, R. W. *Org. Process Res. Dev.* **2021**, *25* (8), 1841-1852.
- [218] Nematollahi, J.; Ketcham, R. *J. Org. Chem.* **1963**, *28* (9), 2378-2380.
- [219] Hubele, A. Bactericidal and fungicidal 1-(dichlorofluoromethylthio)-3-phenyl-2,4-imidazolidinediones. Patent DE 2441601 A1, March 13, 1975.
- [220] Kuehle, E.; Brandes, W.; Rosslenbroich, H. J.; Klauke, E. *N*-Sulfenylated hydantoin. Patent DE 3222523 A1, December 22, 1983.
- [221] Fujinami, A.; Ozaki, T.; Yamamoto, S.; Horiuchi, F.; Akiba, K.; Tanaka, K.; Ooba, S.; Kameda, N.; Ooishi, T.; Nodera, K. 3-(3,5-Dihalophenyl)-2,4-imidazolidinediones. Patent DE 1958183 B2, December 18, 1975.
- [222] Athiel, P.; Alfizar, n.; Mercadier, C.; Vega, D.; Bastide, J.; Davet, P.; Brunel, B.; Cleyet-Marel, J. C. *Appl. Environ. Microbiol.* **1995**, *61* (9), 3216-3220.
- [223] Içli, S. *Org. Magn. Reson.* **1979**, *12* (3), 178-182.
- [224] Lockhart, T. P. *J. Am. Chem. Soc.* **1983**, *105* (7), 1940-1946.
- [225] Phipps, R. J.; Grimster, N. P.; Gaunt, M. J. *J. Am. Chem. Soc.* **2008**, *130* (26), 8172-8174.
- [226] Allen, A. E.; MacMillan, D. W. C. *J. Am. Chem. Soc.* **2011**, *133* (12), 4260-4263.
- [227] Stenczel, T. K.; Sinai, Á.; Novák, Z.; Stirling, A. *Beilstein J. Org. Chem.* **2018**, *14*, 1743-1749.



- [228] Chen, B.; Hou, X.-L.; Li, Y.-X.; Wu, Y.-D. *J. Am. Chem. Soc.* **2011**, *133* (20), 7668-7671.
- [229] Sallio, R.; Payard, P.-A.; Pakulski, P.; Diachenko, I.; Fabre, I.; Berteina-Raboin, S.; Colas, C.; Ciofini, I.; Grimaud, L.; Gillaizeau, I. *RSC Adv.* **2021**, *11* (26), 15885-15889.
- [230] Ichiishi, N.; Canty, A. J.; Yates, B. F.; Sanford, M. S. *Organometallics* **2014**, *33* (19), 5525-5534.
- [231] Modéc, B.; Podjed, N.; Lah, N. Beyond the Simple Copper(II) Coordination Chemistry with Quinaldinate and Secondary Amines. In *Molecules*, 2020; Vol. 25.
- [232] Kozuch, S.; Shaik, S. *Acc. Chem. Res.* **2011**, *44* (2), 101-110.
- [233] Métayer, B.; Angeli, A.; Mingot, A.; Jouvin, K.; Evano, G.; Supuran, C. T.; Thibaudeau, S. *J. Enzyme Inhib. Med. Chem.* **2018**, *33* (1), 804-808.
- [234] Uhr, H.; Boie, C.; Rieck, H.; Krueger, B.-W.; Heinemann, U.; Markert, R.; Vaupel, M.; Kugler, M.; Stenzel, K.; Wachendorff-Neumann, U.; Mauler-Machnik, A.; Kuck, K.-H.; Loesel, P.; Narabu, S.-I. Preparation of aryloxydithiazole and aryloxydithiazine dioxides as pesticides and fungicides. Patent DE 19918294, October 26, 2000.
- [235] Tanaka, S.; Katayama, M. *Nippon Noyaku Gakkaishi* **2000**, *25* (2), 133-139.
- [236] Louzoun Zada, S.; Green, K. D.; Shrestha, S. K.; Herzog, I. M.; Garneau-Tsodikova, S.; Fridman, M. *ACS Infect. Dis.* **2018**, *4* (7), 1121-1129.
- [237] Kirkpatrick, D. L.; Indarte, M. Preparation of *N*-substituted thiazolecarboxamides for inhibiting CNKSR1. Patent US 20160304533, October 20, 2016.
- [238] Brown, A.; Bunnage, M.; Lane, C.; Lewthwaite, R.; Glossop, P.; James, K.; Price, D. Formamide derivatives for the treatment of diseases. Patent US 20050215590 A1, September 29, 2005.
- [239] Vitale, R. M.; Thellung, S.; Tinto, F.; Solari, A.; Gatti, M.; Nuzzo, G.; Ioannou, E.; Roussis, V.; Ciavatta, M. L.; Manzo, E.; Florio, T.; Amodeo, P. *Bioorg. Chem.* **2020**, *105*, 104337.
- [240] Fu, P.; Kong, F.; Li, X.; Wang, Y.; Zhu, W. *Org. Lett.* **2014**, *16* (14), 3708-3711.
- [241] Ogawa, T.; Yamada, H. *N*-styrylphthalimide derivative for organic nonlinear optical material and use thereof. Patent JPH 08176107 A, July 9, 1996.
- [242] Otsu, S.; Ofuku, K.; Kagawa, N. Semiconductor for photoelectric conversion material, photoelectric conversion device, and solar cell. Patent JP 2005019124 A, January 20, 2005.
- [243] de Nanteuil, F.; Waser, J. *Angew. Chem. Int. Ed.* **2013**, *52* (34), 9009-9013.

- [244] Chu, Z.; Tang, Z.; Zhang, K.; Wang, L.; Li, W.; Wu, H.-H.; Zhang, J. *Organometallics* **2019**, *38* (20), 4036-4042.
- [245] Kramer, P.; Schönfeld, J.; Bolte, M.; Manolikakes, G. *Org. Lett.* **2018**, *20* (1), 178-181.
- [246] Susanto, W.; Chu, C.-Y.; Ang, W. J.; Chou, T.-C.; Lo, L.-C.; Lam, Y. *J. Org. Chem.* **2012**, *77* (6), 2729-2742.
- [247] Szudkowska-Frańczak, J.; Hreczycho, G.; Pawluć, P. *Org. Chem. Front.* **2015**, *2* (6), 730-738.
- [248] He, Q.; Chatani, N. *J. Org. Chem.* **2018**, *83* (21), 13587-13594.
- [249] Dai, J.; Ren, W.; Chang, W.; Zhang, P.; Shi, Y. *Org. Chem. Front.* **2017**, *4* (2), 297-302.
- [250] Dai, J.; Ren, W.; Wang, H.; Shi, Y. *Org. Biomol. Chem.* **2015**, *13* (31), 8429-8432.
- [251] Wefer, J.; Lindel, T. *Eur. J. Org. Chem.* **2015**, *2015* (28), 6370-6381.
- [252] Cho, S.-D.; Hwang, J.; Kim, H.-K.; Yim, H.-S.; Kim, J.-J.; Lee, S.-G.; Yoon, Y.-J. *J. Heterocycl. Chem.* **2007**, *44* (4), 951-960.
- [253] Shen, S.-J.; Wang, L.-M.; Gong, G.-M.; Wang, Y.-J.; Liang, J.-Y.; Wang, J.-W. *RSC Adv.* **2022**, *12* (20), 12663-12671.
- [254] Jiang, B.; Shi, M. *Org. Chem. Front.* **2017**, *4* (12), 2459-2464.
- [255] Arndt, M.; Salih, K. S. M.; Fromm, A.; Goossen, L. J.; Menges, F.; Niedner-Schatteburg, G. *J. Am. Chem. Soc.* **2011**, *133* (19), 7428-7449.
- [256] Goossen, L. J.; Blanchot, M.; Brinkmann, C.; Goossen, K.; Karch, R.; Rivas-Nass, A. *J. Org. Chem.* **2006**, *71* (25), 9506-9509.
- [257] Buba, A. E.; Arndt, M.; Goossen, L. J. *J. Organomet. Chem.* **2011**, *696* (1), 170-178.
- [258] Semina, E.; Tuzina, P.; Bienewald, F.; Hashmi, A. S. K.; Schaub, T. *Chem. Commun.* **2020**, *56* (44), 5977-5980.
- [259] Rogers, M. M.; Kotov, V.; Chatwichien, J.; Stahl, S. S. *Org. Lett.* **2007**, *9* (21), 4331-4334.
- [260] Brice, J. L.; Harang, J. E.; Timokhin, V. I.; Anastasi, N. R.; Stahl, S. S. *J. Am. Chem. Soc.* **2005**, *127* (9), 2868-2869.
- [261] Kohler, D. G.; Gockel, S. N.; Kennemur, J. L.; Waller, P. J.; Hull, K. L. *Nat. Chem.* **2018**, *10* (3), 333-340.
- [262] Desai, L. V.; Sanford, M. S. *Angew. Chem. Int. Ed.* **2007**, *46* (30), 5737-5740.
- [263] Bacon, R. G. R.; Karim, A. *J. Chem. Soc., Perkin Trans. 1* **1973**, (0), 278-280.

- [264] Ogawa, T.; Kiji, T.; Hayami, K.; Suzuki, H. *Chem. Lett.* **1991**, *20* (8), 1443-1446.
- [265] Mondal, K.; Patra, S.; Halder, P.; Mukhopadhyay, N.; Das, P. *Org. Lett.* **2023**, *25* (8), 1235-1240.
- [266] Arsenyan, P.; Petrenko, A.; Paegle, E.; Belyakov, S. *Mendeleev Commun.* **2011**, *21* (6), 326-328.
- [267] Steemers, L.; Wijsman, L.; van Maarseveen, J. H. *Adv. Synth. Catal.* **2018**, *360* (21), 4241-4245.
- [268] Bolshan, Y.; Batey, R. A. *Angew. Chem. Int. Ed.* **2008**, *47* (11), 2109-2112.
- [269] Bolshan, Y.; Batey, R. A. *Tetrahedron* **2010**, *66* (27), 5283-5294.
- [270] Lam, P. Y. S.; Vincent, G.; Bonne, D.; Clark, C. G. *Tetrahedron Lett.* **2003**, *44* (26), 4927-4931.
- [271] Jiao, J.-W.; Bi, H.-Y.; Zou, P.-S.; Wang, Z.-X.; Liang, C.; Mo, D.-L. *Adv. Synth. Catal.* **2018**, *360* (17), 3254-3259.
- [272] Li, J.; Zhang, Z.; Wu, L.; Zhang, W.; Chen, P.; Lin, Z.; Liu, G. *Nature* **2019**, *574* (7779), 516-521.
- [273] Hall, D. G. Structure, Properties, and Preparation of Boronic Acid Derivatives. In *Boronic Acids*, Wiley-VCH Verlag & Co. KGaA: Weinheim, 2011, pp 1-133.
- [274] Branca, D.; Ferrigno, F.; Hernando, J. I. M.; Jones, P.; Kinzel, O.; Malancona, S.; Muraglia, E.; Palumbi, M. C.; Pescatore, G.; Scarpelli, R. Preparation of saturated bicyclic heterocyclic derivatives as smo antagonists. Patent WO 2010023480 A1, March 4, 2010.
- [275] Baret, N.; Dulcere, J.-P.; Rodriguez, J.; Pons, J.-M.; Faure, R. *Eur. J. Org. Chem.* **2000**, *2000* (8), 1507-1516.
- [276] Frankland, E.; Duppa, B. F. *Justus Liebigs Ann. Chem.* **1860**, *115* (3), 319-322.
- [277] Frankland, E.; Duppa, B. F. *Proc. R. Soc. Lond.* **1980**, *10* (10), 568-570.
- [278] Frankland, E. *J. Chem. Soc.* **1862**, *15* (0), 363-381.
- [279] António, J. P. M.; Russo, R.; Carvalho, C. P.; Cal, P. M. S. D.; Gois, P. M. P. *Chem. Soc. Rev.* **2019**, *48* (13), 3513-3536.
- [280] Hardouin Duparc, V.; Bano, G. L.; Schaper, F. *ACS Catal.* **2018**, *8* (8), 7308-7325.
- [281] Cox, P. A.; Leach, A. G.; Campbell, A. D.; Lloyd-Jones, G. C. *J. Am. Chem. Soc.* **2016**, *138* (29), 9145-9157.
- [282] Xu, J.; Wang, X.; Shao, C.; Su, D.; Cheng, G.; Hu, Y. *Org. Lett.* **2010**, *12* (9), 1964-1967.
- [283] Wagh, R. B.; Nagarkar, J. M. *Tetrahedron Lett.* **2017**, *58* (48), 4572-4575.

- [284] Demir, A. S.; Reis, Ö.; Emrullahoglu, M. *J. Org. Chem.* **2003**, *68* (26), 10130-10134.
- [285] Liu, S.; Yu, Y.; Liebeskind, L. S. *Org. Lett.* **2007**, *9* (10), 1947-1950.
- [286] Lennox, A. J. J.; Lloyd-Jones, G. C. *Isr. J. Chem.* **2010**, *50* (5-6), 664-674.
- [287] Moon, S.-Y.; Kim, U. B.; Sung, D.-B.; Kim, W.-S. *J. Org. Chem.* **2015**, *80* (3), 1856-1865.
- [288] Vantourout, J. C.; Law, R. P.; Isidro-Llobet, A.; Atkinson, S. J.; Watson, A. J. B. *J. Org. Chem.* **2016**, *81* (9), 3942-3950.
- [289] Zheng, Z.-G.; Wen, J.; Wang, N.; Wu, B.; Yu, X.-Q. *Beilstein J. Org. Chem.* **2008**, *4*, 40.
- [290] Quach, T. D.; Batey, R. A. *Org. Lett.* **2003**, *5* (23), 4397-4400.
- [291] Thomas, A. A.; Zahrt, A. F.; Delaney, C. P.; Denmark, S. E. *J. Am. Chem. Soc.* **2018**, *140* (12), 4401-4416.
- [292] Lennox, A. J. J.; Lloyd-Jones, G. C. *Chem. Soc. Rev.* **2014**, *43* (1), 412-443.
- [293] Cundy, D. J.; Forsyth, S. A. *Tetrahedron Lett.* **1998**, *39* (43), 7979-7982.
- [294] Collman, J. P.; Zhong, M.; Zhang, C.; Costanzo, S. *J. Org. Chem.* **2001**, *66* (23), 7892-7897.
- [295] Akatyev, N.; Il'in, M.; Il'in (Jr.), M.; Peregudova, S.; Peregudov, A.; Buyanovskaya, A.; Kudryavtsev, K.; Dubovik, A.; Grinberg, V.; Orlov, V.; Pavlov, A.; Novikov, V.; Volkov, I.; Belokon, Y. *ChemCatChem* **2020**, *12* (11), 3010-3021.
- [296] Ley, S. V.; Thomas, A. W. *Angew. Chem. Int. Ed.* **2003**, *42* (44), 5400-5449.
- [297] Knecht, T.; Pinkert, T.; Dalton, T.; Lerchen, A.; Glorius, F. *ACS Catal.* **2019**, *9* (2), 1253-1257.
- [298] Zhao, L.; Xu, B.; Ablikim, U.; Lu, W.; Ahmed, M.; Evseev, M. M.; Bashkirov, E. K.; Azyazov, V. N.; Howlader, A. H.; Wnuk, S. F.; Mebel, A. M.; Kaiser, R. I. *ChemPhysChem* **2019**, *20* (6), 791-797.
- [299] Myhill, J. A.; Wilhelmsen, C. A.; Zhang, L.; Morken, J. P. *J. Am. Chem. Soc.* **2018**, *140* (45), 15181-15185.
- [300] Pinto da Silva, L. *J. Phys. Chem. C* **2017**, *121* (30), 16300-16307.
- [301] Liu, J.; Yao, H.; Wang, C. *ACS Catal.* **2018**, *8* (10), 9376-9381.
- [302] Gurung, S. K.; Thapa, S.; Kafle, A.; Dickie, D. A.; Giri, R. *Org. Lett.* **2014**, *16* (4), 1264-1267.
- [303] Budiman, Y. P.; Friedrich, A.; Radius, U.; Marder, T. B. *ChemCatChem* **2019**, *11* (21), 5387-5396.
- [304] Mao, J.; Guo, J.; Fang, F.; Ji, S.-J. *Tetrahedron* **2008**, *64* (18), 3905-3911.

- [305] Zhou, Y.; You, W.; Smith, K. B.; Brown, M. K. *Angew. Chem. Int. Ed.* **2014**, *53* (13), 3475-3479.
- [306] Shinde, D. N.; Trivedi, R.; Krishna, J. V. S.; Giribabu, L.; Sridhar, B.; Khursade, P. S.; Prakasham, R. S. *New J. Chem.* **2018**, *42* (15), 12587-12594.
- [307] Pałasz, A.; Cież, D. *Eur. J. Med. Chem.* **2015**, *97*, 582-611.
- [308] Gazivoda, T.; Raić-Malić, S.; Marjanović, M.; Kralj, M.; Pavelić, K.; Balzarini, J.; Clercq, E. D.; Mintas, M. *Biorg. Med. Chem.* **2007**, *15* (2), 749-758.
- [309] Chernick, E. T.; Ahrens, M. J.; Scheidt, K. A.; Wasielewski, M. R. *J. Org. Chem.* **2005**, *70* (4), 1486-1489.
- [310] Kraihanzel, C. S.; Grenda, S. C. *Inorg. Chem.* **1965**, *4* (7), 1037-1042.
- [311] Naumov, P.; Jovanovski, G.; Ristova, M.; Razak, I. A.; Çkir, S.; Chantrapromma, S.; Fun, H.-K.; Ng, S. W. *Z. Anorg. Allg. Chem.* **2002**, *628* (13), 2930-2939.
- [312] Hergold-Brundic, A.; Grupce, O.; Jovanovski, G. *Acta Crystallogr. Sect. C: Cryst. Struct. Commun.* **1991**, *47* (12), 2659-2660.
- [313] Brown, H. C.; Gupta, S. K. *J. Am. Chem. Soc.* **1975**, *97* (18), 5249-5255.
- [314] Schäfer, P.; Palacin, T.; Sidera, M.; Fletcher, S. P. *Nat. Commun.* **2017**, *8* (1), 15762.
- [315] Batey, R. A.; Thadani, A. N.; Lough, A. J. *J. Am. Chem. Soc.* **1999**, *121* (2), 450-451.
- [316] Wang, Q.; Nilsson, T.; Eriksson, L.; Szabó, K. J. *Angew. Chem. Int. Ed.* **2022**, *61* (46), e202210509.
- [317] Shi, X.; Li, S.; Wu, L. *Angew. Chem. Int. Ed.* **2019**, *58* (45), 16167-16171.
- [318] Chan, D. M. T.; Monaco, K. L.; Li, R.; Bonne, D.; Clark, C. G.; Lam, P. Y. S. *Tetrahedron Lett.* **2003**, *44* (19), 3863-3865.
- [319] Peng, C.; Zhang, W.; Yan, G.; Wang, J. *Org. Lett.* **2009**, *11* (7), 1667-1670.
- [320] Tokunaga, Y.; Ueno, H.; Shimomura, Y.; Seo, T. *Heterocycles* **2002**, *57*, 787-790.
- [321] Korich, A. L.; Iovine, P. M. *Dalton Trans.* **2010**, *39* (6), 1423-1431.
- [322] Shankarananth, V.; Ranganayakulu, D.; Sridhar, C.; Rajasekhar, K. K.; Bhaskar, S. *J. Pharm. Res.* **2011**, *4* (10), 3821-3823.
- [323] Negishi, E.; Wang, G. Hydrometalation and Subsequent Coupling Reactions. In *Category 6, Compounds with All-Carbon Functions*, 1st Edition ed.; de Meijere, A., Ed.; Science of Synthesis, Vol. 47b; Georg Thieme Verlag KG, 2010; pp 909-970. DOI: 10.1055/sos-SD-047-00392.
- [324] Alonos, D. A.; Nájera, C. Product Class 5: Styrenes, Stilbenes, and Other Alk-1-enylbenzenes. In *Category 6, Compounds with All-Carbon Functions*, 1st

- Edition ed.; Siegel, J. S., Tobe, Y., Shinkai, I., Eds.; Science of Synthesis, Vol. 45a; Georg Thieme Verlag KG, 2009; pp 209-244. DOI: 10.1055/sos-SD-045-00154.
- [325] Deng, M.-Z.; Li, N.-S.; Huang, Y.-Z. *J. Chem. Soc., Chem. Commun.* **1993**, (1), 65-66.
- [326] Arentsen, K.; Caddick, S.; Cloke, F. G. N.; Herring, A. P.; Hitchcock, P. B. *Tetrahedron Lett.* **2004**, *45* (17), 3511-3515.
- [327] Burns, A. R.; McAllister, G. D.; Shanahan, S. E.; Taylor, R. J. K. *Angew. Chem. Int. Ed.* **2010**, *49* (32), 5574-5577.
- [328] Seath, C. P.; Fyfe, J. W. B.; Molloy, J. J.; Watson, A. J. B. *Angew. Chem. Int. Ed.* **2015**, *54* (34), 9976-9979.
- [329] Lüthy, M.; Taylor, R. J. K. *Tetrahedron Lett.* **2012**, *53* (27), 3444-3447.
- [330] Kerins, F.; O'Shea, D. F. *J. Org. Chem.* **2002**, *67* (14), 4968-4971.
- [331] McKinley, N. F.; O'Shea, D. F. *J. Org. Chem.* **2004**, *69* (15), 5087-5092.
- [332] Tzschucke, C. C.; Murphy, J. M.; Hartwig, J. F. *Org. Lett.* **2007**, *9* (5), 761-764.
- [333] McGarry, K. A.; Duenas, A. A.; Clark, T. B. *J. Org. Chem.* **2015**, *80* (14), 7193-7204.
- [334] King, A. E.; Ryland, B. L.; Brunold, T. C.; Stahl, S. S. *Organometallics* **2012**, *31* (22), 7948-7957.
- [335] Santana, A. B.; Lucas, S. D.; Gonçalves, L. M.; Correia, H. F.; Cardote, T. A. F.; Guedes, R. C.; Iley, J.; Moreira, R. *Bioorg. Med. Chem. Lett.* **2012**, *22* (12), 3993-3997.
- [336] Walker, M. A. *J. Org. Chem.* **1995**, *60* (16), 5352-5355.
- [337] Jafarpour, F.; Shamsianpour, M.; Issazadeh, S.; Dorrani, M.; Hazrati, H. *Tetrahedron* **2017**, *73* (13), 1668-1672.
- [338] Zhou, Y.; Liang, H.; Sheng, Y.; Wang, S.; Gao, Y.; Zhan, L.; Zheng, Z.; Yang, M.; Liang, G.; Zhou, J.; Deng, J.; Song, Z. *J. Org. Chem.* **2020**, *85* (14), 9230-9243.
- [339] Gandini, A. *Prog. Polym. Sci.* **2013**, *38* (1), 1-29.
- [340] Froidevaux, V.; Borne, M.; Laborbe, E.; Auvergne, R.; Gandini, A.; Boutevin, B. *RSC Adv.* **2015**, *5* (47), 37742-37754.
- [341] Galkin, K. I.; Sandulenko, I. V.; Polezhaev, A. V. *Processes* **2022**, *10* (1), 30.
- [342] St. Amant, A. H.; Lemen, D.; Florinas, S.; Mao, S.; Fazenbaker, C.; Zhong, H.; Wu, H.; Gao, C.; Christie, R. J.; Read de Alaniz, J. *Bioconjugate Chem.* **2018**, *29* (7), 2406-2414.

- [343] Ha, S.; Lee, Y.; Kwak, Y.; Mishra, A.; Yu, E.; Ryou, B.; Park, C.-M. *Nat. Commun.* **2020**, *11* (1), 2509.
- [344] Uno, B. E.; Deibler, K. K.; Villa, C.; Raghuraman, A.; Scheidt, K. A. *Adv. Synth. Catal.* **2018**, *360* (8), 1719-1725.
- [345] Uno, B. E.; Dicken, R. D.; Redfern, L. R.; Stern, Charlotte M.; Krzywicki, G. G.; Scheidt, K. A. *Chem. Sci.* **2018**, *9* (6), 1634-1639.
- [346] Abel, B. A.; McCormick, C. L. *Macromolecules* **2016**, *49* (17), 6193-6202.
- [347] Ravasco, J. M. J. M.; Faustino, H.; Trindade, A.; Gois, P. M. P. *Chem. Eur. J.* **2019**, *25* (1), 43-59.
- [348] Smith, M. E. B.; Caspersen, M. B.; Robinson, E.; Morais, M.; Maruani, A.; Nunes, J. P. M.; Nicholls, K.; Saxton, M. J.; Caddick, S.; Baker, J. R.; Chudasama, V. *Org. Biomol. Chem.* **2015**, *13* (29), 7946-7949.
- [349] Barradas, R. G.; Fletcher, S.; Porter, J. D. *Can. J. Chem.* **1976**, *54* (9), 1400-1404.
- [350] Machida, M.; Machida, M. I.; Kanaoka, Y. *Chem. Pharm. Bull.* **1977**, *25* (10), 2739-2743.
- [351] Khan, M. N. *J. Pharm. Sci.* **1984**, *73* (12), 1767-1771.
- [352] Forte, N.; Livanos, M.; Miranda, E.; Morais, M.; Yang, X.; Rajkumar, V. S.; Chester, K. A.; Chudasama, V.; Baker, J. R. *Bioconjugate Chem.* **2018**, *29* (2), 486-492.
- [353] Ryan, C. P.; Smith, M. E. B.; Schumacher, F. F.; Grohmann, D.; Papaioannou, D.; Waksman, G.; Werner, F.; Baker, J. R.; Caddick, S. *Chem. Commun.* **2011**, *47* (19), 5452-5454.
- [354] Matsui, S.; Aida, H. *J. Chem. Soc., Perkin Trans. 2* **1978**, (12), 1277-1280.
- [355] Altamirano-Espino, J. A.; Sánchez-Labastida, L. A.; Martínez-Archundia, M.; Andrade-Jorge, E.; Trujillo-Ferrara, J. G. *ChemistrySelect* **2020**, *5* (44), 14177-14182.
- [356] Schultz, E. M.; Bolhofer, W. A.; Augenblick, A.; Bicking, J. B.; Habecker, C. N.; Horner, J. K.; Kwong, S. F.; Pietruszkiewicz, A. M. *J. Med. Chem.* **1967**, *10* (4), 717-724.
- [357] Li, J. *J. Chem. Crystallogr.* **2010**, *40* (5), 428-431.
- [358] Guo, Z.; Sui, J.; Ma, M.; Hu, J.; Sun, Y.; Yang, L.; Fan, Y.; Zhang, X. *J. Controlled Release* **2020**, *326*, 350-364.
- [359] Tao, A.; Huang, G. L.; Igarashi, K.; Hong, T.; Liao, S.; Stellacci, F.; Matsumoto, Y.; Yamasoba, T.; Kataoka, K.; Cabral, H. *Macromol. Biosci.* **2020**, *20* (1), 1900161.
- [360] Du, J.-Z.; Li, H.-J.; Wang, J. *Acc. Chem. Res.* **2018**, *51* (11), 2848-2856.

- [361] Lazarou, K. N.; Boudalis, A. K.; Perlepes, S. P.; Terzis, A.; Raptopoulou, C. P. *Eur. J. Inorg. Chem.* **2009**, *2009* (29-30), 4554-4563.
- [362] Díaz-García, D.; Ardiles, P. R.; Prashar, S.; Rodríguez-Diéguez, A.; Páez, P. L.; Gómez-Ruiz, S. *Pharmaceutics* **2019**, *11* (1), 30.
- [363] Lazarou, K. N.; Psycharis, V.; Perlepes, S. P.; Raptopoulou, C. P. *Polyhedron* **2009**, *28* (6), 1085-1096.
- [364] Liu, Y.; Hu, H.; Zhou, J.; Wang, W.; He, Y.; Wang, C. *Org. Biomol. Chem.* **2017**, *15* (23), 5016-5024.
- [365] Xu, J.; Hu, H.; Liu, Y.; Wang, X.; Kan, Y.; Wang, C. *Eur. J. Org. Chem.* **2017**, *2017* (2), 257-261.
- [366] Majce, V.; Kočevár, M.; Polanc, S. *Tetrahedron Lett.* **2011**, *52* (26), 3287-3290.
- [367] Sánchez, A.; Pedroso, E.; Grandas, A. *Eur. J. Org. Chem.* **2010**, *2010* (13), 2600-2606.
- [368] Rebelo, B. A.; Santos, R. B.; Ascenso, O. S.; Nogueira, A. C.; Lousa, D.; Abranches, R.; Ventura, M. R. *Bioorg. Chem.* **2020**, *94*, 103452.
- [369] Ekici, Ö. D.; Li, Z. Z.; Campbell, A. J.; James, K. E.; Asgian, J. L.; Mikolajczyk, J.; Salvesen, G. S.; Ganesan, R.; Jelakovic, S.; Grütter, M. G.; Powers, J. C. *J. Med. Chem.* **2006**, *49* (19), 5728-5749.
- [370] Kumar, P.; Dathu Reddy, Y.; Kumari, Y.; Rama devi, B.; Dubey, P. *Indian J. Chem. - B Org. Med. Chem.* **2014**, *53*, 392-398.
- [371] Kiselev, V. D.; Kashaeva, H. A.; Potapova, L. N.; Kornilov, D. A.; Latypova, L. I.; Konovalov, A. I. *Russ. Chem. Bull.* **2016**, *65* (9), 2202-2205.
- [372] Byrne, A. J.; Bright, S. A.; McKeown, J. P.; O'Brien, J. E.; Twamley, B.; Fayne, D.; Williams, D. C.; Meegan, M. J. *Pharmaceutics* **2020**, *13* (1), 16.
- [373] Gao, L.; Li, G.; Li, X.; Zhang, G.; Zhang, M.; Li, Q.; Ban, S. *Org. Chem. Front.* **2022**, *9* (9), 2390-2395.
- [374] Matysiak, B. M.; Monreal Santiago, G.; Otto, S. *Chem. Eur. J.* **2022**, *28* (40), e202201043.
- [375] Bello, I. A.; Ndukwe, G. I.; Amupitan, J. O.; Ayo, R. G.; Shode, F. O. *Int. J. Med. Chem.* **2012**, *2012*, 148235.
- [376] Zhang, H.; Zhan, X.-Y.; Chen, X.-L.; Tang, L.; He, S.; Shi, Z.-C.; Wang, Y.; Wang, J.-Y. *Adv. Synth. Catal.* **2019**, *361* (21), 4919-4925.
- [377] Srinivasan, E.; Argade, N. *Cheminform* **2003**, *34* (1).
- [378] Pyriadi, T. M.; Ali, F. M. *Polym. Bull.* **1984**, *11* (2), 129-134.
- [379] Begland, R. W.; Hartter, D. R.; Jones, F. N.; Sam, D. J.; Sheppard, W. A.; Webster, O. W.; Weigert, F. J. *J. Org. Chem.* **1974**, *39* (16), 2341-2350.



- [380] Salakhova, R. S.; Mamedov, E. S.; Gadzhily, T. M. *Thermal instability of (ethoxycarbonylisopropenyl)imides of dibasic acids*; Inst. Teor. Probl. Khim. Tekhnol., Baku, USSR, 1984.
- [381] Yuan, W.; Zhu, H.; Cheng, K.; Huang, Z.; Qin, Y.; Yang, J.; Zhu, P. *Nat. Prod. Res.* **2006**, *20* (6), 573-577.
- [382] Luo, F.; Pan, C.; Cheng, J. *Synlett* **2012**, *2012* (3), 357-366.
- [383] Souffrin, A.; Croix, C.; Viaud-Massuard, M.-C. *Eur. J. Org. Chem.* **2012**, *2012* (13), 2499-2502.
- [384] Becker, D.; Kaczmarska, Z.; Arkona, C.; Schulz, R.; Tauber, C.; Wolber, G.; Hilgenfeld, R.; Coll, M.; Rademann, J. *Nat. Commun.* **2016**, *7* (1), 12761.
- [385] Zhou, Z.; Hu, Y.; Wang, B.; He, X.; Ren, G.; Feng, L. *J. Chem. Res.* **2014**, *38* (6), 378-380.
- [386] Citarella, A.; Moi, D.; Pinzi, L.; Bonanni, D.; Rastelli, G. *ACS Omega* **2021**, *6* (34), 21843-21849.
- [387] Brown, K.; Cavalla, J. F.; Green, D.; Wilson, A. B. *Nature* **1968**, *219* (5150), 164-164.
- [388] Tinnis, F.; Stridfeldt, E.; Lundberg, H.; Adolfsson, H.; Olofsson, B. *Org. Lett.* **2015**, *17* (11), 2688-2691.
- [389] Zheng, Y.; Li, X.; Ren, C.; Zhang-Negrerie, D.; Du, Y.; Zhao, K. *J. Org. Chem.* **2012**, *77* (22), 10353-10361.
- [390] Nozaki, K.; Ogg Jr., R. *J. Am. Chem. Soc.* **1941**, *63* (10), 2583-2586.
- [391] Barrios Sosa, A. C.; Yakushijin, K.; Horne, D. A. *J. Org. Chem.* **2002**, *67* (13), 4498-4500.
- [392] Patil, A. D.; Freyer, A. J.; Killmer, L.; Hofmann, G.; Johnson, R. K. *Nat. Prod. Lett.* **1997**, *9* (3), 201-207.
- [393] Park, K. D.; Morieux, P.; Salomé, C.; Cotten, S. W.; Reamtong, O.; Evers, C.; Gaskell, S. J.; Stables, J. P.; Liu, R.; Kohn, H. *J. Med. Chem.* **2009**, *52* (21), 6897-6911.
- [394] Kwon, Y.-D.; Son, J.; Chun, J.-H. *J. Org. Chem.* **2019**, *84* (6), 3678-3686.
- [395] Sauers, C. K. *J. Org. Chem.* **1969**, *34* (8), 2275-2279.
- [396] Carbery, D. R. *Org. Biomol. Chem.* **2008**, *6* (19), 3455-3460.



# Appendix: Paper I-III

## **Paper I:**

Appended is the published paper. The supporting information can be found online with the publication.

## **Paper II:**

Appended are the final draft of the manuscript and the supporting information which are not yet published.

## **Paper III:**

Appended is the published paper. The supporting information can be found online with the publication.



## Paper I

# Cu-catalyzed *N*-3-Arylation of Hydantoins Using Diaryliodonium Salts

Linn Neerbye Berntsen, Ainara Nova, David S. Wragg and Alexander H. Sandtorv

Organic Letters **2020**, *22* (7), 2687-2691.

DOI: 10.1021/acs.orglett.0c00642



# Cu-catalyzed *N*-3-Arylation of Hydantoin Using Diaryliodonium Salts

Linn Neerbye Berntsen, Ainara Nova, David S. Wragg, and Alexander H. Sandtorv\*



Cite This: *Org. Lett.* 2020, 22, 2687–2691



Read Online

ACCESS |



Metrics & More

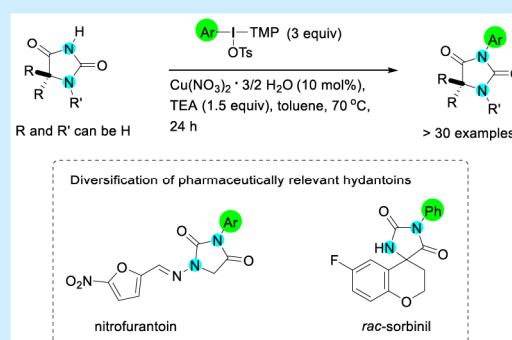


Article Recommendations



Supporting Information

**ABSTRACT:** A general Cu-catalyzed, regioselective method for the *N*-3-arylation of hydantoin is described. The protocol utilizes aryl-(trimethoxyphenyl)iodonium tosylate as the arylating agent in the presence of triethylamine and a catalytic amount of a simple Cu-salt. The method is compatible with structurally diverse hydantoin and operates well with neutral aryl groups or aryl groups bearing weakly donating/withdrawing elements. It is also applicable for the rapid diversification of pharmaceutically relevant hydantoin.



Hydantoin is a heterocyclic scaffold with numerous application areas.<sup>1</sup> The structure has an impressive range of biological activities,<sup>2</sup> likely due to its high density of intermolecular interaction points.<sup>3</sup> It is encountered in several drugs, such as nilutamide, sorbinil, and nitrofurantoin, and constitutes a key molecular component of various agrochemicals.<sup>4</sup> The nucleus also has synthetic versatility,<sup>5</sup> for example, in the preparation of amino acids.<sup>6</sup> Of particular interest are *N*-arylated hydantoin due to their important biological applications (Figure 1).<sup>7</sup>

The primary access point to *N*-arylated hydantoin (and other substituted hydantoin) is through *de novo* cyclization reactions from linear precursors (Scheme 1).<sup>8</sup> A plethora of such transformations is known,<sup>9</sup> and each method has advantages and limitations. The direct functionalization of the hydantoin nucleus offers a complementary approach where

## Scheme 1. Prior Work

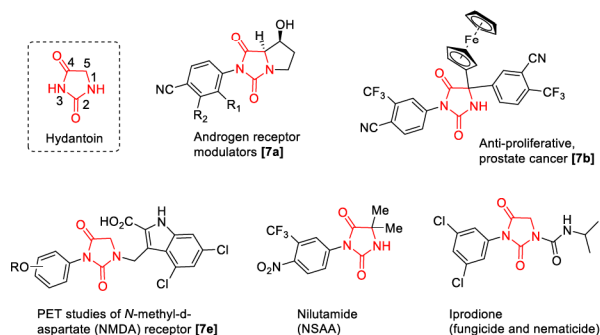
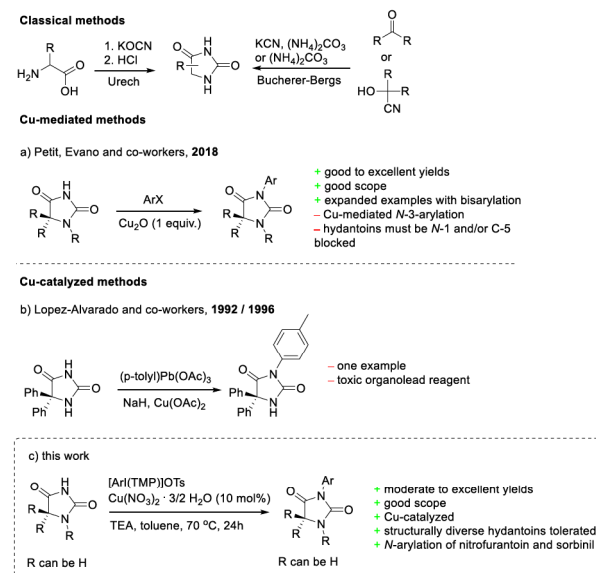


Figure 1. Some *N*-3-arylated hydantoin with biological properties.

Received: February 18, 2020

Published: March 23, 2020

the substituent(s) of interest are chemo- and regioselectively forged onto the ring itself. This scenario allows divergent modifications of hydantoin as well as potentially quicker and cheaper access to such structures. Direct functionalization remains underdeveloped, perhaps due to its challenging nature.<sup>7c,10</sup>

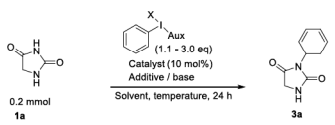
For example, the direct *N*-3-phenylation of unsubstituted hydantoin has, to the best of our knowledge, not been described in the literature.

Recently, a breakthrough was achieved by Petit, Evano, and coworkers (Scheme 1a), who divulged a Cu-mediated *N*-arylation protocol.<sup>11</sup> The method exhibited a good reaction scope and mostly good yields. However, it suffered from two disadvantages: (i) the use of stoichiometric Cu and (ii) clear structural limitations of the hydantoin starting material. Whereas 5,5-disubstituted hydantoin were regioselectively arylated at the *N*-3 position, removing one or both of the C-5 substituents led to significant competing arylation at *N*-1, limiting the substrate scope. The Cu-catalyzed *N*-arylation of hydantoin is largely unexplored, and only sparse and highly specialized examples are reported in the literature (Scheme 1b).<sup>7c,12</sup> Herein we describe a general Cu-catalyzed process for *N*-3-arylation of hydantoin, a complementary method to the current Cu-mediated protocol (Scheme 1).

Diaryliodonium salts<sup>13</sup> have received increasing attention over the past decade,<sup>14</sup> partially due to their ability to transfer aryl groups to nucleophiles.<sup>15</sup> Our reaction discovery process led to the revelation that unsymmetrical iodonium salts regioselectively arylated the *N*-3-position of hydantoin in the presence of a simple copper salt and tertiary amine under mild conditions. In contrast, phenyl iodide was an inefficient arylating agent under Cu-catalyzed conditions and did not successfully couple to the hydantoin nucleus.

An overview of the optimization studies is provided in Scheme 2. The best conditions (entry 1) involved the use of excess aryl(trimethoxyphenyl)iodonium tosylate in the presence of copper(II)nitrate sesquihydrate and triethylamine in toluene at 70 °C for 24 h. Under these conditions, trace amounts (<5%) of the *N*-1-regioisomer were typically

**Scheme 2. Key Controls and Optimization Data for the Reaction**

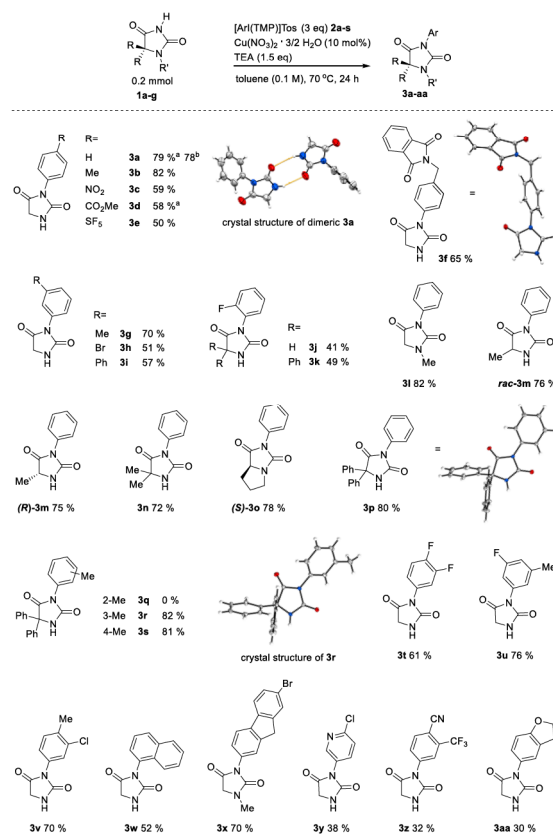


#	X	Aux	Amount of salt (eq.)	Catalyst	Additive / base (eq.)	Solvent	Temp (°C)	Yield (%) <sup>a</sup>
1	OTs	TMP	3.0	Cu(NO <sub>3</sub> ) <sub>2</sub> · 3/2 H <sub>2</sub> O	TEA (1.5)	Toluene	70	79
2	OTs	TMP	1.5	Cu(NO <sub>3</sub> ) <sub>2</sub> · 3/2 H <sub>2</sub> O	TEA (1.5)	Toluene	70	72
3	OTs	TMP	1.1	Cu(NO <sub>3</sub> ) <sub>2</sub> · 3/2 H <sub>2</sub> O	TEA (1.5)	Toluene	70	66
4	OTs	TMP	1.1	Cu(NO <sub>3</sub> ) <sub>2</sub> · 3/2 H <sub>2</sub> O	NaH (1.1) and TEA (0.2)	Toluene	70	67
5	OTf	TMP	3.0	Cu(NO <sub>3</sub> ) <sub>2</sub> · 3/2 H <sub>2</sub> O	TEA (1.5)	Toluene	70	nd
6	OTs	TMP	3.0	-	-	Toluene	70	nd
7	OTs	TMP	3.0	Cu(NO <sub>3</sub> ) <sub>2</sub> · 3/2 H <sub>2</sub> O	-	Toluene	70	nd
8	OTs	TMP	3.0	-	TEA (1.5)	Toluene	70	nd
9	OTs	TMP	3.0	-	NaH (1.0)	Toluene	70	nd
10	OTs	TMP	3.0	-	NaH (2.0)	Toluene	70	nd
11	OTs	TMP	3.0	Cu(NO <sub>3</sub> ) <sub>2</sub> · 3/2 H <sub>2</sub> O	NaH (1.0)	Toluene	70	nd
12	OTs	TMP	3.0	-	TEA (1.5)	Toluene	70	47
13	OTs	TMP	3.0	Cu <sub>2</sub> O	TEA (1.5)	Toluene	70	41
14	Br	TMP	3.0	Cu(NO <sub>3</sub> ) <sub>2</sub> · 3/2 H <sub>2</sub> O	TEA (1.5)	Toluene	70	7
15	OTs	Mes	3.0	Cu(NO <sub>3</sub> ) <sub>2</sub> · 3/2 H <sub>2</sub> O	TEA (1.5)	Toluene	70	60
16	OTs	TMP	3.0	Cu(NO <sub>3</sub> ) <sub>2</sub> · 3/2 H <sub>2</sub> O	TEA (1.5)	DMSO	70	74
17	OTs	TMP	3.0	-	-	Toluene	110	nd
18	OTs	TMP	3.0	Cu(NO <sub>3</sub> ) <sub>2</sub> · 3/2 H <sub>2</sub> O	DMEDA(1.5)	Toluene	70	64
19	OTs	TMP	3.0	-	DMEDA(1.5)	Toluene	70	trace

<sup>a</sup>Yield measured using mesitylene as an internal standard in the <sup>1</sup>H NMR analysis of the crude reaction mixture.

observed as well as small amounts of the corresponding *N,N'*-bisarylated product (3–10%). The process was also efficient and regioselective when the excesses of phenyl-(trimethoxyphenyl)iodonium tosylate was reduced to 1.5 or 1.1 equiv (entries 2 and 3), although the desired target was produced in slightly reduced yield. If a small reduction in yield is tolerable, then the process can therefore be performed with improved atom efficiency. The scope and limitations of the process are shown in Scheme 3.

**Scheme 3. Scope and Limitations of the Catalytic *N*-3-Arylation Process<sup>c</sup>**



<sup>a</sup>5 mol % of catalyst employed. <sup>b</sup>Reaction performed using 1 mmol of diaryl iodonium salt and extended reaction time (31 h). <sup>c</sup>Conditions: Hydantoin 1a–g (0.2 mmol, 1.0 equiv), [ArI(TMP)]Tos 2a–s (0.6 mmol, 3.0 equiv), Cu(NO<sub>3</sub>)<sub>2</sub> · 3/2 H<sub>2</sub>O (0.02 mmol, 0.1 equiv), triethylamine (TEA) (0.3 mmol, 1.5 equiv), and toluene (2 mL).

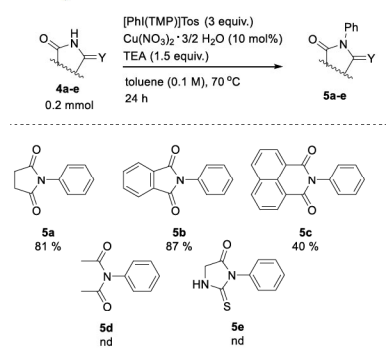
Pleasingly, the *N*-3 arylation proceeded smoothly with structurally diverse hydantoin, including structures lacking substituents on C-5 or *N*-1.<sup>11</sup> Aryl rings bearing neutral or weakly electron-donating/withdrawing groups were efficiently transferred to the *N*-3-position on the hydantoin ring. This trend was also observed for disubstituted aryl rings. The method was sensitive to iodonium salts bearing aryl groups congested at the *o*-position, likely due to steric crowding around the Cu-center in the catalytic process. The relatively small fluoride atom was tolerated, providing the corresponding hydantoin 3j and 3k in moderate yields. The more demanding *o*-methyl group was not tolerated under our conditions, and the coupled product 3q was not observed in the post reaction



mixture. The mild conditions did not cause epimerization at the C-5-position of the hydantoin ring. The coupled chiral hydantoin products (*R*)-**3m** and (*S*)-**3o** were obtained in good yield with stereoretention, as indicated by polarimetric analysis. Strongly electron-poor and electron-rich aryl groups were less efficient substrates (**3c,d,e**), and *N*-3-arylated hydantoins **3y**, **3z**, and **3aa** were isolated in modest yield.

To our delight, the method was also applicable to a small selection of cyclic imide-type structures<sup>16</sup> (Scheme 4) such as

**Scheme 4. N-Arylation of Other N–H Bonds<sup>a</sup>**

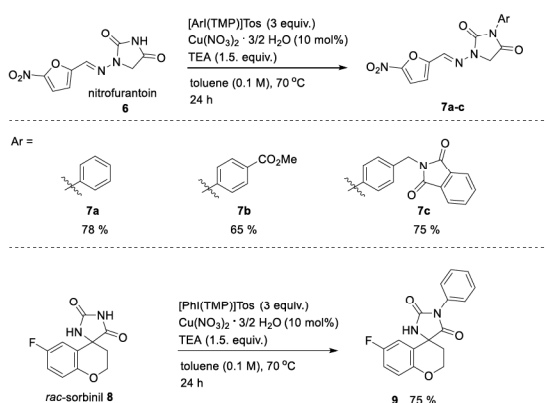


<sup>a</sup>Conditions: Imide **4a–d** (0.2 mmol, 1.0 equiv), [ArI(TMP)]Tos **2a** (0.6 mmol, 3.0 equiv), Cu(NO<sub>3</sub>)<sub>2</sub>·3/2 H<sub>2</sub>O (0.02 mmol, 0.1 equiv), triethylamine (TEA) (0.3 mmol, 1.5 equiv), and toluene (2 mL).

succinimide **4a** and phthalimide **4b**, exemplifying the usefulness of the method in an expanded structural space. The linear imide **4d** did not produce the desired product **5d**, indicating that the method is not applicable to linear imides, likely due to their less constrained conformation compared with cyclic imides. Thiohydantoin **4e** did not react under our conditions.

To illustrate the practicality of the method, the well-known antibiotic drug nitrofurantoin **6**<sup>17</sup> was *N*-3-arylated in good yield, providing a small library of nitrofurantoin derivatives **7a–c** (Scheme 5). The racemate of the aldose reductase inhibitor sorbinil **8**<sup>18</sup> was also *N*-3-arylated in good yield.

**Scheme 5. Regioselective N-Arylation of Pharmaceutically Relevant Agents<sup>a</sup>**

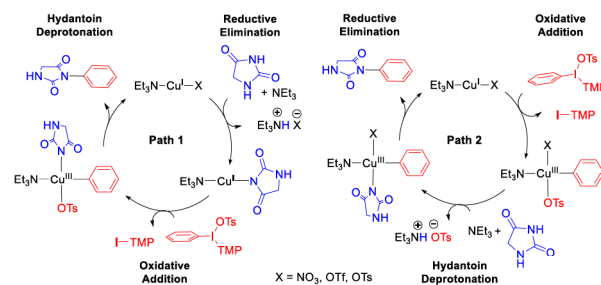


<sup>a</sup>Conditions: hydantoin **6** or **8** (0.2 mmol, 1.0 equiv), [ArI(TMP)]Tos (0.6 mmol, 3.0 equiv), Cu(NO<sub>3</sub>)<sub>2</sub>·3/2 H<sub>2</sub>O (0.02 mmol, 0.1 equiv), triethylamine (TEA) (0.3 mmol, 1.5 equiv), and toluene (2 mL).

These examples illustrate the potential methods for the rapid diversification of pharmaceutically relevant agents and highlight the advantage of direct functionalization.

Two different mechanisms involving the Cu(I)/Cu(III) species could be envisaged for this process (Scheme 6).

**Scheme 6. Two Mechanistic Proposals for the Cu-Catalyzed N-Arylation Process**



Pathway 1 corresponds to the mechanism proposed for Ullman-type C–N bond coupling reactions using aryl iodides.<sup>19</sup> In this process, a Cu(I) species would deprotonate the hydantoin prior to the oxidative addition of the iodonium tosylate. In Pathway 2, the first step would consist of an oxidative addition of the iodonium salt followed by the deprotonation of hydantoin. The latter pathway has been proposed in Cu-catalyzed arylation reactions involving diaryliodonium salts.<sup>20</sup> In both pathways, the final product is formed by reductive elimination of the Cu(III) aryl amido intermediate. The use of Cu(II) precatalyst for Cu(I)-mediated reactions is predated.<sup>21</sup> Both one-electron reduction and disproportionation mechanisms have been proposed for the reduction of Cu.<sup>22</sup> We believe that in the two mechanisms TEA acts as both a Cu ligand and base, driving the deprotonation of hydantoin. This double function was corroborated by using a catalytic amount of TEA and NaH as a base (see entry 4, Scheme 2). The tosylate anion may also play an important role when coordinated to the Cu center, assisting the intramolecular deprotonation of hydantoin at the *N*-3 position, which is the most acidic.<sup>22</sup> This could account for the lower yield observed when using bromide or the less basic OTf anion (see entries 5 and 14, Scheme 2).

In summary, we have reported the first general Cu-catalyzed method for the regioselective *N*-3-arylation of hydantoins. The method utilizes unsymmetrical iodonium salts, a simple Cu salt, and triethylamine under mild conditions. The method is robust and flexible, operates well, with weakly electron-donating and -withdrawing groups, proceeds without epimerization at C-5 of hydantoin, and smoothly arylates structurally varied hydantoins, including pharmaceutically relevant structures such as nitrofurantoin and *rac*-sorbinil. In-depth mechanistic investigations are currently underway.

## ■ ASSOCIATED CONTENT

### Supporting Information

The Supporting Information is available free of charge at <https://pubs.acs.org/doi/10.1021/acs.orglett.0c00642>.

Detailed experimental procedures and full spectroscopic data for all new compounds (PDF)

## Accession Codes

CCDC 1975309, 1975600, 1975603, and 1986195 contain the supplementary crystallographic data for this paper. These data can be obtained free of charge via [www.ccdc.cam.ac.uk/data\\_request/cif](http://www.ccdc.cam.ac.uk/data_request/cif), or by emailing [data\\_request@ccdc.cam.ac.uk](mailto:data_request@ccdc.cam.ac.uk), or by contacting The Cambridge Crystallographic Data Centre, 12 Union Road, Cambridge CB2 1EZ, UK; fax: +44 1223 336033.

## AUTHOR INFORMATION

## Corresponding Author

Alexander H. Sandtorv – Department of Chemistry, University of Oslo, N-0315 Oslo, Norway; [orcid.org/0000-0003-2480-0195](https://orcid.org/0000-0003-2480-0195); Email: [a.h.sandtorv@kjemi.uio.no](mailto:a.h.sandtorv@kjemi.uio.no)

## Authors

Linn Neerbye Berntsen – Department of Chemistry, University of Oslo, N-0315 Oslo, Norway

Ainara Nova – Hylleraas Centre for Quantum Molecular Sciences, Department of Chemistry, University of Oslo, N-0315 Oslo, Norway; [orcid.org/0000-0003-3368-7702](https://orcid.org/0000-0003-3368-7702)

David S. Wragg – Department of Chemistry, University of Oslo, N-0315 Oslo, Norway

Complete contact information is available at:  
<https://pubs.acs.org/10.1021/acs.orglett.0c00642>

## Notes

The authors declare no competing financial interest.

## ACKNOWLEDGMENTS

L.N.B. gratefully acknowledges the Department of Chemistry at the University of Oslo for funding her Ph.D. fellowship. Arild X. Hagen (Department of Chemistry, University of Oslo) is acknowledged for technical assistance with the optimization study, and Brian C. Gilmour (Oslo University Hospital, University of Oslo) is acknowledged for technical assistance in the preparation of diaryliodonium salts. The project has received support from UiO: Life Science and was partially supported by the Research Council of Norway through the Norwegian NMR Platform, NNP (226244/F50). A.N. acknowledges the support from the Research Council of Norway (FRINATEK grant no. 250044 and Center of Excellence grant no. 262695). We acknowledge the use of the Norwegian national infrastructure for X-ray diffraction and scattering (RECX, Research Council of Norway project number 208896).

## REFERENCES

- (1) Konnert, L.; Lamaty, F.; Martinez, J.; Colacino, E. *Chem. Rev.* **2017**, *117*, 13757–13809.
- (2) For some examples, see: (a) Sarges, R.; Goldstein, S. W.; Welch, W. M.; Swindell, A. C.; Siegel, T. W.; Beyer, T. A. *J. Med. Chem.* **1990**, *33*, 1859–1865. (b) Tan, L.; Maji, S.; Mattheis, C.; Zheng, M.; Chen, Y.; Caballero-Diaz, E.; Gil, P. R.; Parak, W. J.; Greiner, A.; Agarwal, S. *Macromol. Biosci.* **2012**, *12*, 1068–1076. (c) Su, M.; Xia, D.; Teng, P.; Nimmagadda, A.; Zhang, C.; Odom, T.; Cao, A.; Hu, Y.; Cai, J. *J. Med. Chem.* **2017**, *60*, 8456–8465. (d) Żesławska, E.; Kincses, A.; Spengler, G.; Nitek, W.; Tejchman, W.; Handzlik, J. *Chem. Biol. Drug Des.* **2019**, *93*, 844–853. (e) Cho, S.; Kim, S.-H.; Shin, D. *Eur. J. Med. Chem.* **2019**, *164*, 517–545. (f) Fetzer, C.; Korotkov, V. S.; Sieber, S. A. *Org. Biomol. Chem.* **2019**, *17*, 7124–7217.
- (3) Mendgen, T.; Steuer, C.; Klein, C. D. *J. Med. Chem.* **2012**, *55*, 743–753.
- (4) Mizuno, T.; Kino, T.; Ito, T.; Miyata, T. *Synth. Commun.* **2000**, *30*, 1675–1688.
- (5) (a) Khazaei, A.; Zolfigol, M. A.; Rostami, A. *Synthesis* **2004**, 2959–2961. (b) Sandtorv, A. H.; Bjørsvik, H.-R. *Adv. Synth. Catal.* **2013**, *355*, 499–507. (c) Leitch, J. A.; Cook, H. P.; Bhonoah, Y.; Frost, C. G. *J. Org. Chem.* **2016**, *81*, 10081–10087. (d) Luo, Z.; Liu, T.; Guo, W.; Wang, Z.; Huang, J.; Zhu, Y.; Zeng, Z. *Org. Process Res. Dev.* **2018**, *22*, 1188–1199.
- (6) (a) Burton, S. G.; Dorrington, R. A. *Tetrahedron: Asymmetry* **2004**, *15*, 2737–2741. (b) May, O.; Verseck, S.; Bommarius, A.; Drauz, K. *Org. Process Res. Dev.* **2002**, *6*, 452–457. (c) Fernandez-Nieto, F.; Mas Rosello, J.; Lenoir, S.; Hardy, S.; Clayden, J. *Org. Lett.* **2015**, *17*, 3838–3841. (d) Abas, H.; Mas-Roselló, Amer, M. M.; Durand, D. J.; Groleau, R. R.; Fey, N.; Clayden, J. *Angew. Chem., Int. Ed.* **2019**, *58*, 2418–2422. (e) Amer, M. M.; Abas, H.; Leonard, D. J.; Ward, J. W.; Clayden, J. *J. Org. Chem.* **2019**, *84*, 7199–7206.
- (7) For some examples, see: (a) Hamann, L. G.; Manfredi, M. C.; Sun, C.; Krystek, S. R., Jr.; Huang, Y.; Bi, Y.; Augeri, D. J.; Wang, T.; Zou, Y.; Betebenner, D. A.; Fura, A.; Seethala, R.; Golla, R.; Kuhns, J. E.; Lupisella, J. A.; Darienzo, C. J.; Custer, L. L.; Price, J. L.; Johnson, J. M.; Biller, S. A.; Zahler, R.; Ostrowski, J. *Bioorg. Med. Chem. Lett.* **2007**, *17*, 1860–1864. (b) Payen, O.; Top, S.; Vessieres, A.; Brule, E.; Plamont, M.-A.; McGlinchey, M. J.; Muller-Bunz, H.; Jaouen, G. *J. Med. Chem.* **2008**, *51*, 1791–1799. (c) Wang, C.; Zhao, Q.; Vargas, M.; Jones, J. O.; White, K. L.; Shackelford, D. M.; Chen, G.; Saunders, J.; Ng, A. C. F.; Chiu, F. C. K.; Dong, Y.; Charman, S. A.; Keiser, J.; Vennerstrom, J. L. *J. Med. Chem.* **2016**, *59*, 10705–10718. (d) Tamura, T.; Noda, H.; Joyashiki, E.; Hoshino, M.; Watanabe, T.; Kinoshita, M.; Nishimura, Y.; Esaki, T.; Ogawa, K.; Miyake, T.; Arai, S.; Shimizu, M.; Kitamura, H.; Sato, H.; Kawabe, Y. *Nat. Commun.* **2016**, *7*, 13384–13398. (e) Bauman, A.; Piel, M.; Höhnemann, S.; Krauss, A.; Jansen, M.; Solbach, C.; Dannhardt, G.; Rösch, F. *J. Labelled Compd. Radiopharm.* **2011**, *54*, 645–656.
- (8) (a) Meusel, M.; Gütschow, M. *Org. Prep. Proced. Int.* **2004**, *36*, 391–443. (b) Konnert, L.; Lamaty, F.; Martinez, J.; Colacino, E. *Chem. Rev.* **2017**, *117* (23), 13757–13809.
- (9) For some recent examples, see: (a) Rajic, Z.; Zorc, B.; Raic-Malic, S.; Ester, K.; Kralj, M.; Pavelic, K.; Balzarini, J.; De Clercq, E.; Mintas, M. *Molecules* **2006**, *11*, 837–848. (b) Zhao, B.; Du, H.; Shi, Y. *J. Am. Chem. Soc.* **2008**, *130*, 7220–7221. (c) Gao, M.; Yang, Y.; Wu, Y.-D.; Deng, C.; Shu, W.-M.; Zhang, D.-X.; Cao, L.-P.; She, N.-F.; Wu, A.-X. *Org. Lett.* **2010**, *12*, 4026–4029. (d) Bogolubsky, A. V.; Moroz, Y. S.; Savych, O.; Pipko, S.; Konovets, A.; Platonov, M. O.; Vasylenko, O. V.; Hurmach, V. V.; Grygorenko, O. O. *ACS Comb. Sci.* **2018**, *20*, 35–43. (e) Saunthwal, R. K.; Cornall, M. T.; Abrams, R.; Ward, J. W.; Clayden, J. *Chem. Sci.* **2019**, *10*, 3408–3412. (f) Declas, N.; Le Vaillant, F.; Waser, J. *Org. Lett.* **2019**, *21*, 524–528. (g) Liu, S. L.; Haung, J.-Y.; Barve, I. J.; Huang, S.-C.; Sun, C.-M. *ACS Comb. Sci.* **2019**, *21* (4), 336–344.
- (10) (a) Hugel, H. M.; Rix, C. J.; Fleck, K. *Synlett* **2006**, 2006, 2290–2292. (b) Bigg, D.; Auvin, S.; Lanco, C.; Prevost, G. Imidazolidine-2,4-dione Derivatives, Their Preparation and Use for Treating Hormone-Dependent Cancer. WO 2010119194 A1, 2010. (c) Cowley, P. M.; McGowan, M. A.; Brown, T. J.; Han, Y.; Liu, K.; Pu, Q.; Wise, A.; Zhang, H.; Zhou, H. Novel Substituted Imidazopyridine Compounds as Inhibitors of indoleamine 2,3-Dioxygenase and/or Tryptophan-2,3-dioxygenase. WO 2017189386 A1, 2017. (d) Qin, X.; Fang, L.; Zhao, J.; Gou, S. *Inorg. Chem.* **2018**, *57*, 5019–5029.
- (11) Thilmany, P.; Gerard, P.; Vanoost, A.; Deldaele, C.; Petit, L.; Evano, G. *J. Org. Chem.* **2019**, *84*, 392–400.
- (12) Preliminary communication: (a) Lopez-Alvarado, P.; Avendano, C.; Carlos Menendez, J. *Tetrahedron Lett.* **1992**, *33*, 6875–6878. Full report: (b) Lopez-Alvarado, P.; Avendano, C.; Menendez, J. C. *J. Org. Chem.* **1996**, *61*, 5865–5870. (c) Suresh, M.; Ravi, S.; Sudhakar, K. Synthesis of Nilutamide and Development of C-N Bond Formation by Reusable Green Catalyst. IN 201741010702, 2017. (d) Pierce, J. M.; Hale, J. J.; Miao, S.; Vachal, P. Substituted-1,3,8-triazaspiro[4.5]decane-2,4-diones. WO2010147776 A1, 2010.

(e) Vachal, P.; Miao, S.; Pierce, J. M.; Guiadeen, D.; Colandrea, V. J.; Wyvratt, M. J.; Salowe, S. P.; Sonatore, L. M.; Milligan, J. A.; Hajdu, R.; Gollapudi, A.; Keohane, C. A.; Lingham, R. B.; Mandala, S. M.; DeMartino, J. A.; Tong, X.; Wolff, M.; Steinhuebel, D.; Kieczkowski, G. R.; Fleitz, F. J.; Chapman, K.; Athanasopoulos, J.; Adam, G.; Akyuz, C. D.; Jena, D. K.; Lusen, J. W.; Meng, J.; Stein, B. D.; Xia, L.; Sherer, E. C.; Hale, J. J. *J. Med. Chem.* **2012**, *55*, 2945–2959.

(13) For some reviews, see, for example: (a) Deprez, N. R.; Sanford, M. S. *Inorg. Chem.* **2007**, *46* (6), 1924–1935. (b) Merritt, E. A.; Olofsson, B. *Angew. Chem., Int. Ed.* **2009**, *48*, 9052–9070. (c) Yusubov, M. S.; Maskae, A. V.; Zhdankin, V. V. *ARKIVOC* **2011**, *2011*, 370–409. (d) Aradi, K.; Tóth, B. L.; Tolnai, G. L.; Novák, Z. *Synlett* **2016**, *27*, 1456–1485. (e) Olofsson, B. *Top. Curr. Chem.* **2015**, *373*, 135–166.

(14) Stuart, D. R. *Chem. - Eur. J.* **2017**, *23*, 15852–15863.

(15) For some recent examples, see: (a) Jalalian, N.; Ishikawa, E. E.; Silva, L. F.; Olofsson, B. *Org. Lett.* **2011**, *13*, 1552–1555. (b) Phipps, R. J.; McMurray, L.; Ritter, S.; Duong, H. A.; Gaunt, M. J. *J. Am. Chem. Soc.* **2012**, *134*, 10773–10776. (c) Sandtorv, A. H.; Stuart, D. R. *Angew. Chem., Int. Ed.* **2016**, *55*, 15812–15815. (d) Bhattarai, B.; Tay, J.-H.; Nagorny, P. *Chem. Commun.* **2015**, *51*, 5398–5401. (e) Modha, S. G.; Greaney, M. F. *J. Am. Chem. Soc.* **2015**, *137*, 1416–1419. (f) Aradi, K.; Mészáros, A.; Tóth, B. L.; Vincze, Z.; Novák, Z. *J. Org. Chem.* **2017**, *82*, 11752–11764. (g) Purkait, N.; Kervefors, G.; Linde, E.; Olofsson, B. *Angew. Chem., Int. Ed.* **2018**, *57*, 11427–11431. (h) Wang, L.; Chen, M.; Zhang, J. *Org. Chem. Front.* **2019**, *6*, 32–35.

(16) Metal-free coupling of imides with unsymmetric iodonium salts is also known: Basu, S.; Sandtorv, A. H.; Stuart, D. R. *Beilstein J. Org. Chem.* **2018**, *14*, 1034–1038.

(17) Wijma, R. A.; Huttner, A.; Koch, B. C. P.; Mouton, J. W.; Muller, A. E. *J. Antimicrob. Chemother.* **2018**, *73*, 2916–2926.

(18) Huang, Q.; Liu, Q.; Ouyang, D. *Med. Chem.* **2019**, *15*, 3–7.

(19) Gurjar, K. K.; Sharma, R. K. *ChemCatChem* **2017**, *9*, 862–869.

(20) (a) Chen, B.; Hou, X.-L.; Li, Y.-X.; Wu, Y.-D. *J. Am. Chem. Soc.* **2011**, *133*, 7668–7671. (b) Ichiishi, N.; Canty, A. J.; Yates, B. F.; Sanford, M. S. *Organometallics* **2014**, *33*, 5525–5534.

(21) Allen, S. E.; Walvoord, R. R.; Padilla-Salinas, R.; Kozłowski, M. *C. Chem. Rev.* **2013**, *113*, 6234–6458.

(22) For similar acetate-assisted deprotonation reactions, see: Davies, D. L.; Macgregor, S. A.; McMullin, C. I. *Chem. Rev.* **2017**, *117*, 8649–8709.



## Paper II

# A Mechanistic Study of the Cu-catalyzed *N*-arylation of Hydantoins with Aryl(TMP)iodonium Salts

Linn Neerbye Berntsen and Ainara Nova

*Draft of the Manuscript*



## Paper III

# Cu-catalyzed C(sp<sup>2</sup>)-N-bond Coupling of Boronic Acids and Cyclic Imides

Linn Neerbye Berntsen, Thomas Nordbø Solvik, Kristian Sørnes, David S. Wragg  
and Alexander H. Sandtorv

Chemical Communications **2021**, *57*, 1359-7345.

DOI: 10.1039/D1CC04356K










## Cu-catalyzed C(sp<sup>2</sup>)-N-bond coupling of boronic acids and cyclic imides†

 Cite this: *Chem. Commun.*, 2021, 57, 11851

 Received 9th August 2021,  
 Accepted 19th October 2021

DOI: 10.1039/d1cc04356k

[rsc.li/chemcomm](http://rsc.li/chemcomm)

 Linn Neerbye Berntsen,  Thomas Nordbø Solvi, Kristian Sørnes,  David S. Wragg and Alexander H. Sandtorv \*

A general Cu-catalyzed strategy for coupling cyclic imides and alkenylboronic acids by forming C(sp<sup>2</sup>)-N-bonds is reported. The method enables the practical and mild preparation of (*E*)-enimides. A large range of cyclic imides are allowed, and di- and tri-substituted alkenylboronic acids can be used. Full retention was observed in the configuration of the alkene double bond in the coupled products. The method is also applicable for preparing *N*-arylimides, using arylboronic acids as coupling partners. The usefulness of this strategy is exemplified by the convenient derivatization of the chemotherapy medication 5-fluorouracil, the nucleoside uridine and the anti-epileptic drug phenytoin.

Enimides (Fig. 1) are functional groups found in *N*-sulfonylurea isosteres,<sup>1</sup> biologically active structures,<sup>2,3</sup> functional materials,<sup>4</sup> and natural products such as the parazoanthines A-E.<sup>5</sup> They are also building blocks in synthesis of complex structures,<sup>6</sup> polycyclic architecture,<sup>7</sup> and β-2-amino acid derivatives.<sup>8</sup>

The growing interest in the enamide moiety has catalyzed a recent spurt of attention for methodology appropriate for its construction (Fig. 2).<sup>9</sup> In reactions where the enamide C(sp<sup>2</sup>)-N-bond is formed, only a few strategies are known. The main access point is the Ru-catalyzed hydroimidation strategy, wherein imides and alkynes are condensed (Fig. 2, strategy 1).<sup>10</sup> Drawbacks include the use of an expensive Ru-catalysts, and the structural limitations imposed. A second approach involves the Cu-mediated coupling of imides and vinylic halides (Fig. 2, strategy 2).<sup>11</sup> This strategy is only applicable to phthalimide, and therefore specialized. Other examples are substrate specific.<sup>12,13</sup>

The Chan-Lam<sup>14</sup> inspired Cu-catalyzed process using alkenyl boron coupling partners, is an attractive route to enimides for several reasons: (i) the availability of alkenylboronic reagents<sup>15</sup> provide synthetic flexibility, (ii) the use of an inexpensive Cu-catalyst is attractive, and (iii) a potentially larger structural diversity

of enimides is conceivable, compared to Ru-methods currently used. Thus far, only highly substrate dependent examples are known,<sup>16</sup> but a general method has not been reported before now.

Our endeavors were initiated as shown in Table 1. Due to our ongoing interest<sup>17</sup> in the pharmaceutically relevant hydantoin framework,<sup>18</sup> hydantoin **1a** was used as a model substrate, with styrylboronic acid **2a** as reagent. The optimal conditions (entry #1) involved the use of excess reagent **2a** (3.0 equiv.) with copper(II)triflate and pyridine in ethanol at 25 °C. Less expensive Cu-salts may also be effective (#2 and 3). The process was also effective using 2.0 equiv. of the reagent (entry #4), so less reagent can be employed if a slight reduction in yield is acceptable. Our investigations uncovered that the process was inefficient in aprotic solvents such as DMF and toluene (entries #6 and 7), and that the use of base/ligand was of paramount importance. Surprisingly, triethylamine (entry #8) performed poorly compared to pyridine. Strong, non-nucleophilic bases (entries #9 and 11) were also ineffective. The complete optimization study can be found in the ESI.†

We next investigated the scope and limitations of the method, Scheme 1. Complete retention of the configuration

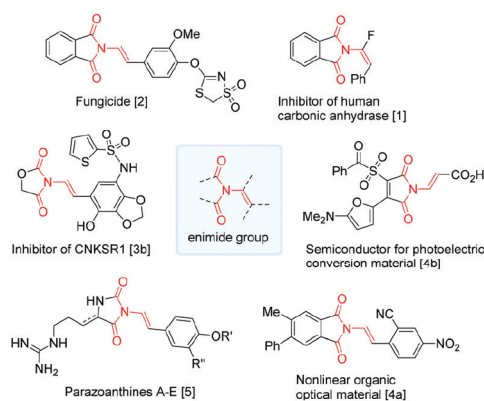
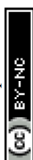


Fig. 1 Some examples of cyclic enimides.

Department of Chemistry, University of Oslo, Oslo N-0315, Norway.

 E-mail: [a.h.sandtorv@kjemi.uio.no](mailto:a.h.sandtorv@kjemi.uio.no)

† Electronic supplementary information (ESI) available. CCDC 2099681, 2099682, 2099683, 2099684 and 2099686. For ESI and crystallographic data in CIF or other electronic format see DOI: 10.1039/d1cc04356k



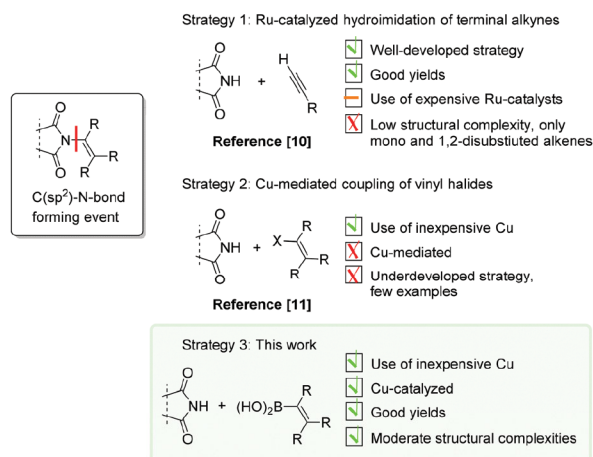


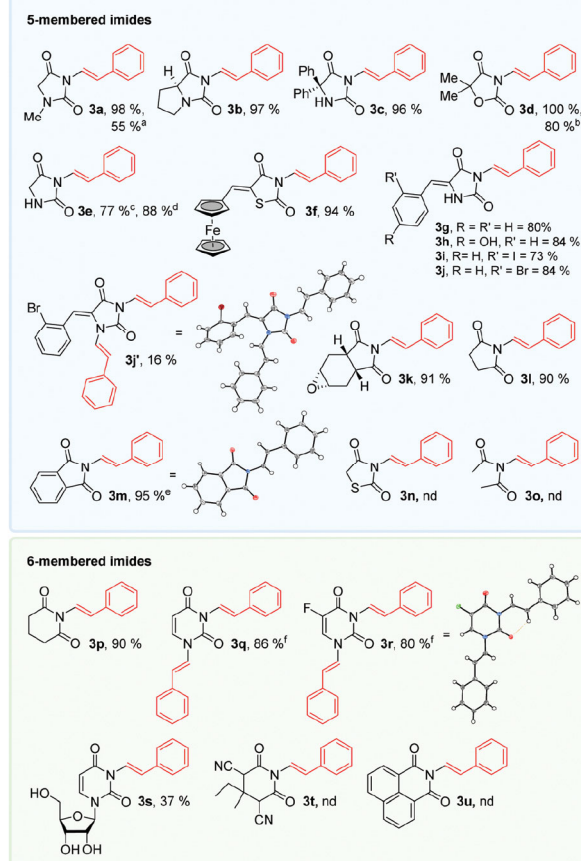
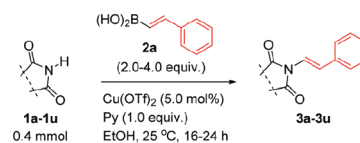
Fig. 2 Prior developments in the area of C(sp<sup>2</sup>)-N-bond formation.

Table 1 Reaction optimization

#	Catalyst	2a (equiv.)	Additive/base (equiv.)	Solvent	Time (h)	Yield <sup>a</sup> (%)
1	Cu(OTf) <sub>2</sub>	3.0	Py (1.0)	EtOH	9/15	98/97 <sup>b</sup>
2	Cu(NO <sub>3</sub> ) <sub>2</sub> <sup>c</sup>	3.0	Py (1.0)	EtOH	24	96
3	CuCl	3.0	Py (1.0)	EtOH	24	95
4	Cu(OTf) <sub>2</sub>	2.0	Py (1.0)	EtOH	24	94
5 <sup>d</sup>	Cu(OTf) <sub>2</sub>	1.0	Py (1.0)	EtOH	24	71
6	Cu(OTf) <sub>2</sub>	3.0	Py (1.0)	DMF	24	26
7	Cu(OTf) <sub>2</sub>	3.0	Py (1.0)	PhMe	24	0
8	Cu(OTf) <sub>2</sub>	3.0	Et <sub>3</sub> N (1.0)	EtOH	24	8
9	Cu(OTf) <sub>2</sub>	3.0	<i>t</i> -BuOK (1.0)	EtOH	18	22
10	—	3.0	<i>t</i> -BuOK (2.0)	EtOH	24	0
11	Cu(OTf) <sub>2</sub>	3.0	LiHMDS (1.0)	EtOH	18	3

Conditions: *N*-Methylhydantoin **1a** (0.20 mmol, 1.0 equiv.), boronic acid **2a** (as specified), catalyst (0.010 mmol, 0.050 equiv.), additive/base (as specified) in solvent (as specified, 1 mL). <sup>a</sup> <sup>1</sup>H NMR yield using mesitylene as internal standard. <sup>b</sup> Isolated yield. <sup>c</sup> The (hemi)pentahydrate salt was used. <sup>d</sup> Reaction performed at 40 °C.

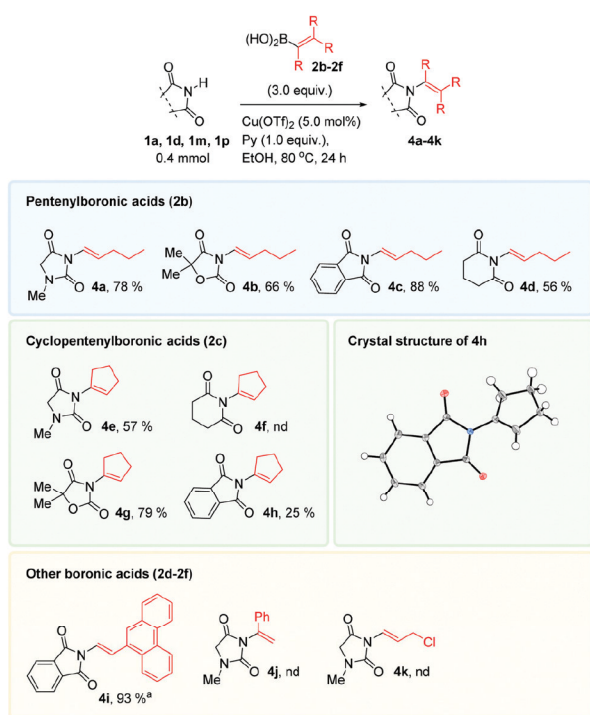
of the alkene double bond was observed in all cases. The anti-epileptic drug phenytoin **1c** was conveniently derivatized in excellent yield. Hydantoin **1e** was also smoothly alkenylated. The aldol adduct **1h** was smoothly *N*-3-alkenylated and not *O*-alkenylated, in excellent yield. We typically observed *N*-1, *N*-3-bisalkenylated hydantoin byproducts in these reactions, such as the disubstituted hydantoin **3j'**. Phthalimide **3m** and glutarimide **3p** were obtained in excellent yields. Uracils are privileged structures in drug discovery.<sup>19</sup> Uracil **1q**, the chemotherapy medication 5-fluorouracil **1r** and the nucleoside uridine **1s** were bis-alkenylated to **3q**, **3r** and **3s**, respectively. These results show that the method can conjugate drugs and nucleosides and provide uracils cumbersome to access.<sup>20</sup> Lastly, 2,4-thiazolidinedione **1n** was unreactive, but the ferrocenyl derivative **3f** was obtained in excellent yield.



Scheme 1 Imide scope of the reaction. Conditions: imide **1a–1u** (0.40 mmol, 1.0 equiv.), boronic acid **2a** (1.2 mmol, 3.0 equiv.), Cu(OTf)<sub>2</sub> (0.020 mmol, 0.050 equiv.), pyridine (0.40 mmol, 1.0 equiv.) and EtOH (2 mL). <sup>a</sup> (*E*)-Styryl-9-BBN was used as coupling partner. <sup>b</sup> CuCl (5.0 mol%) was used as catalyst. <sup>c</sup> 2.0 equiv. boronic acid **2a** was used. <sup>d</sup> Reaction performed at 1.5 mmol scale. <sup>e</sup> Reaction performed at 0.40 and 1.0 mmol scale. <sup>f</sup> 4.0 equiv. boronic acid **2a** was used.

The method is applicable to cyclic imides, and not linear imides, as imide **1o** failed to react under our conditions. As suggested by Wasielewski *et al.*<sup>21</sup> the carbonyl groups can adopt a parallel, coplanar conformation<sup>22</sup> and may chelate to Cu(II)-ions. The chelation is likely detrimental for the coupling reaction.

A selection of alkenylboronic acids **2b–2f** were next investigated with some imides, Scheme 2. The performance of the coupling reaction varied. The 1-pentenyl reagent **2b** transferred in good to moderate yields, depending on the imide substrate. The cyclopentenyl coupling partner **2c** was challenging, likely imposing a high steric demand in relevant Cu-species in the catalytic cycle. The coupled product **4g** was obtained in good yield, but the six membered product **4f** was not detected.



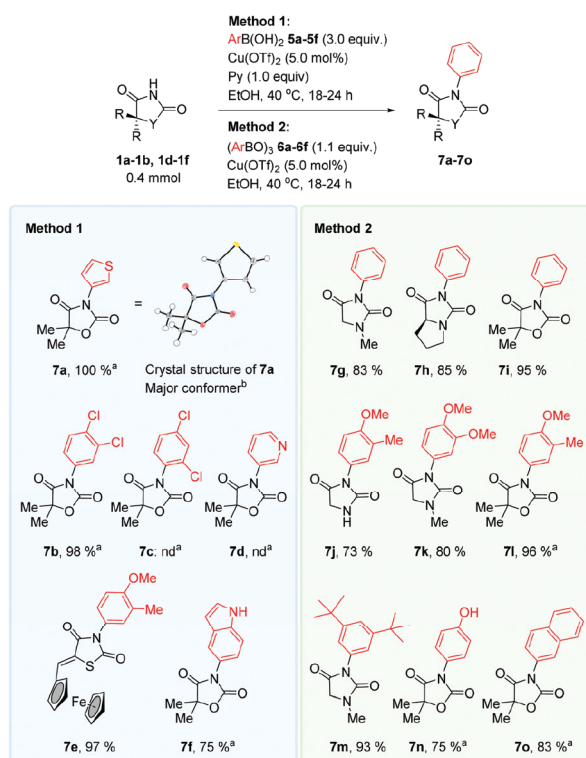
**Scheme 2** Alkenylboronic acid scope. Conditions: imide **1a**, **1d**, **1m** or **1p** (0.40 mmol, 1.0 equiv.), boronic acid **2b–2f** (1.2 mmol, 3.0 equiv.), Cu(OTf)<sub>2</sub> (0.020 mmol, 0.050 equiv.), pyridine (0.40 mmol, 1.0 equiv.) and EtOH (2 mL). <sup>a</sup> Reaction performed at 0.18 mmol scale at 25 °C.

The 1,1,2-trisubstituted alkenes obtained, are not currently accessible employing the Ru-catalyzed methods mentioned in the introduction.

Our earlier work<sup>17</sup> spurred an interest in employing arylboronic acids for *N*-arylation. Although the Cu-catalyzed or -mediated arylation of imides has been documented earlier,<sup>23</sup> the use of such conditions is sparingly described<sup>24</sup> using the pharmaceutically relevant hydantoin, 2,4-oxazolidinedione and related frameworks as substrates.

The method was high yielding and tolerable to diverse aryl groups, Scheme 3. The reaction performance varied if the arylboronic acid (method 1), or the corresponding anhydride (triarylboroxine, method 2) was employed. It is not possible to draw a conclusion as to which method operates best with which substrate. The pyridine likely has several key functions, such as being a Cu-ligand, acting as a base, and stabilizing boroxines *in situ*.<sup>25</sup>

The method smoothly transferred electron-rich aryl groups to form products such as **7j**, **7k**, **7l**, **7m** and **7n** in mostly excellent yields. Electron-rich heterocyclic fragments were also efficiently coupled. The thiophenyl product **7a** was obtained in excellent yield, and the indolyl product **7f** was obtained in good yield. The pyridinyl product **7d** was not obtained. The electron-poor 3,4-dichlorophenyl group coupled to afford product **7b** in excellent yield, whereas the 2,4-dichlorophenyl group did not couple. We attribute this to the steric hindrance of the



**Scheme 3** Scope of *N*-arylation. Method 1: hydantoin **1a**, **b** or **1d–1f** (0.40 mmol, 1.0 equiv.), boronic acid **5a–5f** (1.2 mmol, 3.0 equiv.), Cu(OTf)<sub>2</sub> (0.020 mmol, 0.050 equiv.), pyridine (0.020 mmol, 1.0 equiv.) in EtOH (2 mL). Method 2: hydantoin **1a**, **b** or **1d–1f** (0.40 mmol, 1.0 equiv.), boroxine **6a–6f** (0.44 mmol, 1.1 equiv.), Cu(OTf)<sub>2</sub> (0.020 mmol, 0.050 equiv.). <sup>a</sup> Reaction performed on 0.14 mmol scale. <sup>b</sup> Only the major conformer of the thiophene-ring is shown.

chlorine atom in the 2-position of the aryl group. Electronically neutral phenyl and naphthyl groups coupled in good yields.

L. N. B. and T. N. S. acknowledge the Department of Chemistry at the University of Oslo for funding their PhD fellowships. George Peletis is acknowledged for performing initial experiments on the *N*-arylation chemistry of hydantoin. The project has received support from UiO: Life Science and was partially supported by the Research Council of Norway through the Norwegian NMR Platform, NNP (226244/F50). We acknowledge the use of the Norwegian national infrastructure for X-ray diffraction and scattering (RECX, Research Council of Norway project number 208896).

## Conflicts of interest

There are no conflicts to declare.

## Notes and references

- B. Metayer, A. Angeli, A. Mingot, K. Jouvin, G. Evano, C. T. Supuran and S. Thibaudeau, *J. Enzyme Inhib. Med. Chem.*, 2018, **33**, 804–808.
- H. Uhr, C. Boie, H. Rieck, B.-W. Krueger, U. Heinemann, R. Market, M. Vaupel, M. Kugler, K. Stenzel, U. Wachendorff-Neumann, A. Mauler-Machnik, K.-H. Kuck, P. Loesel and S.-I. Narabu,

- Preparation of aryloxydithiazole and aryloxydithiazine dioxides as pesticides and fungicides, Patent DE 19918294, 2000.
- 3 (a) A. D. Brown, M. E. Bunnage, C. A. L. Lane, R. A. Lewthwaite, P. A. Glossop, K. James and D. A. Price, Preparation of formylamino hydroxyphenyl phenylacetamide derivatives as  $\beta 2$  adrenoceptor agonists, Patent US 20050215590 A1, 2005; (b) D. L. Kirkpatrick and M. Indarte, Preparation of N-substituted thiazolecarboxamides for inhibiting CNKSR1, Patent US 20160304533 A1, 2016; (c) S. Louzoun Zada, K. D. Green, S. K. Shrestha, I. M. Herzog, S. Garneau-Tsodikova and M. Fridman, *ACS Infect. Dis.*, 2018, **4**, 1121–1129.
  - 4 (a) T. Ogawa and H. Yamada, Preparation of N-styrylphthalimide derivatives as nonlinear organic optical materials, Patent JP 08176107, 1996; (b) S. Otsu, K. Ofuku and N. Kagawa, Semiconductor for photoelectric conversion material, photoelectric converter, and photoelectrochemical cell, Patent, JP 2005019124, 2003.
  - 5 N. Cachet, G. Genta-Jouve, E. L. Regalado, R. Mokriani, P. Amade, G. Culioli and O. P. J. Thomas, *J. Nat. Prod.*, 2009, **72**(9), 1612–1615.
  - 6 (a) E. Alacid and C. Najera, *Adv. Synth. Catal.*, 2008, **350**, 1316–1322; (b) W. Susanto, C.-Y. Chu, W. J. Ang, T.-C. Chou, L.-C. Lo and Y. Lam, *J. Org. Chem.*, 2012, **77**, 2729–2742; (c) F. de Nanteuil and J. Waser, *Angew. Chem., Int. Ed.*, 2013, **52**, 9009–9013; (d) J. Szudkowska-Frątczak, G. Hreczycho and P. Pawluć, *Org. Chem. Front.*, 2015, **2**, 730–738; (e) E. Landagaray, M. Ettaoussi, M. Rami, J. A. Boutin, D.-H. Caignard, P. Delagrange, P. Melynyk, P. Berthelot and S. Yous, *Eur. J. Med. Chem.*, 2017, **127**, 621–631.
  - 7 (a) S. K. Murphy, M. Zeng and S. B. Herzon, *Science*, 2017, **356**, 956–959; (b) P. Kramer, J. Schonfeld, M. Bolte and G. Manolikakes, *Org. Lett.*, 2018, **20**, 178–181.
  - 8 J. Dai, W. Ren, W. Chang, P. Zhang and Y. Shi, *Org. Chem. Front.*, 2017, **4**, 297–302.
  - 9 (a) Z. J. Song, M. D. Tellers, P. G. Dormer, D. Zewge, J. M. Janey, A. Nolting, D. Steinhuebel, S. Oliver, P. N. Devine and D. M. Tschaen, *Org. Process Res. Dev.*, 2014, **18**, 423–430; (b) H. Lingua, F. Vibert, D. Mouysset, D. Siri, M. P. Bertrand and L. Feray, *Tetrahedron*, 2017, **73**, 3415–3422; (c) W.-M. Cheng, R. Shang and Y. Fu, *Nat. Commun.*, 2018, **9**, 5215–5223; (d) W. Lin, W. Li, D. Lu, F. Su, T.-B. Wen and H.-J. Zhang, *ACS Catal.*, 2018, **8**, 8070–8076.
  - 10 (a) L. J. Goossen, M. Blanchot, C. Brinkmann, K. Goossen, R. Karch and A. J. Rivas-Nass, *Org. Chem.*, 2006, **71**, 9506–9509; (b) M. Arndt, K. S. M. Salih, A. Fromm, L. J. Goossen, F. Menges and G. Niedner-Schatteburg, *J. Am. Chem. Soc.*, 2011, **133**, 7428–7449; (c) A. E. Buba, M. Arndt and L. J. Goossen, *J. Organomet. Chem.*, 2011, **696**, 170–178; (d) E. Semina, P. Tuzina, F. Bienewald, A. S. K. Hashmi and T. Schaub, *Chem. Commun.*, 2020, **56**, 5977–5980.
  - 11 (a) R. G. R. Bacon and A. Karim, *J. Chem. Soc., Perkin Trans. 1*, 1973, 278–280; (b) T. Ogawa, T. Kiji, K. Hayami and H. Suzuki, *Chem. Lett.*, 1991, 1443–1446.
  - 12 D. G. Kohler, S. N. Gockel, J. L. Kennemur, P. J. Waller and K. L. Hull, *Nat. Chem.*, 2018, **10**, 333–340.
  - 13 (a) L. V. Desai and M. S. Sanford, *Angew. Chem., Int. Ed.*, 2007, **46**, 5737–5740; (b) Z. Song and W. Yi, *Adv. Synth. Catal.*, 2016, **358**, 2727–2732.
  - 14 J. Q. Chen, J. H. Li and Z. B. Dong, *Adv. Synth. Catal.*, 2020, **362**, 3311–3331.
  - 15 (a) R. J. Perner, C.-H. Lee, M. Jiang, Y.-G. Gu, S. DiDomenico, E. K. Bayburt, K. M. Alexander, K. L. Kohlhaas, M. F. Jarvis, E. L. Kowaluk and S. S. Bhagwat, *Bioorg. Med. Chem. Lett.*, 2005, **14**, 2803–2807; (b) G. A. Molander, L. N. Cavalcanti, B. Canturk, P.-S. Pan and L. E. Kennedy, *J. Org. Chem.*, 2009, **74**, 7364–7369; (c) J. Hu, B. Cheng, X. Yang and T.-P. Loh, *Adv. Synth. Catal.*, 2019, **361**, 4902–4908.
  - 16 (a) Y. Bolshan and R. A. Batey, *Angew. Chem., Int. Ed.*, 2008, **47**, 2109–2112; (b) J.-W. Jiao, H.-Y. Bi, P.-S. Zou, Z.-X. Wang, C. Liang and D.-L. Mo, *Adv. Synth. Catal.*, 2018, **360**, 3254–3259; (c) L. Steemers, L. Wijsman and J. H. van Maarseveen, *Adv. Synth. Catal.*, 2018, **360**, 4241–4245; (d) J. Li, Z. Zhang, L. Wu, W. Zhang, P. Chen, Z. Lin and G. Liu, *Nature*, 2019, **574**, 516–521.
  - 17 L. Neerby Berntsen, A. Nova, D. S. Wragg and A. H. Sandtorv, *Org. Lett.*, 2020, **22**, 2687–2691.
  - 18 (a) L. Konnert, F. Lamaty, J. Martinez and E. Colacino, *Chem. Rev.*, 2017, **117**, 13757–13809; (b) P. Thilmany, P. Gerard, A. Vanoost, C. Deldaele, L. Petit and G. Evano, *J. Org. Chem.*, 2019, **84**, 394–400.
  - 19 A. Palasz and D. Ciez, *Eur. J. Med. Chem.*, 2015, **97**, 582–611.
  - 20 R. Dalpozzo, A. De Nino, L. Maiuolo, A. Procopio, R. Romeo and G. Sindona, *Synthesis*, 2002, 172–174.
  - 21 E. T. Chernick, M. J. Ahrens, K. A. Scheidt and M. R. Wasielewski, *J. Org. Chem.*, 2005, **70**, 1486–1489.
  - 22 C. S. Kraihanzel and S. C. Grenda, *Inorg. Chem.*, 1965, **4**, 1037–1042.
  - 23 Z.-G. Zheng, J. Wen, N. Wang, B. Wu and X. Q. Yu, *Beilstein J. Org. Chem.*, 2008, **4**, 40.
  - 24 H. M. Hügel, C. J. Rix and K. Fleck, *Synlett*, 2006, 2290–2292.
  - 25 A. L. Korich and P. M. Iovine, *Dalton Trans.*, 2010, **39**, 1423–1431.

